

JANUARY 1989
ENVIRONMENTAL SCIENCE & TECHNOLOGY

ES&T



ts of

**Renewable
energy sources**
page 10

POLLUTION BUSTERS

When you're a leader in the defense industry, you're concerned with environmental protection. Our concern has given rise to a variety of opportunities in all phases of compliance, control and management.

Our team of pollution busters includes: Safety & Environmental Engineers and Specialists; Regulatory Specialists; Permit Specialists; and Groundwater Remediation Specialists.

This is how our team operates. Our Safety & Environmental professionals provide monitoring support in the areas of waste waters, soil, groundwater and air. They conduct investigations and formulate compliance programs to minimize pollution impact and prevent problems. And, they represent Lockheed in these matters with respective regulatory agencies.

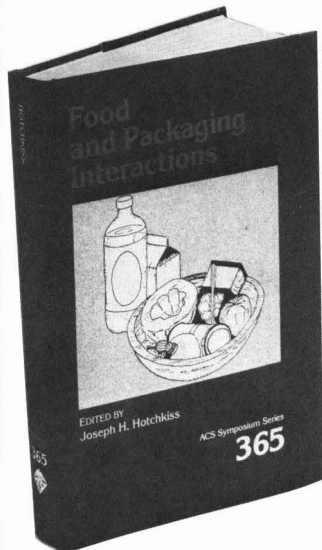
Our Regulatory Specialists analyze and evaluate new and changing environmental requirements, monitoring the pulse of key legislation to provide impact analyses to management. While our Permit Specialists identify and schedule permitting requirements for all Facility Engineering projects and track the status of all permits.

Specialists in groundwater and soil remediation assess contamination; interface with regulatory agencies; and coordinate technical studies and remedial plans.

Get on the team that keeps our business clean and enjoy the benefits of a Fortune 500 company. Just send your resume to J. Sims, Professional Staffing, Lockheed Missiles & Space Company, Dept. 557KAJS, P.O. Box 3504, Sunnyvale, CA 94088-3504. We are proud to be an equal opportunity, affirmative action employer. U.S. citizenship may be required.

 **Lockheed Missiles & Space Company**
Giving shape to imagination.

Food and Packaging Interactions



GAIN

The Professional Edge WITH MEMBERSHIP IN THE AMERICAN CHEMICAL SOCIETY

- Keep up-to-date with weekly copies of **CHEMICAL AND ENGINEERING NEWS**
- Enjoy substantial discounts on subscriptions to ACS's internationally respected, authoritative journals and publications
- Network with your fellow scientists at local, regional and national meetings
- Enhance your career opportunities with ACS employment services
- Save on insurance and retirement plans and tax deferred annuity programs
- Discover the latest advances in your discipline with a first-year-free Division membership

Learn why 9 out of 10 ACS members renew year after year. Gain the Professional Edge: Join ACS now. For further information write or send the coupon below or call TOLL FREE 1-800-424-6747

American Chemical Society
1155 Sixteenth St., N.W.
Washington, DC 20036

YES! Please send information on the advantages of joining the ACS.

Name _____
Address _____

I am most interested in the following science(s): _____

The last decade has seen a rapid evolution in the methods and materials used to package foods. This new book is the first to examine the impact changes in food packaging technology can have on the food itself. You'll learn how packaging affects the quality, safety, shelf life, and nutritional contents of food. You'll benefit from the experiences of leading research groups studying food and packaging interactions. You'll gain important knowledge on the mechanisms by which packaging interacts with food, including:

- permeability
- migration
- processing
- flavor permeability and sorption
- package performance

Food and Packaging Interactions will prove invaluable to food scientists in general, and to all packaging technologists in the food processing and packaging industries.

Joseph H. Hotchkiss, *Editor, Cornell University*

Developed from a symposium sponsored by the Division of Agricultural and Food Chemistry of the American Chemical Society

ACS Symposium Series No. 365
306 pages (1988) Clothbound
ISBN 0-8412-1465-4 LC 88-1273
US & Canada \$64.95 Export \$77.95

Order from: American Chemical Society
Distribution Office Dept. 82
1155 Sixteenth St., N.W.
Washington, DC 20036

or CALL TOLL FREE

800-227-5558
and use your credit card!

Editor: William H. Glaze
Associate Editor: John H. Seinfeld
Associate Editor: Philip C. Singer

ADVISORY BOARD

Roger Atkinson, Joan M. Daisey, Fritz H. Frimmel, Nicholas E. Gallopoulos, George R. Helz, Ronald A. Hites, James Leckie, Donald Mackay, Ralph Mitchell, Walter J. Weber, Jr., Alexander J. B. Zehnder, Richard G. Zepp

WASHINGTON EDITORIAL STAFF

Managing Editor: Stanton S. Miller
Associate Editor: Julian Josephson

MANUSCRIPT REVIEWING

Manager: Monica Creamer
Associate Editors: Yvonne D. Curry,
Diane Scott

Assistant Editor: Marie C. Wiggins

MANUSCRIPT EDITING

Journals Editing Manager: Mary E. Scanlan
Assistant Editor: Lorraine Gibb

Director, Operational Support:

C. Michael Phillippe

GRAPHICS AND PRODUCTION

Production Manager: Leroy L. Corcoran
Art Director: Alan Kahan
Designer: Peggy Corrigan
Production Editor: Jennie Reinhardt

PUBLICATIONS DIVISION

Director: Robert H. Marks
Head, Special Publications Department:
Randall E. Wedin

Head, Journals Department: Charles R. Bertisch

ADVERTISING MANAGEMENT

Centcom, Ltd.
For officers and advertisers, see page 36.

Please send *research* manuscripts to Manuscript Reviewing, *feature* manuscripts to Managing Editor. For editorial policy, author's guide, and peer review policy, see the January 1989 issue, page 29, or write Monica Creamer, Manuscript Reviewing Office, *ES&T*. A sample copyright status form, which may be copied, appears on the inside back cover of the January 1989 issue.

Environmental Science & Technology, ES&T (ISSN 0013-936X), is published monthly by the American Chemical Society at 1155 16th Street, N.W., Washington, D.C. 20036. Second-class postage paid at Washington, D.C., and at additional mailing offices. POSTMASTER: Send address changes to *Environmental Science & Technology*, Membership & Subscription Services, P.O. Box 3337, Columbus, Ohio 43210.

SUBSCRIPTION PRICES 1989: Members, \$33 per year; nonmembers (for personal use), \$61 per year; institutions, \$212 per year. Foreign postage, \$10 additional for Canada and Mexico, \$18 additional for Europe including air service, and \$27 additional for all other countries including air service. Single issues, \$18 for current year, \$2 for prior years. Back volumes, \$225 each. For foreign rates add \$2 for single issues and \$10 for back volumes. Rates above do not apply to nonmember subscribers in Japan, who must enter subscription orders with Maruzen Company, Ltd., 3-10 Nihon bashi 2 chome, Chuo-ku, Tokyo 103, Japan. Tel: (03) 272-7211.

COPYRIGHT PERMISSION: An individual may make a single reprographic copy of an article in this publication for personal use. Reprographic copying beyond that permitted by Section 107 or 108 of the U.S. Copyright Law is allowed, provided that the appropriate per-copy fee is paid through the Copyright Clearance Center, Inc., 27 Congress St., Salem, Mass. 01970. For reprint permission, write Copyright Administrator, Publications Division, ACS, 1155 16th St., N.W., Washington, D.C. 20036.

REGISTERED NAMES AND TRADEMARKS, etc., used in this publication, even without specific indication thereof, are not to be considered unprotected by law.

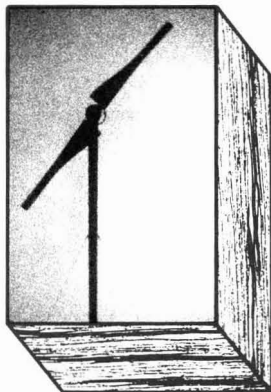
SUBSCRIPTION SERVICE: Orders for new subscriptions, single issues, back volumes, and microform editions should be sent with payment to Office of the Treasurer, Financial Operations, ACS, 1155 16th St., N.W., Washington, D.C. 20036. Phone orders may be placed, using Visa, Master Card, or American Express, by calling the ACS Sales Office toll free at (800) 227-5558 or Member and Subscriber Services at (614) 447-3776 or toll free (800) 333-9511 from anywhere in the continental U.S. (In the Washington, D.C., area call 872-4363.) Changes of address, subscription renewals, claims for missing issues, and inquiries concerning records and accounts should be directed to Manager, Member and Subscriber Services, ACS, P.O. Box 3337, Columbus, Ohio 43210. Changes of address should allow six weeks and be accompanied by old and new addresses and a recent mailing label. Claims for missing issues will not be allowed if loss was due to insufficient notice of change of address, if claim is dated more than 90 days after the issue date for North American subscribers or more than one year for foreign subscribers, or if the reason given is "missing from files."

The American Chemical Society assumes no responsibility for statements and opinions advanced by contributors to the publication. Views expressed in editorials are those of the author and do not necessarily represent an official position of the society.

ES&T CONTENTS

Volume 23, Number 1, January 1989

FEATURES



10 **Renewable energy development.** It has many environmental benefits. Vic Phillips and Patrick Takahashi, University of Hawaii, Honolulu, HI.



14 **The drinking-water additives program.** The National Sanitation Foundation evaluates all types of products in contact with drinking water. Nina I. McClelland, David A. Gregorka, and Betsy D. Carlton, National Sanitation Foundation, Ann Arbor, MI.

REGULATORY FOCUS

27 **An environmental agenda for the new administration.** Alvin L. Alm lists some tasks he believes the incoming Bush administration should carry out.

VIEWS

20 **Living in a glass house.** Douglas G. Cogan examines adverse climatic changes that human activities may cause.

23 **Toxic trade with Africa.** Arti K. Vir looks at shipments of hazardous waste for disposal in Africa.

25 **Acid deposition: A paper tiger.** *ES&T's* Stan Miller observes that efforts to control acid rain in the United States have so far produced a plethora of papers.

DEPARTMENTS

- 3 Editorial
 - 4 Guest editorial
 - 5 Letters
 - 7 Currents
 - 22 Environmental index
 - 26 Books
 - 28 Advisory Board
 - 29 Editorial Policy
 - 33 Classified
 - 36 Consulting services directory
- IBC Copyright release form

UPCOMING

Overview of major health effects of tropospheric ozone
Changes in the chemistry of surface water

RESEARCH

■ 39 **Photooxidation of probe compounds sensitized by crude oils in toluene and as an oil film on water.** Rainer G. Lichtenhaler, Werner R. Haag,* and Theodore Mill
The effect of crude oil residues on

ESTHAG 23(1)1-128 (1989)
ISSN 0013 936X

Cover: Mark B. Thompson
Credits: p. 6, Lisa Damerst; pp. 10-12, courtesy Vic Phillips; p. 14, John Heiny; p. 20, M.J. Davis Design

the photolyses of a variety of model crude oil components in toluene is studied.

46

Continuous flow method for simultaneous determination of monochloramine, dichloramine, and free chlorine: Application to a water purification plant. Toyooki Aoki

A system with three double-tube separation units is proposed for the continuous, simultaneous determination of monochloramine, dichloramine, and free chlorine in water.

51

Transport of microspheres and indigenous bacteria through a sandy aquifer: Results of natural- and forced-gradient tracer experiments. Ronald W. Harvey,* Leah H. George, Richard L. Smith, and Denis R. LeBlanc

The results of the comparative transport of bacteria, bromine, and microspheres in groundwater is presented.

57

On the distribution of atmospheric polychlorinated biphenyl congeners between vapor phase, aerosols, and rain. J. C. Duinker* and F. Bouchertall

Fourteen chromatographically well-separated PCB congeners are analyzed in filtered air, in particulates, and in rain collected simultaneously in an urban area.

62

Characterization of chlorophenol and chloromethoxybenzene biodegradation during anaerobic treatment. Sandra L. Woods,* John F. Ferguson, and Mark M. Benjamin

The removal of chlorinated phenols, catechols, guaiacols, and veratroles during continuous anaerobic treatment is described.

68

Biodegradation of trace concentrations of substituted phenols in granular activated carbon columns. Gerald E. Speitel Jr.,* Chih-Jen Lu, Mukesh Turakhia, and Xian-Jin Zhu

Biodegradation of *p*-nitrophenol, 2,4-dichlorophenol, and pentachlorophenol is investigated over the concentration range of 1–25 µg/L.

75

Measurements of the gas/particle distributions of atmospheric organic compounds. Mary P. Ligocki and James F. Pankow*

The gas/particle distributions of polycyclic aromatic hydrocarbons and other organic compounds are measured at ground level in Portland, OR, and the Oregon coast.

83

Distribution of polychlorinated biphenyl congeners and other halocarbons in whole fish and muscle among Lake Ontario salmonids. Arthur J. Niimi* and Barry G. Oliver

Concentrations of PCB congeners vary widely in four Lake Ontario salmonid species although percent contribution of each congener to total concentration is similar among species.

89

Characteristics of radioactive particles released from the Chernobyl nuclear reactor. R. G. Cuddihy,* G. L. Finch, G. J. Newton, F. F. Hahn, J. A. Mewhinney, S. J. Rothenberg, and D. A. Powers.

Particles from the Chernobyl nuclear reactor accident are analyzed to evaluate the long-term human exposure risks.

95

Increases in the polynuclear aromatic hydrocarbon content of an agricultural soil over the last century. Kevin C. Jones,* Jennifer A. Strafford, Keith S. Waterhouse, Edward T. Furlong, Walter Giger, Ronald A. Hites, Christian Schaffner, and A. E. Johnston

Soil samples collected from Rothamsted Experimental Station in southeast England at various times since the mid-1800s and up to the present are analyzed for polynuclear aromatic hydrocarbons.

101

Evaporation times and rates of specific hydrocarbons in oil spills. Warren Stiver, Wan Ying Shiu, and Donald Mackay*

A method is presented for estimating the residence time of specific hydrocarbons in an oil spill.

106

A new gas-phase nitric acid calibration system. Linda J. Nunnermacker,* Russell R. Dickerson, Alan Fried, and Robert Sams

A new calibration source of gaseous nitric acid based on the conversion of HCl(g) to HNO₃ on solid AgNO₃(s) is developed.

110

Paleolimnological evidence for trace-metal sensitivity in scaled chrysophytes. Sushil S. Dixit,* Aruna S. Dixit, and R. Douglas Evans

A stratigraphic study of scaled chrysophyte microfossils (golden-brown algae) in the sediments of three Sudbury, Ontario, lakes is initiated to examine their sensitivity to increased trace-metal pollution.

115

Oxidative co-oligomerization of guaiacol and 4-chloroaniline. Kathleen E. Simmons, Robert D. Minard, and Jean-Marc Bollag*

The formation of a complex between a humus constituent and a pesticide derivative by enzymes and an abiotic catalyst provides a model reaction for incorporation of xenobiotics into humus materials.

121

Physical and chemical behavior of stabilized sewage sludge blocks in seawater. Chih-Shin Shieh* and Frank J. Roethel

The results indicate that the stabilized sewage sludge blocks maintain their structural integrity in seawater and would be classified as a nonhazardous material.

125

Theoretical and experimental evidence for artifact particulate matter formation in electrical aerosol analyzers. Arthur W. Stelson

Artifact aerosol formation from sulfur dioxide within an electrical aerosol analyzer is demonstrated and attributed to hydroxyl radical generation within the instrument.

*To whom correspondence should be addressed.

■ This article contains supplementary material in microform. See ordering instructions at end of paper.

A progress report

I am pleased to take this opportunity, at the beginning of my second year as editor, to announce some major developments in the journal. First, we are announcing changes in the types of research articles we will publish and the elimination of the Notes category. Formerly Notes were "shorter research reports of unusual significance or studies of small scope." The Editorial Advisory Board recommended, and the editors concurred, that studies of small scope can be handled in short articles but that a new category is needed to emphasize rapid communication of results of unusual quality and significance. Our revised editorial policy, found later in this issue, includes such a new category: Research Communications. Effective immediately we will accept manuscripts that meet our stated criteria for this category. We have made every effort to develop a system that will expedite the publication of Communications, including the provision for handling manuscripts by FAX. Our goal is publication within 12 weeks of receipt, providing there are no major revisions required. There will be no quota on the number of Research Communications published each month.

We are also continuing to make efforts to decrease the time from receipt to publication of all research articles. Our data suggest that we have made progress in this area in 1988, but the record is still spotty. I continue to have grave concerns about time to publication, and assure authors that we will continue to do whatever is necessary to make *ES&T* a leader, not a laggard, in this respect.

In addition to other strong appointments to the Advisory Board, we are pleased to announce in this issue the expansion of the *ES&T* Advisory Board to include two new members in environmental biology. Professor Ralph Mitchell of Harvard University and Professor Alexander Zehnder of the Agricultural University at Wageningen bring to our board areas of expertise

which have been missing. Their appointment signifies the editors' determination to cover the important developments in the area of environmental biology and biochemistry that are changing the face of environmental science.

Finally, we also welcome in this issue another new talent, Alvin Alm. He will replace Richard Dowd as author of the Regulatory Focus column in the front section of the journal. Mr. Alm brings to this position experience in government and the private sector. Most recently, he was the Chair of the Research Strategies Committee of the EPA Science Advisory Board, whose report promises to make a major impact on the agency. Mr. Alm will continue to cover domestic public policy issues, but in addition he will give enhanced coverage of international environmental developments. Managing Editor Stan Miller and his staff will focus increasingly on international news and features, which we feel is appropriate for a journal of the stature of *ES&T*.

I continue to be open to your suggestions on the ways in which *ES&T* can better serve the environmental science professions.

R. H. Glaze



Rallying behind pollution prevention

All the recent talk about apparently new global environmental problems—such as acid rain, global warming, garbage disposal, and infectious waste—has not focused national interest on pollution prevention instead of control. America's emphasis on using more and better technology to control pollutants after they have been produced has weakened taboos against producing pollutants. Negotiating safe or acceptable levels of pollution institutionalizes its production and implies approval of it. This pollution control strategy has resulted in environmental policy gridlock rather than a major policy debate on prevention versus control. The upcoming 20th anniversary of Earth Day in 1990 offers an opportunity to put the policy spotlight on pollution prevention.

Calls for more recycling of garbage and toxic waste miss the point that any handling and management of waste is never as safe or beneficial as avoiding the generation of the waste in the first place. Discussions of finding substitutes for chlorofluorocarbons (CFCs) to combat stratospheric ozone depletion fail to articulate that that solution is a preventive measure and that control measures used after CFCs are produced are far less effective. In the debate on how to reduce coal power plant emissions to fight acid rain, the choice between burning dirty coal and controlling air emissions versus using a cleaner raw material or energy source to eliminate them—another pollution prevention tactic—is not fully described. The comparative analyses ignore the fact that the options are different *qualitatively*.

The most effective, expeditious reductions in pollution have always come from practicing prevention—notably by banning chemicals and products such as DDT, PCBs, and leaded gasoline. Despite concern about severe economic dislocations, there is little evidence that they have occurred. Even now, the replacement of CFCs seems to be moving rapidly. A threat to health or environment does not have to be predicted for pollution prevention to be practiced. Pollution prevention can be used successfully after a cause of an environmental threat is identified if preventive measures

can be conceived and differentiated from control measures. An emphasis on prevention favors monitoring and analysis to detect problems early, before they become acute.

If pollution prevention became the environmental protection paradigm, then it would be routinely used to respond to environmental threats. Pollution control measures would be seen as inferior and used only in those cases where preventive measures had not yet been identified. Commitment to pollution prevention does not imply a belief that that all pollution can be eliminated.

If using pollution prevention were easy, we would have been using it already. Because prevention is not easy to use, we need to make it an issue of public policy debate, to make room for it on crowded agendas, and to acknowledge that we need a better, more cost-effective strategy and paradigm to achieve comprehensive environmental protection. Pollution prevention needs to evolve from a theoretical, philosophical concept sometimes practiced in an atmosphere of crisis to an explicit, commonly valued and applied tool used for all environmental problems.

Two recent actions at the Environmental Protection Agency, following several reports on waste reduction and pollution prevention, signal that this evolution is beginning. A recent report by EPA's Science Advisory Board concluded: "In addition to the current emphasis on federally mandated controls that are put in place to clean up pollutants after they have been generated, the Agency must develop a strategy that emphasizes the reduction of pollution before it is generated. A strategic shift in emphasis from control and clean-up to anticipation and prevention is absolutely essential to our future physical, environmental, and economic health" (1).

Even before the report was issued, EPA had formed an Office of Pollution Prevention. Several bills introduced in Congress proposed high status for such an office; however, funding for the office is low.

Now, the challenge is to build nationwide support for

(continued on p. 5)

ES&T LETTERS

Editorial comment

In the July 1988 issue of this journal a paper was published entitled "Sorption of 2,3,7,8-Tetrachlorodibenzo-*p*-dioxin to Soils from Water/Methanol Mixtures" (Vol. 22, pp. 819-825). In the original version of the paper, three authors were listed: R. W. Walters, the corresponding author, A. Guiseppi-Elie, and J. C. Means. Dr. Means' name was removed from the list of authors during the final stages of the review process by action of the corresponding author. There is currently a dispute between Dr. Walters and Dr. Means regarding this action. The editors of *ES&T* refuse to allow the journal to be used as a forum for this argument or to act as judges in the dispute. *ES&T*, like all scholarly journals, must rely on the ethical standards of authors, especially corresponding authors, in decisions regarding joint authorship. The editors will continue to assume that the responsibility for such decisions remains with corresponding authors.

William H. Glaze
Editor, *ES&T*

Arctic agreement?

Dear Sir: In the September *ES&T* article, "Finland's Environmental Trends" (Vol. 22, No. 9), you referred on page 1002 to an agreement to conduct joint studies of arctic regions, including the fate, transport, and effects of pollutants. This agreement, according to the article, was signed in March by Finland, the United States, Canada, Denmark, Norway, the Soviet Union, and Sweden. As a researcher involved in studying trace contaminants in the Arctic I immediately contacted a colleague at Environment Canada to seek further information. Unfortunately, he was unaware of an agreement being signed although he did attend a meeting of the International Arctic Science Committee in Stockholm in March. He stated that although an agreement was discussed and a recommendation was made to form an international committee for cooperation and coordination, nothing formal was signed.

Dennis J. Gregor

Head, Surveys and Interpretation Division
Environment Canada, Ottawa, ON
K1A 0H3

The author replies:

My information concerning the agreement came to me in March 1988 from

Jerry Brown, National Science Foundation, Washington, DC 20550, USA, telephone (202) 357-7817. He attended the meeting that gave birth to the arctic agreement in his capacity as head of the Arctic Research and Policy Staff, Division of Polar Programs. As I understood him, an actual agreement was made. When I used the phrase, "signed an agreement," I meant that a document was generated and agreed to by all parties. I did not use the term "signed," in the formal diplomatic sense. You might wish to contact Dr. Brown or the meeting's host, Bert Bolin of the Swedish Academy of Sciences in Stockholm, telephone 08-753-12-28, for further information. I am sure that either of these gentlemen can help you locate the Canadian you seek to contact.

Julian Josephson

Associate Editor, *ES&T*

Laboratory performance

Dear Sir: I read with interest the October feature article, "A Comparison of Laboratory Performance" (*ES&T*, Vol. 22, No. 10, p. 1121). The authors quite accurately point out the importance of establishing good communication with

(continued on p. 6)

(from p. 4)

these initial steps. If public and private resources shift from pollution control to prevention, then we will have more tangible evidence that the prevention paradigm is taking hold. In the coming months there is an historic opportunity for leaders in government, industry, and public interest groups to select pollution prevention as the theme for the 20th anniversary of Earth Day in 1990. Doing so could rekindle the spiritual and moral lift Earth Day gave the nation, firmly plant pollution prevention in the national consciousness, and overcome mere lip service in key institutions. Fearing that technology may not be harnessed fast enough to avert catastrophe and lacking confidence in current environmental programs, Americans are ready for pollution prevention.

References

- (1) *Future Risk: Research Strategies for the 1990s*; U.S. Environmental Protection Agency. U.S. Government Printing Office: Washington, DC, 1988; SAB-EC-88-040.



Joel S. Hirshhorn is senior associate at the Congressional Office of Technology Assessment in Washington, DC.

(from p. 5)

commercial laboratories. It is likewise important that laboratories communicate accurately with clients. To that end, I feel compelled to communicate to your readers a significant issue raised by the article.

There is no "National Certification" program. In the guest editorial, "Selecting Environmental Analytical Laboratories," Lawrence Keith suggests that clients request information from the laboratory concerning national certification. The feature story authors used EPA-CLP (Contractor Laboratory Program) participation as a quality determination category. This would lead the reader to conclude that EPA-CLP participation represents national certification. I was surprised that the article passed EPA's scrutiny because the CLP program is not, in fact, a national certification program.

Carla Dempsey, of EPA's Office of Emergency and Remedial Response (Superfund), pleaded with participants at a hazardous waste conference in Norfolk, Virginia, in May 1988 to recall that the "C" in CLP does not stand for certification. In addition, Bob Booth, Senior Service Advisor at EPA for Region III, stated at a conference organized by the American Council of Independent Laboratories (ACIL) in Atlantic City, NJ, on May 21, 1988, that "... the agency has never sold the CLP as a certification program."

The lack of a national certification program is a significant issue for many laboratories that work in multiple states. Each state, and often local governments and regulatory agencies as well, has its own independent certification program. To work in a particular area, a laboratory must comply with the prevailing certification requirements. These programs are repetitious, time-consuming, and costly, and frequently provide little quality assurance.

The problem is exacerbated by the de facto certification status the CLP program enjoys. Many laboratory users believe CLP certification is the same as national certification and therefore mistakenly believe that a CLP laboratory provides higher quality data. With the strict performance criteria demanded by EPA contracts (failure to comply results in mandatory penalties), non-EPA work can take a back seat.

For member firms of the ACIL, national certification has been an important issue for years. Many firms have supported the efforts of a private sector group known as the American Association for Laboratory Accreditation (A2LA). However, the lack of user concern for a national program, coupled with the political complexities of state programs, has made A2LA's

struggle difficult. While A2LA has a credible program in place, only 20 environmental laboratories are currently accredited by A2LA, and recognition of the program by regulation is non-existent.

For laboratories and laboratory users alike, there is hope in the recent formation of the Consortium for Quality Environmental Data (CQED). A growing group of private industries, trade associations, and laboratories is bringing the issue of national certification into the limelight. When the political and technical issues surrounding this important topic are resolved, a national certification program may be available that can appropriately be used as one criterion for evaluating and selecting environmental analytical laboratories.

For further information on A2LA, contact John Locke, 656 Quince Orchard Road, #704, Gaithersburg, MD 20878. For details on CQED, contact ACIL, 1725 K Street, Washington, DC 20006; (202) 887-5872.

Steven S. Fisher
President, Brown and Caldwell
Laboratories
Emeryville, CA 94608

The authors reply:

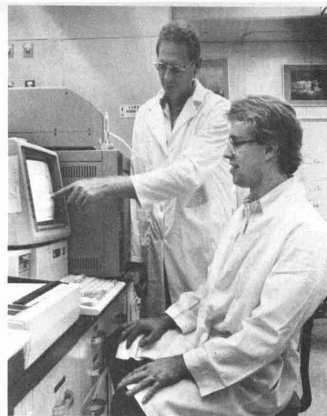
As authors of the feature article, "A Comparison of Laboratory Performances," we do not agree that the readers of our article will conclude that EPA-CLP participation represents "national certification." Indeed, if we believed that participation in EPA-CLP indicates national certification, there would not have been a need for this laboratory evaluation study. The 0.6% (2 points \times .3 weight) contribution to the overall score is recognition that EPA-CLP participation is not sufficient to judge a laboratory's performance.

We agree, however, that a certification of commercial laboratories is essential for the future of environmental monitoring.

Phyllis C. Pei
Julie H. Einerson
Sandia National Laboratories
Albuquerque, NM 87185

The guest editor replies:

Use of the term "national" in my statement, "... request a copy of its [a laboratory's] Quality Assurance plan, as well as information concerning state and national certification," was intended in the broad sense of U.S. government versus state government "certifications." Perhaps my meaning would have been clearer if I had used the word "federal"—my statement did not refer to the EPA-CLP, nor was such reference intended. For example, Ra-



dian Corporation has a U.S. Navy "certification" and a U.S. Army Corps of Engineers "validation," participates in federal WP and WS audits, and possesses a dozen state certifications and approvals, with five more state certifications pending.

Mr. Fisher is entirely correct in his assessment that the lack of a uniform, nationwide certification program is a significant issue for laboratories that work in multiple states. The redundancy of paperwork, performance evaluation analyses, and reports is expensive in time and money for laboratories that accept samples from several states. For example, our Austin, Texas, laboratory has state certifications or approvals from California, Oklahoma, and New York, in addition to an annual audit by the state of Texas. At the same time our Raleigh, North Carolina, laboratory has certifications, approvals, or audits by Texas, Delaware, Oklahoma, New York, and North Carolina, but not California. Our California laboratory is certified, approved, or audited by Oklahoma, Texas, and of course, California.

A true nationwide certification would be useful, however, only if all states would recognize it and accept it in place of their own systems. A recent nonexhaustive telephone poll by Radian found that 39 states require certifications for drinking-water analyses, and eight require certifications for nonpotable water analyses. State-imposed entropy is rapidly increasing and a vital question is whether the states would accept a national certification for environmental laboratories, if it existed, in place of their own approval systems. We need to hear representatives of state environmental laboratory certification agencies address this problem and give their opinions.

Lawrence H. Keith
Radian Corporation
Austin, TX 78720

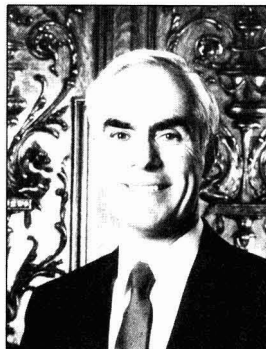
tors that currently are exempt from state regulations because they existed before these rules took effect, and may require them to retrofit controls. Bradley adds that state authorities have the power to mandate this NO_x control policy with no additional legislative or other approval. NES-CAUM's members are Connecticut, Maine, Massachusetts, New Hampshire, New Jersey, New York, Rhode Island, and Vermont.

In Florida, more than 90% of the population depends on groundwater for drinking water supplies. The same is true in Hawaii, Idaho, Mississippi, Nebraska, and New Mexico. The only part of the United States in which no one is dependent on groundwater is the District of Columbia. The next lowest dependence—20–29%—is found in Colorado and Rhode Island. The national average still is more than 50%. Arizona has dropped from over 90% to about 65% dependence on groundwater because of completion of the Central Arizona aqueduct. Revised information on groundwater dependence will be published later this year in *The Water Encyclopedia* by the groundwater consulting firm of Geraghty & Miller (Plainview, NY).

New Jersey Gov. Thomas Kean suggested Nov. 15 that no more wetland acreage should be drained or developed than is being created or restored. He told the National Wetlands Policy Forum that the long-term goal should be "an increasing inventory of wetlands." As an example of the potential usefulness of wetlands, Kean listed natural flood control in New Jersey's Passaic River valley. Because the wetlands have been destroyed for development, it will cost New Jersey \$1.5 billion to provide artificial flood control, Kean noted. The forum was organized by The Conservation Foundation (Washington, DC) at the request of EPA administrator Lee Thomas. Its report contains more than 100 recommendations for preserving wetlands.

Pennsylvania Gov. Robert Casey has signed legislation establishing a state Superfund. The new law (HB 1852), signed Oct. 18 and effective Dec. 17, enables Pennsylvania to step up the cleanup of hazardous waste sites on the National Priority List and to clean up sites that do not qualify for federal aid. The law also gives responsible parties a chance to clean up waste sites voluntarily before the state begins legal action. About \$30 million a year will come from 0.5% of the state's \$0.0095

capital stock and corporate franchise tax. An additional \$50 million will come from the state's general fund during the next two years. Pennsylvania officials hope to clean up 250 of the state's worst sites during the next 12 years.



Casey: Signed state Superfund law

AWARDS

The American Ground Water Trust invites undergraduate students to apply for scholarship support. Scholarship applications must be submitted by April 1, 1989. The amount of the scholarship is determined annually by the board of trustees of the trust; in recent years each scholarship carried a stipend of \$2000. The trust has awarded 26 scholarships since the beginning of the program in 1975. To receive an application, candidates must send a stamped, self-addressed envelope to The American Ground Water Trust, Scholarship Program, 6375 Riverside Drive, Dublin, OH 43017.

VIEWPOINT

Indoor radon is a problem but not a crisis like asbestos, even though it is a major concern among home builders, according to John Spears, an indoor air quality researcher for the National Association of Home Builders (Washington, DC). He said that builders can evaluate sites by studying soil types and permeability and by measuring radon in nearby homes. During construction, builders can seal off radon entry pathways. Spears says that correcting a radon problem in a single-family home can cost about \$1500, but removing asbestos, which he believes is more dangerous to health than radon, can cost \$10,000 or more and is much harder to accomplish. He recommends that the United States study the Swedish approach to radon removal, which, he says, "is 10 years ahead of ours."

The environment was a minor concern of voters during the 1988 election, despite reports in the popular media, Richard Wirthlin of the Wirthlin Group (Washington, DC), suggested. He told a Chemical Manufacturers Association Chemical Forum luncheon audience Nov. 10 that the principal concern, by far, was drugs. Nevertheless, Wirthlin forecast that the environment will regain importance as an issue from 1988 to 1992. "The American public believes that clean air and water are basic rights. Also, voters are going to be strongly concerned with progress in the cleanup of toxic waste sites and about what is being done to mitigate the greenhouse effect." He predicts that these could be major election issues in 1992.

SCIENCE

Anaerobic bacteria that degrade polychlorinated biphenyls (PCBs) are present in nature, James Tiedje and his colleagues at Michigan State University report in the Nov. 4, 1988, issue of *Science*. The bacteria work by removing chlorine atoms from PCBs; Tiedje suggests that this action may give the bacteria the energy they need for growth. He adds that these microbes prefer to attack the most toxic of the PCBs. In laboratory experiments, Tiedje and his team found the anaerobes living in Hudson River (NY) sediments contaminated with PCBs. After 16 weeks, the PCBs they studied were degraded to less toxic substances that aerobic microbes could decompose easily. The team isolated one microbe called DCB1, which easily dechlorinates the environmental contaminant chlorobenzoate. The scientists' findings appear to contradict the conventional wisdom that such dechlorinating microbes do not exist.

TECHNOLOGY

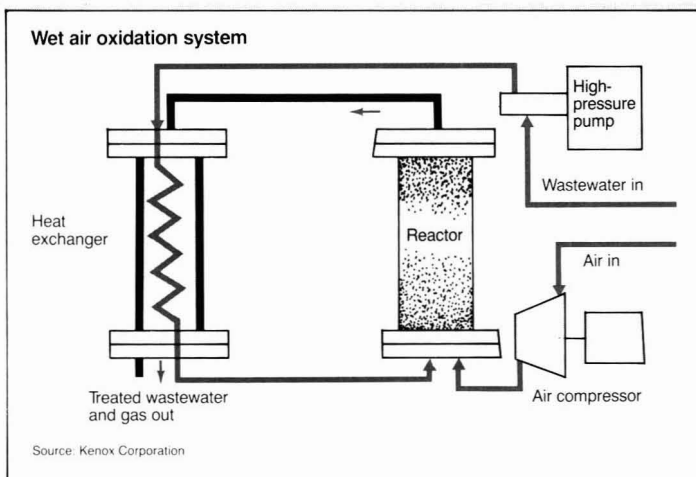
Plumes of contaminants in groundwater can be tracked with trace inorganics, according to Ilhan Olmez of the Massachusetts Institute of Technology. The technique uses signatures of elements not modified during their passage through groundwater. Rare earth elements (REEs) are one example. Although their concentrations attenuate during transport, the ratio between their concentrations remains constant. Olmez explains that the ratio between the concentrations of two REEs measured at a monitoring well will match the ratio measured at the source where the contamination originated,

thereby incriminating the source. The analysis technique used is neutron activation analysis, which Olmez says is sensitive and reliable, but he acknowledges that its use requires access to a nuclear research reactor.

Toxic fumes generated during soldering operations in the electronics industry can be removed with an air purification system made by Kemper GmbH (Vreden, West Germany). EPA and OSHA require the abatement of these fumes, which are suspected carcinogens, in the workplace. The fume-laden air is extracted through a nozzle and connecting hose that convey the fumes into the system. A series of filters traps particles as fine as $0.1 \mu\text{m}$ with a 99.997% removal, according to Kemper spokesmen. An activated carbon filter adsorbs gases and odors. The cleaned air then can be recirculated to the workplace or vented outside. Spent filters are returned to Kemper for disposal.

A way to store intermittent, diffuse solar energy may be with Magnesium hydride, according to spokesmen for Bomin-Solar (Lörrach, West Germany). Solar energy is concentrated at a focal point at which temperatures exceed 400°C . Hot hydrogen is released from the magnesium hydride, and its heat can be tapped for cooking, heating water, or process heat. The cooled hydrogen recombines with the magnesium to form magnesium hydride in a closed system, and the process starts all over again with only minute energy losses and an efficiency near 90%, according to Bomin-Solar spokesmen. They say that in a hot, arid area, the prototype system, containing a 3-m^2 mirror, produces 21 kW/day of solar energy. The spokesmen add that conventional systems with a 3-m^2 mirror would produce only 2 kW/day of energy.

A variant of wet air oxidation can detoxify a wide range of priority pollutants and reduce chemical oxygen demand (COD) to required levels, says Brad Stott of Kenox (North York, ON, Canada). After pH adjustment, the waste stream enters the reactor at about 15 gal/min. The waste is then heated to 410°F under pressure of 600 psig for 35–55 min to destroy oxidizable material. Next, the waste leaves the reactor and is treated with lime to precipitate heavy metals. The cleaned effluent is then combined with other cleaned plant effluent and sent to sewer lines, according to Stott. He adds that COD



is reduced by 80–90% and that the system can treat sludges and slurries from chemical, pulp and paper, and many other industries. He says that the system has operated at demonstration scale for more than two years at a drum reclamation facility in Mississauga, ON, Canada.

BUSINESS

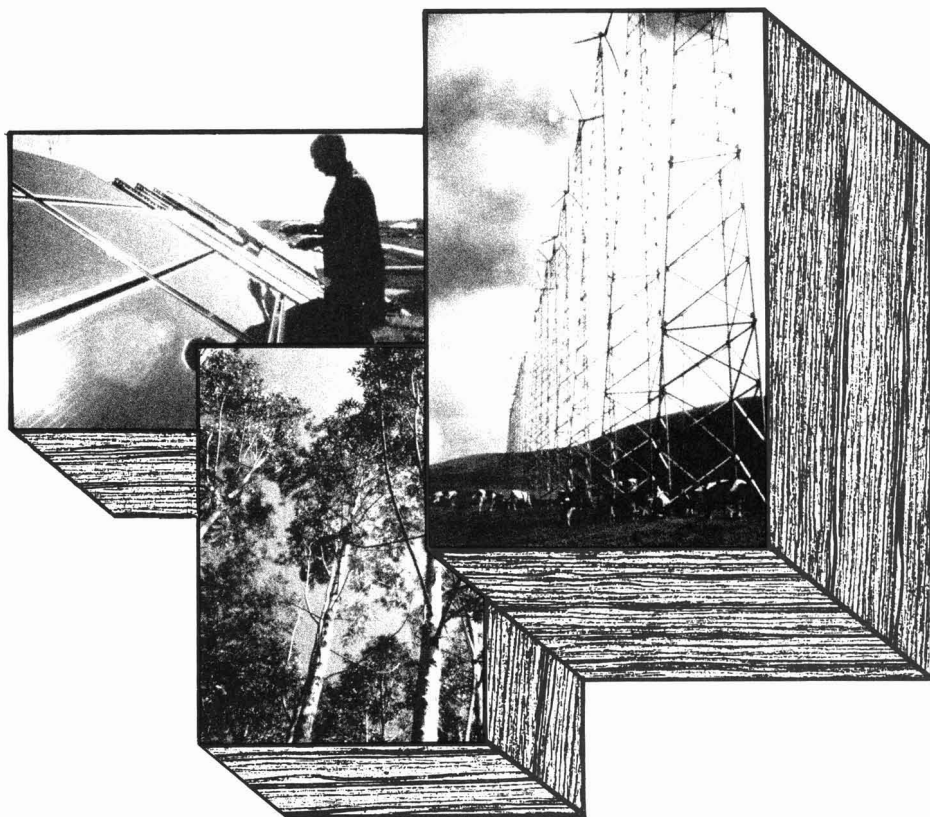
Clement Associates (Fairfax, VA) has received a 5-year, \$16-million contract with the Agency for Toxic Substances and Disease Registry to evaluate the health effects of hazardous waste contaminants. Clement president Elizabeth Anderson says that the work "will provide primary toxicological information for health practitioners and the general public on the potential adverse health effects associated with chemicals found at uncontrolled waste sites." She adds that the contract "also will enable us to focus in greater detail on the inherent chemical, toxicological, and environmental properties of each chemical." Emphasis will be placed on human health implications of data developed and on identifying data gaps, according to Anderson.

Groundwater Technology (GT, Norwood, MA) has announced a system able to remove chlorinated solvents, degreasers, and other denser-than-water hydrocarbons from the bottom of an aquifer. The system, known as Chlorinated Probe Scavenger, consists of a submersible pump and a special probe that can distinguish between dense, nonaqueous-phase liquids (DNAPLs) and water. The intake is placed entirely in the DNAPL layer, guaranteeing the recovery of 100% water-free liquid, according to GT spokesmen. The

hydrocarbon is collected by an intake cartridge and fed through a flexible hose to a stainless-steel reservoir. When enough of the hydrocarbon has been collected, it is pumped to a surface-level collecting tank. The company markets one system for wells 20 ft deep or less and another for wells up to 100 ft deep.

Norton Chemical Process Products (Akron, OH) has licensed its gas purification process to clean medium-Btu gas generated in a landfill in Kearny, NJ. The landfill will produce 7.2 scf (scf = standard ft³) of gas that has a heat value of about 565 Btu/scf. The gas will be cleaned by what Norton calls its SELEXOL solvent gas process, which will remove trace amounts of chlorinated hydrocarbons from a natural gas produced by the anaerobic digestion of municipal wastes in the landfill. No heat is needed to regenerate the solvent; thus, energy requirements are "significantly reduced," according to Norton spokesmen. The landfill gas facility is expected to start up in August 1989.

Hunter Biosciences (HBIO, Raleigh, NC) has developed portable biotreatment systems to clean up gasoline spills from leaking underground storage tanks. These systems use selected gasoline-degrading bacteria together with water, oxygen, and nutrients; the microbes consume the waste. The system is marketed under the name PetroClean. HBIO president Jason Caplan says that gasoline station sites can be cleaned up 5–10 times faster than they can with air stripping and carbon adsorption, and that cleanup costs can be 50–90% lower because hauling and land disposal of contaminated soil are not needed.



Renewable energy development

It has many environmental benefits

Vic Phillips
Patrick Takahashi
University of Hawaii
Honolulu, HI 96822

Not long ago, coal miners would lower a canary in a cage by a rope down into a mine shaft to determine the presence of poisonous gases. After a while, they would pull up the cage and check the canary's condition. If the bird was alive, they knew they could safely enter the mine. If the bird was dead (or, in miners' parlance, "shafted"), they then went back to the pet store. For the coal miners, the canary served as an indica-

tor of benign or harmful conditions in their working environment.

Today, we use more sophisticated, super-sensitive electronic "canaries" that can detect trace amounts of toxic materials in our environment to alert us to the dangers to which we have exposed ourselves. Our acutely discerning canaries are now telling us that our health and habitat are deteriorating. How can we resolve this plight? We can convert to technologies based on abundant, benign, renewable energy resources such as biomass, geothermal, hydroelectric, ocean thermal, solar, and wind.

Compatibility with the environment

The Hawaii Natural Energy Institute (HNEI) was established in the wake of

the global oil price shock of 1973 to help Hawaii achieve energy self-sufficiency for economic security. Its mission is to develop local, renewable energy resources to replace imported oil with little or no degradation of Hawaii's unique, fragile ecosystems. Therefore, an integral component of HNEI's research efforts has been environmental protection. Energy-related environmental studies conducted by HNEI over the past 14 years indicate that in comparison with conventional alternatives, renewable energy development clearly has environmental benefits.

For example, although trace amounts of hydrogen sulfide, mercury, and radon can be found in geothermal emissions, they generally are obscured by normal background levels because of

natural outgassing from nearby vents and fracture zones. Siegel and her colleagues (1) report that vigorous native forests exist over an area of at least 25,000 hectares around the Kilauea volcano in Hawaii and that pastures, gardens, parks, forests, and a major wildlife refuge exist near Rotorua, New Zealand, despite continuous exposure to daily geothermal emissions or "natural steam." By contrast, coal combustion typically results in a greater threat to air quality than does geothermal power production, especially in SO₂, NO₂, CO₂, and particulates. Although there are essentially no geothermal emissions of these combustion products, ammonia, hydrocarbons, and hydrogen sulfide are present in geothermal fluid. These materials, however, can be removed without undue difficulty.

The compatibility of wind power and the environment occasionally has been questioned. For example, a concern about birds flying into windmills may be raised when wind farms are erected in mountain passes and migratory flyways; however, in the isolated Hawaiian Islands this problem does not exist. Birds face much greater danger from pollution and loss of habitat caused by traditional energy operations than they do from windmills.

In the case of ocean thermal energy conversion (OTEC), cold, low-pathogen, nutrient-rich water from depths of 500–1000 m is pumped to the surface to generate electricity, produce fresh water for drinking, and stimulate the growth of organisms in land-based aquaculture or offshore mariculture. Preliminary findings indicate a positive effect of OTEC discharges on marine fishery productivity.

"Growing methanol" (i.e., thermochemically converting fast-growing, short-rotation trees and grasses harvested from energy plantations into methanol) can directly benefit the environment. Vehicles such as racing cars fueled with methanol demonstrate superior engine performance; they give off fewer pollutants than vehicles operating on gasoline or diesel fuels. Moreover, the CO₂ released by combustion of methanol produced from biomass feedstocks does not contribute to global warming via the greenhouse effect, because the release of carbon equals the uptake of carbon in a cycle of combustion and photosynthesis.

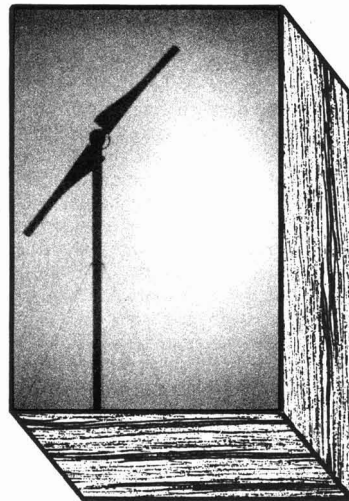
Threats of traditional technologies

The foregoing are just a few examples of the compatibility of renewable energy technologies with the environment. Traditional nonrenewable energy technologies, by contrast, significantly disrupt the environment, resulting in

both obvious and hidden costs to the environment and to the economy and health of our society.

The potentially dangerous natural substances, such as heavy metals and fossil fuels, that used to be covered with a protective layer of soil or that otherwise remained effectively undisturbed and isolated from us, are now in the air we breathe, the water we drink, and the food we eat. We have further disrupted nature by introducing synthetic materials such as plastics, chlorofluorocarbons, agricultural and industrial chemicals, and plutonium (2–5). One symptom of this threat to our environment is the disappearance of wild species (6). Because we live on the same planet, the disappearance of species indicates that we humans might also become endangered.

Many environmental problems stem from fossil- and nuclear-energy production and use. Familiar examples are air pollutants from motor vehicles and coal-fired power plants, oil spills from supertankers, and radioactive wastes from nuclear facilities. Whenever raw materials from the environment are



converted into more readily usable products for human convenience, such as jet fuel or refrigerators, there are environmental impacts. The severity of the impact depends on the technology used and the rate at which the conversion is accomplished. The current challenge is to choose technologies that concurrently minimize environmental impacts and maximize profits (7).

As people increasingly demand environmental protection to safeguard their health, the costs of protecting the environment during energy production will be passed on to the consumer in the form of higher prices (8). As a result, renewable energy technologies, which have the clear advantage environmen-

tally, are now becoming competitive with traditional, nonrenewable energy technologies in the marketplace, particularly when the social and environmental costs previously not included in the market price are incorporated. Americans want a clean, healthy, safe environment, and more and more often they are choosing to pay for damage prevention rather than for cleanup. Moreover, citizens throughout the world are demanding environmentally compatible energy and food production technologies, such as agroforestry and other integrated projects to protect agricultural land, fuel wood sources, and watersheds.

Although we are concerned with the plight of endangered species and their habitats, we are more attentive to direct environmental impacts on humans. As we grow more aware of our power over the environment and of how intimately our species is connected to all other species in the ecosphere, we perceive that we must broaden our concept of the environment to include our society.

Within this larger environmental framework, we need to make economic and technological decisions that increase our options, ensure the sustainability of the life support system on our planet, and promote the security of our future. Our environment, then, includes the system of nature (or ecosphere) and the system of human interactions (or society).

Benefits of renewable energy

The three principal attributes of renewable energy technologies are flexibility, sustainability, and security.

Flexibility. Because of their flexibility, local renewable energy resources can be locally controlled for local needs. Citizens can democratically choose which technologies and what scale of production are most efficient, economical, and environmentally sound for the services they want (9).

Renewable energy resources also can be appropriately matched to the task required. For example, why waste an expensive, concentrated form of energy such as electricity for heating domestic water when direct sunlight is sufficient? Incorrectly matching the energy quality (the ability of the energy to perform the work of a specific task) with the task to be accomplished is like cutting butter with a chainsaw—it is inefficient and wasteful (10). Modular designs for natural resource development projects can be used to help solve several problems at the same time. For instance, the production of energy, by-product fertilizer, and food; the cleanup of air and water; and the treatment of waste can be accomplished by the same integrated operation. The conversion from energy to

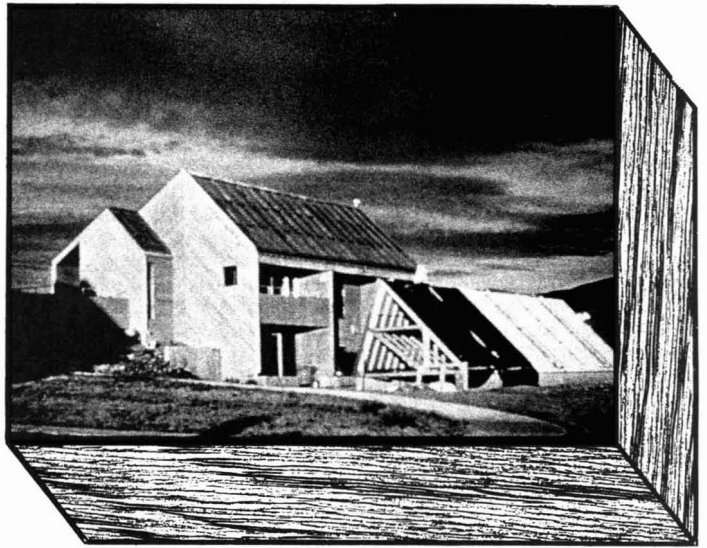
synergy is a welcome alternative to supply-side strategies that have jeopardized our environment and have squandered our one-time bonanza of fossil fuels (11, 12).

Moreover, increased energy efficiency and conservation efforts, such as cogeneration of industrial process heat and electricity, plugging leaks in buildings with added insulation, weather stripping and storm windows, and improved fuel economy in automobiles, are cost-effective alternatives to the mere provision of more energy. Bockris and Dandapani (13) report that per capita energy consumption and income are linearly related up to an energy consumption rate of about 6 kW per person; above that rate, the increase in energy consumption does not affect average income. The implication for the United States and other developed nations is that an energy saving of up to 40% is possible through conservation, with no significant decrease in the standard of living.

Sustainability. The second important benefit of natural energy development is sustainability. Renewable energy resources are replenished by natural processes if we do not destroy the means of their renewal (by overloading or oversimplifying ecosystems so that they no longer can function normally), or if we do not use the resources too rapidly. These resources are rate-limited, not supply-limited as are coal, oil, and natural gas.

By living on our "annual income" of energy from the sun rather than on our "savings account" of fossil fuels, we would not be threatened with shortages. "Balancing the budget," a familiar battle cry in Washington these days, makes good sense in energy development as well as in business and government. Renewable energy development allows the economy to grow in goods and services (i. e., those products, including clean air and water, whose manufacture and use promote the welfare of producers and consumers) by reducing "bads and disservices" (i. e., those by-products and side effects that impair the welfare of workers and end-users, including exposure to toxic chemicals and emissions) (14).

Renewable energy technologies also help maintain the integrity of the life support system of our planet. Because the chemistry of their conversion is essentially the same as the chemistry of metabolism of living organisms, renewable energy technologies are compatible with life processes. This life support system, which is powered by the sun, consists of the 5 million-10 million species currently interacting with the physical environment of our planet. All life forms on Earth have the



same basic recipe: Add water and sunlight to a DNA filling inside a protein crust. Each species, however, contains a package of DNA with unique instructions for living on Earth. Furthermore, each species is vitally dependent on all of the other species.

This interdependency of organisms in the ecosphere is illustrated by the relationship between green plants, animals, and microbes. Green plants produce food and oxygen through the process of photosynthesis; animals, including humans, consume the food and oxygen and release carbon dioxide and water through the process of enzymatic combustion; and microbes decompose dead tissues and restore the chemical balance between producers and consumers by recycling nutrients back into the system. All of this general house-keeping operates on sunshine and is done free of charge. Renewable energy technologies gently tap into the planet's natural system of energy production, waste management, water purification, air conditioning, mineral recycling, detoxification, and soil building (15-17).

Sustainable energy technologies are those that convert raw materials to usable forms of energy without destroying the ecosystems from which the natural resources originated. The construction and operation of renewable energy facilities affect the environment far less destructively than do petroleum, coal, oil shale, and nuclear facilities (18). Even greater environmental advantages exist during the energy utilization process that converts usable energy to useful work. For example, there are no net accumulations of carbon dioxide to increase the Earth's temperature, no toxic emissions, and no large piles of slag and radioactive wastes. Energy systems

based on renewable energy resources can provide an ample supply of high-quality fuels on a sustainable basis.

Security. The third benefit of renewable energy development is security. From the global perspective, the use of renewable energy technologies greatly reduces the probability of large-scale disasters such as the greenhouse effect, acid-rain toxicity, radioactive spills or accidents, and the threat of nuclear terrorism or war. Because renewable energy systems are self-sufficient, they reduce political pressure for military intervention to obtain foreign oil and benefit our economy instead of foreign economies (19). Renewable energy technologies decrease health and safety hazards and enhance environmental quality in urban and rural workplaces and communities.

Renewable energy developments create jobs and expand the local economy. For example, positions are created for agronomists or foresters in the production of biomass energy; for engineers in integrated process design and operation of systems for conversion to useful energy products; and for service-sector employees in the distribution of renewable energy products to local end-users. Renewable energy enterprises keep dollars circulating in the community longer and free dollars previously spent on foreign oil for other purposes.

Engines powered by renewable fuels such as methanol from biomass, hydrogen from geothermally powered electrolysis of water, or electricity from photovoltaic panels operate cleaner than do gasoline and diesel engines. Diverse renewable energy resources are available locally that can provide financial security and a clean, healthy environment for future generations.

Data and education needed

In addition to sound technical know-how, two components are essential to the success of any renewable energy development project. The first is the need for environmental baselines. It is vital to establish what ecological resources exist and how they contribute to functioning of the ecosystem being considered for development. This is especially true for remote, pristine areas. Even in "restored" areas, which were once severely disrupted, data are necessary to confirm ecological improvements resulting from the discontinuation of unsustainable operations, from site rehabilitation, and from the changeover to renewable energy operations.

The other critical component is that people be educated about the benefits of renewable energy development and included in the decision-making process. It is imperative to explain to governmental and business leaders and the public how renewable energy technologies can enable us to prosper within the natural limitations of the ecosphere. This means making accurate information available to all parties, opening channels of communication between potentially opposing groups, and including all parties in the decision-making process from the beginning.

The promise of renewable energy

Renewable energy technologies offer flexible, affordable, locally available, and sustainable alternatives to fossil and nuclear fuels. They improve environmental protection during the extraction and utilization of energy. Perhaps most importantly, renewable energy development would increase our security, promote peace, and free us from the threat of environmental disaster and war over resources (resulting from the struggle between the "haves" versus the "have-nots").

Renewable energy development would provide jobs and financial security for our families and friends, benefit our health and personal safety, and offer us freedom from the diseases and debilitation brought about by industrial pollution. Ultimately, it would enhance the democratic values and individual freedom we cherish.

Acknowledgments

This article was reviewed for suitability as an *ES&T* feature by David M. Armstrong, University of Colorado, Boulder, CO 80309.

References

- (1) Siegel, B. Z. et al. In *Natural and Man-Made Hazards*; El-Sabbh, M. I.; Murty, T. S., Eds.; D. Reidel Publishing Co.: Hingham, MA, 1988; pp. 589-97.
- (2) Brown, L. R. *Building a Sustainable Society*; W. W. Norton: New York, 1981.
- (3) Carson, R. *Silent Spring*; Houghton-Mifflin: Boston, 1962.
- (4) Commoner, B. *The Closing Circle: Nature, Man and Technology*; Alfred A. Knopf: New York, 1971.
- (5) Schell, J. *The Fate of the Earth*; Alfred A. Knopf: New York, 1982.
- (6) Myers, N. *A Wealth of Wild Species: Storehouse for Human Welfare*; Westview Press: Boulder, CO, 1983.
- (7) Miller, G. T. *Living in the Environment: An Introduction to Environmental Science*; Wadsworth: Belmont, CA, 1985.
- (8) Commoner, B. *The Poverty of Power: Energy and the Economic Crisis*; Alfred A. Knopf: New York, 1976.
- (9) Schumacher, E. F. *Small Is Beautiful: Economics as if People Mattered*; Harper and Row: New York, 1973.
- (10) Lovins, A. B. *Soft Energy Paths: Toward a Durable Peace*; Ballinger: Cambridge, MA, 1977.
- (11) Odum, H. T. *Environment, Power, and Society*; Wiley-Interscience: New York, 1971.
- (12) Ophuls, W. *Ecology and the Politics of Scarcity: Prologue to a Political Theory of the Steady State*; W. H. Freeman: San Francisco, 1977.
- (13) Bockris, J. O.; Dandapani, B. *Int. J. Hydrogen Energy* **1987**, *12*, 439-44.
- (14) Daly, H. E. *Steady-State Economics*; W. H. Freeman: San Francisco, 1977.
- (15) Erhlich, P. R.; Mooney, H. A. *BioScience* **1983**, *33*, 248-54.
- (16) Myers, N. *Environment* **1980**, *22*, 6-13.
- (17) Woodwell, G. M. *BioScience* **1974**, *24*, 81-87.
- (18) Hayes, D. Presented to the American Association for the Advancement of Science, San Francisco, Jan. 1980.
- (19) Lovins, A. B.; Lovins, L. H. *Brittle Power: Energy Strategy for National Security*; Brick House: Andover, MA, 1982.



Vic Phillips (l) is the manager of bioresources and environmental research at the Hawaii Natural Energy Institute (HNEI) of the University of Hawaii at Manoa (Honolulu). He coordinates an international effort to remediate global warming and is involved in a project to replace fossil fuels with methanol from biomass. Previously, Phillips was at the University of Colorado Laboratory of Mountain Ecology where he worked on the revegetation of former mining operations and on baseline ecological studies for mining and hydroelectric projects. He has a Ph.D. in ecology from the University of Colorado.

Patrick Takahashi (r) is director of HNEI and director of the Energy and Resources Division of the Pacific International Center for High Technology Research. He has degrees in chemical engineering through the Ph.D. from Stanford University and Louisiana State University.

ENVIRONMENTAL SCIENTISTS AND ENGINEERS ...

ORDER YOUR COPIES OF THE MOST REQUESTED SPECIAL REPORTS FROM ES&T

Introducing three series made available by ES&T covering major areas in environmental science. You'll want to order all three!

Cancer Risk Assessment (32pp)

This special report explores the various scientific topics of public concern to regulate chemicals in the environment. Among the topics you'll find covered to help you manage the risk and communicate the results of risk assessment are:

- Being more realistic about chemical carcinogenesis
- Exposure assessment
- Cancer dose-response extrapolations
- Physiological pharmacokinetic modeling
- And more ...

Wastewater Treatment (48pp)

Update your knowledge of the latest processes for the treatment of wastewater with this in-depth report. You'll find topics such as these ...

- Removing particles in water and wastewater
- Removing dissolved organic contaminants from water
- Removing dissolved inorganic contaminants from water
- Anaerobic wastewater treatment
- To name a few ...

Computer Usage in Engineering (13pp)

Utilize the power of the computer to bridge the gap between engineers and public decision-makers with this report that briefs you on the computer basics and then discusses new trends and applications, such as artificial intelligence, and their potential impact on environmental engineering. You'll also see how personal computers might change the practice of environmental engineering in the future, and much more.

BULK RATES AVAILABLE!

ALL SERIES MUST BE PRE-PAID BY CHECK OR MONEY ORDER.

TO ORDER, send check or money order with name, address, telephone number, and quantity of each series to:

American Chemical Society
P.O. Box 57136
West End Station
Washington, DC 20037
(202) 872-4363

RATES FOR EACH SERIES

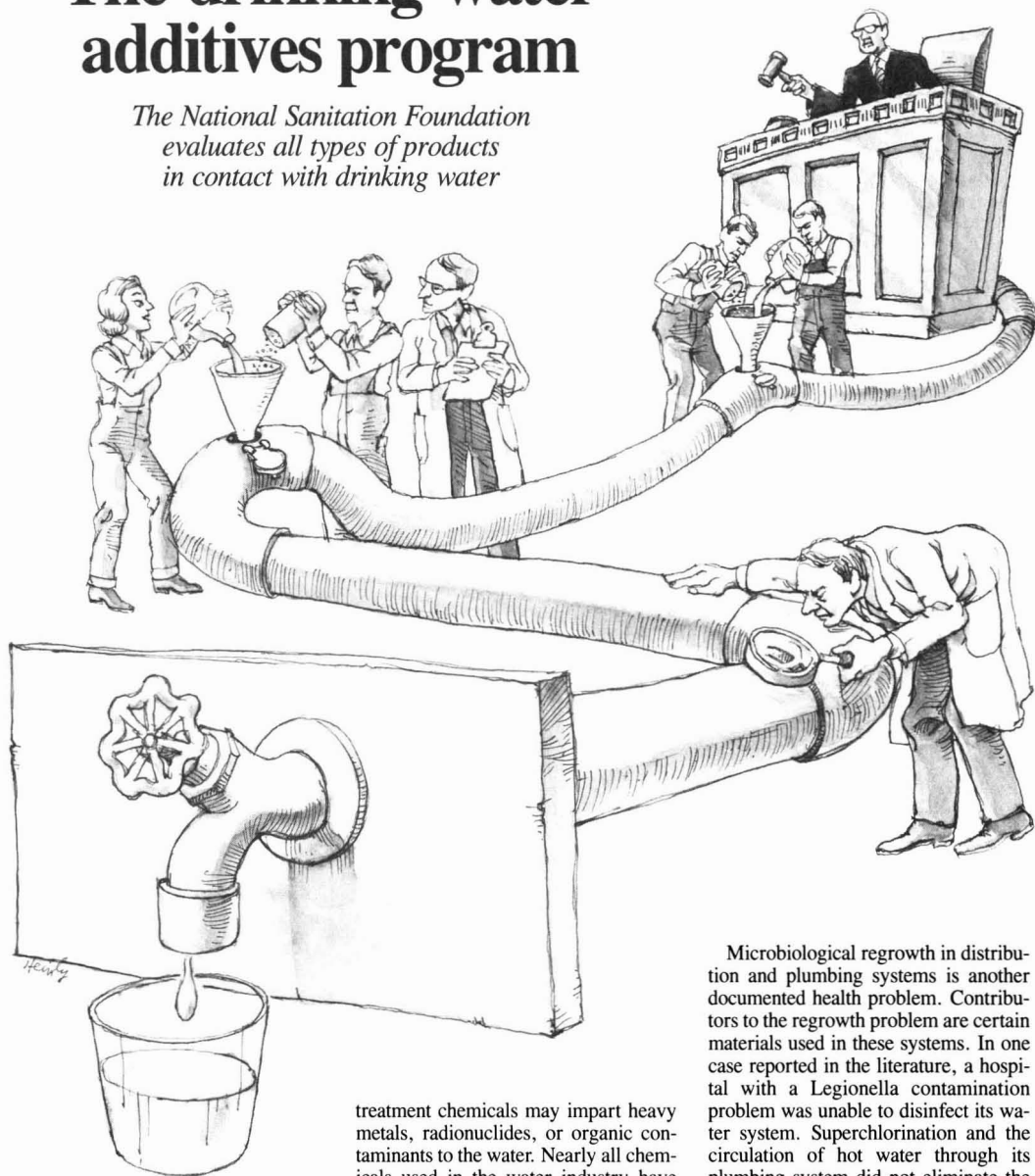
1 copy \$10.00 ea.
2-5 copies \$ 5.00 ea.
6 and above \$ 4.00 ea.

Foreign payment must be made in U.S. dollars by international money order, UNESCO coupons, or U.S. bank draft.

Foreign orders add 20% of total order cost for shipping/handling.
Please allow 4-6 weeks for delivery.

The drinking-water additives program

The National Sanitation Foundation evaluates all types of products in contact with drinking water



Nina I. McClelland
David A. Gregorka
Betsy D. Carlton
National Sanitation Foundation
Ann Arbor, MI 48106

Additives to drinking water come in many forms. While improving the overall quality of water, some water

treatment chemicals may impart heavy metals, radionuclides, or organic contaminants to the water. Nearly all chemicals used in the water industry have trace levels of contaminants associated with them, and depending on the source and production method, contamination of the water supply may or may not be threatened. Another source of additives to water supplies is the materials used in distribution and plumbing systems, such as coatings, pipes, gaskets, and valves. Significant levels of inorganic and organic chemical contaminants may leach or be extracted from metal and synthetic materials used in drinking-water systems.

Microbiological regrowth in distribution and plumbing systems is another documented health problem. Contributors to the regrowth problem are certain materials used in these systems. In one case reported in the literature, a hospital with a *Legionella* contamination problem was unable to disinfect its water system. Superchlorination and the circulation of hot water through its plumbing system did not eliminate the regrowth problem. The source of the problem was eventually traced to natural rubber fittings used in the hospital's water distribution system. All were replaced with a less biologically active material, and the regrowth problem was solved. Today the National Sanitation Foundation (NSF) has many current and prospective programs that are focused on drinking-water quality. They include a series of standards for devices that treat drinking water at the point of use and the point of entry;

standards for plastics piping systems and for flexible membrane liners used in reservoirs and aqueducts; and certification of bottled water, packaged ice, and drinking-water treatment laboratories.

Under its Safe Drinking Water Act authority, EPA has been evaluating additives products. States, water utilities, and others have relied on EPA's opinions to make decisions about accepting or rejecting additives products for use in public water systems. Resource constraints and other demands have limited EPA's activities to issuing new advisory opinions for products that are virtually identical to products previously reviewed. Recognizing the shortcomings of the current program; the likelihood of no increases in future program funding; and the needs of states, public water systems, and manufacturers for the evaluation of additives products, EPA requested proposals for the establishment of a voluntary, third-party, private-sector additives program. EPA required that voluntary consensus standards be developed, and that the successful bidder offer a program of third-party certification based on the standards.

As a result of the proposal, NSF entered into a cooperative agreement with EPA to develop a voluntary, third-party, private-sector program for evaluating drinking-water additives. NSF has led this effort through a unique consortium approach, which includes the American Water Works Association Research Foundation (AWWARF), the Conference of State Health and Environmental Managers (COSHEM), and the Association of State Drinking Water Administrators (ASDWA). In September 1987, the American Water Works Association (AWWA) joined the team. EPA intends that this new third-party program replace EPA's existing additives advisory program, as announced by the agency in the *Federal Register* on July 7, 1988.

Existing standards

There are several existing NSF performance standards for products used in contact with drinking water, and numerous product or materials standards are available from the AWWA, the American Society of Sanitary Engineering (ASSE), the American Society for Testing and Materials (ASTM), and others. AWWA and ASSE performance standards complement current and proposed NSF health effects standards. Other NSF standards, such as Standard 14 (plastic piping components), reference ASTM and other standards for performance. By Joint Committee decision, the new NSF additives standards relate to real and potential *health effects* associated with products used to treat,

store, and distribute drinking water. They are *not performance* standards, and do not reference performance requirements.

Standards development

Various working and advisory groups and committees were established to develop the new standards. These groups—which included representatives from industry, regulatory agencies, water utilities, other product users and specifiers, and public interest groups—played a major role in defining and developing the additives program.

A steering committee was responsible for overall policy setting, grant administration, the formal program work plan, and program coordination. It did not, however, become involved in standards writing or balloting. This group was chaired by the principal investigator (NSF), and includes representatives of EPA, AWWARF, ASDWA, COSHEM, and AWWA.

Standards and criteria were developed through NSF's established voluntary consensus standards development process. Task groups drafted requirements for the product categories, in-

cludes input from all concerned parties, balanced participation, a means for adjudicating negatives, and an appeals process.

Scope of standards

The additives program has produced two standards. One addresses direct additives and includes all chemicals used in drinking-water treatment and in water well drilling. The second deals with indirect additives, including all materials in contact with drinking water during its treatment, storage, transmission, and distribution. Specific sections of each standard deal with variabilities of each product type, including degree or extent of exposure to drinking water. The Health Effects Task Group had primary responsibility for maintaining consistent requirements for all products, based on sound, scientific principles of public health.

Toxicology requirements

The toxicological requirements under Standards 60 and 61 are predicated on protecting the public health through careful consideration of both the additive product or material and the con-

"The new NSF additives standards relate to real and potential health effects."

cluding protective materials; pipes and related products; joining and sealing materials; mechanical devices; process media; coagulation and flocculation chemicals; disinfection and oxidation chemicals; chemicals for corrosion and scale control and softening, precipitation, sequestering, and pH adjustment; and miscellaneous treatment applications.

A Health Effects Task Group addressed toxicological and risk considerations. A Peer Review Group of experts in toxicology and analytical chemistry was established to bring additional expertise and an added level of review to the effort. Requirements drafted by the Health Effects Task Group were reviewed and approved by the Peer Review Group.

The NSF standards development methodology is consistent with American National Standards Institute (ANSI) guidelines, and NSF is "an accredited ANSI standards organization." This is one of two available classes of ANSI accreditation. NSF's standards are accepted by ANSI without additional ballot. In conformance with the Office of Management and Budget A-119 guidelines and ANSI requirements, NSF of-

taminants or impurities the product or material could contribute. The principle of commensurate effort is central to the toxicology evaluation approach. This principle states that the amount of data required to determine the safety of an additive should be proportional to the additive's potential for causing adverse health effects. The basic precepts of toxicology suggest that the potential for any substance to cause an adverse health effect is related to the level of exposure or dose. Therefore, more data are required for high-exposure, high-risk additives than for low-exposure, low-risk additives.

The Drinking Water Additives Program standards are consistent with federally regulated drinking-water standards. For regulated contaminants, the maximum allowable level (MAL) described in Standards 60 and 61 is based on the EPA regulated maximum contaminant level (MCL), with the MAL equal to 10% of the MCL. The 10% level was chosen to account for multiple sources of one contaminant. This is consistent with the approach taken in the National Academy of Sciences' Water Chemicals Codex. The U.S. Food and Drug Administration (FDA) em-

employs similar estimations of source contributions from various types of products in its regulation of food additives. For unregulated contaminants, a maximum drinking-water level (MDWL) is calculated, based on toxicology data and appropriate risk assessment

models, and adjusted for the exposure concentration of the contaminant at the tap.

The toxicology evaluation procedures in Standards 60 and 61 are similar to those used by FDA in its evaluation of food additives. Both systems use

exposure concentrations in grouping additives for evaluation. Under the Drinking Water Additives Program, the exposure concentration ranges associated with each toxicity testing category are as follows:

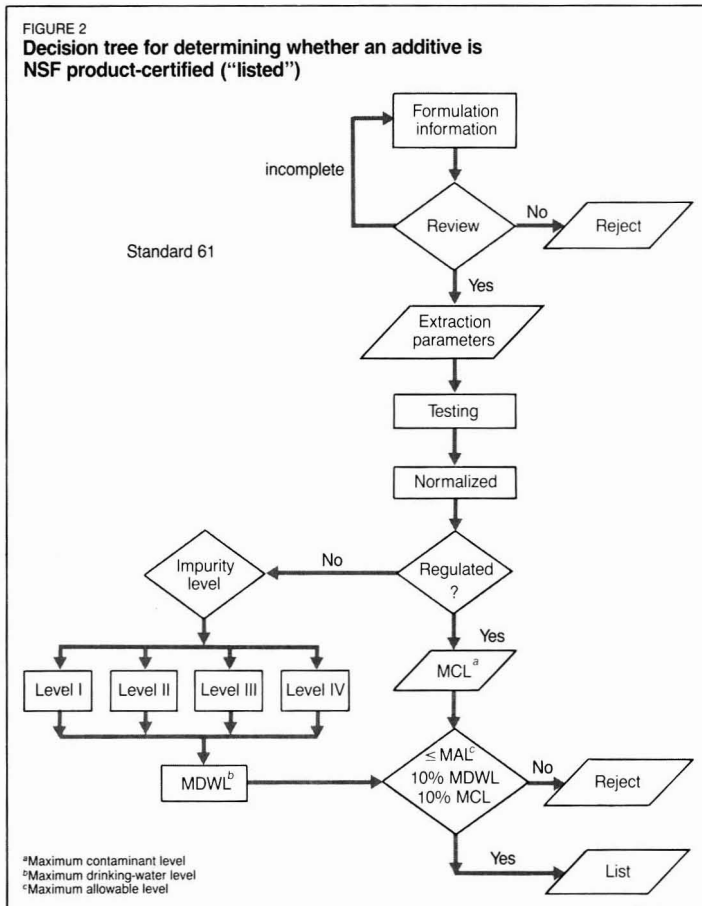
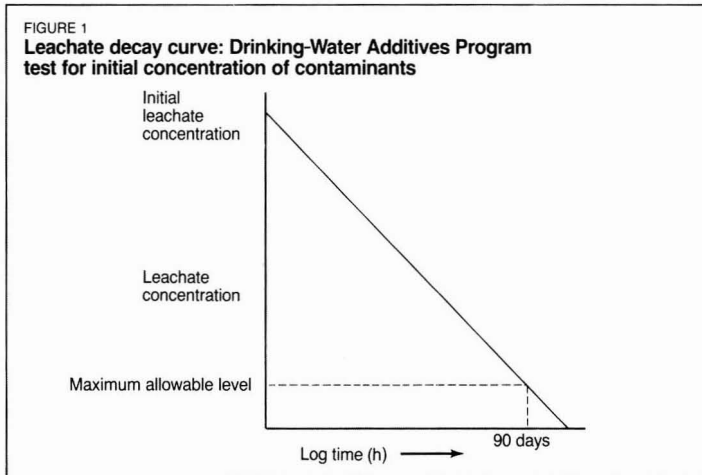
- Category Level I < 10 ppb
- Category Level II ≥ 10 ppb < 50 ppb
- Category Level III ≥ 50 ppb < 1000 ppb
- Category Level IV ≥ 1000 ppb

Practical considerations were used in the selection of exposure concentration limits for the four testing categories. For example, most noncarcinogenic substances are regulated at concentrations between 10 and 1000 ppb. It is therefore important that the potential for target-organ toxicities (toxic effects on specific organs in the body) of any substances present in tap water within this range be characterized prior to permitting this substance in a drinking-water system. Similarly, the mutagenic potential of an additive (as predictor of carcinogenic potential) needs to be determined at or below the 10 ppb range at which most carcinogenic substances are regulated.

The toxicity testing requirements in each exposure category build on the requirements of the exposure level below it. In the first category (< 10 ppb), short-term tests for genetic toxicity and carcinogenic potential are required. The Ames *Salmonella* gene mutation test, with and without microsomal activation, and a mammalian chromosomal aberration test, such as a mouse microsomal assay, would fulfill these requirements. In Category II, in addition to the Category I genotoxicity tests, a subchronic study in rodents (using an oral exposure route) is required. To further define potential toxicities, Category III requires reproductive and developmental toxicity as well as teratology studies, in addition to the Category I and II genotoxicity and subchronic studies. When the exposure level is greater than or equal to 1000 ppb (Category IV), a long-term cancer bioassay (preferably in rodents and preferably by the oral route) is required in addition to the previously described studies.

Special studies may be conducted to support the use of an additive in any exposure category. If data from reputable laboratories are currently available, new studies may not be required solely for certification under Standard 60 or 61.

Data provided by the required toxicity tests are used to calculate the MDWL for unregulated contaminants. For noncarcinogens, the calculation is based on the no-observed-adverse-effect level (NOAEL) of the most appropriate endpoint in the most sensitive test



species. If no NOAEL is determined, the MDWL may be calculated based on the lowest-observed-adverse-effect level.

Although the primary focus of the toxicology evaluation approach to drinking-water additives is low-level chronic exposure, this approach also provides for products with intermittent application or implementation (e.g., tank coatings), which may impart high-level but short-term (acute) contaminant concentrations to the water. In these product-class-specific cases, health concerns center primarily on adverse reproductive or developmental effects. Required testing depends on the initial concentration of the contaminant and the slope of the leachate decay curve as determined in laboratory testing (see Figure 1). Acute toxicity testing with expanded toxicology end points may be required in rodents unless the initial concentration is below the MAL. The concentration of the contaminant at 90 days then determines which of the four toxicity testing categories previously described is appropriate.

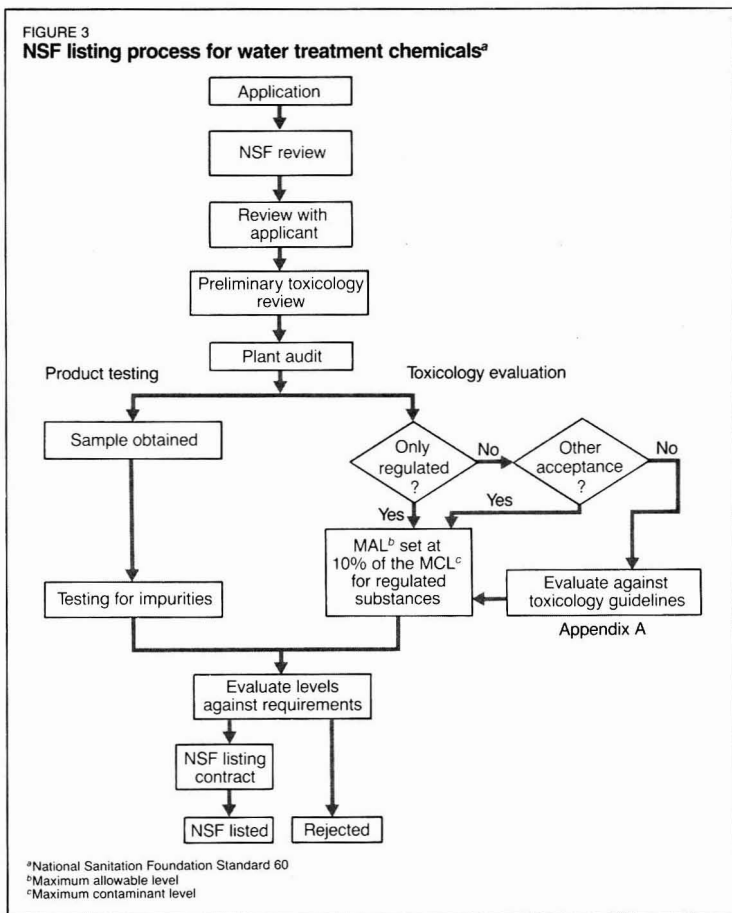
The formulation review and toxicology evaluation approach is illustrated in Figure 2. Formulation review and laboratory extraction testing data each provide an interactive segment of the overall drinking water additives evaluation. An initial formulation review is performed, from which the contaminants of interest may be determined. The extractant levels of these contaminants are obtained from laboratory testing. These laboratory-based concentrations are then used to calculate exposure levels and determine if the contaminant is below regulated levels or which toxicity category testing level is applicable. The appropriate toxicology data are reviewed and an MDWL calculated for the contaminant(s) prior to reaching a certification decision.

Product certification

The second objective of the program is to implement the use of the product through product certification. NSF is now offering product certification (NSF Listing) based on the requirements of its standards.

Other groups may also offer product evaluation based on the standards, and some manufacturers may choose to certify their products themselves. Whatever approach is selected by manufacturers, AWWARF will maintain and make available a directory of all products certified as meeting the standards. The list will include trade name, manufacturer, and certifying entity. AWWARF will not make judgments on the reliability of the certifying entity.

Regulatory officials and product us-



ers will determine the type of product certification adequate to meet their needs, whether it is the NSF Listing Program, independent laboratory testing, manufacturer's self-certification, or some other certification mechanism. For most of these products, the chief regulatory responsibility lies with state drinking-water administrators.

Testing, evaluation, and listing of products will be performed for a fee by NSF for manufacturers requesting these services. The fee structure is determined by the technical requirements of the standards, and the program is structured to be self-supporting.

The increase in product prices and water rates caused by the evaluation services is expected to be very small. For example, annual testing, evaluation, and listing fees for a lime manufacturer are estimated to be about \$2,015 per year. First year costs, because of the nonrecurring standards development fee (\$6,000) and an initial formulation review fee, are significantly higher. However, by amortizing the first year cost over five years and adding it to the annual cost, a total an-

nual cost of about \$4,200 is projected. Assuming an average lime company sells 25,000 metric tons to the water industry, NSF's product certification would cost about 17 cents per metric ton. (Lime sells to water utilities for about \$55 per metric ton.)

The Listing procedure

NSF has a single goal under its Listing Program, that is, ensuring the integrity of its registered certification marks. To ensure fulfillment of NSF's legal and moral responsibilities, a formal Listing procedure has been established, and contracts are signed with listed participants. There are seven major steps in the Listing process: application, preliminary toxicology review, initial audit, product testing and toxicology evaluation, listing, follow-up audit and testing (as required), and enforcement. Figure 3 shows the process flow.

As a first step in the application process, manufacturers interested in having a product listed contact NSF in Ann Arbor and describe their products in detail. If available, descriptive litera-

**Receive your personal
subscription
to C&EN as part
of your membership
when you join ACS**

The subscription to C&EN you now pay \$40 a year for will be yours as part of your membership, when you join ACS.

And that's only one of the benefits!

Consider a few of the others:

- National Meetings—at special member rates
- Local and Regional meetings to meet your colleagues, learn what is going on in your area
- Divisional Meetings and publications to keep pace with your specific disciplines
- Professional Development Courses at special member rates
- Substantial member savings on 22 ACS journals and periodicals
- Impressive insurance and retirement benefits

Find out how to receive your **personal subscription to C&EN** along with other member benefits. Write, use coupon below, or **CALL 1-800-ACS-5558**

American Chemical Society
1155 Sixteenth Street, N.W.
Washington, DC 20036

YES!

Please send me details on how to receive my personal subscription to C&EN as well as other advantages of membership in ACS

Name _____
Address _____
City _____
State, ZIP _____

ture is submitted by the manufacturer to help identify the relevant standard(s) against which the product is evaluated. NSF returns an application package for completion. All product information is strictly confidential. NSF's records cannot be accessed by other parties, even through the Freedom of Information Act.

Following a preliminary toxicology review, the next step is the initial plant quality assurance (QA) audit and product evaluation. The plant is audited following receipt of a signed application, acceptance of formulation information, toxicological review, and payment of initial fees. NSF will not share toxicology data. Manufacturers wishing to share such data may mutually arrange to do so, but without the direct involvement of NSF. Although there is no blanket acceptance or grandfathering of previously accepted products, health effects data and prior regulatory acceptance may be considered in the toxicology evaluation process.

Next, the product is tested and evaluated. For special cases, testing and evaluation may occur in the field, or at the manufacturer's plant. If the product fully complies with the applicable standard, listing may be authorized. If the product does not comply with the standard, a report documenting all points of noncompliance is forwarded to the manufacturer. Each point of noncompliance must be corrected before the product can be listed.

When listing is authorized, the manufacturer receives official notice and authorization to use the NSF Mark. The official listing, together with the Mark on the product, may be used to verify to regulatory agencies and users that the product complies with an NSF standard. The listing is included in NSF's on-line database and in the next published listing book, and is widely distributed. Unless otherwise requested by the company, NSF also arranges for publication of NSF listed products in the AWWARF directory.

During periodic, unannounced, follow-up audits, qualified personnel re-examine the listed product to ensure that it is equivalent to the item tested, or that only authorized changes have been made; to verify that the product continues to be in compliance with the standard; to review quality control procedures and records; and to select product samples for repeat testing as appropriate.

Manufacturers outside the United States may also use NSF's listing services. Products may be submitted for evaluation against any current NSF standard, using the procedure described. The NSF Mark, when authorized, may be used regardless of where

products are produced or marketed. Audits of production facilities and product testing and evaluation are required at the same frequency for domestic and international program participants.

In its various programs, there are currently more than 150 NSF-listed manufacturers in Australia, Brazil, Canada, Chile, Costa Rica, Denmark, Dominican Republic, England, Finland, France, Germany, Honduras, Hungary, Italy, Israel, Japan, Korea, Kuwait, Mexico, The Netherlands, Puerto Rico, Saudi Arabia, Spain, Sweden, and Taiwan.

NSF welcomes inquiries from regulators, manufacturers, water utilities, and others with an interest in the drinking-water additives standards or NSF's Listing Program for direct and indirect additives products.



Nina I. McClelland is chairman, president, and chief executive officer of NSF. McClelland is a graduate of the University of Toledo (B.S., 1951 and M.S., 1963), and received her Ph.D. from the University of Michigan in environmental chemistry in 1968. She has recently served as a member of the National Academy of Sciences Committee on Water Treatment Chemicals, and as a member of the EPA National Drinking Water Advisory Council.



David A. Gregorka is assistant to the president and director of the NSF drinking-water additives program. Gregorka has a B.S. from the University of Rochester (1973), an M.S. from the University of Michigan (1974), and an M.B.A. from the University of Michigan (1988). He administers NSF Listing programs for products and materials covered by the standards.

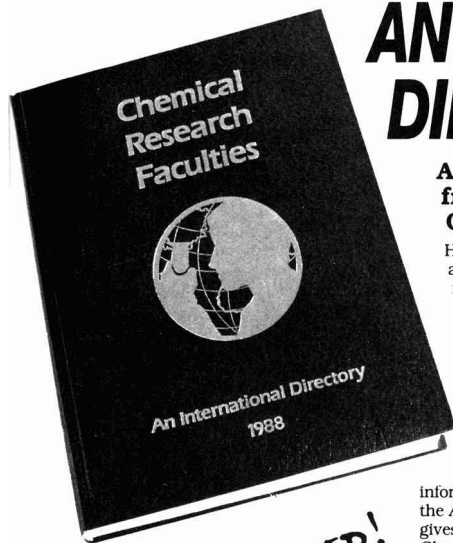


Betsy D. Carlton is a toxicologist for the drinking-water additives program of NSF. Carlton received her Ph.D. in developmental biology from the University of Cincinnati in 1977. She is responsible for toxicology and risk assessment for the drinking-water additives Listing programs.

CHEMICAL RESEARCH FACULTIES

AN INTERNATIONAL DIRECTORY, 1988

More than a third ALL-NEW information!



UPDATED!

\$159.95 in the U.S. and Canada
\$191.95 in all other countries

An invaluable resource from the American Chemical Society.

Here it is—all the information you need about chemical research and researchers at universities around the world, gathered into one volume.

Chemical Research Faculties: An International Directory contains a wealth of facts on more than 11,500 faculty members and 1922 departments in 107 countries. And it's a book no academic institution or chemically oriented business can afford to be without.

Designed to provide the same type of information on an international scale that the ACS *Directory of Graduate Research* gives for U.S. and Canadian schools, *Chemical Research Faculties: An International Directory* includes listings for chemistry, chemical engineering, biochemistry, pharmaceutical/medicinal chemistry, and toxicology.

It offers informative statistical tables on graduate programs worldwide. Organizes data on 72 chemical and chemical engineering societies in 54 nations. And is

cross-referenced three ways—by faculty, institution, and research subject—for easy use.

The 1988 edition has been expanded by a full third—and includes listings for toxicology departments and chemical engineering societies.

Indispensable for industry and academia alike.

If you're involved in chemical research, *Chemical Research Faculties: An International Directory* can keep you abreast of the latest developments in your area of specialization.

If you advise graduate students, it can help you steer them toward the programs they're seeking.

And if you're in a business even remotely related to chemical research, just one of the thousands of leads this book contains could pay for the purchase price many times over.

Why not fill out the attached order form right now? Or call 800/227-5558 and charge your VISA, MasterCard, American Express, or Diners Club/Carte Blanche.

And let *Chemical Research Faculties: An International Directory* open up a whole new world of professional possibilities.

ORDER FORM

- YES! Please rush me my copy of the new international directory!

	U.S./		
QTY:	CANADA	EXPORT	TOTAL
Chemical Research Faculties: An International Directory, 1988 Edition	\$159.95	\$191.95	_____
	AMOUNT ENCLOSED _____		

- I have enclosed a check for \$_____ payable to the American Chemical Society.
- Purchase Order # _____ enclosed.
- Charge my VISA MasterCard American Express Barclaycard Access Diners Club/ Carte Blanche.

Name of cardholder _____
Account # _____
Expires _____ Interbank # _____ (MasterCard and Access)
Signature _____

Note: Please allow four to six weeks for delivery. Foreign payment must be made in U.S. currency by international money order, UNESCO coupons, or U.S. bank draft. Order through your local bookseller or directly from the American Chemical Society. Orders from individuals must be prepaid.

PLEASE SHIP BOOKS TO:

Name _____
Address _____

TO ORDER IN THE U.S., CALL (800) 227-5558. **262**

MAIL THIS ORDER FORM TO: American Chemical Society
Distribution Office, Department 262
P.O. Box 57136
West End Station
Washington, D.C. 20037

- Please send me more information about the ACS *Directory of Graduate Research 1987*, which gives similar data for U.S. schools.

Departmental Information

includes address and phone number, name of department head, advanced degrees offered, and principal areas of research.

Guide to Chemical Research Institutions lists all countries, universities, and departments in order of appearance, providing an overview of each section.

Statistical Tables

provide for each country the number of master's and doctoral degrees conferred in 1985 and 1986 as well as the number of full-time faculty, post-doctoral appointments, and students enrolled in advanced degree programs.

Faculty Information

includes name, year of birth, title, degrees (with years and institutions), areas of specialization, current research, and recent publications.

Four Organizational Sections

break down listings into chemistry, chemical engineering, biochemistry, pharmaceutical/medicinal chemistry, and toxicology.

Chemical Society Information

lists address, principal officer, publications, purpose, organizational structure, and number of members.

Faculty Index

helps you keep up with colleagues' moves and learn more about others in your area of specialization.

Institutional Index

provides a merged alphabetical listing that lets you find institutions known by name but not location.

Index of Research Subjects

helps you locate universities, departments, and individuals doing research related to your own.

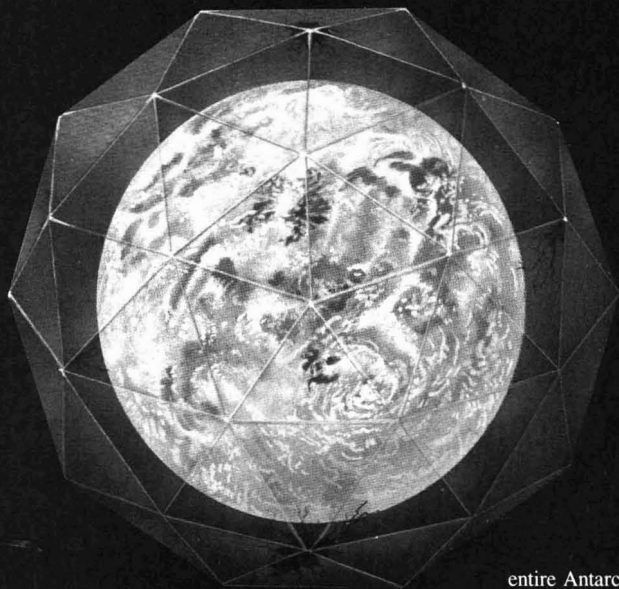


FREE TELEPHONE ORDERING

1-800-227-5558

Washington, D.C. area residents call 872-8065 or 872-8066

Living in a glass house



By Douglas G. Cogan

Nineteen eighty-eight may be remembered as the year the Earth struck back. Scorching summer heat had us flocking to the beaches, but medical waste and other tide-swept garbage kept us out of the water. Lack of rainfall parched crops, sapped hydropower, even made washing the family car a luxury. While we waited anxiously for a change in the weather, NASA scientists informed us that more of the same—or worse—is in the long-range forecast. Within our lifetimes, they predicted, the climate will become hotter and the sun's rays more deadly than at any time in human history.

These twin atmospheric perils—the greenhouse effect and ozone depletion—are better understood if we envision the Earth as a fragile glass house. It's as if the planet were protected by a floating network of special window panes that filter out the sun's harmful ultraviolet light while retaining some of its radiant heat. Spanning the globe in a seamless web, these window panes form a giant geodesic dome under which all life, save that in the deep oceans, has evolved.

Three years ago, an orbiting satellite known as Nimbus 7 provided the first tangible evidence that the exterior of the glass house is falling into disrepair. It revealed a gaping hole in the Earth's basement window—the ozone layer over Antarctica—which spreads from the South Pole each year, at the beginning of austral spring, and engulfs the

entire Antarctic continent by early October. Although the damage seems to repair itself as spring turns to summer, it is a patch-up job at best. Since 1979, all latitudes more than 60° south of the equator have sustained ozone declines of 5% or more throughout the year. And at its worst, the hole covers an area twice the size of the continental United States, with depletion exceeding 50% at its center (1).

In 1988, signs emerged of hairline fractures in window panes throughout the glass house—even around the main living quarters in the Northern Hemisphere. A careful review of nearly 20 years of ground-based and satellite instrument data confirmed a year-round ozone loss of 3% across densely populated regions of North America, Europe, and the Soviet Union, and a wintertime loss of 4.7%. Perhaps more troubling is that sophisticated computer models had indicated that such a decline would not occur until well into the 21st century.

A hole in the attic?

As we enter 1989, the search is on for another ozone hole—this time in the attic of the glass house. One hundred



Douglas G. Cogan

atmospheric scientists and their support crew will be spending the next six weeks in and around Stavanger, Norway, a city of 85,000 inhabitants along the North Sea. Situated only 10° south of the Arctic Circle, Stavanger is strategically important for two reasons. First, it lies at the edge of a cold-weather band that extends from Greenland to Russia, where stratospheric temperatures can plummet to below -80 °C—cold enough to gasify dry ice. Second, Stavanger has a large military airfield that can accommodate a specially equipped DC-8 and an ER-2, a modified U-2 spy plane.

These NASA aircraft were the workhorses of the Antarctic Airborne Ozone Expedition (AAOE) of 1987. That expedition, in combination with extensive ground-based and satellite monitoring, identified three necessary elements for the development of an ozone hole. First, the atmosphere over one of the poles needs to wind itself up in a tight spiral—a polar vortex—that is virtually impenetrable by outside air masses. Second, stratospheric temperatures inside the vortex need to fall below -80 °C to freeze out droplets of nitric acid and below -85 °C to turn water vapor into ice. If the vortex is sufficiently cold and stable, the resulting particles—thought to be nitric acid trihydrate wrapped in a thick coat of ice—fall out of the ozone layer before evaporating in the troposphere several kilometers below (2).

That leaves the lower stratosphere practically defenseless against ozone depletion, provided that the third element is in place: elevated levels of chlorine. Without nitric acid to sequester chlorine in inactive reservoirs of chlorine nitrate and hydrogen chloride, chlorine free radicals are able to attack ozone from the time sunlight returns to the pole at the end of winter until the polar vortex breaks up later in the spring. This heterogeneous (surface-catalyzed) process allows one chlorine atom to destroy tens of thousands of ozone molecules before the carnage is over.

An Arctic ozone hole is not likely to be as severe as the one in the Antarctic, however. The Northern Hemisphere is considerably warmer on average and the North Pole is less prone to the development of a well-contained polar vortex. Even so, the necessary elements exist for accelerated depletion of the Arctic ozone layer. Stratospheric temperatures there occasionally fall below -80 °C. This permits the formation of polar stratospheric clouds (PSCs) that freeze out nitric acid, although they appear 10 times less frequently than in the Antarctic.

More importantly, tests conducted

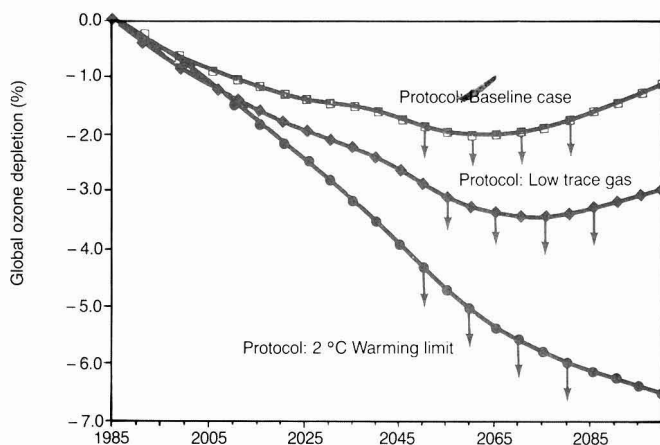
last winter in the Arctic found abundances of chlorine dioxide, a proxy for the free radicals involved in ozone depletion, at 10 times the level suggested in models of homogeneous chemistry. In addition, abundances of nitrogen dioxide, an inhibitor of chlorine's ozone-depleting capabilities, were among the lowest measured anywhere in the Earth's atmosphere. This strongly suggests that heterogeneous chemical reactions already are taking place in the Arctic (3). Nevertheless, this year's Arctic expedition may be unable to locate an ozone hole. The one in the Antarctic last year was weaker than expected, breaking up six weeks earlier than it did in 1987. Scientists attribute this to unusually dynamic weather patterns, which pushed the polar vortex off the South Pole into regions with more sunlight, allowing the vortex to

warm up and diminishing the presence of PSCs. If the same kind of dynamic forces are at work in the Arctic this winter, PSCs there may not form at all—leaving scientists with the unwelcome prospect of having to repeat the Arctic experiments.

Putting the house in order

Sixteen months from now the Montreal Protocol will be reviewed. This international agreement, signed by nearly four dozen nations since September 1987, calls for a 50% cut in production of fully halogenated chlorofluorocarbons (CFCs) by 1998. But an analysis of the Protocol by the U.S. Environmental Protection Agency suggests that its implementation hardly will protect the ozone layer (4). On the contrary, EPA found that chlorine levels in the atmosphere are likely to tri-

FIGURE 1
Simulated global average total column ozone depletion:
Protocol scenario with alternative trace gas assumptions



Note. Arrows indicate that ozone depletion estimates may be underestimated.

Assumptions

Protocol: United States participation; 94% participation in other developed nations; 65% participation in developing nations. Use of compounds not covered by the Protocol grows at the rates in the No Controls scenario. Growth rates among nonparticipants are reduced to 37.5% (developed nations) and 50% (developing nations) of their baseline values. Compound use assumed constant after 2050.

Other trace gases—annual growth rates

Baseline scenario	Low scenario	2 °C Warming limited (1985–2075) ^a
CH ₄ : 0.017 ppm	CH ₄ : 0.01275 ppm (75% of the base scenario value)	CH ₄ : 0.24%
N ₂ O: 0.2%	N ₂ O: 0.15%	N ₂ O: 0.06%
CO ₂ : at the 50th percentile rate reported by NAS (about 0.6%/yr)	CO ₂ : at the 25th percentile rate reported by NAS (about 0.4%)	CO ₂ : 0.15%

^aAssuming a 3 °C climate sensitivity to doubled CO₂, trace gas growth is limited so that projected equilibrium warming equals 2 °C by 2075.

ple—from 2.7 parts per billion in volume to 8 ppbv in 2075—even if all nations in the world were to abide by terms of the agreement (an unlikely proposition). The EPA study also concluded that stabilizing chlorine at its present concentration in the atmosphere (which itself may be too high) would require an immediate ban on production of CFCs and halons as well as a freeze on the production of methyl chloroform. (Halons are bromine-based fire extinguishants. The Montreal Protocol calls for a freeze on production of these compounds by 1992. Methyl chloroform is a widely used chlorinated solvent; its use is not restricted by the Protocol.)

Last October, scientists meeting at The Hague under the auspices of the United Nations Environment Program (UNEP) agreed to conduct a six-month assessment that may influence the outcome of the treaty negotiations in 1990. The assessment will be broken into four parts, reflecting the state of knowledge on: (1) the chemistry and physics of ozone depletion; (2) UV-B health effects on humans, plants, and animals; (3) the availability of substitutes for products made with or containing CFCs; and (4) economic impacts of more stringent controls.

The UNEP assessment, due out this summer, may contain promising news. Several chemical companies expect to have commercial plants producing CFC substitutes by 1990. (Chronic toxicity tests are likely to delay market introduction of several substitutes until at least 1992, however.) The world's largest producer of CFCs, Du Pont, is optimistic enough about the development of alternatives that it has pledged to end production of fully halogenated CFCs

by the year 2000. In fact, companies that produce 60% of the world's CFCs have pledged their support for a complete phase-out of the ozone-depleting compounds.

Other sections of the UNEP assessment may contain bad news, however. Beyond pointing out the inadequacy of present control measures, the assessment may take a longer look at the relationship between ozone depletion and the greenhouse effect. Past industrial activity has committed the Earth to at least 0.5 °C of warming over the next century (5). Since the warming will be accentuated at the poles, permafrost may thaw and release molecular methane hydrates from the soil. Oxidation of that methane, in turn, would increase the amount of water vapor in the atmosphere. The greenhouse effect also is likely to trap more heat in the troposphere and possibly reduce temperatures in the lower stratosphere. The combination of more airborne water vapor and reduced stratospheric temperatures could increase the presence of PSCs—even in portions of the globe where they are not found now. Evidence also is mounting that sulfuric acid droplets, derived from power plant emissions and volcanic eruptions, could foster surface-catalyzed ozone depletion away from the poles.

The most sobering prospect of all is that efforts to limit future global warming may have their own adverse consequences on the ozone layer. EPA estimates that measures taken to hold global warming to an increase of 2 °C by 2075 could triple the ultimate rate of ozone depletion (4). This would result largely because of the reduced nitrogen oxide emissions and comparatively warmer stratospheric tempera-

tures, which, absent PSC considerations, facilitate ozone depletion.

As more is learned about mankind's complex relationship with the sky, the perception is growing that Earth's dwellers do indeed live inside a glass house. This recognition may change the way society behaves inside the house and may promote new respect for its fragile exterior. The outcome of negotiations to revise the Montreal Protocol will tell whether this new perspective is shaping global environmental policy.

References

- (1) "Executive Summary"; Ozone Trends Panel Report, National Aeronautics and Space Administration: Washington, DC, March 1988.
- (2) Monastersky, R. *Science News* **1988**, *134*(16), 249-51.
- (3) Solomon, S. et al. *Science* **1988**, *242*, 550-55.
- (4) Hoffman, J. S.; Gibbs, M. J. *Future Concentrations of Stratospheric Chlorine and Bromine*; U.S. Environmental Protection Agency, U.S. Government Printing Office: Washington, DC, 1988.
- (5) Jaeger, J. *Developing Policies for Responding to Climatic Change*; World Meteorological Organization: Geneva, Switzerland, 1988, WMO/TD-No. 225.

Douglas G. Cogan is author of Stones in a Glass House: CFCs and Ozone Depletion, a chronicle of the development of regulations to protect the ozone layer. Mr. Cogan has coauthored reports on energy conservation and renewable energy and is presently engaged in a study of corporate responses to the greenhouse effect. He is a senior analyst with the Investor Responsibility Research Center, Inc.; (202) 939-6500. Stones in a Glass House is available for \$35. Paid orders may be sent to IRRIC, 1755 Massachusetts Ave., N.W., Suite 600, Washington, DC 20036.

Environmental Index

Year the change in the ozone concentration over Antarctica was observed: 1977

Year the change in the ozone concentration over Antarctica was reported in the scientific literature: 1985

Year measurements of chlorofluorocarbons in the atmosphere were first made: 1970

Atmospheric lifetime of CFC-11 (CCl₃F): 75 years

Atmospheric lifetime of CFC-12 (CCl₂F₂): 110 years

Definition of atmospheric lifetime of a chlorofluorocarbon: average time between release to the atmosphere and eventual destruction in the stratosphere

Sources are listed on page 26.

Toxic trade with Africa

By Arti K. Vir

A new kind of trade has been taking place between some western industrialized nations and certain African countries. Toxic and radioactive waste shipped out from the West are being dumped on African soil. Often this is a silent trade. In some cases, however, contractual agreements have been made with African governments.

As environmental and safety laws in Europe and the United States become increasingly stringent and as the cost of disposal of hazardous waste has mounted up to \$2500 per ton, dumpers, or "waste merchants" as they have come to be known, are turning to poor and easily accessible African territories. This year, several countries in West Africa received offers from the United States and Europe. One of these countries will get only \$2.50 per ton. But to nations that are drowning economically, this is an attractive deal.

Many African nations have been outraged by this new assault. Nigeria has been at the forefront in denouncing waste dumping in Africa, and is particularly concerned because Benin, its neighbor to the west, has agreed to accept radioactive wastes from France. At the Organization of African Unity (OAU) summit held in May this year in Addis Ababa, Ethiopia, President Babangida of Nigeria declared, "No government, no matter the financial inducement, has the right to mortgage the destiny of future generations of African children."

Ironically, about a week after the OAU summit, toxic waste of foreign origin was discovered in Nigeria. The discovery was made on June 2, after a letter was received by the Nigerian government from eight Nigerian students in Pisa, Italy. The students, alerted by reports in local Italian newspapers, wrote to their government warning that waste from Italy was being dumped in Nigeria.

According to reports, the waste drums, weighing about 3800 tons, were found stored at a site in Koko, Nigeria, a port town of about 5000 inhabitants. The cargo had arrived from Italy in five



Arti K. Vir

shipments between August 1987 and May 1988.

When the owner of the waste site, Mr. Sunday Nana, was questioned, he said he had no knowledge of the contents of the drums and that over the last five years he had been renting out portions of his land to various importers for storing their merchandise. In this case he identified the importer of the drums as Mr. Gianfranco Raffaelli, an Italian businessman. Raffaelli, a Nigerian resident for many years, imported the wastes in collaboration with Irukpen Construction Company, a Nigerian firm with which he was closely connected. He falsified and forged documents and permits for importing the drums. Raffaelli slipped out of Nigeria on June 2 after newspapers reported the discovery of the Koko dump.

The government arrested 15 Nigerians in connection with the scandal; an Italian accomplice, Desiderio Perazzi, is being held in jail. A special tribunal will be set up to try this case. On the morning of June 14, Nigerian newspaper headlines read "Culprits may face firing squad" and "Death penalty likely."

The government also seized an Italian merchant ship, the *M. V. Piave*, on June 10 in order to transport the wastes back to Italy. The Nigerian ambassador to Rome was recalled. The Minister of Justice and the Attorney General have said the matter will go to the International Court of Justice at The Hague if Italy does not remove the toxic wastes.

The dump site was sealed off and a team of experts studied the area and took samples for analysis. Experts

from other countries, including Britain and the United States, were asked to assist in the investigation. Initial surveys of the site showed that many of the drums were damaged, leaking, and emitting an odor. Recent reports say about 4000 of the drums were old and rusted and some were swelling because of the heat. Scientists have determined that many of the drums contain volatile solvents and there is a risk of fire or explosion that would produce highly toxic smoke. Some drums are marked with the letters "R," "D," "X," and the skull and crossbones symbol. Chemical name markings include "Polychlorodifenile" (PCBs), "fluorosilicate," "erocitus," and "rheo 53."

It has been reported that among the waste at the Koko site, methyl melamine waste originated from Dyno-Cyanamid of Norway, dimethyl and ethylacetate formaldehyde came from Italian chemical manufacturers, and PCBs came from Elma, a Turin-based electromechanical plant. The experts' reports have conflicted to some degree, but the presence of highly toxic PCBs has been confirmed. Also, the Japanese Atomic Energy Research Agency reported that three of the drums contain a highly radioactive material.

On July 6, 150 workers started re-packaging the waste into containers for removal. On July 12, three workers suffered severe chemical burns while moving the drums. Doctors at the site reported that some of the crew were vomiting blood and had been hospitalized, and one man had been partially paralyzed. On July 30 the *M.V. Karin B* sailed to Italy carrying the first 2270-ton load of toxic waste from the Koko dump site. The second shipment of waste, which carried all the remaining containers out, left Koko on August 15th aboard the *M.V. Deep Sea Carrier*. However, because land within a radius of about 500 m from the dump site has been declared unsafe, concern over surface and groundwater contamination remains. Scientists will be doing continuous environmental monitoring at and around the site for the next three years. Also, the local hospital is being

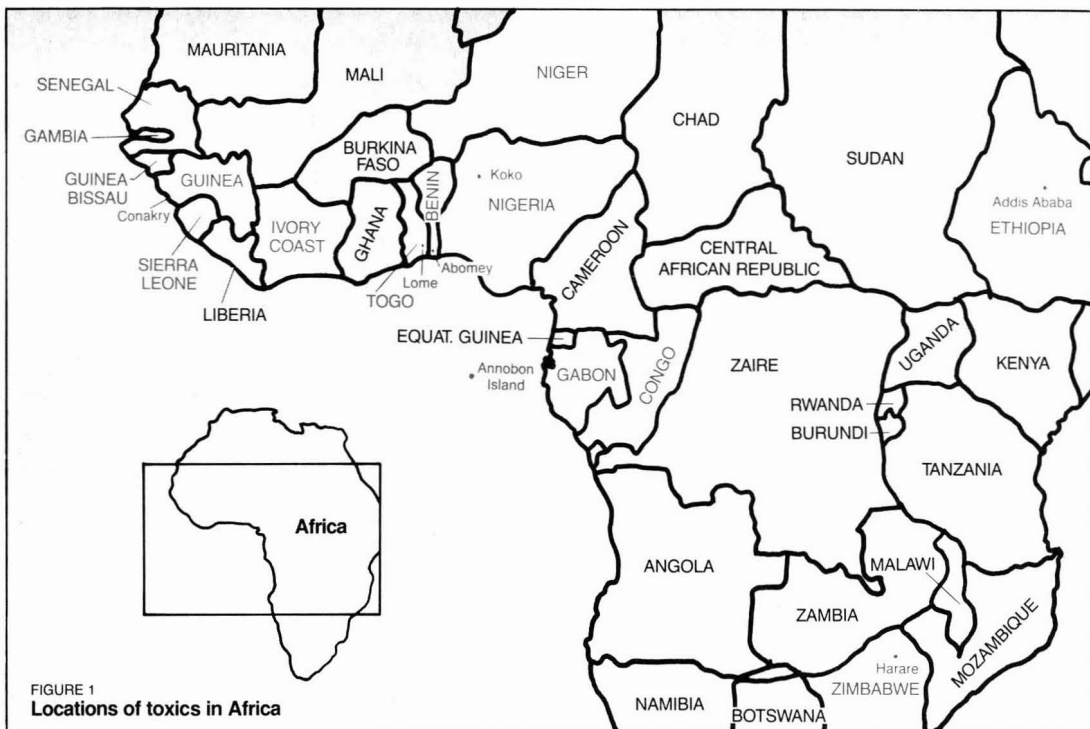


FIGURE 1
Locations of toxics in Africa

upgraded so it can monitor health effects on the Koko residents.

Nigeria has received international attention because of the scandal at Koko, but this is only one of many occurrences in Africa. In early June, as Nigerian papers carried headlines almost daily on the waste dumping from Italy, many other reports of this kind of activity surfaced, and by mid-June, some of the weekly African journals, including *West Africa* and *African Concord*, were carrying cover stories and special reports on this toxic terrorism. The involvement of several countries in this new trade was revealed.

Another case of dumping occurred in Guinea. In March of this year, a Norwegian shipping company dumped 15,000 tons of material labeled "raw material for bricks" in a quarry on Kassa Island, off the mainland capital of Conakry, Guinea. On June 8, newspapers reported that the island's vegetation was drying up and dying. The cause, the Guinean government discovered, was the dumped cargo that was in fact incinerator ash from a municipal incinerator in Philadelphia.

The Guinean government called for immediate removal of the waste and on June 10 arrested Norway's Honorary Consul, Mr. Sigmund Stromme. He was also a director in the Norwegian-Guinean company Guinomar that imported the waste. The shipment was the first of a total of 85,000 tons of waste

Guinea was to receive. Stromme was charged with forging documents in order to bring in the shipment. On June 21 a Norwegian freighter arrived in Guinea to take away the 15,000 tons of incinerator ash, and by July 2 it was reported to have removed all the waste. According to Greenpeace, there is a long list of countries involved in this toxic waste trade. Allegedly there was a contract with a Dutch shipping company under which Congo was to receive solvent, paint, pesticide sludge, and chemical waste from the United States and Europe amounting to a million tons between June 1988 and May 1989 for a fee of \$84 million. In May Congo retracted this agreement.

On February 9 of this year, Guinea-Bissau signed a five-year contract with two British companies to receive as landfill 15 million tons of waste from tanning and pharmaceutical industries for a payment of \$600 million. The wastes would come from the United States and Europe. This contract has now been canceled.

South Africa received two shipments in 1986 of 60 drums each of mercury-laced sludge waste from New Jersey that was to have been recycled to reclaim the mercury.

At least 1500 gallons of hazardous waste from armed forces agencies in the United States were dumped in a phosphate mine pit in Zimbabwe. The exporters from the United States, Jack

and Charles Colbert, were sentenced in February 1988 to 13 years' imprisonment for fraudulent business practices. Of the shipment, 274 drums were falsely labeled as cleaning fluids.

Africa Analysis reported that a U.K. company has a 10-year license to dump 10 million drums of waste from Europe on Annobon Island in Equatorial Guinea for a fee of \$1.6 million (1).

West African Hotline reported that President Bongo of Gabon met with Denison Mining Corporation in 1987 and agreed to take uranium tailing waste from its mines in Colorado (1).

Sierra Leone newspapers reported that Freetown received a shipment of toxic ash, cadmium, chromium, mercury, and lead from a U.S. ship, the *Bark*, in March. The cargo was transferred to the U.S.-affiliated Sierra Rutile mine.

In January 1988, a contract was made between Benin and Sesco Ltd. in Gibraltar to deliver up to five million tons per year of nonnuclear industrial waste from North America and Europe and will pay Benin \$2.50 per ton. Another agreement was made in January between France and President Kerekou of Benin by which France will pay Benin \$18 million for hazardous wastes. Three cargo vessels are on their way from France to Benin carrying the first consignment of waste, including cyanide, asbestos, and high-level radioactive material.

On August 3, newspapers reported that two towns in Benin had received large amounts of radioactive waste from the Soviet Union between 1984 and 1986. Some was buried at Canna, under the tarmac of a military airfield that was being built by the Soviets. The work at the airfield ceased two years ago when the Soviets moved out of Benin. Another dumping ground for the Soviet radioactive waste was at Dan. Both dumping areas are in the historic Abomey region. A shipment of nuclear waste was brought into Benin by a Benin marine vessel from Le Havre in northern France and has been buried also in the Abomey area.

The list of countries continues: Senegal, Ethiopia, and Niger have been approached with offers to trade in hazardous goods.

The widespread practice of toxic waste dumping in Africa has been strongly condemned and was addressed at the Economic Community of West African States (ECOWAS) meeting held in June at Lome, Togo. The 16 member countries passed a resolution calling for stiff penalties for the toxic waste dumpers. Some of the countries have already started instituting laws prohibiting dumping. Ivory Coast adopted a law in July that provides for

Amount offered to the Congo this year to accept 100,000 tons of Europe's toxic waste: \$7,063,500. Source: *Harper's Magazine*, October 1988, p. 15.

fines up to \$1.6 million and prison sentences up to 20 years. Gambia has passed a bill setting penalties of 5 to 40 years of imprisonment. Nigeria and Congo are now putting together anti-dumping laws as well. In addition, African countries have been urged to set up monitoring systems or a "dump watch" to look out for potential dumpers.

Many countries around the world, now alerted, are refusing to off-load toxic cargo. It has been reported that a ship carrying 10,000 tons of waste from Philadelphia has been sailing around since August 1986 because its cargo has been rejected by the Bahamas, Honduras, Haiti, the Dominican Republic, and Guinea Bissau. The Italian Green Party has reported that a Syrian-registered ship, *Zanoobia*, sailed around the world for more than a year looking for a place to discharge its load of chemical wastes, and eventually had

to return without success to Marina de Carrara, Italy, where it had started.

Public outcry, antidumping laws, and monitoring systems should act as deterrents for toxic waste dumpers. The re-entrations of dumping contracts by Congo and Guinea Bissau and the demands by Nigeria and Guinea that foreign governments remove illegally dumped hazardous materials from their territories are warnings to industrial nations to keep waste away from African shores.

References

- (1) Ayadike, O. *West Africa*, June 20, 1988, p. 1109.

Arti K. Vir received a B.S. in biology in 1981 from Lafayette College in Pennsylvania and an M.S. in environmental science in 1983 from Hunter College of the City University of New York. Vir has worked for the environmental consulting firm of Wapora, Inc. and Edwards and Kelsey, Inc. and as an environmental scientist for the New York State Attorney General's office. Vir lives in West Africa; she has traveled in the Ivory Coast, Ghana, Togo, Benin, and Nigeria. She plans to be in Africa for the next few years and will continue to travel and write.

Acid deposition: A paper tiger

By Stanton S. Miller

This nation is controlling acid rain with paper. At the outset the Reagan administration opted not to control acid deposition, because the science was not all in. Then in 1980, Congress established a 10-year program to get the facts; by enacting the Energy Security Act of 1980, Public Law 96-294, Congress initiated the National Acid Precipitation Assessment Program (NAPAP).

This year, 27 state-of-the-art science and technology reports will become available that will analyze the causes, effects, controls, and costs of acidic deposition. Produced at a cost of about \$400 million of federal tax revenues and prepared and authored by about 100 specialists, these reports will become available in November 1989. But the results in these reports will be more than decision-makers can handle. Perhaps the decision-makers will not be

able to see the policy implications for the facts. Nevertheless, an Integrated Assessment Report, the final assessment report from the NAPAP, will be available in September 1990.

Meanwhile, at a public review meeting in mid-November this year in Washington, DC, NAPAP received comments on its draft assessment plan. The final plan will be published this month. But the uncertainty level in the forthcoming science and technology reports is a main concern. A classification system has been adopted to evaluate and rank the scientific information. Codes from zero to four stars will be used to assess the information in the 27 reports; these codes are intended to help the public and the policy-makers understand the assessments. A four-star rating indicates the highest level of confidence in the accuracy of that section of the report; a zero rating indicates the lowest level of confidence in the facts.

It will not be an easy task for peer-review scientists to evaluate this information and to choose ratings for it.

James R. Mahoney, director of the program and moderator at the public meeting, says, "This rating will not replace formalized error and careful interpretive statements, but it will enhance communication between science and the public." When these reports become available in November, confidence levels will be included.

For those who can wait, a 5-day international conference is planned for November 1989 to review the 27 reports. Meanwhile, what priority President-elect Bush places on this key environmental problem will be interesting to watch.

Stanton S. Miller is the managing editor of ES&T.

Pollution Threat of Heavy Metals in Aquatic Environments. Geoffrey Mance. Elsevier Applied Science Publishers, Crown House, Linton Road, Barking, Essex IG11 8JU, England, U.K. 1987. xii + 372 pages. \$86.50, cloth.

Reviewed by Jorma Heinonen, Counselor for Science and Technology, Embassy of Finland, Washington, DC 20045.

One admirable feature of *Pollution Threat of Heavy Metals in Aquatic Environments* is that it points up the need for substantial improvements in the quality control of many kinds of environmental data, especially if these data are to be used to set standards. Moreover, the author explains why an appreciation of the limitations of such data and of the scientific knowledge and research that generated the data is crucial to any evaluation of these standards. This book refers mainly to water quality standards that are being developed as a result of environmental legislation by members of the European Community.

The book consists of 11 chapters. The first chapter presents a history of the study of the effects of metals in aquatic ecosystems, with an emphasis on the damage caused by the methylation of mercury by aquatic organisms. Chapter 2 briefly discusses laboratory techniques for toxicity testing and the basic weaknesses and practical limitations of testing protocols.

The next three chapters alone could make up a book. They lucidly discuss the toxicity of 11 metals to various types of freshwater and marine fauna, primarily fish. The author acknowledges that the information presented does not represent an exhaustive survey of the literature. Rather, he obtains it from sampling and analyses whose general methodology he has evaluated and deemed to be scientifically adequate.

I am somewhat mystified by the author's statement, "There are few re-

views of the toxicity of mercury to freshwater fish and the available information from studies that are methodologically sound are few." For example, selected reviews made by experts on mercury were compiled in a booklet published in 1972 (*J*). It includes a survey on the quality of mercury analyses.

Chapter 6 is a good summary of 10 major factors in toxicity, supported by ample data. The author states that the generalization that salmonid species of fish are more sensitive to toxic substances than are nonsalmonid species often is ill-founded. He adds that although salmonid species are more sensitive to cadmium and chromium, the reverse may be true for other contaminants. In other cases, a lack of data prevents any reasonable comparison from being made.

Thus the thesis of this book that previous generalizations were based on inadequate scientific data seems convincing. Premature generalizations and oversimplifications unfortunately are common in environmental issues even among research scientists. For instance, on the basis of empirical observations, it has been widely asserted that when a waterway begins to become contaminated, the salmonid species are the first to disappear. A more recent example of hastily drawn conclusions is the discussions on the fate of the North Sea seal population.

Chapters 7 and 8 deal with freshwater and tidal water field studies, respectively. They also consider the difficulties in working under the uncontrolled conditions normally encountered in field studies. The introduction to Chapter 7 and the discussion in both chapters of field tests and of the literature are well-presented. These chapters would have been enhanced, however, by a more thorough comparison of laboratory and field testing procedures.

The subject matter of Chapter 9, bioaccumulation, could just as well have been placed after Chapter 6.

The author deserves credit for em-

phasizing, in Chapter 10, the different roles standards may have. He summarizes how standards are developed. It would have been helpful, however, if he had stressed how laborious and sophisticated a process standard development can be and that the establishment of standards always has a political dimension as well.

Chapter 11 deals with international controls. The book, however, discusses mostly the experience, developments, and results obtained in the United Kingdom, and, to a lesser extent, in other countries of the European Community. Thus, the discussion primarily covers the North Sea. Because it is unique, I think the author should have mentioned the Baltic Sea—a small, isolated, shallow sea with brackish water.

Pollution Threat of Heavy Metals in Organic Environments presents its information clearly, which qualifies it to serve as a data base. More significantly, however, the book helps the reader appreciate the complexity of the factors that govern the environment for living organisms. One of its messages is that there is a need for better data, which must come from accelerated research by scientists concerned about quality. The book is valuable for people dealing with environmental research, pollution control, and regulatory issues.

Reference

- (1) "Mercury Contamination in Man and his Environment," Technical Report Series No. 137, International Atomic Energy Agency: Vienna, Austria, 1972.

Environmental Index Source Box

- (1), (2) Rowland, F. S. *Earth's Atmosphere in the Twenty-First Century*. Carolina Environmental Essay Series, VIII; The Institute for Environmental Studies. The University of North Carolina at Chapel Hill, 1987, p. 21.
- (3) *ibid.*, p. 12.
- (4)-(6) *ibid.*, p. 14.

An environmental agenda for the new administration



Alvin L. Alm

The four-year term awaiting President-elect Bush may seem like a long time in which he can pursue his policy agenda. History shows, however, that a president's legislative and budgetary program is at its most powerful very early in the term. The actions taken in the first few months of a new administration can establish its direction and tone. Although it is a period of great opportunity, the first year of a new administration is also a dangerous period for policy formulation because the new team has not worked together and the weak and strong links are not yet known and tested.

Because of my recent participation in the quadrennial preparation of transition papers—in my case for the American Agenda project of Presidents Carter and Ford—I have entered the fray, providing unsolicited, but I hope sagacious, advice to the new president. My list of recommendations stems from the fundamental assumption that timely action is necessary to use the full power of the presidency during the honeymoon. My recommendations focus only on those issues that are fundamentally presidential, not on those that can be dealt with by agency heads. I recommend the following:

1. *Elevate waste prevention and reduction to the primary environmental goal of the new administration.* Unless the United States pursues a strong waste prevention and reduction strategy, our pollution problems will continue to overwhelm us. We will merely move pollution from the air and water to land and then back again. Population and economic growth will tax the assimilative capacity of the environment, and we will simply never catch up. One

form of waste prevention, energy conservation, has already demonstrated what can be done. For the past 15 years, the U.S. GNP has grown by 40%, but energy use is about the same. Product substitution and process changes could actually roll back hazardous waste generation.

2. *Attack global warming comprehensively.* Global warming, the so-called greenhouse effect, could affect the very habitability of the planet. Caused by carbon dioxide emissions, chlorofluorocarbons, and other greenhouse gases, as well as deforestation, global warming presents an unprecedented challenge to scientists, civil servants, and those in the energy industry and other sectors of a majority of the nations. No environmental problem requires greater international cooperation and a wider range of actions.

To attack global warming, the new president should designate responsibilities for research, coordination, and action options. For example, the Secretary of Energy could develop options for reducing carbon dioxide emissions; the Council on Environmental Quality (CEQ) or the White House could take responsibility for overall coordination; and the Office of Science and Technology Policy, CEQ, or EPA could coordinate research.

The president should also develop an international strategy to slow down the causes of global warming that would include a new global warming convention and other mechanisms for international cooperation. The global warming problem will be with us for centuries. But, now that political understanding of the issue has burst like a bombshell, it is time to begin the long-term battle to stabilize the planet.

3. *Create a Department of the Environment by upgrading EPA and adding functions of the National Oceanic and Atmospheric Administration (NOAA).* Because of its size and importance, EPA deserves to be a cabinet department. The argument for upgrading EPA to cabinet status would be strengthened if certain NOAA functions for coastal zone management, marine pollution, and atmospheric sciences were added to EPA's functions. A department strengthened along these lines would have greater capabilities in these criti-

cal areas and would have more clout than the current EPA.

4. *Greatly strengthen EPA's long-term Research and Development Program.* A recent Science Advisory Board (SAB) panel recommended a comprehensive set of reforms for EPA's R&D programs. Two of the recommendations require decisions by the new administration. The first is whether to create an Environmental Research Institute, a contractor-operated institution that would conduct ecological research and monitoring. The second is whether to commit to a substantial long-term increase in funding of EPA's R&D programs; the SAB panel recommended a doubling of funds over a five-year period. A commitment along these lines would greatly help identify and reduce environmental risk.

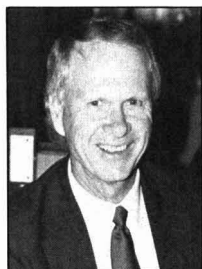
These are only a few of the recommendations set forth in the transition paper I prepared. In addition, I recommended the following:

- \$1 billion annual purchase of land for National Parks, National Seashores, scenic trails and other open space;
- a concerted attack on pollution at federal facilities;
- a blue-ribbon panel review of the Superfund program; and
- development of an affirmative set of recommendations on the Clean Air Act.

It is easy to make sweeping recommendations when one has no responsibility for budgetary and political tradeoffs. I recognize that there are budgetary pressures facing the new president; however, these environmental initiatives do not appear unreasonable. The public and the Congress are demanding action. If the president is not perceived as providing that leadership, the Congress will quickly fill the gap. In my opinion, the president has the opportunity to seize the initiative on some of the issues posed above, or to follow the inexorable force of public pressure.

Alvin L. Alm is president and CEO of Alliance Technology Corp., an environmental engineering and consulting firm with headquarters in Bedford, MA. Alm served as deputy administrator of EPA from 1983 to 1985.

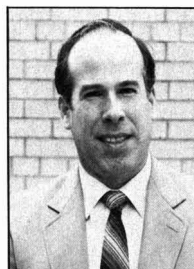
ES&T's 1989 Advisory Board



Dr. William H. Glaze
Editor
University of
California, Los Angeles



Dr. John H. Seinfeld
Associate Editor (air)
California Institute of
Technology

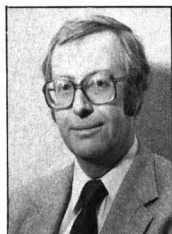


Dr. Philip C. Singer
Associate Editor (water)
University of North
Carolina

William H. Glaze, editor, has announced the appointment of three new members to the *ES&T* advisory board. **Joan M. Daisey** is a staff scientist in the indoor environment program of the Lawrence Berkeley Laboratory (Berkeley, CA). Her research interests encompass airborne toxic organic compounds in indoor and outdoor environments, and their origin, nature, and atmospheric reactions. **Ralph Mitchell** is Gordon McKay Professor of applied biology at Harvard University. His research interests include microbial processes on

surfaces, the microbial transport of metals through subsoils, and the degradation of hazardous organics in biofilm reactors. **Alexander J. B. Zehnder** is chairman of the department of microbiology at the Agricultural University in Wageningen, The Netherlands. His research interests are in environmental microbiology.

Board members serve three-year terms. The last year of each member's term is noted in parentheses.



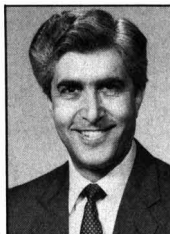
Dr. Roger Atkinson
University of
California, Riverside
(1990)



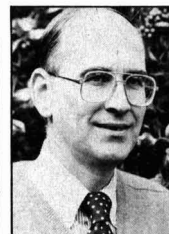
Dr. Joan M. Daisey
Lawrence Berkeley
Laboratory
(1991)



Dr. Fritz H. Frimmel
Technical University
of Munich
(1989)



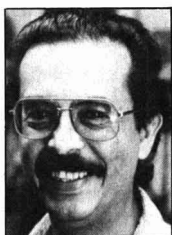
**Nicholas E.
Gallopoulos**
General Motors
Research Laboratories
(1990)



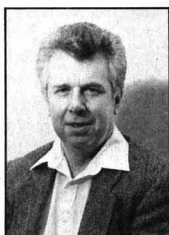
Dr. George Helz
University of Maryland
(1989)



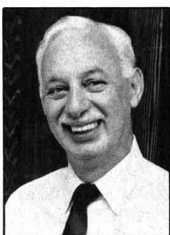
Dr. Ronald A. Hites
Indiana University at
Bloomington
(1990)



Dr. James Leckie
Stanford University
(1989)



Dr. Donald Mackay
University of Toronto
(1989)



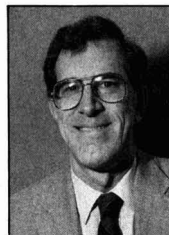
Dr. Ralph Mitchell
Harvard University
(1991)



Dr. Walter J. Weber, Jr.
University of Michigan
(1991)



**Dr. Alexander J. B.
Zehnder**
Agricultural University
of Wageningen
(1991)



Dr. Richard G. Zepp
EPA
(1991)

Editorial Policy

Environmental Science & Technology reports on aspects of the environment and its control by scientific, engineering, and political means. Contributed materials may appear as feature articles, critical reviews, current research papers, research communications, and correspondence. Central to the evaluation of all contributions is a commitment to provide the readers of *ES&T* with scientific information and critical judgments of the highest quality. For the convenience of authors, the specific nature of each type of contribution is outlined below.

Feature articles. A manuscript submitted for publication as a feature article should present useful discussion and opinion on important research directions in environmental science, developing technology, environmental processes, and social, political, or economic aspects of environmental issues. Each manuscript undergoes review by qualified peers as well as by the editors for the purpose of balance and elimination of inappropriate bias. Review criteria include significance of the scientific issue or process described, quality and succinctness of the text, and identification of potential research needs. Strict requirements for documentation of results, completeness of data, and originality, such as those applicable to research manuscripts, are not included in the review criteria for feature articles.

Views. A manuscript submitted for publication as a view should be objective, not an advertisement for a product or method, and should comment on a timely event or development. Views are *not* news items, but insightful commentaries on timely environmental topics. The manuscript should be about 1000 words long. The manuscript will be reviewed by members of the *ES&T* advisory board or reviewers to judge the suitability of its publication in *ES&T*.

Critical reviews. Critical reviews are thoroughly documented, peer-reviewed assessments of selected areas of the environmental science research literature for the purpose of identifying critical research needs. Criteria for acceptability include current importance of the field under review, thoroughness of the literature coverage, clarity of text, and adequacy of research need identification.

Current research papers. The research pages of *ES&T* are devoted to the publication of critically reviewed papers concerned with the fields of water, air, and waste chemistry, and with other scientific and technical fields that are relevant to the understanding and management of the water, air, and land environments. Contributed research papers, in general, describe complete and fully interpreted results of original research.

Environmental Science & Technology seeks to publish papers of an original and significant nature. Originality should be evidenced by new experimental data, new interpretations of existing data, or new theoretical analysis of environmental phenomena. Significance will be interpreted with respect to the breadth of impact of the reported findings. Manuscripts reporting data of a routine nature that do not offer heretofore

unavailable important information or do not substantially augment already available data will be declined publication in *ES&T*. The scope of the reported data in ambient monitoring studies should be such that broad conclusions applicable to more than the particular local scale are possible.

All research articles emphasizing analytical methodology for air or water analysis must include substantial application to environmental samples. *ES&T* faces some overlap with other journals in this area, and articles that do not contain, in the editors' judgment, a significant emphasis on environmental analysis will be returned to the authors for submission elsewhere.

Manuscripts should be prepared with strict attention to brevity. The vast majority of articles are expected to be fewer than four published pages. Processing time will be shortened if the editors do not have to return manuscripts to be condensed.

Research Communications. Research Communications are short research reports describing results of unusual significance. The subject of the communication should be of such importance and the report of such quality that rapid publication is warranted. Communications are expected to be preliminary reports that will be followed by a more detailed publication. The communication should be no longer than two printed pages including figures, tables, and references. Every effort should be made to keep the length substantially below this maximum, such as by avoiding a lengthy introductory section. The Experimental Section should be as brief as possible, giving only essential details. An abstract should be sent with the communication for publication in *Chemical Abstracts*, but it will not be published in *ES&T*. See Current Research Author's Guide for directions for preparation of Abstracts. Communications will be reviewed expeditiously and published as rapidly as possible. To ensure prompt attention to their manuscript, authors should consider sending Communications by FAX to the ACS Manuscript Office (FAX# 202-872-6325) or sending it by express courier. A FAX number for return communications should be included, if available. If minor revisions are required, manuscripts will be returned to authors as expeditiously as possible and should be returned to ACS headquarters within two weeks. The need for major revision is just cause for rejection of the Communication.

Correspondence is a significant comment on work published in the research section of *ES&T*. Comments should be received within six months of date of publication of the original article. The authors of the original article ordinarily will be allowed to reply.

Send manuscripts to: *Environmental Science & Technology*, 1155 16th St., N.W., Washington, D.C. 20036. Address feature and views manuscripts to Managing Editor; research manuscripts to Manager, Manuscript Office. Include a signed copyright status form, a copy of which appears in the January issue.

Peer review in *ES&T*

Characteristics of *ES&T*

ES&T stands out among American Chemical Society journals in that it combines both a magazine and a journal. Only one other ACS publication contains this combination—our sister publication, *ANALYTICAL CHEMISTRY*. Because of the hybrid nature of our publication, it serves a large and diverse audience.

Central to the evaluation of all contributions to *ES&T* is a commitment to provide our readers with scientific information of the highest quality. The publication seeks the most significant, original, and broadly applicable types of articles for its current research section. A vast number of persons review original manuscript contributions and indicate in their evaluations the originality and scientific validity of the work, as well as the appropriateness of the material for our publication.

The Editor and Associate Editors, who are located at the University of California, Los Angeles, the University of North Carolina, and the California Institute of Technology, are fully responsible for all material published in *ES&T*. This policy is a general one applicable to all editors of American Chemical Society publications. The 12 members of the Advisory Board are chosen by the editor to provide input to *ES&T*'s operation. The members are chosen to represent various constituent groups in the research and reader communities and serve three-year terms. Although the editors seek advice and help from individuals in the scientific community and from advisory groups, it is ultimately the editors' responsibility to provide editorial direction, set editorial policies, and make individual publication decisions.

The Washington editorial staff handling the current research section is responsible for the day-to-day operation of the peer review system. All editorial staff members have chemistry or related science degrees.

General guidelines and overall editorial policies set by the editor form the basis for evaluating reviewers' comments on research articles submitted for the current research section.

A look at Peer Review

Each manuscript submitted to the current research section is assigned to a particular staff member and to the editor or associate editor who are then jointly responsible for the manuscript—including choosing reviewers, screening manuscripts to determine whether the papers may fall outside of *ES&T*'s scope, and communicating ultimate acceptance or rejection.

Three reviewers are carefully selected for each paper, based on the subject matter of the paper, the experts available in a given area, and knowledge of the habits of proposed reviewers. Thus, known slow reviewers are avoided when possible. Potential reviewers for each paper are identified through various means, one of which involves a computer search of subjects that reviewers have indicated are their areas of expertise. Reviewers are normally asked to respond within three weeks, and if they are late, reminders are sent. Late review notifications are generated and dispatched as mailgrams on a weekly basis.

When the reviews come in, they are examined and evaluated by the staff editor. If the reviewers do not agree on the

disposition of the paper, or if the technical and scientific strengths or shortcomings of the work have not been adequately addressed, an additional reviewer may be selected.

Copies of the reviews (at least two) and the manuscripts are sent by FAX to the editor or an associate editor, who provides oversight for the entire operation and makes final decisions about manuscript disposition. The subject matter of the manuscript determines which editor will receive the file. Although all letters are written in the editorial office, the editors examine all materials and decide on the course of action, which is then conveyed to the staff editor.

If the editor or associate editor has recommended revision of the manuscript, the staff editor goes over the paper carefully in a "pre-edit" check to aid the author in revising the manuscript.

Tips for authors of papers submitted to *ES&T*

- Prepare your paper with the audience of the publication in mind. Papers prepared for other journals are likely to need some revision to make them suitable for *ES&T*.
- Clearly state in the introduction the purpose of the work and put the work in perspective with earlier work in the area. This may appear obvious, but authors often fail to clearly state the purpose and significance of their work.
- Write concisely. The vast majority of articles are expected to be fewer than five published pages. Long manuscripts are looked at much more closely and critically both by reviewers and editors. Do not repeat information or figures or tables that have appeared elsewhere. Use illustrative data rather than complete data where appropriate.
- Suggest names of possible reviewers for your paper. You may also suggest the names of persons whom you do not want to review the paper. The editors try to use at least one reviewer who has been suggested by authors. This cannot be assured, however, since specific reviewers may not be available for reviewing or may already be overloaded.
- Follow the Current research author's guide, published in every January issue.

If your manuscript is rejected

- Read the reviews carefully. If the reviewers have "missed the point," as authors often claim, consider how the presentation can be clarified and improved to make the point clear. If reviewers have not understood, it is unlikely that readers will understand.
- Is the manuscript, after all, more suitable for another journal?
- Is the work sufficiently complete, or do you need to do more work before seeking publication?
- If you feel strongly that the paper has not been judged fairly, then carefully revise the manuscript, taking into account the reviewers' criticisms, and send the manuscript to the editorial office with a rebuttal letter asking that the manuscript be reconsidered. Provide an itemized list of changes made in the manuscript in response to reviewer comments, as well as objective rebuttals to the criticisms with which you do not agree.

Current research author's guide

This manuscript preparation guide is published to aid authors in writing, and editors and reviewers in expediting the review and publication of research manuscripts in *Environmental Science & Technology*, including full research articles and communications. For a detailed discussion with examples of the major aspects of manuscript preparation, please refer to *The ACS Style Guide* (1986).

Title

Use specific and informative titles. They should be as brief as possible, consistent with the need for defining the subject of the paper. If trade names are used, give generic names in parentheses. Key words in titles assist in effective literature retrieval.

Authorship

List the first name, middle initial, and last name of each author. Omit professional and official titles. Give the complete mailing address where work was performed. If present address of author is different, include the new information in a footnote. In each paper with more than one author, the name of the author to whom inquiries should be addressed carries an asterisk. The explanation appears on the contents page.

Abstracts

An abstract, which will appear at the beginning of each paper, must accompany each manuscript. Authors' abstracts frequently are used directly for *Chemical Abstracts*. Use between 100 and 150 words to give purpose, methods or procedures, significant new results, and conclusions. Write for literature searchers as well as journal readers.

Text

Consult a current issue for general style. Assume your readers to be professionals not necessarily expert in your particular field. Historical summaries are seldom warranted. However, documentation and summary material should be sufficient to establish an adequate background. Divide the article into sections, each with an appropriate heading, but do not oversectionalize. The text should have only enough divisions to make organization effective and comprehensible without destroying the continuity of the text. Keep all information pertinent to a particular section within that section. Avoid repetition. Do not use footnotes; include the information in the text.

Introduction. Discuss relationship of your work to previously published work, but do not repeat. If a recent article has summarized work on the subject, cite the summarizing article without repeating its individual citations.

Experimental details. Apparatus: List devices only if of specialized nature. Reagents: List and describe preparation of special reagents only. Procedure: Omit details of procedures that are common knowledge to those in the field. Brief highlights of published procedures may be included, but details must be left to literature cited. Describe pertinent and critical factors involved in reactions so that the method can be reproduced, but avoid excessive description.

Results and discussion. Be complete but concise. Avoid nonpertinent comparisons or contrasts.

Manuscript requirements

Five complete legible copies of the manuscript are required. They should be typed double or triple spaced on 22 × 28 cm paper, with text, tables, and illustrations of a size that can be mailed to reviewers under one cover. Duplicated copies will be accepted only if very clear.

If pertinent references are unpublished, furnish copies of the work or sufficient information to enable reviewers to evaluate the manuscript.

In general, graphs are preferable to tables if precise data are not required. When tables are submitted, however, they should be furnished with appropriate titles and should be numbered consecutively in Roman numeral style in order of reference in the text. Double space with wide margins, and prepare tables in a consistent form, each on a separate 22 × 28 cm sheet.

Submit original drawings (or sharp glossy photographic prints) of graphs, charts, and diagrams prepared on high-quality inking paper. All lines, lettering, and numbering should be sharp and unbroken. If coordinate paper is used, use blue cross-hatch lines because no other color will "screen out."

Typed lettering does not reproduce well: Use black India ink and a lettering set for all letters, numbers, and symbols. On 20 × 25 cm copy, lettering should be at least 0.32 cm high. Lettering on copy of other sizes should be in proportion. Label ordinates and abscissas of graphs along the axes and outside the graph proper. Do not use pressed wax for numbering or lettering.

Photographs should be supplied in glossy print form, as large as possible, but preferably within the frame of 20 × 25 cm. Sharp contrast is essential.

Number all illustrations consecutively using Arabic numerals in the order of reference in the text. Include a typed list of captions and legends for all illustrations on a separate sheet. If drawings are mailed under separate cover, identify by name of author and title of manuscript. Advise editor if drawings or photographs should be returned to the author. Color reproduction is possible provided the author bear all incremental charges. An estimate of these charges will be given upon request. A letter acknowledging the author's willingness to defray the cost of color reproduction should accompany.

Nomenclature

The nomenclature should correspond, as closely as possible, to that used by other ACS primary publications (refer to *The ACS Style Guide*).

Use consistent units of measure (preferably SI). If nomenclature is specialized, include a "Nomenclature" section at the end of the paper, giving definitions and dimensions for all terms. Write out names of Greek letters and special symbols in margin of manuscript at point of first use. If subscripts and superscripts are necessary, place them accurately. Avoid trivial names. Trade names should be defined at point of first use (registered trade names should begin with a capital letter). Identify typed letters and numbers that could be misinterpreted, for example, one and the letter "l," zero and the letter "O."

Formulas and equations

Chemical formulas should correspond to the style of ACS publications. Chemical equations should be balanced and numbered consecutively along with mathematical equations. The mathematical portions of the paper should be as brief as possible, particularly where standard derivations and techniques are commonly available in standard works.

Safety

Authors are requested to call special attention—both in their manuscripts and in their correspondence with the editors—to safety considerations such as explosive tendencies, precautionary handling procedures, and toxicity.

Acknowledgment

Include essential credits in an "Acknowledgment" section at the end of the text, but hold to an absolute minimum. Give meeting presentation data or other information regarding the work reported (for example, financial support) in a note following Literature Cited.

References

Literature references should be numbered and listed in order of reference in text. They should be listed by author, patentee, or equivalent. In the text, just the number should be used, or the name should be followed by the number. "Anonymous" is not acceptable for authorship. If the author is unknown, list the reference by company, agency, or journal source. Do not list references as "in press" unless they have been formally accepted for publication. Give complete information, using abbreviations for titles of periodicals as in the *Chemical Abstracts Service Source Index, 1907-1984*.

For periodical references to be considered complete, they must contain authors' surnames with initials, journal source, year of issue, volume number, and the first and last page

numbers of the article. Consult *The ACS Style Guide* for reference style.

Supplementary material

Extensive tables, graphs, spectra, calculations, or other material auxiliary to the printed article will be included in the microfilm edition of the journal. Identify supplementary material as to content, manuscript title, and authors. Three copies of the supplementary material, one in a form suitable for photoreproduction, should accompany the manuscript for consideration by the editor and reviewers. The material should be typed on white paper with black typewriter ribbon or printed on high quality (300 dpi) laser printer. If individual characters for any of the material, computer or otherwise, are broken or disconnected, the material is definitely unacceptable.

Figures and illustrative material should preferably be original high-contrast drawings or good prints of originals. Optimum size is 22 × 28 cm. Minimum acceptable character size is 1.5 mm. The caption for each figure should appear on the same piece of copy with the figure. Be sure to refer to supplementary material in text where appropriate.

Supplementary material may be obtained in photocopy or microfiche form at nominal cost. Material of more than 20 pages is available in microfiche only. Photocopy or microfiche must be stated clearly in the order. Prepayment is required. See instructions at the end of individual papers.

The supplementary material is abstracted and indexed by Chemical Abstracts Service.

Subscribers to microfilm editions receive, free, the supplementary material in microfiche form from individual papers in any particular issue. For information, contact Microforms Program at the ACS in Washington, D.C., or call (202) 872-4554.

Research Communications. Please refer to Editorial Policy for guidelines on research communications.

INDUSTRIAL & ENGINEERING CHEMISTRY RESEARCH



Editor Donald R. Paul *Univ. of Texas, Austin*

Quality information that gives you the leading edge

The American Chemical Society offers you the interdisciplinary research journal in the broad field of chemical engineering and industrial chemistry.

In this one professional journal you will find reports on—fundamental and theoretical aspects of chemical engineering—recent work on design methods and their applications—current and future products involving chemical engineering processes—process design and development—new technologies—special updates on timely symposia—specialty selected topics.

**Don't miss a single issue!
Subscribe TODAY!**

Volume 28 (1989) ISSN 0888-5885 CODEN: IECRED

ACS Members	U.S.	Canada & Mexico	Europe Air-service Included	All other countries. Air Service Incl.
1 Year	\$ 55	\$ 70	\$ 82	\$101
2 Years	\$ 99	\$129	\$153	\$191
Nonmember	\$321	\$336	\$348	\$367

Member rates are for personal use only. Subscriptions are based on a calendar year. Foreign payment must be made in U.S. currency by international money order, UNESCO coupons, or U.S. bank draft, or order through your subscription agency. For nonmember rates in Japan, contact Maruzan Co., Ltd. This publication is available on microfilm, microfiche, and the full text is available online on STN International.

Call Toll free in the U.S. at **1-800-227-5558** for credit card orders, or write: American Chemical Society, Marketing Communications Department, 1155 Sixteenth Street, NW, Washington, DC 20036.

Telex: 440159 ACSPUI or 892582 ACSPUBS
Cable address: JEICHEM



ENVIRONMENTAL SCIENCE & TECHNOLOGY

Enter your own monthly subscription to ES&T and be among the first to get the most authoritative technical and scientific information on environmental issues.

YES! I want my own one-year subscription to ENVIRONMENTAL SCIENCE & TECHNOLOGY at the rate checked below:

1989	U.S.	Canada & Mexico	Europe	All Other Countries
Published Monthly	<input type="checkbox"/> \$ 33	<input type="checkbox"/> \$ 43	<input type="checkbox"/> \$ 51	<input type="checkbox"/> \$ 60
ACS members:	<input type="checkbox"/> \$ 61	<input type="checkbox"/> \$ 71	<input type="checkbox"/> \$ 79	<input type="checkbox"/> \$ 88
Nonmembers-Personal	<input type="checkbox"/> \$ 212	<input type="checkbox"/> \$ 222	<input type="checkbox"/> \$ 230	<input type="checkbox"/> \$ 239
Nonmembers-Institutional				

Payment Enclosed (Payable to American Chemical Society)

Bill Me Bill Company

Charge my VISA/MasterCard

Diners Club/Carte Blanche

Card No. _____

Expires _____ Interbank No. _____ (M/C)

Signature _____

Name _____

Title _____ Employer _____

Address Home Business _____

City, State, Zip _____

Employer's Business: Manufacturing Academic Government Other _____

Member rates are for personal use only.

Subscriptions outside the U.S., Canada, and Mexico are delivered via air service.

Foreign payment must be made in U.S. currency by international money order, UNESCO coupons, or U.S. bank draft. Orders accepted through your subscription agency. For nonmember rates in Japan, contact Maruzen Co., Ltd. Please allow 45 days for your first copy to be mailed. Redeem until December 31, 1989.

680 **MAIL THIS POSTAGE-PAID CARD TODAY!** 4831R



ENVIRONMENTAL SCIENCE & TECHNOLOGY

Enter your own monthly subscription to ES&T and be among the first to get the most authoritative technical and scientific information on environmental issues.

YES! I want my own one-year subscription to ENVIRONMENTAL SCIENCE & TECHNOLOGY at the rate checked below:

1989	U.S.	Canada & Mexico	Europe	All Other Countries
Published Monthly	<input type="checkbox"/> \$ 33	<input type="checkbox"/> \$ 43	<input type="checkbox"/> \$ 51	<input type="checkbox"/> \$ 60
ACS members:	<input type="checkbox"/> \$ 61	<input type="checkbox"/> \$ 71	<input type="checkbox"/> \$ 79	<input type="checkbox"/> \$ 88
Nonmembers-Personal	<input type="checkbox"/> \$ 212	<input type="checkbox"/> \$ 222	<input type="checkbox"/> \$ 230	<input type="checkbox"/> \$ 239
Nonmembers-Institutional				

Payment Enclosed (Payable to American Chemical Society)

Bill Me Bill Company

Charge my VISA/MasterCard

Diners Club/Carte Blanche

Card No. _____

Expires _____ Interbank No. _____ (M/C)

Signature _____

Name _____

Title _____ Employer _____

Address Home Business _____

City, State, Zip _____

Employer's Business: Manufacturing Academic Government Other _____

Member rates are for personal use only.

Subscriptions outside the U.S., Canada, and Mexico are delivered via air service.

Foreign payment must be made in U.S. currency by international money order, UNESCO coupons, or U.S. bank draft. Orders accepted through your subscription agency. For nonmember rates in Japan, contact Maruzen Co., Ltd. Please allow 45 days for your first copy to be mailed. Redeem until December 31, 1989.

680 **MAIL THIS POSTAGE-PAID CARD TODAY!** 4831R

CLASSIFIED SECTION



STAFF TOXICOLOGIST

The Research and Environmental Affairs Department of Texaco, Inc. is inviting applications for a staff position in toxicology at the Corporate Research facility in Beacon, New York. The position offers a challenging opportunity to conduct health hazard evaluations for petroleum and chemical products, designing research studies and conducting environmental risk assessments. The successful candidate should have an MS or Ph.D. in Toxicology or related disciplines and demonstrated capabilities in conducting bioassays. Two to five years experience preferred.

Please send your resume in confidence to:

**Employee and
Public Relations Department
Texaco Inc.
P. O. Box 509
Beacon, N.Y. 12508**

An Equal Opportunity/Affirmative Action Employer. Applicants who are not legally authorized to work in the United States need not apply.

POSTDOCTORAL POSITION

The Division of Exposure Assessment within the Department of Environmental and Community Medicine, UMDNJ-Robert Wood Johnson Medical School, in association with the UMDNJ-Rutgers University Environmental and Occupational Health Sciences Institute, requires an individual to conduct modeling research on human exposure to pollutants from multi-media pathways, and statistical analyses of diverse databases. The work will be eventually tied into joint programs conducted by the Division and members of the Toxicology program interested in bioavailability and biomarkers. This position is associated with our new NIEHS center. Candidates should send resumes and names of references to: **Dr. Paul J. Lioy, Department of Environmental and Community Medicine, University of Medicine and Dentistry of New Jersey-Robert Wood Johnson Medical School, (EST), 675 Hoes Lane, Piscataway, NJ 08854-5635.**

The UMDNJ is an Affirmative Action/
Equal Employment Opportunity Employer M/F/H/V.



Risk Assessment Opportunities

HLA is an expanding, dynamic firm providing environmental services related to hazardous and solid waste disposal facilities and the remediation of contaminated sites. As a result of our growth, we offer exceptional opportunities in our Novato, CA location.

Environmental Toxicology

Requires 4-8 years' experience in public health and environmental risk impacts from hazardous waste sites using EPA methodologies.

Fate and Transport

Requires 4-8 years' experience with strong chemistry background and familiarity with hazardous chemical fate and transport issues.

Aquatic Toxicology

Requires 8-10 years' experience in evaluation of environmental effects of hazardous chemicals on fresh water ecosystems. Consulting engineering experience is required.

Quality and dependability are HLA traditions. They will continue to be the foundation of our professional practice. We offer competitive compensation, benefits, and a team-oriented environment. Submit resume and salary history to: HLA Staffing, Dept. CA, P.O. Box 578, Novato, CA 94948. EOE, M/F/H/V.

Harding Lawson Associates

Denver • Houston • Dallas • Phoenix • Anchorage • Honolulu • San Francisco Bay Area • Southern California • Reno • Sacramento • Princeton, NJ

ASSISTANT/ASSOCIATE PROFESSOR OZONE RESEARCH

The Division of Exposure Assessment of the Department of Environmental and Community Medicine of UMDNJ-Robert Wood Johnson Medical School in association with the UMDNJ-Rutgers University Environmental and Occupational Health Sciences Institute (EOHSI), requires an individual with research experience to develop and/or apply mathematical models on ozone chemistry with particular emphasis on applications in New Jersey. He/She will also conduct research on mechanisms and fate of ozone and other products, and provide linkages to human exposure models. Applicants should possess a Doctoral level degree, and have a record of competitive grant funding from EPA, etc. The successful candidate should have interest in training students and teaching in advanced courses within the joint UMDNJ-Rutgers University graduate programs. The position will be funded through the newly created Ozone Research Center within the EOHSI. Candidates should send curriculum vitae and three letters of reference to: **Dr. Paul J. Lioy, Department of Environmental and Community Medicine, University of Medicine and Dentistry of New Jersey-Robert Wood Johnson Medical School, (EST), 675 Hoes Lane, Piscataway, NJ 08854-5635.**

The UMDNJ is an Affirmative Action/
Equal Employment Opportunity Employer M/F/H/V.



ROUX

ROUX ASSOCIATES INC

GEOCHEMIST

Roux Associates Inc. is a rapidly growing ground-water consulting firm with offices in California and the Northeast. We specialize in the investigation and remediation of ground-water related problems for large chemical and petroleum companies.

We currently have a position open for a geochemist in our Huntington, New York office. Responsibilities include the management of sampling programs, data evaluation, report preparation and presentations to clients. Some travel would be required to assist with projects in our other offices.

Applicants must have a M.S. or a Ph.D. in chemistry or geochemistry and a minimum of three years experience with an environmental consulting firm. Salary is commensurate with qualifications.

In addition to a competitive compensation and benefits package, we offer a stimulating professional environment and exceptional career growth opportunities.

Please send your resume and salary requirements, in confidence, to William Sarni at:

ROUX ASSOCIATES INC

The Huntington Atrium
775 Park Avenue, Suite 255
Huntington, NY 11743



(800) 227-5558 (U.S. only)



NO POSTAGE
NECESSARY
IF MAILED
IN THE
UNITED STATES

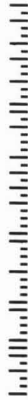
BUSINESS REPLY MAIL

FIRST CLASS PERMIT NO. 10094 WASHINGTON, D.C.

POSTAGE WILL BE PAID BY ADDRESSEE

American Chemical Society

Marketing Communications Department
1155 Sixteenth Street, N.W.
Washington, D.C. 20077-5768



(800) 227-5558 (U.S. only)



NO POSTAGE
NECESSARY
IF MAILED
IN THE
UNITED STATES

BUSINESS REPLY MAIL

FIRST CLASS PERMIT NO. 10094 WASHINGTON, D.C.

POSTAGE WILL BE PAID BY ADDRESSEE

American Chemical Society

Marketing Communications Department
1155 Sixteenth Street, N.W.
Washington, D.C. 20077-5768



CLASSIFIED SECTION

HAZARDOUS WASTE PROFESSIONALS

EBASCO is an Industry Leader in Engineering, Construction and Environmental Consulting. We are seeking Hazardous Waste Professionals at all levels throughout our Western Regional Operations.

We are particularly interested in **Group Leaders and Project Managers** with experience in Hazardous Waste Remedial Design. State registration (CE) and Construction experience is highly desirable.

Our Western offices are in Anchorage, Alaska; Bellevue, Washington; Denver, Colorado; Sacramento, San Francisco and Santa Ana, California.

Please send resume and location preference to:

R. D. Roda
Regional Administrator
Personnel & Services
EBASCO SERVICES INC.
3000 W. MacArthur Blvd.
Santa Ana, CA 92704

An Equal Opportunity
Employer M/F/H/V

EBASCO

An ENSECH Engineering and Construction Company

ENVIRONMENT/ENERGY. Energy Resource Administrator, State of Maryland, Power Plant & Environmental Review Division. Unclassified position. Performs engineering, economic, and environmental evaluations of existing and future power plants. Advanced degree required (Ph.D. preferred, Master's degree plus experience equivalent to doctorate may be acceptable) in a physical or life science or engineering discipline. Training or experience in one of the following areas is desirable: energy supply, applied ecology, engineering, physics, mathematics, and earth sciences as it relates to the power or energy industry. Candidates should demonstrate substantial administrative or managerial experience and detailed familiarity with relevant environmental regulations. Complete State Benefit Package; location: Annapolis, MD. Salary \$37,868 to \$49,790, commensurate with qualifications. Apply (with resume, technical writing sample, and names and current phone numbers of three references) before 15 January 1989 to James M. Telt, Director, Power Plant and Environmental Review Division, Tawes State Office Building (B-3), Annapolis, MD 21401. Minority applicants are encouraged to apply. The State of Maryland is an equal opportunity employer.

USDA, Agricultural Research Service, U.S. Salinity Laboratory, Riverside, California, has opening for interdisciplinary: Agricultural Engineer, Soil Scientist, Hydrologist, GS-11/12, to plan, conduct, and report research related to the transport of water and dissolved constituents in saturated-unsaturated soils. Serves as a member of a team of scientists developing integrated models predicting the behavior of salts and toxic elements in irrigated and non-irrigated agricultural soils. Objectives of the research is to quantify the basic physical, chemical and biological processes controlling the movement of water, salts and toxic substances in the subsurface, and to develop models for predicting water flow and solute transport in and below the root zones of the salt-affected soils. Applicants must need specific educational requirements and professional experience directly related to position. Ph.D. or equivalent in soil science, soil physics, hydrology, agricultural engineering, or related field, is desired. Must be U.S. citizen. GS-11/12. Salary range: \$27,716-\$43,181 per annum, commensurate with qualifications and experience. For program questions, please contact Dr. Rien van Genuchten, USDA-ARS, U.S. Salinity Laboratory, 4500 Glenwood Drive, Riverside, California 92501 (714-369-4847). For qualification requirements and application procedures, please contact Cathleen Emuto, USDA-ARS Personnel Division, Room 403, Bldg. 003, BARC-West, Beltsville, MD 20705 (301-344-3138). Applications must be postmarked by January 13, 1989. Applications must be coded 9W010.

GRADUATE STUDY in ENVIRONMENTAL SCIENCE AND ENGINEERING at Oregon Graduate Center. Highly qualified, motivated students sought for aggressive research in transport and fate of organic and inorganic contaminants, atmospheric chemistry and physics, aquifer remediation, microbial ecology and physiology, biodegradation, biogeochemistry, analytical environmental chemistry, numerical modeling, estuarine and coastal studies, elemental cycling in terrestrial ecosystems. Intensive research experience, state-of-the-art instrumentation, maximal student-faculty interaction. Assistantships with tuition remission available to qualified Ph.D. applicants. Write: Carl D. Palmer, ES&E, OGC, 19600 N.W. von Neumann Dr., Beaverton, OR 97006, (503)-690-1197.

ENVIRONMENTAL ORGANIC GEOCHEMIST

PTI Environmental Services, a west coast consulting firm, seeks an individual with a graduate degree in chemistry, chemical oceanography, or a related environmental science with experience in analytical organic chemistry (knowledge of EPA/CLP procedures desirable) and organic geochemistry (transport and fate of organic compounds in aquatic systems). Excellent writing and speaking skills are essential. Responsibilities will include geochemical data analysis and interpretation, and specialized QA/QC reviews. Send resume and salary requirements to: **PTI Environmental Services, Attn: TG/11/88/EST, 3625 132nd Ave. S.E., Suite 301, Bellevue, WA 98006.** EOE.

USDA, Agricultural Research Service, U.S. Salinity Laboratory, Riverside, California, has opening for Interdisciplinary: Soil Scientist/Chemist/Geoquatic Chemist/Chemical Oceanography/Environmental Chemist, GS-11/12, to plan, conduct, and report research related to: 1) developing a quantitative understanding of the chemical-organic complexation processes that control the reactions and mobility of trace elements in saline, irrigated soils for purposes of preventing or minimizing ground water pollution with trace elements from irrigated agriculture, and 2) establishing the influence of organics on clay dispersion, aggregation and permeability of sodic soils. Must be able to cooperate and communicate with other project scientists in related areas of soil/water chemistry and physics in order to carry out this team-oriented research. Summary Qualifications: BS or higher degree in one of the physical or life sciences with specific course requirements or equivalent combination of education/experience plus 3 years of professional experience. Applicants must need specific educational requirements and professional experience directly related to position. Desired: Ph.D. or equivalent in Soil Science, Geoquatic Chemistry, Chemical Oceanography or Environmental Chemistry with courses in organic and physical chemistry. Must be U.S. citizen. Salary is \$27,716-\$36,032 for GS-11 and \$33,218-\$43,181 per annum for GS-12, commensurate with qualifications and experience. For information on program, contact Dr. James D. Rhoades, (714) 369-4816, Research Leader, U.S. Salinity Laboratory, 4500 Glenwood Drive, Riverside, California 92501. Contact Cathleen Emuto, (301) 344-3138 for qualification requirements and application procedures, or write to her at USDA-ARS-Personnel Division, Room 403, Bldg. 003, BARC-West, Beltsville, MD 20705. An Equal Opportunity Employer. Applications must be postmarked by January 23, 1989. Applications must be coded 9W012.

CLASSIFIED ADVERTISING RATES

Rate based on number of insertions used within 12 months from date of first insertion and not on the number of inches used. Space in classified advertising cannot be combined for frequency with ROP advertising. Classified advertising accepted in inch multiples only.

Unit	1-T	3-T	6-T	12-T	24-T
1 inch	\$105	\$100	\$95	\$90	\$85

(Check Classified Advertising Department for rates if advertisement is larger than 10".)

SHIPPING INSTRUCTIONS: Send all material to

**Environmental Science & Technology
Classified Advertising Department**
500 Post Road East
P.O. Box 231
Westport, CT 06881
(203) 226-7131

USE THE CLASSIFIED SECTION

CLASSIFIED ADVERTISING RATES

Rate based on number of insertions used within 12 months from date of first insertion and not on the number of inches used. Space in classified advertising cannot be combined for frequency with ROP advertising. Classified advertising accepted in inch multiples only.

Unit	1-T	3-T	6-T	12-T	24-T
1 inch	\$105	\$100	\$95	\$90	\$85

(Check Classified Advertising Department for rates if advertisement is larger than 10".)

SHIPPING INSTRUCTIONS:

Send all material to

**Environmental Science &
Technology
Classified Advertising
Department
500 Post Road East
P.O. Box 231
Westport, CT 06881
(203) 226-7131**

Environmental Scientists and Engineers

Positions open at all levels: recent B.S. graduates with excellent academic record to Ph.D. with 10+ years' relevant experience. Degrees should be in Environmental or Civil Engineering, Chemistry, Toxicology, Public Health or related disciplines. Course work or expertise in some of the following technical areas is required:

- Exposure and risk assessment/human health and ecological studies
- Computer skills in data bases, spreadsheets, graphics, GIS
- Aquatic/environmental chemistry
- Multimedia chemical transport and fate modeling/air dispersion modeling

Prior consulting or agency experience is a plus. These positions require highly technical work and offer rapidly increasing management responsibility. Focus of the work is on chemical data interpretation related to hazardous waste sites, sanitary landfills, resource recovery plants, industrial and occupational settings. Studies are conducted for a national clientele which is a balance of private and public sectors. **Please send resumes to:**

Gradient Corporation

44 Brattle Street, Cambridge, MA 02138

Environmental Health

The Program in Social Ecology at the University of California, Irvine is recruiting for an assistant professor, tenure track, position in the area of Environmental Health. Applicants should have received a Ph.D. in environmental sciences, organic chemistry, molecular genetics or biochemistry. The successful candidate will have demonstrated experience in laboratory or field research related to environmental health sciences. Ability to teach statistics and environmental testing methodology is desirable.

The Program in Social Ecology grants B.A., M.A., and Ph.D. degrees. The 30 full-time faculty have multidisciplinary interests and expertise in environmental sciences, public health, demography, urban planning, environmental law, human development, and environmental psychology. The Social Ecology Building houses four laboratories: air pollution monitoring, water quality, microbial ecology and bioremediation laboratory, radiocarbon dating and environmental chemistry laboratory, a full-scale Environmental Simulation Laboratory, and an ultraclean room is under construction.

Candidates should submit a letter of application, curriculum vitae, and names of 3 referees to:

**Dr. Betty H. Olson
Environmental Health Search Committee
Program in Social Ecology
University of California
Irvine, CA 92717**

Closing date for applications is January 15, 1989. The University of California is an Equal Opportunity/Affirmative Action Employer.

ENVIRONMENTAL/CIVIL ENGINEERS

NATIONWIDE opportunities available in: **Water Quality, Solid and Hazardous Waste Management, Toxicology, Hydrogeology and Geotechnology.** All Fees employer paid. Contact: **James E. Iannoni & Assoc., P.O. Box 66, Hampton, CT 06247 (203) 455-0151.**

ENVIRONMENTAL ENGINEERING INDUSTRIAL HYGIENE

Positions of responsibility are available in several geographic locations. Well established consulting firm with a solid growth plan needs experienced engineers, scientists, and C.I.H.'s. Opportunities in real estate environmental audit, GC mass spec operations (Finnegan), asbestos program management, environmental, I.H. and ecological section leaders; environmental field engineers and technicians. Priority consideration given to candidates for Branch Manager and Department Manager positions.

Submit resume and salary history to **W. G. Sublette, Environmental Protection Systems, 100 Galleria Parkway, Suite 1000, Atlanta, Ga., 30080** for confidential consideration.

SENIOR FACULTY POSITION IN ENVIRONMENTAL SCIENCES, UNIVERSITY OF CALIFORNIA, LOS ANGELES.

Faculty Position in Environmental Science and Engineering, School of Public Health. Upper level tenure-track appointment in the Interdepartmental Environmental Science and Engineering Program and, jointly, in the Division of Environmental and Occupational Health Sciences. The candidate should have the potential to be director of the ESE program. Research and teaching in an environmentally pertinent area of biology, microbiology, chemistry, biochemistry, as broadly defined. The ESE Program emphasizes the relationship between science and public policy, so a demonstrated interest in this relationship plus an outstanding record of research in a specialized area is required. Opportunity to participate in the M.S. and Ph.D. training programs of the Division and for interaction with engineers and basic scientists from other departments such as Biology, Microbiology, Biological Chemistry, Chemistry, Engineering, Earth Sciences, etc. Send curriculum vitae, statement of research and teaching goals, and names of three references by March 15, 1989 to: Robert A. Mah, Chair, ESE Search Committee, School of Public Health, UCLA, Los Angeles, CA 90024. UCLA is an affirmative action, equal opportunity employer. Women and minorities are encouraged to apply.


professional consulting services directory

Cenref Labs

BRIGHTON CO. (303) 659-0497
(800) 634-0497
LIBERAL, KS (316) 624-4292

ENVIRONMENTAL TESTING

Priority Pollutants • PCB's
RCRA Hazardous Waste Analyses
Drinking Water • Wastewater
Pesticides • Sludge • CLP
Engine Emission Monitoring



**GERAGHTY
& MILLER, INC.**
Ground-Water Consultants

125 East Bethpage Road
Plainview, New York 11803
(516) 249-7600
Offices Located Nationwide

CONSULTING GROUND WATER
GEOLOGISTS AND ENGINEERS

ROUX ASSOCIATES INC

THE HUNTINGTON ATRIUM
775 PARK AVENUE, SUITE 255
HUNTINGTON, NEW YORK 11743
516 673-7200

CHERRY HILL NEW JERSEY 609 424-3993
EAST GRANBY CONNECTICUT 203 653-8021
CONCORD CALIFORNIA 415 686-8747

WARNING SYSTEM SERVICES

PLANNING AND EVALUATION OF
EMERGENCY WARNING SYSTEMS

David N. Keast
Principal Consultant

657 Westford Street
Carlisle, MA 01741
(617) 369-8872 (Area Code 508 after July 16, 1988)

THE CONSULTANT'S DIRECTORY

UNIT	Six Issues	Twelve Issues
1" X 1 col.	\$60	\$55
1" X 2 col.	115	105
1" X 3 col.	170	145
2" X 1 col.	115	105
2" X 2 col.	210	190
4" X 1 col.	210	190

ENVIRONMENTAL
SCIENCE &
TECHNOLOGY
500 Post Road East
P.O. Box 231
Westport, CT 06881

ANSARA, BICKFORD & FISKE
RECRUITMENT COUNSEL TO
The Environmental / Chemical Industry

We have successfully advanced the careers of the following Environmental & Chemical professionals through our nationwide relationship with hundreds of quality firms: Chemists "GC, AA, ECT." • Remediation Specialists • Water Supply Engineers • Risk Assessment Specialists • Waste Water Engineers • Toxicologists • Industrial Hygienists • Landfill Specialists • Chemical Specialist • Hydrogeologists • Environmental Marketing • Air Monitoring Specialists • Hazardous Waste Specialists • Many Project Manager Positions

Submit your resume to:
Peter Ansara
c/o Ansara, Bickford & Fiske
P.O. Box 239, 1111 Elm St.
West Springfield, MA 01090
Client companies assume all fees. Confidentiality assured. (413) 733-0791 / Fax(413) 731-1486



INDEX TO THE ADVERTISERS IN THIS ISSUE

ADVERTISERS	PAGE NO.	Advertising Management for the American Chemical Society Publications	Westport, Ct. Edward M. Black, CENTCOM, LTD., 500 Post Road East, P.O. Box 231, Westport, Ct 06880 (Area Code 203) 226-7131
American Society for Testing and Materials	OBC	CENTCOM, LTD. <i>President</i> Thomas N. J. Koerwer <i>Executive Vice President</i> James A. Byrne <i>Senior Vice President</i> Benjamin W. Jones <i>Clay S. Holden, Vice President</i> Robert L. Voepel, Vice President Joseph P. Stenza, Production Director 500 Post Road East P.O. Box 231 Westport, Connecticut 06880 (Area Code 203) 226-7131 Telex No. 643310 Fax No. (203) 454-9939	Cleveland, OH. John Guyot, CENTCOM, LTD., 325 Front St., Berea, OH 44017 (Area Code 312) 234-1333
Brookhaven National Laboratory	OBC	ADVERTISING SALES MANAGER Bruce Poorman	Chicago, Ill. Michael J. Pak, CENTCOM, LTD., 540 Frontage Rd., Northfield, Ill 60093 (Area Code 312) 441-6383
Lockheed Missiles & Space Co.	IFC	ADVERTISING PRODUCTION MANAGER Jay S. Francis	Houston, Tx. Michael J. Pak, CENTCOM, LTD., (Area Code 312 441-6383)
		SALES REPRESENTATIVES	San Francisco, Ca. Paul M. Butts, CENTCOM, LTD., Suite 1070, 2672 Bayshore Frontage Road, Mountainview, CA 94043 (Area Code 415) 969-4604
		Philadelphia, Pa. Patricia O'Donnell, CENTCOM, LTD., GSB Building, Suite 405, 1 Belmont Ave., Bala Cynwyd, Pa. 19004 (Area Code 215) 667-9666	Los Angeles, Ca. Clay S. Holden, CENTCOM, LTD., 3142 Pacific Coast Highway, Suite 200, Torrance, CA 90505 (Area Code 213) 325- 1903
		New York, N.Y. Patricia O'Donnell, CENTCOM, LTD., 60 E. 42nd Street, New York 10165 (Area Code 212) 972-9660	Boston, Ma. Edward M. Black, CENTCOM, LTD., (Area Code 203) 226-7131
			Atlanta, Ga. Edward M. Black, CENTCOM, LTD., (Area Code 203) 226-7131
			Denver, Co. Paul M. Butts, CENTCOM, LTD., (Area Code 415) 969-4604

Choosing a graduate school?

Need to know who's doing research critical to yours?

*New edition
just published!*

The ACS Directory of Graduate Research 1987

All the information you need on chemical research and researchers at universities in the U.S. and Canada . . . in a single source.

Includes listings for chemistry, chemical engineering, biochemistry, pharmaceutical/medicinal chemistry, clinical chemistry, and polymer science.

Lists universities with names and biographical information for all faculty members, their areas of specialization, titles of all papers published within last two years, and individual telephone numbers.

Provides a statistical summary of academic chemical research—with information by department on numbers of full- and part-time faculty, postdoctoral appointments, graduate students, and M.S. and Ph.D. degrees granted.

What you'll find inside . . .

. . . information on . . .

- 668 academic departments
- 11,569 faculty members
- 62,591 publication citations

. . . listings for . . .

- chemistry
- chemical engineering
- biochemistry
- pharmaceutical/medicinal chemistry
- clinical chemistry
- polymer science

1345 pages (1987) Clothbound

Price:

US & Canada **\$50.00**

Export **\$60.00**

No academic institution or chemically oriented business can afford to be without the ACS Directory of Graduate Research 1987! Order today by calling toll free (800) ACS-5558 or using the coupon below.

Please send me _____ copy(ies) of the ACS Directory of Graduate Research 1987.
Price: U.S. & Canada \$50.00, Export \$60.00

Payment enclosed (make checks payable to American Chemical Society).

Purchase order enclosed. P.O. # _____

Charge my: MasterCard/VISA American Express Access Barclaycard
 Diners Club/Carte Blanche

Account # _____

Expires _____ Interbank # (MC and ACCESS) _____

Name of cardholder _____ Phone # _____

Ship books to:
Name _____

Address _____

City, State, Zip _____

ORDERS FROM INDIVIDUALS MUST BE PREPAID. Prepaid and credit card orders receive free postage and handling. Please allow 4-6 weeks for delivery.

Mail this order form with your payment or purchase order to:
American Chemical Society, Distribution Office, Dept. 705,
P.O. Box 57136, West End Station, Washington, DC 20037.

New Titles

from the
American
Chemical
Society

It's the Good Book!

Biotechnology and Materials Science Chemistry for the Future

Biotechnology and materials science—two different fields unified through the science of chemistry. Now you can get a better understanding of these two disciplines and their tremendous impact on technology. This new book presents discussions of exciting advances by outstanding researchers in these pivotal fields. Learn the history behind present-day biotechnology and see where advances are predicted. Look at the progress being made in new recombinant DNA technology and materials produced by high-technology. Written in non-technical language, this 11-chapter book is beautifully illustrated in full color. Scientist and non-scientist alike will find this book both informative and enjoyable.

Mary L. Good, Editor

Jacqueline K. Barton, Associate Editor

135 pages (1988)

Cloth: US & Canada **\$24.95** Export **\$29.95**

ISBN 0-8412-1472-7

Paper: US & Canada **\$14.95** Export **\$17.95**

ISBN 0-8412-1473-5

New edition of the ACS best-seller!

Cancer: The Outlaw Cell Second Edition

Completely revised and updated! This new book consists of articles on the most promising research and clinical treatment from leading scientists in the field. Special emphasis is on the basic concepts for biology and medicine, new developments, and an appraisal of advances in non-surgical modes of therapy used in treatment. Beginning with an overview, this 14-chapter book includes subjects such as the genetic basis of cancer, cancer and the immune response, angiogenesis, and immunotherapy. *Cancer: The Outlaw Cell* is an easy-to-understand book for anyone interested in cancer research and medicine.

Richard E. LaFond, Editor

306 pages. (1988)

Cloth: US & Canada **\$29.95** Export **\$35.95**

ISBN 0-8412-1419-0

Paper: US & Canada **\$19.95** Export **\$23.95**

ISBN 0-8412-1420-4

How to use statistics in research...

Practical Statistics for the Physical Sciences

Learn how to get the information you need from research data with this dynamic new book on statistical procedures. Written in understandable, easy-to-follow steps, this book teaches you the concepts underlying the use of statistics in research. Worked-out examples are provided to illustrate each procedure, and commonly-used formulas, tables, and reference information are also included. No prior knowledge of statistics is necessary to use this practical "how-to" book. *Practical Statistics for the Physical Sciences* is a comprehensive reference—vital to anyone who works with statistical data.

Larry L. Havlicek and **Ronald D. Crain**

522 pages. Cloth. (1988)

US & Canada **\$59.95** Export **\$71.95**

ISBN 0-8412-1453-0

Implementing a GLP program...

Good Laboratory Practices An Agrochemical Perspective

Requirements for good laboratory practices (GLP) are here to stay! Learn how to implement a GLP program that meets federal standards with this new book. You'll get an overview of good laboratory practices from EPA, academic, and industrial perspectives. You'll become familiar with current practices, probable changes, what needs to be done, why, and how to do it. With 19 chapters, this book will give you a better understanding of GLP standards with regard to compliance, quality assurance, and standard operating procedures. Also included is the text of the proposed FIFRA Generic Good Laboratory Practices Standards. An excellent guide for anyone involved in the implementation of a GLP program.

Willa Y. Garner and **Maureen Barge**, Editors

ACS Symposium Series 369

168 pages. Cloth. (1988)

US & Canada **\$39.95** Export **\$47.95**

ISBN 0-8412-1480-8

Send your purchase order or payment to **American Chemical Society, Distribution Office Dept. 147, P.O. Box 57136, Washington, DC 20037.** Or call toll-free **(800) 227-5558.**

Photooxidation of Probe Compounds Sensitized by Crude Oils in Toluene and as an Oil Film on Water

Rainer G. Lichtenhaler[†]

Senter for Industriforskning, P.O. Box 350 Blindern, 0314 Oslo 3, Norway

Werner R. Haag* and Theodore Mill

Chemistry Laboratory, SRI International, Menlo Park, California 94025

■ The effect of crude oil residues on the photolyses of a variety of model crude oil components in toluene was studied. 3,6-Dimethylphenanthrene and dibenzothiophene photolyses were not sensitized, but rather were slower at high residue concentrations due to light screening. 2,6-Di-*tert*-butyl-4-methylphenol was used as a probe for peroxy radicals; a wavelength-averaged quantum yield of 0.002 was estimated for a crude oil diluted with toluene. Di-*n*-butyl sulfide, tetramethylethylene, and α -terpinene were used as probes for singlet oxygen both in toluene solution and in pure oil films on water. Singlet oxygen quantum yields were estimated to range from 0.5 to 0.8 at 366 nm for a variety of crude oils in toluene. In pure films on water, apparent quantum yields were 3 orders of magnitude lower, but $^1\text{O}_2$ concentrations in sunlight were still high enough to oxidize reactive compounds such as alkylated olefins and alkyl sulfides on a time scale of minutes to hours. The present results suggest that $^1\text{O}_2$ is not a significant source of peroxy radicals, and therefore, direct photolytic initiation must be involved. Equations are presented for estimating singlet oxygen and peroxy radical quantum yields by use of actinometers that are consumed in first-order fashion.

Introduction

The fate of crude oil compounds released to the aqueous environment is of concern because of their acute and chronic harmful effects on ecological systems. These effects include direct toxicity, phototoxicity of biosorbed compounds (1, 2), and formation of toxic peroxidic products by photolysis (3, 4).

A complex sequence of events occurs following an oil spill to a water surface (5): (1) The oil spreads rapidly to produce nonhomogeneous films of <0.01–3 mm thickness. (2) Volatile components rapidly evaporate leaving behind only compounds of boiling point greater than ~250 °C. (3) A small fraction dissolves into the water. (4) Photooxidation produces polar and partly mutagenic peroxidic products, which tend to partition into the aqueous phase. (5) Water-in-oil emulsions form, causing an increase in viscosity and stabilization of the film. (6) After significant

oxidation, dispersion, or dilution, insoluble refractory materials form aggregates and remain floating or slowly sink.

Photolytic decomposition of crude oils and formation of toxic products has been attributed to direct photolysis, singlet oxygenation, and radical oxidation, but the relative importance of these pathways has not been quantified (3–6). Larson and Hunt (3, 6) proposed that peroxides are initially formed by $^1\text{O}_2$ reactions and then photolyze to initiate radical chains. They demonstrated that β -carotene inhibits the formation of peroxides and suggested tentatively that this was due to quenching of singlet oxygen; however, one cannot rule out the possibility that radical pathways were also quenched.

Crude oils vary in composition, but they generally consist of about 75% aliphatics and 25% aromatics; a majority of these can be organic sulfur compounds if sulfur content is high (range <1%–14%) (3, 5, 7). Lesser amounts of phenols and nitrogen-containing compounds are also present (5, 8). These different components are expected to photooxidize by different pathways. We describe below experiments using a variety of substrates as probes to estimate the relative importance of direct photolysis, oxy radical oxidation, and singlet oxygenation in the presence of crude oil residues in dilute solution. An effort is made to extrapolate the results to the optically thick conditions found in most oil slicks in the environment.

Experimental Procedures

Materials. All chemicals were reagent grade or better, obtained from commercial sources. Crude oil samples were received from various oil companies and distilled under vacuum to yield straight run residues with bp ≥ 360 °C at 1 atm. In the case of oil-film-on-water experiments, a less viscous residue (Ekofisk; bp ≥ 210 °C) was used to allow rapid spreading on the water surface. Arabian Heavy residue was separated into maltenes (*n*-hexane-soluble fraction, 91.5% by weight) and asphaltenes (8.5% by weight) by standard methods (9).

Photolyses. Toluene solutions (5 mL) of acceptor compounds, with or without sensitizers (total residue, maltenes, or asphaltenes), in 12-mm-o.d. borosilicate glass tubes were irradiated in a carousel with 366 ± 40 nm light generated and filtered (glass plates) from a 400-W medi-

[†]Present address: Norwegian Institute for Water Research, P.O. Box 333 Blindern, 0314 Oslo 3, Norway.

Table I. Effect of Arabian Heavy Residues and Methylene Blue on the Photolyses of Various Model Crude Oil Components

compd (μM)	sensitizer ^a (mg/L)	α_{350} , cm^{-1}	solvent	$10^5 k_{\text{expt}}$, s^{-1}	lamp
DMP (100)	none		toluene	2.7	Hg
	asph (3.44)	0.1		2.7	
	asph (138)	6		0.0	
	malt (24.4)	0.1		2.4	
	malt (2440)	10		0.0	
	none		98:2 tol/MeOH	0.0	Xe ^b
DBT (100)	m. blue (4.2)			≤ 0.5	
	none		toluene	21	Xe
	none		hexane	7.7	
	malt (97.5)	0.4		5.4	
	none		99:1 hex/MeOH	7.7	
DBS (500)	malt (97.5)	0.4		5.4	
	none		toluene	≤ 0.8	Hg
	asph (3.44)	0.1		3.2	
	malt (24.4)	0.1		8.6	
	none		98:2 tol/MeOH	6	Xe ^b
TME (100)	m. blue (4.2)			110	
	none		toluene	≤ 52	Xe
	malt (32.5)	0.1		1340	
α -terp (100)	none		toluene	≤ 85	Xe
	malt (32.5)	0.1		2170	
BHT (100)	none		toluene	$\sim 14^c$	Xe
	malt (32.5)	0.1		46	
	asph (2.86)	0.1		38.5	
	tot res (13.5)	0.1		38.0	
	malt (32.5)	0.1	benzene	53	
tetralin (500)	none		hexane	0.43	Xe
	malt (32.5)	0.1		1.2	
	none		benzene	0.4	
	malt (32.5)	0.1		0.4	
	malt (32.5)	0.1	toluene	0.0	

^a Abbreviations: asph, asphaltenes; malt, maltenes; tot res, total residue; m. blue, methylene blue; hex, *n*-hexane; tol, toluene. ^b With $\text{K}_2\text{Cr}_2\text{O}_7$ filter to remove light below 550 nm. ^c 1 mM BHT.

um-pressure mercury lamp (10).

Sunlight-simulating irradiations were performed by holding the tubes stationary 30 cm in front of a 350-W xenon lamp. The intensity reaching the tubes was ~ 5 times that of noon, summer, 38°N sunlight as measured by an EG&G ElectroOptics 460-1A laser power meter equipped with a 460-2 silicon detector (300–1000 nm), or ~ 3 times greater as measured by *p*-nitroacetophenone/pyridine actinometry (10) in borosilicate glass (300–400 nm). Filters for removing light from the xenon lamp below 400 nm consisted of 8 cm of 0.05 M NaNO_2 , and for removing that below 550 nm, 8 cm of 0.14 M $\text{K}_2\text{Cr}_2\text{O}_7$. In the case of optically thick solutions irradiated with the xenon lamp, magnetic stirring was applied to achieve uniform photolysis.

Tests for oxygen dependence of photolyses were performed by purging solutions for ca. 5 min with oxygen or nitrogen. A fan kept the tube temperature at $28 \pm 3^\circ\text{C}$.

Photolyses in sunlight were carried out on petroleum films prepared by allowing 0.5 mL of residue to spread on a 2-cm-deep layer of water in a 6.5-cm-i.d. glass Petri dish, which was wedged in a cork ring and floated in a bucket of water for cooling. The oil formed a circular film with a diameter of 4.0 cm, resulting in an average thickness of 0.44 mm and total sunlight absorbance up to ~ 700 nm.

Analyses. At appropriate time intervals, samples were analyzed by GLC/FID using a 12-m methyl polysiloxane coated capillary column. Internal standards, added after irradiations, were chosen to elute close to acceptor compounds. In film experiments, *n*-nonadecane, already present in the oil, served as internal standard. No loss of nonadecane was observed during the 5-min sunlight exposures performed here, in contrast to the photooxidation of hexadecane reported by Tjessel et al. (11) during week-long irradiations. The film was sampled by inserting

a glass capillary tube and taking up the adhering residue in 10–15 μL of chloroform.

Data Evaluation. In all cases, data were fitted to a first-order regression by plotting the log of the relative concentration versus time and obtaining the experimental rate constant (k_{expt}) from the slope. Losses of 2,6-di-*tert*-butyl-4-methylphenol (BHT) were also treated as zero-order kinetics by plotting concentration versus time. Generally excellent first-order behavior was observed, except for BHT which exhibited an order between zero and one. All rate constants are reported in units of s^{-1} (and M s^{-1} for BHT) and have estimated 95% confidence intervals of $\pm 15\%$.

Results and Discussion

Effect of Residues on Photolyses. Table I shows the effect of Arabian Heavy residues on the solution photolyses of several model acceptor compounds (A) similar to those which might be present in crude or refined oil and which were expected to be selective for the various photooxidative processes. Abbreviations are as follows: 3,6-dimethylphenanthrene (DMP), dibenzothiophene (DBT), di-*n*-butyl sulfide (DBS), tetramethylethylene (TME), α -terpinene (α -terp), 2,6-di-*tert*-butyl-4-methylphenol (BHT), and tetralin (tetr). The residues had no sensitizing effect on the photolyses of DMP or DBT but, rather, caused inhibition at high residue concentrations where light screening became important. Thus, to a first approximation, the photolyses of such compounds will occur by direct light absorption in an oil film. Using *p*-nitroacetophenone/pyridine actinometry (10), we estimate a direct photolysis quantum yield of 0.003 ± 0.001 at 366 nm for DMP in toluene, uncorrected for the differences in refractive indexes of the solvents. The remaining compounds absorb little light at wavelengths above 300 nm,

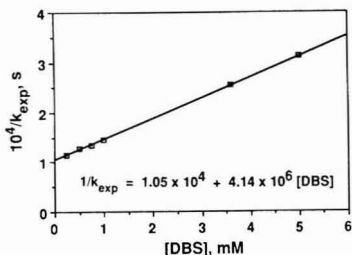
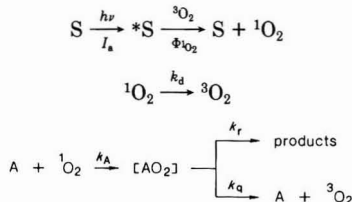


Figure 1. Stern-Volmer plot of DBS photooxidation sensitized by maltenes.

and their photolyses occur predominantly by sensitized processes.

Tests for $^1\text{O}_2$ Intermediacy. Singlet oxygen reaction kinetics may be visualized by the following scheme:



where I_a is the rate of light absorption in einstein $\text{L}^{-1} \text{s}^{-1}$ and $\Phi_{^1\text{O}_2}$ is the quantum yield of $^1\text{O}_2$ formation (for theoretical discussion see ref 12-15). The rate of and rate constant for loss of acceptor A are

$$-d[\text{A}]/dt = I_a \Phi_{^1\text{O}_2} [k_r[\text{A}]/(k_d + k_A[\text{A}])] \quad (1)$$

$$k_{\text{exptl}} = I_a \Phi_{^1\text{O}_2} [k_r/(k_d + k_A[\text{A}])] \quad (2)$$

Experiments are preferably run at low $[\text{A}]$, where $k_A[\text{A}] \ll k_d$, yielding $k_{\text{exptl}} = I_a \Phi_{^1\text{O}_2} (k_r/k_d)$, and first-order behavior is observed.

Products. DBS photooxidized in toluene in the presence of maltenes or residue to give nearly quantitative yields of di-*n*-butyl sulfoxide and small amounts of sulfone. This is supportive of a $^1\text{O}_2$ mechanism (16); oxy radical attack would be expected to occur at a C-H bond. However, other processes could also account for this result, such as oxidation by hydroperoxides.

Oxygen and Sensitizer Dependence. At low sensitizer concentration ($<50 \text{ mg/L}$ maltenes), the rate of DBS photooxidation was unaffected by purging with O_2 but totally inhibited under N_2 , as required for either oxy radical oxidation or singlet oxygenation. This excludes direct triplet sensitizer reactions (17). Methylene blue, a known $^1\text{O}_2$ sensitizer, had a profound accelerating effect (Table I).

DBS Self-Inhibition. Figure 1 is a Stern-Volmer plot (inverse of eq 2) for self-inhibition by DBS, using initial rates to determine k_{exptl} . It yields a value of 395 ± 8 for k_A/k_d from the slope/intercept. Taking $k_d = 3.7 \times 10^4 \text{ s}^{-1}$ for toluene (13), we calculate $k_A = 1.5 \times 10^7 \text{ M}^{-1} \text{ s}^{-1}$ for DBS in this solvent, in reasonable agreement with literature values of 1.0×10^7 and $1.4 \times 10^7 \text{ M}^{-1} \text{ s}^{-1}$ in CHCl_3 and MeOH , respectively (13, 18) [the latter value being corrected to $k_d = 1.0 \times 10^5 \text{ s}^{-1}$ in MeOH (12, 13)]. Thus, good evidence is obtained that maltene sensitization of DBS photolysis occurs via $^1\text{O}_2$.

Solvent Isotope Effect. $^1\text{O}_2$ reactions are generally much faster in deuterated solvents than in the corresponding protonated solvents because the former quench $^1\text{O}_2$ more slowly (12, 13). The ratio of experimental rate

Table II. Deuterium Isotope Effect on Maltene-Sensitized Photolysis Rate Constants for DBS and BHT^a

compd	concn, μM	solvent	$10^4 k_{\text{exptl}}, \text{s}^{-1}$	$k^{\text{D}}/k^{\text{H}}$	
				exptl	calcd ^b
DBS	100	benzene	5.8	13.3	13.5
		benzene- d_6	77		
	500	benzene	5.8	3.7	5.6
		benzene- d_6	15.6 ^c		
	100	toluene	5.3	8.1	8.3
		toluene- d_8	43		
500	toluene	5.3	2.1	4.2	
	toluene- d_8	11 ^c			
BHT	100	toluene	4.6	1.9	11.7
		toluene- d_8	8.9		

^a Irradiated in Xe lamp in presence of 32.5 mg/L Arabian Heavy maltenes. ^b Calculated as by eq 3 by using $k'_d = 1.4 \times 10^5 \text{ s}^{-1}$ in benzene- d_6 , $k'_d = 3.1 \times 10^5 \text{ s}^{-1}$ in toluene- d_8 , and in both benzene and toluene $k_d = 3.7 \times 10^4 \text{ s}^{-1}$; $k_A = 1.5 \times 10^7 \text{ M}^{-1} \text{ s}^{-1}$ for DBS, and $k_A = 7 \times 10^5 \text{ M}^{-1} \text{ s}^{-1}$ for BHT (12, 13). ^c Initial rate constant; rate constant increases as DBS is depleted and has lesser effect on $^1\text{O}_2$ lifetime.

Table III. Solvent Dependence of Maltene-Sensitized Photolysis Rate Constant for DBS^a

solvent ^b	ϵ, D	$10^5 k_{\text{exptl}}, \text{s}^{-1}$	$10^6 k_r, \text{M}^{-1} \text{s}^{-1}$	k_r/k_A ^d
hexane	1.89	5.13	0.16	0.011
99:1 hex/MeOH	2.20	53	1.7	0.11
benzene	2.27	53	1.7	0.11
toluene	2.38	53	1.7	0.11
99:1 tol/MeCN	2.78	116	3.7	0.25
99:1 tol/MeOH	2.70	230	7.4	0.50
98:2 tol/MeOH	2.98	460	15	1.0

^a DBS (500 μM) irradiated in Xe lamp in presence of 32.5 mg/L Arabian Heavy maltenes. ^b Hex, *n*-hexane; tol, toluene. ^c Dielectric constant, for mixtures calculated assuming linear additivity. ^d Calculations based on $k_r = 1.7 \times 10^6 \text{ M}^{-1} \text{ s}^{-1}$ in toluene (determined relative to TME by using $k_r = 4.2 \times 10^7 \text{ M}^{-1} \text{ s}^{-1}$ and assuming $k_A = 1.5 \times 10^7 \text{ M}^{-1} \text{ s}^{-1}$ independent of solvent).

constants from eq 2 in deuterated and protonated solvents is then

$$k^{\text{D}}/k^{\text{H}} = (k_d + k_A[\text{A}]) / (k'_d + k_A[\text{A}]) \quad (3)$$

where k'_d is the quenching rate constant for the deuterated solvent.

Table II shows the solvent isotope effects observed for DBS and BHT. For DBS, the agreement between the experimental value of $k^{\text{D}}/k^{\text{H}}$ and that predicted from eq 3 is adequate, thus indicating a $^1\text{O}_2$ mechanism. (The data at 500 μM DBS are less precise because $k_A[\text{A}] \approx k'_d$, resulting in non-first-order behavior in deuterated solvents.) For BHT, the results indicate that its loss does not occur by singlet oxygenation. These results are expected in view of the reported selectivity of alkyl sulfides for singlet oxygenation and BHT for peroxy radical reactions (12, 19, 20).

Solvent Polarity Effect on DBS Photooxidation. The rate of oxidation of alkyl sulfides by $^1\text{O}_2$ increases rapidly with increasing solvent polarity because a greater fraction of interactions involves chemical reaction compared to physical quenching (16). Table III shows this effect for maltene-sensitized photooxidation of DBS, again consistent with a $^1\text{O}_2$ mechanism. Effects of solvent polarity on peroxy radical oxidation rates are expected to be much less marked (21) or be in the opposite direction (22).

Inhibition by BHT. Addition of 3 mM BHT caused less than a factor of 2 reduction in the DBS photooxidation rate. Because BHT reacts 10^4 times faster than alkyl

Table IV. Initial Rate Constants for Sensitized Photolyses of TME and BHT as a Function of Residue Fraction (Arabian Heavy)^a

compd	resid fractn	[S], mg/L	$10^8 k_{\text{exptl}}^b$ s ⁻¹	$10^5 k_{\text{exptl}}/[S]$, L mg ⁻¹ s ⁻¹	wt fractn	calcd contrib to $10^9 k_{\text{exptl}}/[S]^c$, L mg ⁻¹ s ⁻¹
TME	maltenes	32.5	1300	40	0.915	37
	asphaltenes	2.86	390	133	0.085	11
	total residue	13.5	590	43		48
BHT	maltenes	32.5	28	0.86	0.915	0.79
	asphaltenes	2.86	23	8.0	0.085	0.68
	total residue	13.5	22	1.6		1.5

^aTME or BHT (100 μM) in toluene irradiated in Xe lamp with optically matched solutions ($\alpha_{366} = 0.1 \text{ cm}^{-1}$). ^bAfter correction for contribution by direct photolysis. These values are proportional to quantum yields. ^cProduct of value in column 5 times value in column 6.

sulfides with ROO^{*} and causes termination (19, 20), complete inhibition would have been expected if ROO^{*} were the oxidant for DBS. Three millimolar BHT should not affect (<5%) the concentration of ¹O₂ (12).

¹O₂ Rate Constants. Two olefins, α-terp and TME, exhibited a relative rate of 1.6 ± 0.2 for photooxidation sensitized by maltenes in toluene, from which we calculate a k_t of $(6.8 \pm 0.9) \times 10^7 \text{ M}^{-1} \text{ s}^{-1}$ for α-terp [based on a k_t of $4.2 \times 10^7 \text{ M}^{-1} \text{ s}^{-1}$ for TME (12)], reasonably close to the value of $4.3 \times 10^7 \text{ M}^{-1} \text{ s}^{-1}$ reported by Monroe (13) in chloroform and consistent with a ¹O₂ oxidation of these two compounds sensitized by maltenes. Therefore, we have assumed below that their photolytic consumption in crude oil residues is due to ¹O₂ because of their high ¹O₂ rate constants and low photolysis and radical oxidation rate constants (19).

Similarly, from the relative rate data in Tables I and II, we calculated k_t for DBS to be $(1.7 \pm 0.3) \times 10^6 \text{ M}^{-1} \text{ s}^{-1}$ in toluene and benzene (see Table III). From the relative rates of oxidation of DMP and DBS in the presence of methylene blue in 98:2 toluene/MeOH (Table I), we calculate $k_t \leq 6.7 \times 10^4 \text{ M}^{-1} \text{ s}^{-1}$ for DMP based on $k_t = 1.5 \times 10^7 \text{ M}^{-1} \text{ s}^{-1}$ for DBS in this solvent (Table III).

Quantum Yields (Φ) of ¹O₂ Formation. To determine Φ_{O₂}, the rate constant (k^{sens}) of DBS photooxidation in 366-nm light was compared to the direct photolysis rate constant (k^{dir}) of a *p*-nitroanisole/pyridine (PNA/pyr) actinometer having a quantum yield Φ_{PNA} adjusted to 0.0057 (10). In both cases, the total absorbance was ≤0.1 at 366 nm. Under these conditions

$$\Phi_{\text{O}_2} = k^{\text{sens}} k_{\text{dPNA}} \Phi_{\text{PNA}} / k^{\text{dir}} k_{\text{r}\alpha} \quad (4)$$

where ϵ_{PNA} is the molar extinction coefficient of PNA and α is the absorbance of the sensitizing solution (in cm^{-1}). Thus, a quantum yield for production of ¹O₂ of 0.6 ± 0.2 at 366 nm was obtained for the Arabian Heavy maltene fraction in toluene (uncorrected for differences in solvent refractive index). From this, the quantum yield of inter-system crossing is ≥0.6, which is in the range of values for many aromatic hydrocarbons (23). Thus, as expected, the aromatic components of the crude residue appear to be responsible for ¹O₂ formation.

¹O₂ Quantum Yields as a Function of Wavelength Ranges, Crude Residue Fractions, and Crude Residue Origins. Wavelength Ranges. Preliminary experiments showed that the ¹O₂ quantum yield (maltene-sensitized) at 400–550 nm is a factor of ~4 lower than at 300–400 nm and decreases further above 550 nm. Similar findings have been reported for humic and fulvic acids (17), which are also polychromophoric, natural organic materials.

Crude Residue Fractions. Rate constants for TME photooxidation were used to evaluate the relative contribution of the crude oil fractions to the total ¹O₂ production

Table V. Rate Constant for DBS Photooxidation and Relative Quantum Yields for ¹O₂ Production for Crude Residues of Various Geographical Origins^a

crude oil origin	[S], ^b mg/L	$10^4 k_{\text{exptl}}^c$, s ⁻¹	rel quantum yield ^c
Arabian Heavy ^d	13.5	1.93	1
Iranian Light ^d	12.0	2.41	1.25
Es Sider ^d	19.0	2.14	1.11
Forties ^e	16.9	1.58	0.82
Statfjord ^e	23.7	2.03	1.05
Ekofisk ^e	24.5	1.67	0.86
Nigerian Forcados ^f	42.8	2.57	1.33

^aDBS (500 μM) in toluene irradiated in Xe lamp. ^bSensitizer: total residue, in optically matched ($\alpha_{366} = 0.1 \text{ cm}^{-1}$). ^c k_{exptl} relative to Arabian Heavy. Absolute quantum yields at 366 nm may be estimated by multiplying by 0.6, the value obtained in the Hg lamp for Arabian Heavy maltenes, the fraction that contributes the most to singlet oxygen formation. ^dMiddle East. ^eNorth Sea. ^fAfrica.

(Table IV). The asphaltenes absorbed ~11 times more light than the maltenes (on a weight basis) but were ~3 times less efficient in producing ¹O₂. The relative contributions of maltenes and asphaltenes to ¹O₂ production are approximately additive ($k_{\text{exptl}}/[S] = 0.43 \pm 0.07 \text{ L mg}^{-1} \text{ s}^{-1}$ observed for the total residue versus $0.48 \pm 0.07 \text{ L mg}^{-1} \text{ s}^{-1}$ calculated from the sum of the fractions).

Crude Residue Origins. Table V shows that crude oil residues of different geographical origins exhibit similar quantum yields for ¹O₂ production. Therefore, in optically thick films (>100 μm) in which essentially all incident sunlight up to 800 nm is absorbed, ¹O₂ production will be approximately independent of the crude oil origin. However, absorption coefficients varied much more strongly (by a factor of 3.5), and therefore under optically thin conditions, the Iranian Light would absorb the most light and produce the most ¹O₂.

Effect of Sensitizer Concentration on ¹O₂ Formation. In an attempt to extrapolate our laboratory results to those expected in an actual film, we studied the rate of DBS photooxidation as a function of sensitizer concentration. Figure 2 shows that the observed rate constant increased proportionally to the sensitizer concentration when total absorbance was low and then became independent of sensitizer concentration at high concentrations where all light at 366 nm was absorbed. This independence of rate constant implies that crude oil components do not significantly reduce the lifetime of ¹O₂ at concentrations up to 40 g/L, or ~4% crude oil in toluene. However, independence was observed only in an oxygen atmosphere or with rapid stirring. In air without stirring, the rate constant actually decreased with increasing sensitizer concentration, indicating that oxygen diffusion limits the formation of ¹O₂ under these conditions. These data

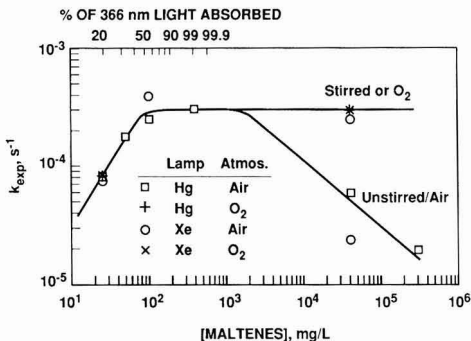


Figure 2. DBS photooxidation rate constant vs sensitizer concentration. Values obtained with the Xe lamp have been divided by 3.37 to normalize them to the Hg lamp conditions.

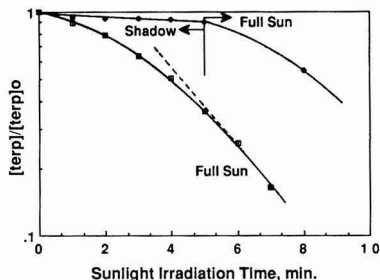


Figure 3. α -Terpinene disappearance in an Ekofisk ($\geq 210^\circ\text{C}$) film (0.44 mm) on water. Note log scale.

suggest that, in actual oil films, photooxidation rates may be limited by mass transport of oxygen from air when films are thick, but are less limited as the film spreads and increases its surface-to-volume ratio.

Film Experiments. In film experiments, α -terpinene was used in place of DBS in order to minimize volatilization losses, and a lower boiling ($\geq 210^\circ\text{C}$) Ekofisk residue was used in place of the Arabian Heavy in order to allow easier spreading of the film. Figure 3 shows the rate of sunlight photooxidation of $500\ \mu\text{M}$ α -terpinene in a 0.44-mm-thick film on water. This high concentration of α -terpinene was needed to allow reasonable analysis in the crude mixture. A possible reason for the curvature of the plot is the competition of α -terpinene with the solvent for quenching of $^1\text{O}_2$ during the initial portion, which decreases as the α -terpinene is consumed. This assertion assumes a k_r of $7 \times 10^7\ \text{M}^{-1}\ \text{s}^{-1}$ for α -terpinene in the residue (as measured in toluene) and a k_d of $3.7 \times 10^4\ \text{s}^{-1}$ in the residue by analogy to hexane and toluene solvents, a mixture of which serves as a model for crude oils save for the difference in viscosity. We have, however, not yet been able to verify these assumptions. Using the later portion of the curve with the presumption that the α -terpinene no longer affects the lifetime of $^1\text{O}_2$, we find $k_{\text{exptl}} = (5 \pm 1) \times 10^{-3}\ \text{s}^{-1}$, or a half-life of ~ 2 min and $[^1\text{O}_2] = 8 \times 10^{-11}\ \text{M}$ in the bulk film. By dividing by the light screening factor S_λ (14, 24) at 400 nm, we calculate that at the surface of the film $k_{\text{exptl}} = 0.4\ \text{s}^{-1}$ and $[^1\text{O}_2] = 6 \times 10^{-9}\ \text{M}$.

These data can be used to estimate $\Phi_{^1\text{O}_2}$ in the film. At low $[A]$ and assuming total sunlight absorbance (up to 700 nm), eq 2 reduces to

$$\Phi_{^1\text{O}_2} = k_{\text{exptl}} I_d k_d / k_r \sum W_\lambda = (6 \pm 2) \times 10^{-4} \quad (5)$$

where $I_a = \sum W_\lambda / jD$, $\sum W_\lambda / j$ is the incident light intensity in einstein $\text{L}^{-1}\ \text{s}^{-1}$, taken from Zepp and Cline (25), and

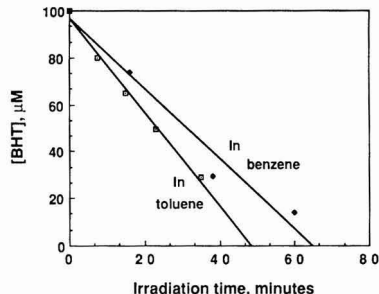


Figure 4. Total ROO^* formation rate as measured by the BHT photooxidation rate in the Xe lamp with 32.5 mg/L Arabian Heavy maltenes in benzene or toluene solvent.

D is the film thickness in centimeters. This $\Phi_{^1\text{O}_2}$ for the Ekofisk film is 3 orders of magnitude lower than the value of 0.6 estimated for the Arabian Heavy maltene fraction in dilute solution under optically thin conditions in the 366-nm Hg lamp. The drop in $\Phi_{^1\text{O}_2}$ cannot be due to differences in type of crude (Table V); it is most likely a result of higher local light absorption rates, which cause rapid local oxygen depletion, and of the higher viscosity, which reduces the O_2 diffusion rate. Both of these reduce the efficacy of energy transfer to ground-state O_2 . $\Phi_{^1\text{O}_2}$ for polymer-bound rose bengal is reported to decrease 2–4-fold with a 25% increase in solvent viscosity (26). The residue used in the film experiments had a viscosity of 1.3 P at 27°C , which is 250 times higher than that of toluene (0.0053 P at 30°C). The results in Figure 2 show that local oxygen depletion occurs at high absorbance even in toluene solution where the viscosity is much lower than in the film. Other factors may also be operative, such as k_r being lower in the film due to slower diffusion of acceptor and $^1\text{O}_2$ and k_d being higher in the crude oil than in toluene.

Tests for ROO^* and RO^* Intermediacy. BHT and tetralin were used to probe for peroxy and alkoxy radical oxidation because they react very slowly with $^1\text{O}_2$ (12) and because they have widely different rate constant ratios for the former two oxidants (19, 20, 27–29). For $t\text{-BuOO}^*$ $k_{\text{BHT}}/k_{\text{tetralin}} = 5000$, and for $t\text{-BuO}^*$ $k_{\text{BHT}}/k_{\text{tetralin}} = 12$ (see supplementary material). From Table I, the observed rate constant ratio in toluene was $\gg 200$; the tetralin loss rate was near zero after correction for direct photolysis. This implies that the RO^* concentration was very low ($\leq 3 \times 10^{-13}\ \text{M}$) in benzene or toluene and that RO^* had negligible contribution to the sensitized BHT or DBS losses. The high reactivity of ROO^* with BHT ($1 \times 10^4\ \text{M}^{-1}\ \text{s}^{-1}$) suggests that ROO^* is the major oxidant.

ROO^* Quantum Yields and Steady-State Concentrations. Quantum Yields. The production rate R_i of peroxy radicals is equal to the loss rate of BHT assuming BHT traps all the peroxy radicals:

$$-d[\text{BHT}]/dt = R_i/2 \quad (6)$$

The factor of 2 accounts for the consumption of two ROO^* by each BHT (20). Figure 4 shows that the maltene-sensitized BHT loss is approximately linear as expected from eq 6. However, the data in Figure 4 fit nearly as well to first-order kinetics, i.e., the order was between zero and one. This indicates that $100\ \mu\text{M}$ BHT is scavenging a large fraction but not all peroxy radicals. The average initial BHT loss rate observed after subtracting the direct photolysis rate was $\geq 2 \times 10^{-8}\ \text{M}\ \text{s}^{-1}$ from which $R_i \geq 4 \times 10^{-8}\ \text{M}\ \text{s}^{-1}$. This rate of initiation implies that all sensitizer molecules in these solutions are transformed to peroxy radicals in ~ 1 h in the Xe lamp (assuming an average

molecular weight of 250 for the maltenes), although it is possible that some radical pairs collapse back to starting materials in the absence of BHT. In actual oil films, conversion to peroxy radicals may be limited by oxygen mass transfer, since the dissolved oxygen concentration of 2–3 mM (23) is much less than that of a ~5 M neat organic liquid.

These data may be used to estimate $\Phi_{\text{ROO}\cdot}$, the quantum yield of peroxy radical formation. The initiation rate is related to the quantum yield by

$$R_i = I_a \Phi \quad (7)$$

Writing two such equations for $\text{ROO}\cdot$ and $^1\text{O}_2$ and ratioing, one obtains

$$\Phi_{\text{ROO}\cdot} = \Phi_{^1\text{O}_2} [R_i(\text{ROO}\cdot) / R_i(^1\text{O}_2)] \quad (8)$$

$R_i(^1\text{O}_2)$ is calculated from the steady-state assumption and the values of k_d and $[^1\text{O}_2]$ (the latter from the observed TME loss rate constant; for calculation see ref 14) in toluene with 32.5 mg/L maltenes in the Xe lamp:

$$R_i(^1\text{O}_2) = k_d[^1\text{O}_2] = (3.7 \times 10^4 \text{ s}^{-1})(3 \times 10^{-10} \text{ M}) = 1 \times 10^{-5} \text{ M s}^{-1} \quad (9)$$

Using $R_i(\text{ROO}\cdot) = 4 \times 10^{-8} \text{ M s}^{-1}$ and $\Phi_{^1\text{O}_2} = 0.6$, eq 8 yields $\Phi_{\text{ROO}\cdot} = 0.002 \pm 0.001$. The large estimated error results because $\Phi_{^1\text{O}_2}$ applies to 366 nm while the R_i values apply to broad wavelength Xe lamp irradiation. The value nevertheless serves to show that the average quantum yield for peroxy radicals is 2–3 orders of magnitude lower than for singlet oxygen.

The data in the lower half of Table IV indicate the relative contribution of maltenes and asphaltenes to the total peroxy radical production. The quantum yields for the two fractions appear to be about the same, and therefore the quantum yield for the total residue is also ~0.002. Although the asphaltenes absorb 10 times as much light, they represent only 10% of the total weight and therefore the two fractions contribute equally to the total $\text{ROO}\cdot$ production.

ROO \cdot Steady-State Concentrations. Using eq 10 with $R_i \geq 4 \times 10^{-8} \text{ M s}^{-1}$ and $2k_t = 3 \times 10^8 \text{ M}^{-1} \text{ s}^{-1}$ for benzylperoxys (derived from toluene) (30), we calculate $[\text{ROO}\cdot]_{\text{ss}} \geq 1 \times 10^{-8} \text{ M}$ in the

$$[\text{ROO}\cdot]_{\text{ss}} = (R_i/2k_t)^{1/2} \quad (10)$$

absence of BHT in toluene with 32.5 mg/L maltenes in Xe lamp radiation. This calculation assumes that the maltenes have no effect on the termination rate and thus on $[\text{ROO}\cdot]_{\text{ss}}$ in toluene. Despite their lower quantum yield of formation, peroxy radicals are more abundant than $^1\text{O}_2$ under these conditions ($[^1\text{O}_2] = 3 \times 10^{-10} \text{ M}$, see above), because their destruction rate is much lower. No value of $[\text{ROO}\cdot]_{\text{ss}}$ can be estimated in benzene since the $\text{ROO}\cdot$ lifetime is not known in the absence of BHT.

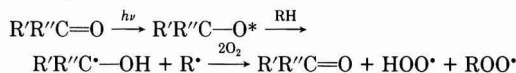
At present there is no way to extrapolate these results to estimate peroxy radical concentrations in oil films because the termination rate in crude oils is unknown. Unfortunately, we could not measure BHT consumption rates in neat films because the oil components caused analytical interferences. However, because termination is a second-order process, one may expect $[\text{ROO}\cdot]_{\text{ss}}$ to be lower in films where high light absorption rates cause higher local concentrations of peroxy radicals. Nevertheless, the high initiation rates indicate that radical oxidation will be important. Measurements of initiation rates, propagation rate constants, and oxygen uptake rates of crude oil films in sunlight will be needed to more fully characterize the system.

Importance of $^1\text{O}_2$ for $\text{ROO}\cdot$ Initiation. A simple calculation suggests that $^1\text{O}_2$ is not important for production of $\text{ROO}\cdot$ by maltenes in toluene. As described above, maltenes had no significant effect on the $^1\text{O}_2$ lifetime at concentrations up to ~40 g/L. From this we calculate a maximum average maltene interaction rate constant k_A of $90 \text{ L g}^{-1} \text{ s}^{-1}$ (or $2 \times 10^4 \text{ M}^{-1} \text{ s}^{-1}$ assuming a molecular weight of 250). The total rate of interaction of maltenes with $^1\text{O}_2$ is

$$R \leq k_A[\text{maltenes}][^1\text{O}_2] = 9 \times 10^{-10} \text{ M s}^{-1} \quad (11)$$

for 0.033 g/L maltenes and $3 \times 10^{-10} \text{ M } ^1\text{O}_2$. This value is 40 times lower than the minimum $\text{ROO}\cdot$ production rate of $4 \times 10^{-8} \text{ M s}^{-1}$. In addition, if radical formation resulted from $^1\text{O}_2$ -produced hydroperoxides, then BHT consumption should accelerate as the concentration of peroxides increases, contrary to the observed results.

Thus, direct photoinitiation appears to dominate over $^1\text{O}_2$ -induced $\text{ROO}\cdot$ production. However, this conclusion has yet to be tested for actual crude oil films. Direct initiation may occur by processes such as photoionization, homolytic bond fission, or excitation of carbonyls:



Direct Photolysis Rates in the Film. Direct photolyses of DMP and DBT will be slower in oil films than in dilute solution due to competitive light absorption by the oil components. This will occur if the film is thicker than ~10 μm and absorbs most of the light below 400 nm.

Using $\Phi = 0.003$ (see above) in the equations of Zepp and Cline (25), we calculate a direct photolysis rate constant of $1 \times 10^{-7} \text{ s}^{-1}$ for DMP in the Ekofisk film under noon, summer sunlight at 40° N. The same calculation for an optically thin film or at the film surface yields a rate constant of $3 \times 10^{-5} \text{ s}^{-1}$, or 300 times higher. Thus, direct photolysis rates may be strongly inhibited in actual oil films, and $^1\text{O}_2$ or radical pathways may dominate. However, we have observed that absorbing oil components are slowly bleached by exposure to light and therefore direct photolysis rates will increase with time.

Conclusions

Crude oil components are very efficient producers of singlet oxygen in dilute toluene solution ($\Phi_{^1\text{O}_2}$ in the range 0.5–0.8) and moderately efficient producers of peroxy radicals ($\Phi_{\text{ROO}\cdot} = 0.002$). Alkoxy radical formation rates were too low to measure under the present conditions. Direct photolysis was the major transformation pathway for the polycyclic compounds dibenzothiophene and 3,6-dimethylphenanthrene.

In neat films, apparent $^1\text{O}_2$ quantum yields are 3 orders of magnitude lower because high absorbance causes local oxygen depletion, and possibly because high viscosity slows diffusion of oxygen and substrate, or because the lifetime of $^1\text{O}_2$ or its triplet precursor is shorter in neat oils. $^1\text{O}_2$ concentrations in actual films in sunlight are high enough to oxidize reactive components such as alkythianes and thiolanes (7) in a few hours. The limiting step in oxidation of oil films appears to be transport of oxygen into the film.

The mechanism of oxy radical formation remains unclear, but our results suggest that $^1\text{O}_2$ is not a significant source of radicals compared to direct photolysis. Because peroxy radical formation also requires oxygen, it is probably also less efficient in neat oils. This effect remains to be quantified. Direct photolyses will also be slower in oil films, to an extent dependent upon the absorption spectrum of the compound and the film thickness. The ob-

servation by others (11) that alkanes are oxidized after long irradiation times also implies that oxy radicals are formed and are the dominant oxidants for compounds not sensitive to direct photolysis or $^1\text{O}_2$.

Diagnostic tests for $^1\text{O}_2$ and ROO^* in undiluted crude oils await measurements of rate constants for processes in viscous fluids including triplet lifetimes, $^1\text{O}_2$ quenching, $^1\text{O}_2$ reaction with substrates, ROO^* propagation, and ROO^* termination.

Acknowledgments

Janet Sandell performed the viscosity measurements.

Supplementary Material Available

The derivation for estimating single oxygen yields by use of actinometers consumed in a first-order fashion and a summary of the rate constants used (3 pages) will appear following these pages in the microfilm edition of this volume of the journal. Photocopies of the supplementary material from this paper or microfiche (105 × 148 mm, 24× reduction, negatives) may be obtained from Microforms Office, American Chemical Society, 1155 16th St., N.W., Washington, DC 20036. Full bibliographic citation (journal, title of article, authors' names, inclusive pagination, volume number, and issue number) and prepayment, check or money order for \$10.00 for photocopy (\$12.00 foreign) or \$10.00 for microfiche (\$11.00 foreign), are required.

Registry No. DMP, 1576-67-6; DBT, 132-65-0; DBS, 544-40-1; TME, 563-79-1; BHT, 128-37-0; α -terp, 99-86-5; tetr, 119-64-2; O_2 , 7782-44-7; methylene blue, 61-73-4.

Literature Cited

- (1) Kagan, J.; Kagan, E. D.; Kagan, I. A.; Kagan, P. A.; Quigley, S. *Chemosphere* **1985**, *14*, 1829-1834.
- (2) Oris, J. T.; Giesy, J. P. *Environ. Toxicol. Chem.* **1986**, *5*, 761-768.
- (3) Larson, R. A.; Hunt, L. L.; Blankenship, D. W. *Environ. Sci. Technol.* **1977**, *11*, 492-496.
- (4) Østgaard, K.; Aarberg, A.; Klungsoyr, J.; Jensen, A. *Water Res.* **1987**, *21*, 155-164.
- (5) Tjessem, K.; Aarberg, A. *Chemosphere* **1983**, *12*, 1373-1394.
- (6) Larson, R. A.; Hunt, L. L. *Photochem. Photobiol.* **1978**, *28*, 553-555.
- (7) Sinninghe-Damsté, J. S.; De Leeuw, J. W.; Kock-van Dalen, A. C.; De Zeeuw, M. A.; De Lange, F.; Rupstra, W. I. C.; Schenck, P. A. *Geochim. Cosmochim. Acta* **1987**, *51*, 2369-2391.
- (8) Guseinov, M. M.; Zeinalov, E. B.; Trifel, B. Y.; Velieva, K. U.; Mastaliova, K. A. *Dokl. Akad. Nauk. Az. SSR* **1984**, *40*, 39-44; *Chem. Abstr.* **1984**, *101*, 194718n.
- (9) *IP Standards for Petroleum and its Products*, IP Method 143/57; Institute of Petroleum: London, 1972.
- (10) Dulin, D.; Mill, T. *Environ. Sci. Technol.* **1982**, *16*, 815-820.

- (11) Tjessem, K.; Kobberstad, O.; Aarberg, A. *Chemosphere* **1983**, *12*, 1395-1406.
- (12) Wilkinson, F.; Brummer, J. G. *J. Phys. Chem. Ref. Data* **1981**, *10*, 809-999.
- (13) Monroe, B. M. In *Singlet O₂*; Frimer, A. A., Ed.; CRC: Boca Raton, FL, 1985; Vol. 8, pp 177-224.
- (14) Haag, W. R.; Hoigné, J. *Environ. Sci. Technol.* **1986**, *20*, 341-348.
- (15) Haag, W. R.; Hoigné, J.; Gassmann, E.; Braun, A. M. *Chemosphere* **1984**, *13*, 631-640.
- (16) Foote, C. S.; Peters, J. W. *J. Am. Chem. Soc.* **1971**, *93*, 3795-3796.
- (17) Zepp, R. G.; Schlotzhauer, P. F.; Sink, R. M. *Environ. Sci. Technol.* **1985**, *19*, 74-81.
- (18) Xu, D.; Xu, B.; Cui, G.; Wu, S. *Huaxue Tongbao* **1985**, *2*, 17-19.
- (19) Hendry, D. G.; Mill, T.; Piszkiwicz, L.; Howard, J. A.; Eigenmann, H. K. *J. Phys. Chem. Ref. Data* **1974**, *3*, 937-978.
- (20) Howard, J. A.; Furimsky, E. *Can. J. Chem.* **1973**, *51*, 3738-3745.
- (21) Hendry, D. G.; Russell, G. A. *J. Am. Chem. Soc.* **1964**, *86*, 2368-2371.
- (22) Zaikov, G. E.; Maizus, Z. K. In *Oxidation of Organic Compounds*; Gould, R. F., Ed.; Advances in Chemistry 75; American Chemical Society: Washington, DC, 1968; pp 150-164.
- (23) Murov, S. L. *Handbook of Photochemistry*; Marcel Dekker: New York, 1973; pp 49-51.
- (24) Zepp, R. G. In *The Handbook of Environmental Photochemistry*; Hutzinger, O., Ed.; Springer-Verlag: Berlin, 1982; Vol. 2, part B, pp 19-41.
- (25) Zepp, R. G.; Cline, D. M. *Environ. Sci. Technol.* **1977**, *11*, 359-366.
- (26) Paczkowski, J.; Neckers, D. C. In *Organic Phototransformations in Nonhomogeneous Media*; Fox, M. A., Ed.; ACS Symposium Series 278; American Chemical Society: Washington, DC, 1985; pp 223-242.
- (27) Ingold, K. U. *Can. J. Chem.* **1963**, *41*, 2816-2825.
- (28) Choo, K. Y.; Benson, S. W. *Int. J. Chem. Kinet.* **1981**, *13*, 833-844.
- (29) Mill, T.; Hendry, D. G. In *Comprehensive Chemical Kinetics*; Bamford, C. H., Tipper, C. F. H., Eds.; Elsevier: Amsterdam, 1980; pp 50-52.
- (30) Howard, J. A. In *Advances in Free Radical Chemistry*; Williams, G. H., Ed.; Academic: New York, 1972; Vol. 4, Chapter 2, pp 49-173.

Received for review February 24, 1988. Accepted June 30, 1988. This work was supported by SRI International and the Senter for Industriforskning. We thank the Norwegian council for Scientific and Industrial Research for a fellowship and the Senter for Industriforskning for granting R.G.L. a sabbatical leave to perform this work.

Continuous Flow Method for Simultaneous Determination of Monochloramine, Dichloramine, and Free Chlorine: Application to a Water Purification Plant

Toyoaki Aoki

Laboratory of Environmental Chemistry, College of Engineering, University of Osaka Prefecture, Mozu-umemachi, Sakai 591, Japan

■ A system with three double-tube separation units, each with an inner tube of microporous PTFE and an outer tube of PTFE, is proposed for the continuous, simultaneous determination of monochloramine, dichloramine, and free chlorine in water. The quantitative reaction between chloramines and iodide was used in order to quantify conveniently the chlorine species as available chlorine. Chloramines and chlorine above 0.1 mg of Cl_2/L can be determined by the present method. Inorganic chloramines (ammonia derived) and chloroamino acids (amino acid derived) can be distinguished by the present method. From the application of this method at a water purification plant, the dynamic behavior of chloramines and free chlorine has become apparent. Dichloramine is degraded appreciably by sunlight; it decomposes to produce slight amounts of free chlorine in the course of purification.

Introduction

Chlorine has been used extensively for disinfection in water treatment. In Japan, residual concentrations of free chlorine in drinking water supplies must be greater than 0.1 mg of Cl_2/L . Chloramines (most commonly NH_2Cl and NHCl_2) are formed in the process of disinfecting water containing ammonia by chlorination. Analytical determination of chlorine species in water should be able to differentiate between free chlorine and chloramines. One of the most commonly used methods for chlorine determination is the DPD (*N,N*-diethyl-*p*-phenylenediamine) method. It has been shown by Cooper et al. that DPD reacts directly with free chlorine and monochloramine (1-3). Thus, the presence of chloramines interferes with the determination of free chlorine in this method. Furthermore, free chlorine reacts with nitrogenous organic compounds, such as amino acids, to form a variety of organic chloramines, reducing the formation of inorganic chloramines. Ram et al. reported that the organic chloramines lead to false positive tests for the determination of free chlorine (4, 5). Furthermore, conventional methods for measuring chloramines cannot distinguish between inorganic chloramines and organic chloramines as reported by Issac and Morris (6) and Wolfe et al. (7).

We previously reported on continuous flow methods for determining free chlorine (8), ammonia and nitrate (9), and aqueous ozone (10) utilizing a tubular microporous PTFE membrane to separate volatile compounds such as Cl_2 , NH_3 , and O_3 . Our previous method (11) indicated that simultaneous determination of monochloramine and dichloramine could be performed by measuring the absorbance at each λ_{max} . However, the determination of free chlorine in the presence of chloramines was not possible, since chloramines absorb UV radiation at the λ_{max} of free chlorine.

This paper presents a continuous flow method for simultaneous determination of monochloramine, dichloramine, and free chlorine in water. The problem mentioned above is eliminated by the application of reactions specific to each species and the oxidation of iodide ion by each species. The water to be tested is fed into three separate

channels, each of which lead to separation units with inner tubes made of microporous PTFE. Specific reagents are mixed with the sample in each unit so that only monochloramine permeates into the inner tube in the first unit while monochloramine and dichloramine permeate into the inner tube in the second unit. In the third unit, all of the free chlorine is converted to monochloramine so that the amount of chloramines that permeate into the inner tube represents the total amount of the three chlorine species. Since only the volatile species permeate the PTFE membrane, interference by nonvolatile organic chloramines, such as chloroamino acids, is prevented.

As an application of this method, the amounts of chlorine species were determined during the treatment of water at a purification plant.

Experimental Section

Reagents. Stock solutions of free chlorine were prepared from 7% sodium hypochlorite diluted to 0.1 M. The stock solutions were standardized by the iodine-thiosulfate method.

Monochloramine was prepared from solutions of ammonium chloride and free chlorine, both of which had been adjusted to pH 10 with NaOH prior to mixing according to the procedures of Chapin (12) and Issac and Morris (13). The ammonia to chlorine molar ratio was maintained at 1.03:1.00. The monochloramine stock concentration was determined spectrophotometrically from the absorbance at 244 nm according to the method of Trofe et al. (14) prior to each experiment.

Dichloramine was prepared from solutions of ammonium chloride and free chlorine, both of which had been adjusted to pH 5.0 with acetate buffer solution. The free chlorine solution was poured slowly over 2 min into the ammonia solution while stirring rapidly. The chlorine to ammonia molar ratio was maintained at 1.80:1.0. The dichloramine stock concentration was determined spectrophotometrically from the absorbance at 295 nm (14). Each chloramine solution was prepared fresh daily.

Buffers with pH values in the range 6.0-10.5 were prepared with H_3PO_4 and NaOH, while acetic acid and NaOH were employed to prepare buffers with pH values between 4.5 and 6.0.

All reagents were of analytical reagent grade except the sodium hypochlorite which was of reagent grade. Doubly distilled water was used in the preparation of all solutions, the second distillation being carried out in an all-Pyrex still.

Apparatus and Procedure. A flow diagram of the apparatus is shown in Figure 1. Sample and reagent solutions were propelled by peristaltic pumps (P1-P3) through Tygon tubing (L1-L9). Separation units, S1-S3, were used for the determination of the monochloramine, the sum of monochloramine and dichloramine, and the sum of monochloramine, dichloramine, and free chlorine, respectively. The construction of the separation units was the same as that described in a previous paper (5). The outer tube (3.5 mm o.d. and 2.5 mm i.d.) was made of PTFE, and the inner tube (1.8 mm o.d. and 1.0 mm i.d.)

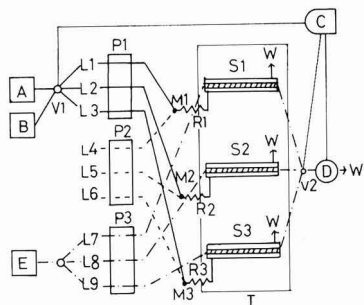


Figure 1. Schematic diagram of continuous flow system. A (L1-L3), sample (each at 5.0 mL/min); B, 2 N H₂SO₄; P1-P3, peristaltic pump; L4, 10 mM KBr containing 0.5 M NaOH (at 0.5 mL/min); L5, 50 mM NaNO₂ at pH 6.8 (at 0.5 mL/min); L6, 50 mM NH₄Cl at pH 6.8 (at 0.5 mL/min); E (L7-L9), 10 mM KI at pH 5.0 (each at 0.5 mL/min); M1-M3, mixing point; R1-R3, reaction coil (PTFE tubing 2.0 mm i.d., 3.0 mm o.d., length 1 m); S1-S3, separation units (inner: microporous PTFE tubing 1.0 mm i.d., 1.8 mm o.d. outer: PTFE tubing 2.5 mm i.d., 3.5 mm o.d., length 0.5 m); V1-V2, electromagnetic valve; D, UV detector; C, microcomputer; T, water bath; W, waste.

was made of microporous PTFE. The length of each separation unit was 500 mm. The sample (A) was fed into three channels (L1-L3) at an electromagnetic valve (V1). The flow rates for each channel were adjusted to the same value (5 mL/min) by the pump (P1).

The sample pumped through L1 was mixed with a solution of 10 mM KBr containing 0.5 M NaOH to decompose the free chlorine and the dichloramine in the sample. The residual monochloramine permeates through the microporous PTFE membrane into the inner tube at the separation unit (S1). The sample passed through L2 was mixed with a solution of 50 mM NaNO₂ buffered at pH 6.8 (L5). In this case, monochloramine and dichloramine remained in the sample and permeated through the microporous PTFE membrane into the inner tube at S2. At the third separation unit (S3), the sample pumped through L3 was mixed with a solution of 50 mM NH₄Cl buffered at pH 6.8 (L6). Ammonia reacts with the free chlorine to form monochloramine which permeates through the microporous PTFE membrane along with the original monochloramine and dichloramine in the sample.

A solution of 10 mM KI buffered at pH 5.0 (L7-L9) was passed through the inner tube of each separation unit. The reaction product between the chloramines and iodide flowed to an electromagnetic valve (V2) which was turned every 5 min to divert the reaction product from each separation unit alternatively to a flow cell (D) where the absorbance at 288 nm was measured by an UV detector (Model UVIDEC 1001V, Japan Spectroscopic Co.). The UV absorbances from the detector were fed to a 16-bit microcomputer (Model PC9800VM2, Japan Electronic Co.), and the UV absorbances during the last 1 min in every 5 min were integrated and averaged. The UV absorbances corresponding to monochloramine alone, the sum of monochloramine and dichloramine, and the sum of monochloramine, dichloramine, and free chlorine were thus obtained at three consecutive 5-min intervals and subtracted from one another to calculate the UV absorbances corresponding to each chlorine species. The concentrations were determined with calibration curves predetermined from standard solutions and were stored in a disk.

The separation units (S1-S3) were inserted into a water bath (T) which circulated by the sample water.

The surfaces of the microporous PTFE tubes (S1-S3) were automatically cleaned for 20 min every 8 h by

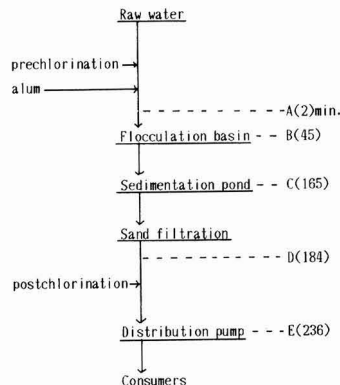


Figure 2. Schematic diagram of the Niwakubo water purification plant. A-E, sampling sites. Numbers in parentheses indicate arrival times from the prechlorination point in minutes.

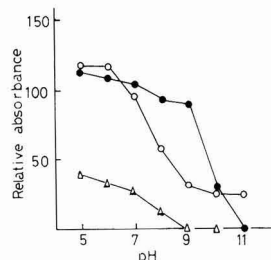


Figure 3. Permeation of chlorine species through a microporous PTFE tube. Concentration of chlorine species, 7.0 mg of Cl₂/L: O, monochloramine; ●, dichloramine; Δ, free chlorine.

switching the sample to 2 N H₂SO₄ at the computer-controlled electromagnetic valve (V1).

Site Description. The Niwakubo water purification plant is operated by the Water Works Department of Osaka Prefecture Government. The treatment scheme used is based on the sequences shown in Figure 2. The water supply rate is 5500-9900 m³/h. Chlorine gas and alum were used as disinfectant and flocculant, respectively. The time required by water to flow from the prechlorination point to the distribution pump is ~4 h. The sampling sites are shown in Figure 2 as A-E, with the arrival times from the prechlorination point in parentheses.

Results and Discussion

Permeability of Chloramines and Free Chlorine. The effect of pH on the permeation of chloramines and free chlorine in pH buffer solutions without KBr, NaNO₂, or NH₄Cl through microporous PTFE is shown in Figure 3. The permeability of each species decreased as the pH of the buffer solution increased.

Above pH 9, all of the free chlorine is converted to ionic species OCl⁻, which cannot permeate through microporous PTFE. Below pH 9, the amount of HOCl, which is volatile and thus permeates through the membrane, increases with decreasing pH. The decrease in the permeation of monochloramines with the increase of pH seems to be due to low permeability in alkaline media. Many studies have shown that the dichloramine readily undergoes decomposition when the pH of the solution is increased (15-17).

Since the permeation of monochloramine was nearly equal to that of dichloramine at pH 6.8, as shown in Figure 3, it was chosen as the optimum pH of the reagent solutions in the separation systems of S2 and S3, eliminating

Table I. Optimization of Concentration of Reagents

reagent ^a		relative intensity		
		free chlorine ^b	mono-chloramine ^b	dichloramine ^b
5 mM	NO ₂ ⁻	41	94	106
	NH ₃	96	101	103
10 mM	NO ₂ ⁻	20	99	104
	NH ₃	98	98	102
20 mM	NO ₂ ⁻	7	102	105
	NH ₃	97	101	101
50 mM	NO ₂ ⁻	0	98	103
	NH ₃	101	100 ^c	102

^a Reagent solutions containing NO₂⁻ (or NH₃) buffered at pH 6.8. ^b Concentrations of free chlorine and chloramines are 7.0 mg of Cl₂/L. ^c Absorbance obtained from monochloramine is defined as 100.

the necessity to consider the difference in permeabilities of the chloramines in the calculations. Since the permeability of free chlorine existing as HOCl at this pH was lower than that of chloramines, excess ammonia was used to convert the free chlorine to monochloramine. This conversion in the third channel further eliminates the consideration of the difference in permeabilities of the free chlorine and the chloramines.

The permeabilities of the chloramines increased with an increase in temperature at the separation units. However, the permeabilities could be maintained constant by inserting the separation units (S1-S3) into a water bath which circulated the sample, the water temperature of which was constant within ± 0.2 °C during a 24-h period.

Optimization of Reagent Concentration. Johnson et al. studied the kinetics of haloamines in the presence of bromide (18, 19). They reported that the half-life for monochloramine was observed to be 3-4 h at pH 7.8 in artificial seawater containing 25 mM bromide and the disappearance of monochloramine decreased with the increase in pH. The reaction product of bromide seems to be bromate, BrO₃⁻, according to Szabo and Csanyi (20) and Carpenter and Macalady (21). In a previous study, we found that bromide ion reacts selectively with free chlorine and dichloramine but the reaction between bromide and monochloramine in alkaline media with pH higher than 11 is very slow (11). The dichloramine (1 mM) was completely decomposed within 1 min in the presence of bromide (1 mM) at pH 11.3, while the monochloramine remained completely unreacted. Therefore, a solution of 10 mM KBr containing 0.5 M NaOH was used as the reagent (L4) in the separation system of S1 given in Figure 1.

Free chlorine may be decomposed with an excess of nitrite. Table I shows that the amount of free chlorine decreased with increasing nitrite concentration and at 50 mM NO₂⁻ all of the free chlorine in the sample was decomposed. The amounts of chloramines remained constant within experimental error even at this nitrite concentration. The optimum concentration of nitrite in the reagent mixed with the sample at separation unit S2 was thus selected to be 50 mM.

Free chlorine may be converted to monochloramine with an excess of ammonia. Table I shows that addition of ammonia does not affect the amount of chloramines, and thus 50 mM ammonia was chosen as the reagent solution for separation unit S3. At the concentration of 50 mM ammonia adjusted to pH 6.8, all of the free chlorine could be converted to monochloramine within 2-3 min.

The chloramines, remaining in the solution after the reaction with the reagents, permeates through microporous

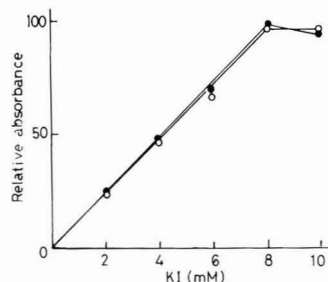


Figure 4. Optimization of iodide concentration in an inner solution buffered at pH 5.0. Concentration of chloramines, 7.0 mg of Cl₂/L: O, monochloramine; ●, dichloramine.

Table II. Relative Absorbances for Chloramines and Free Chlorine at Each Separation System

system	relative absorbance ^a		
	NH ₂ Cl ^b	NHCl ₂ ^b	Cl ₂ ^b
S1	100	0.5	0.0
S2	100	134.3	0.0
S3	100	109.6	93.8

^a Absorbance obtained from monochloramine in each system is defined as 100. ^b Concentrations of chloramines and free chlorine are 14 mg of Cl₂/L.

PTFE tubes into the iodide solution stream buffered at pH 5.0. It was found that iodide ions react quantitatively with chloramines to form I₃⁻ whose absorbance was measured at 288 nm. Figure 4 shows that for sample solutions containing mono- or dichloramines with the same chlorine concentration (7.0 mg of Cl₂/L), the absorbance values at 288 nm increased with increasing iodide and became constant when the iodide concentration was more than 8 mM. It was found that when 10 mM iodide was used as the inner solution, the absorbance values at 288 nm were the same for both mono- and dichloramine solutions with the same chlorine concentration. Thus, in order to determine the chloramines and the free chlorine in the sample solutions, a 10 mM iodide solution buffered at pH 5.0 was used as the inner solution (L7-L9).

Under the experimental conditions described above, the relative absorbances for each chlorine species were measured at each separation unit and are shown in Table II. The concentration of each chlorine species in standard solutions was 14.0 mg of Cl₂/L, which was the maximum concentration found in field measurements at the water purification plant. It is clear from Table II that the amount of monochloramine alone, the total amount of mono- and dichloramine, and the total amount of monochloramine, dichloramine, and free chlorine were selectively measured in systems S1-S3, respectively. The differences of the relative absorbances were corrected in determining the concentration of each species with the computer.

Analytical Performance. The absorbances at 288 nm were proportional to the concentration from 0.1 mg of Cl₂/L for monochloramine, 0.02 mg of Cl₂/L for dichloramine, and 0.02 mg of Cl₂/L for free chlorine to 71 mg of Cl₂/L for all of the chlorine species. The present analyzer was calibrated once a week with standard monochloramine, dichloramine, and free chlorine solutions with a chlorine concentration of 3.55 mg of Cl₂/L. The relative standard deviations over 8 weeks ($n = 8$) were 9.4, 7.4 and 6.5%, respectively. On the other hand, the relative standard deviations during 1 day ($n = 5$) were 1.5, 3.2, and 3.3% at 1.77 mg of Cl₂/L, respectively.

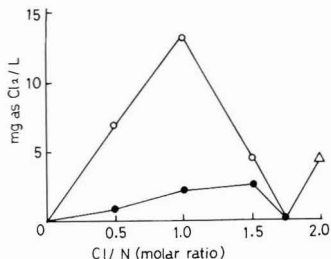


Figure 5. Breakpoint chlorination of ammonia at pH 6.8. Concentration of ammonia, 0.2 mM: O, monochloramine; ●, dichloramine; Δ, free chlorine.

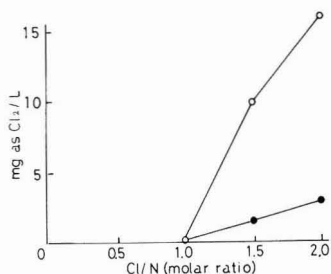


Figure 6. Breakpoint chlorination of alanine at pH 6.8. Concentration of alanine, 0.2 mM: O, monochloramine; ●, dichloramine.

Calcium, magnesium, sulfate, chloride, nitrate, and phosphate, each at a concentration of 50 mg/L, did not interfere with the present method.

Breakpoint Chlorination of Ammonia and Alanine. The chlorinations of alanine at pH 6.8 was examined as an example of when an organic chloramine is formed and compared with the chlorination of ammonia by using the present analyzer. Figure 5 shows the changes of chloramine and free chlorine concentrations as a function of Cl_2/NH_3 molar ratio with the ammonia concentration held constant at 0.2 mM. The patterns shown in Figure 5 are typical of the breakpoint chlorination of ammonia.

The chlorination of 0.2 mM alanine is shown in Figure 6. Below a Cl_2 /alanine molar ratio of 1.0, chloramine and free chlorine were not produced. In this range, the predominant species is chloroalanine. The formation and decomposition of chloroalanine have been studied in detail by Stanbro and Smith (22). The decomposition products have been shown to be ammonia, acetaldehyde, carbon dioxide, and chloride ion. Above a Cl_2 /alanine molar ratio of 1.0, it appears that the ammonia produced from the chloroalanine was chlorinated to form chloramines.

These facts demonstrate that the chloroalanine does not permeate through the microporous PTFE membrane. Similar results as described above were observed with glycine, aspartic acid, glutamic acid, and lysine. The present method, therefore, is not interfered with by chloroamino acid and this suggests that inorganic chloramines (ammonia derived) and chloroamino acids (amino acid derived) may be distinguished, a condition that was proposed by Wolfe et al. (7) as necessary in the analysis of chlorine in water.

Application to a Water Purification Plant. The amount of chlorine in treated water is usually controlled at the Niwakubo water purification plant by measuring ammonia in the pretreated water and the residual chlorine at site B (as shown in Figure 2) with an amperometric analyzer. The present analyzer was operated at the plant beginning on December 1986 through March 1987. Water

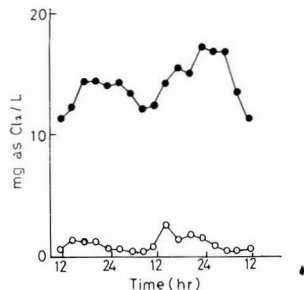


Figure 7. Diurnal variations of chloramines and free chlorine at site A (December 27-29, 1986). O, monochloramine; ●, dichloramine.

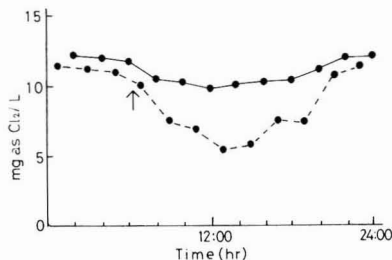


Figure 8. Dichloramine diurnal profiles at site A (—) and at site B (---) (January 29, 1987). Arrow marks the time of sunrise.

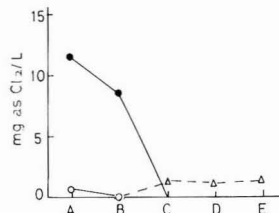


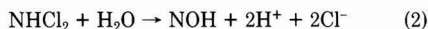
Figure 9. Site variations of mono-chloramine (O), dichloramine (●), and free chlorine (Δ) (December 6, 1986).

from each of the sampling sites (A-E as shown in Figure 2) was sampled without filtration.

Diurnal profiles for chloramines and free chlorine at site A are shown in Figure 7. The arrival time from the prechlorination point to site A is only 2 min. The concentration of ammonia in a pretreated water was 1.81 mg of N/L. Therefore, if all of the ammonia was converted to dichloramine, the concentration of dichloramine should be 18 mg of Cl_2 /L. The concentration of dichloramine was much higher than that of monochloramine and reached its maximum near midnight, while free chlorine was not detected. This suggests that the amount of chlorine is controlled prior to the breakpoint.

The diurnal profiles for dichloramine at sites A and B are shown in Figure 8. The hourly average for the amount of dichloramine was based on measurements performed every 15 min. Relatively high concentrations were observed during the night at both sites. In contrast, the concentrations were at a minimum near midday. It appears that the degradation of dichloramines is affected by sunlight, since the pH and the temperature of water were kept constant at 6.3 ± 0.1 and 8.1 ± 0.2 °C, respectively, during the day at both sites. It might be due to the difference in sunlight duration that the degradation of dichloramine at site B was higher than that at site A, since the arrival times from the prechlorination to sites A and B were 2 and 45 min, respectively.

Figure 9 shows the site variations of the measured chloramines and free chlorine. The amount of chloramines decreased with increasing arrival time from the pre-chlorination point. Free chlorine, on the other hand, appeared at site C and at the following sites where the chloramines disappeared. This suggests that dichloramines decompose only slightly to produce free chlorine. This phenomenon was reported by Wei and Morris (15), Saunier and Selleck (16), and Terashima and Ikawa (17). Wei and Morris proposed that dichloramine is decomposed by the following reactions:



The free chlorine (HOCl) produced from reaction 1 reacts rapidly with the monochloramine to give dichloramine according to the following reaction:



This can explain the fact that free chlorine appears after the decomposition of the monochloramine.

Conclusion

The present continuous flow method enables simultaneous determination of monochloramine, dichloramine, and free chlorine in water. The present method allows monitoring of mono- and dichloramine, which interfere with the conventional methods for determination of free chlorine. This is particularly advantageous in water purification plants.

Studies on the photodecomposition of chloramines and free chlorine using this method are now being carried out in detail, and the result will be published later.

Acknowledgments

We are grateful to Yasushi Kanda of the Chromato Science Co. for the construction of the present analyzer. We thank Masao Takenaka and Shoichi Kaji of the Water Works Department of Osaka Prefecture Government for agreeing to take samples. Acknowledgment is also given to Youichiro Nakamori for helping to obtain a part of the data.

Registry No. PTFE, 9002-84-0; water, 7732-18-5; chlorine, 7782-50-5; monochloramine, 10599-90-3; dichloramine, 3400-09-7.

Literature Cited

- (1) Cooper, W. J.; Sorber, C. A.; Meier, E. P. *J.—Am. Water Works Assoc.* **1975**, *67*, 34–39.
- (2) Guter, K. J.; Cooper, W. J.; Sorber, C. A. *J.—Am. Water Works Assoc.* **1974**, *66*, 38–48.
- (3) Moore, H. E.; Garmendia, M. J.; Cooper, W. J. *Environ. Sci. Technol.* **1984**, *18*, 348–353.
- (4) Ram, N. M.; Morris, J. C. *Environ. Int.* **1980**, *4*, 397–405.
- (5) Ram, N. M.; Malley, J. P., Jr. *J.—Am. Water Works Assoc.* **1984**, *76*, 74–81.
- (6) Isaac, R. A.; Morris, J. C. *Environmental Impact and Health Effects: Volume 3. Transfer of Active Chlorine between Nitrogenous Substances*; Ann Arbor Science: Ann Arbor, MI, 1980.
- (7) Wolfe, L. R.; Ward, R. N.; Olson, H. B. *Environ. Sci. Technol.* **1985**, *19*, 1192–1195.
- (8) Aoki, T.; Munemori, M. *Anal. Chem.* **1983**, *55*, 209–212.
- (9) Aoki, T.; Uemura, S.; Munemori, M. *Environ. Sci. Technol.* **1986**, *20*, 515–517.
- (10) Aoki, T. *Anal. Lett.* **1988**, *21*, 835–842.
- (11) Zhang, D.; Aoki, T.; Munemori, M. Proceedings of the 49th Annual Meeting of the Japan Chemical Society, 1984; p 230.
- (12) Chapin, R. M. *J. Am. Chem. Soc.* **1931**, *53*, 912–920.
- (13) Isaac, R. A.; Morris, J. C. *Environ. Sci. Technol.* **1983**, *17*, 738–742.
- (14) Trofe, W. T.; Inman, W. G., Jr.; Johnson, J. D. *Environ. Sci. Technol.* **1980**, *14*, 544–549.
- (15) Wei, W. I.; Morris, J. C. In *Chemistry of Water Supply Treatment and Distribution*; Rubin, A. J., Ed.; Ann Arbor Science: Ann Arbor, MI, 1974; pp 297–332.
- (16) Saunier, M. B.; Selleck, E. R. *J.—Am. Water Works Assoc.* **1979**, *71*, 164–172.
- (17) Terashima, K.; Ikawa, K. *Jpn. Water Works Assoc.* **1983**, *52*, 33–42.
- (18) Trofe, W. T.; Inman, G. W.; Johnson, J. D. *Environ. Sci. Technol.* **1980**, *14*, 544–549.
- (19) Inman, G. W.; Johnson, J. D. *Environ. Sci. Technol.* **1984**, *18*, 219–224.
- (20) Szabo, Z. G.; Csanyi, L. *Anal. Chim. Acta* **1952**, *6*, 208–211.
- (21) Carpenter, J. H.; Macalady, D. L. *Environmental Impact and Health Effects: Chemistry of Halogens in Sea Water*; Ann Arbor Science: Ann Arbor, MI, 1978; Vol. 1.
- (22) Stanbro, D. W.; Smith, D. W. *Environ. Sci. Technol.* **1979**, *13*, 446–450.

Received for review September 3, 1987. Revised manuscript received May 13, 1988. Accepted May 20, 1988.

Transport of Microspheres and Indigenous Bacteria through a Sandy Aquifer: Results of Natural- and Forced-Gradient Tracer Experiments

Ronald W. Harvey* and Leah H. George

U.S. Geological Survey, Water Resources Division, Menlo Park, California 94025

Richard L. Smith

U.S. Geological Survey, Water Resources Division, Arvada, Colorado 80002

Denis R. LeBlanc

U.S. Geological Survey, Water Resources Division, Boston, Massachusetts 02114

■ Transport of indigenous bacteria through sandy aquifer sediments was investigated in forced- and natural-gradient tracer tests. A diverse population of bacteria was collected and concentrated from groundwater at the site, stained with a DNA-specific fluorochrome, and injected back into the aquifer. Included with the injectate were a conservative tracer (Br^- or Cl^-) and bacteria-sized (0.2–1.3- μm) microspheres having carboxylated, carbonyl, or neutral surfaces. Transport of stained bacteria and all types and size classes of microspheres was evident. In the natural-gradient test, both surface characteristics and size of microspheres affected attenuation. Surface characteristics had the greatest effect upon retardation. Peak breakthrough of DAPI-stained bacteria (forced-gradient experiment) occurred well in advance of bromide at the more distal sampler. Transport behavior of bacteria was substantially different from that of carboxylated microspheres of comparable size.

Introduction

Transport of bacteria through groundwater has long been a concern to Public Health officials (1) and is becoming an increasingly important issue in waste management. In addition to the biological contamination of water supply wells, transport of bacteria may result in the "seeding" of aquifer sediments downgradient of contamination sources with bacteria acclimated to and capable of degrading refractory organic compounds. Degradation of highly mobile and persistent organic contaminants in aquifer sediments may be further enhanced by cotransport with free-living (unattached) bacteria. Therefore, transport of bacteria may have implications not only to placement of water supply wells but to practices of groundwater recharge using direct injection of waste water, to on-land disposal of organic wastes, and to a number of proposals for in situ biological treatment of organically contaminated aquifers. Models have been developed that describe transport of bacteria through porous media (2, 3), but experimental data are scarce.

We describe here a study on the transport of indigenous groundwater bacteria through sandy aquifer sediments. Many aspects of this problem are best investigated in the field, since sediment columns in the laboratory cannot duplicate actual structure of aquifer sediments (4). Findings from an earlier investigation suggested that transport of bacteria affected bacterial distribution within a plume of organically contaminated groundwater (5). The first objective of this study was to examine transport of bacteria under more controlled conditions. To accomplish this, morphologically diverse populations of bacteria were collected and concentrated from the contaminant plume, labeled with a DNA-specific fluorescent marker, reintroduced into aquifer sediments, and monitored as they

Table I. Test Parameters and Conditions for Small-Scale Transport Experiments

parameters	forced gradient		natural gradient
	sampler A	sampler B	
Groundwater Conditions			
ambient flow, m/day	0.3–0.5		0.3–0.5
temperature, °C	10 ± 2		11 ± 2
conductivity, μS	60		345
dissolved oxygen, mg/L	9		<0.1
DOC, mg/L	<1		1–2
Injection			
volume, L	200		75
rate, L/min	95		0.5
duration, h	0.03		2.5
bromide, mg/L	1525		
chloride, mg/L			1425
Tracer Breakthrough ^a			
bromide, mg/L	187	34	
chloride, mg/L			100
C/C ₀	0.123	0.022	0.065
time, days	0.04	0.27	21
av velocity, m/day	41	12	0.33

^a At peak concentrations.

moved downgradient. Several types and sizes of well-characterized, bacteria-sized fluorescent microspheres were employed to simultaneously investigate potential effects of surface characteristics and cell size upon transport of bacteria. A second objective was to assess the suitability of the microspheres as analogues for bacteria in transport experiments.

Methods

Injection Tests. Two types of small-scale, groundwater tracer experiments were employed to examine transport of bacteria and bacteria-sized microspheres through a sandy, freshwater aquifer on Cape Cod, MA. A divergent (forced-gradient) test was run in June 1986 at U.S. Geological Survey well site F393, and a natural-gradient test was run in October 1986 at well site F347. The aquifer sediments, which were deposited in layers as glacial outwash, contain little clay and are composed largely of quartz and feldspar. Mean grain size, average porosity, and hydraulic conductivity are ~0.5 mm, 0.38, and ~0.1 cm/s, respectively (6). Groundwater conditions and test parameters are listed in Table I.

In the forced-gradient experiment, a radially divergent flow field was formed by continuous pumping of groundwater from a supply well (50 m downgradient) into an injection well, which was screened 10.0–11.2 m below land surface (BLS) (Figure 1A) in an area of uncontaminated groundwater (7). Depth to water was ~5 m. The injectate

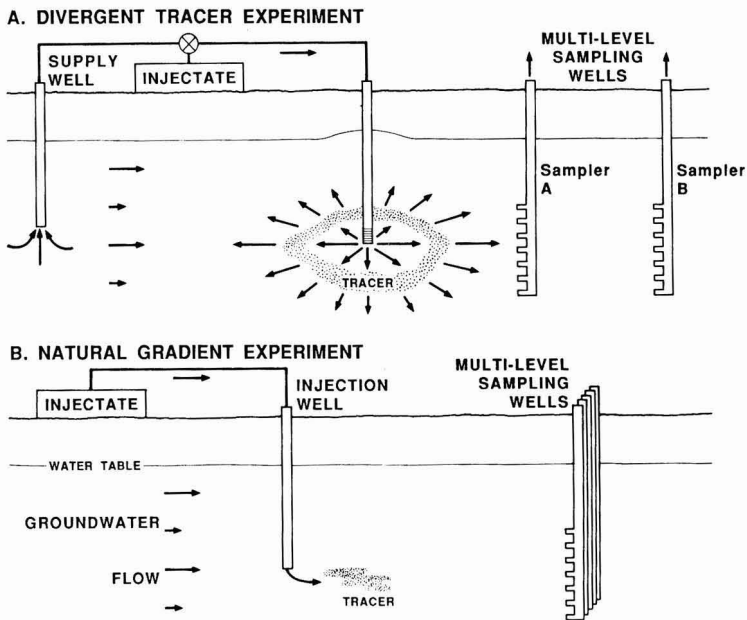


Figure 1. Schematic representation of the divergent (forced-gradient) (A) and natural-gradient (B) groundwater tracer tests.

was added as a short pulse to the injection stream. Stained groundwater bacteria, 0.2-, 0.7-, and 1.2- μm (diameter) fluorescent, carboxylated microspheres (Polysciences, Warwick, PA), and a conservative tracer (bromide) were monitored as they moved with the radial flow past multilevel sampling devices (MLSD) located 1.7 (sampler A) and 3.2 m (sampler B) from the injection well. The MLSD were constructed from 3.2-cm (diameter) poly(vinyl chloride) (PVC) pipe that encase a number of screened, 6.5-mm (diameter) polyethylene (PE) tubes. The PE tubes exit the PVC pipe into surrounding aquifer sediments along a vertical transect at $\sim 0.3\text{-m}$ intervals. Groundwater samples (500 mL from 11.3 m BLS) were taken every 5 min at sampler A and every 15 min at sampler B. The sampled layer was opposite the injection interval and was where bromide breakthrough was most significant in a previous test (7).

In the natural-gradient tracer experiment, fluorescent, bacteria-sized microspheres of differing types and diameters and chloride (used as a conservative tracer) were injected into the plume of contaminated groundwater (6) 500 m downgradient from a treated-sewage infiltration bed. Microspheres in the 0.23, 0.53, 0.91, and 1.35- μm (diameter) size class were composed of carboxylated latex. Microspheres in the 0.6- μm size class were plain latex and had uncharged surfaces. The 0.84- μm microspheres were polyacrolein and had carbonyl surface groups. The microspheres and chloride were added slowly to the aquifer at 8.5 and 9.1 m BLS and monitored as they moved with the natural groundwater flow past a row of MLSD (6.9 m downgradient) set perpendicular to the direction of groundwater (Figure 1B). Groundwater samples (500 mL) were collected at 1-day intervals from a sampling port 9.1 m BLS. Earlier tests with chloride (unpublished data) guided selection of the MLSD and sampling depth. During both natural- and forced-gradient tracer tests, measurements of conservative tracers at several ports ensured that samples were collected at appropriate times and depths to capture maximum breakthrough of microspheres and, in the forced-gradient test, bacteria.

Bacteria. A stainless steel submersible pump (Model SP81; Keck Geophysical Instruments, Inc., Okemos, MI) connected to Teflon tubing was used to collect groundwater from a screened, PVC observation well (5.0-cm diameter, 250- μm slot width) located 250 m (1.6 years groundwater travel time) downgradient from an on-land, treated-sewage infiltration bed. A morphologically diverse population of bacteria was concentrated on-site from 1000 L of collected groundwater into 1–2 L using a stacked-sheet, tangential-flow filtration device (Pelicon model concentrator, Millipore Corp., Bedford, MA). Recovery of bacteria was somewhat low (18%), likely due to irreversible entrapment of bacteria on the filters. Recovered bacteria (largely rod-shaped, 0.2–1.6 μm long) were stained with the fluorochrome, 4',6-diamidino-2-phenylindole (DAPI; Sigma Chemical Co., No. D1388) at 5 μM (final concentration) for 3 h and added to 200 L of uncontaminated groundwater to dilute the stain below its threshold staining concentration. Stained bacteria were injected back into the aquifer after being held for 24 h at 4 $^{\circ}\text{C}$. Samples collected downgradient were kept at 4 $^{\circ}\text{C}$, and counts of DAPI-stained bacteria were made within 48 h.

Analyses. Bromide (forced-gradient tracer test) was measured in the field with a specific ion electrode and later in the laboratory by ion chromatography (Waters Model ILC-1 ion/liquid chromatograph; Waters ICP-A column with borate gluconate buffer at 1.2 mL/min and 25 $^{\circ}\text{C}$). Chloride (natural-gradient tracer test) was measured with a specific ion electrode, which had been calibrated with a chlorimeter. Preparations for enumeration of DAPI-stained bacteria and fluorescent microspheres were made with 100–200 mL of sample in order to obtain good counting statistics. The DAPI-stained bacteria and carboxylated microspheres in these samples both fluoresced under incident UV and/or blue light and were differentially enumerated on black Nuclepore filters (0.2- μm pore size, 25-mm diameter) with a Leitz Dialux 20 microscope, fitted for epifluorescence as described by Harvey et al. (8). DAPI-stained bacteria and 0.7- μm (diameter) carboxylated microspheres (forced-gradient test) and 0.91- and 0.5- μm

Table II. Relative Breakthrough, Maximum Dimensionless Concentration, Retardation Factor, and Attenuation for Bacteria and Different Size Classes of Carboxylated Microspheres in the Forced-Gradient Test (Sampler A)

diam, μm	type	RB, %	$(C/C_0)_{\text{max}}$	RF ^a	atten, %
0.2	microsphere	0.01	2.7×10^{-6}	NC	99.9
0.7	microsphere	0.01	5.2×10^{-6}	NC	99.9
1.2	microsphere	0.01	7.8×10^{-6}	NC	99.9
0.2-1.6	bacteria	0.74	7.8×10^{-4}	~ 1.0	99.3
		2.61 ^b	6.3×10^{-6}	0.8 ^b	97.4

^aNC, not calculated because time of peak breakthrough could not be determined accurately. ^bSampler B.

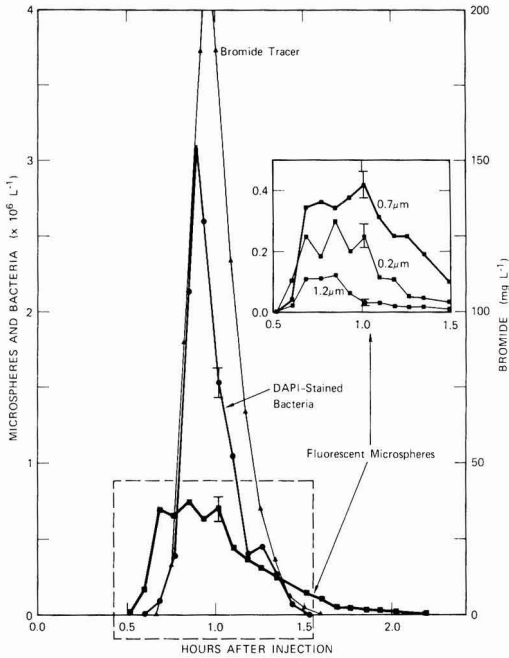


Figure 2. Concentration histories for bromide, DAPI-stained bacteria, and fluorescent microspheres (0.2, 0.7, and 1.2- μm diameter) at the closest sampler in the forced-gradient test.

(diameter) carboxylated microspheres (natural-gradient test) were counted under UV excitation (340–380 nm). Microspheres in other size classes were counted under incident blue light (390–490 nm).

Transport of bacteria and microspheres was evaluated from observed concentration histories (C vs time at sampling points downgradient) and from the following parameters: maximum dimensionless concentration, relative breakthrough, attenuation, and retardation. Maximum dimensionless concentration, $(C/C_0)_{\text{max}}$, was calculated as the ratio of the highest concentration observed in samples collected downgradient to that present in the injectate. Relative breakthrough for bacteria and each class of microsphere was calculated as the integral of dimensionless concentration history normalized to that of the conservative tracer:

$$\% \text{ RB} = \left[\frac{\int_{t_0}^{t_f} \frac{C(t)}{C_0} dt}{\int_{t_0}^{t_f} \frac{[\text{Tr}]_t}{[\text{Tr}]_0} dt} \right] \times 100$$

where C_0 and $[\text{Tr}]_0$ are microsphere and tracer (Cl⁻ or Br⁻) concentrations in the injectate, $C(t)$ and $[\text{Tr}]_t$ are concentrations at time t , and t_0 and t_f are elapsed times from injection to the beginning and end of breakthrough. The percentage of bacteria and microspheres that were immobilized during transport through aquifer sediments, referred to herein as attenuation, was calculated as $100 - \% \text{ RB}$. Retardation factors (RF) were calculated as ratios of time required to reach peak abundance for the microspheres or bacteria to time to peak concentration for the conservative tracer.

Results

Forced-Gradient Test. Concentration histories of carboxylated microspheres, DAPI-stained bacteria, and bromide for sampler A are shown in Figure 2. Concentration histories for DAPI-stained bacteria and bromide

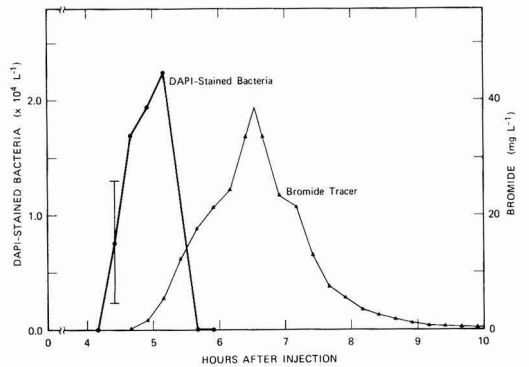


Figure 3. Concentration histories for bromide and DAPI-stained bacteria at the more distal sampler in the forced-gradient test.

were remarkably similar. Peak abundances of both bromide and stained bacteria occurred 0.9–1.0 h after injection. Also, both concentration histories exhibited single peaks and declines to undetectable levels ~ 1.6 h after injection. However, the center of mass of bromide appeared to lag marginally behind that of the stained bacteria. The portion of total breakthrough occurring within the first hour following injection was 66% for DAPI-stained bacteria as compared to 55% for bromide.

Concentration histories for the microspheres differed substantially from those of bacteria and bromide. Carboxylated microspheres [0.2, 0.7, and 1.2 μm (diameter); Figure 2 inset] reached near-maximal abundance before bromide was detected and were present at least 30 min after bromide and stained bacteria had declined to undetectable levels. Microspheres appearing before and after detectable breakthrough of bacteria and bromide accounted for $\sim 15\%$ of total breakthrough. Microspheres were attenuated by aquifer sediments to a greater degree than the bacteria (Table II). Values of $(C/C_0)_{\text{max}}$ were ~ 100 , 150, and 290-fold lower for the 1.2, 0.7, and 0.2- μm (diameter) microspheres, respectively, as compared with stained bacteria in spite of the overlap in size. Relative breakthrough of the microspheres was ~ 70 –200-fold lower than for the bacteria.

Concentration histories of bacteria and bromide appearing at sampler B are depicted in Figure 3. Although numbers of DAPI-stained bacteria at this more distal sampler were near the lower level of detection, peak abundance of stained bacteria appeared to precede the maximum concentration of bromide by ~ 1 –2 h. However, there was still substantial overlap in the concentration histories. Microspheres were detected in samples collected at sampler B, but were below levels required for quantification. Peak abundances of bromide and stained bacteria declined 5- and 113-fold, respectively, relative to break-

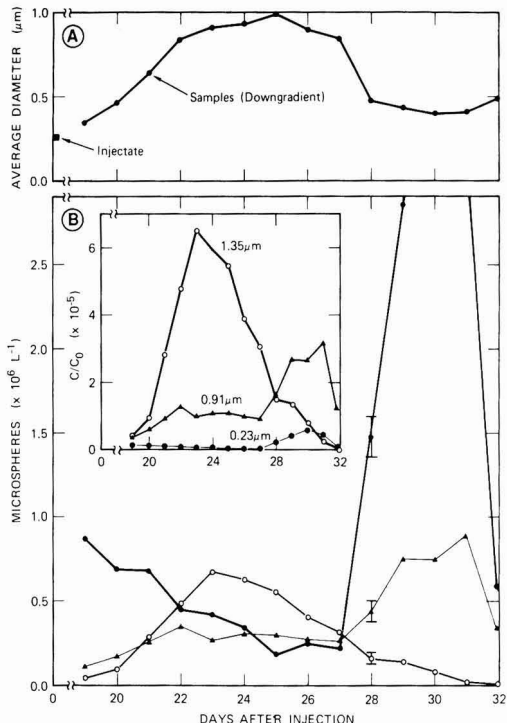


Figure 4. Average microsphere diameter (A) and concentration histories (B) for 0.23, 0.91, and 1.35- μm diameter carboxylated microspheres in the natural-gradient test. Dimensionless concentration history is depicted in the inset.

Table III. Relative Breakthrough, Maximum Dimensionless Concentration, Retardation Factor, and Attenuation for Different Size Classes and Compositions of Microspheres in the Natural-Gradient Test

diam, μm	type	RB, %	$(C/C_0)_{\text{max}}$	RF	atten, %
0.23	carboxylated	0.01	5.9×10^{-6}	1.4	99.9
0.53	carboxylated	0.04	4.4×10^{-5}	1.4	99.9
0.91	carboxylated	0.06	2.7×10^{-5}	1.4	99.9
1.35	carboxylated	0.12	6.5×10^{-5}	1.1	99.8
0.6	uncharged	0.05	1.1×10^{-5}	~ 1.0	99.9
0.85	polyacrolein	3.11	2.3×10^{-3}	1.3	96.9

through at the closest sampler.

Natural-Gradient Test. Concentration histories for 0.23, 0.91, and 1.35- μm (diameter) carboxylated microspheres at 6.9 m downgradient from the injection well are shown in Figure 4B. Values of $(C/C_0)_{\text{max}}$ and relative breakthrough for the carboxylated microspheres generally increased with sphere diameter and were, respectively, 11- and 17-fold higher for the largest as compared with the smallest size class. However, attenuation in aquifer sediments between injection well and MLSD was $\geq 99.8\%$ for all size classes. The increase in relative breakthrough with increasing microsphere diameter resulted in a large average microsphere size (up to 1.0- μm diameter) in samples collected downgradient as compared to the injectate population (0.3 μm) (Figure 4A).

The effects of surface characteristics upon retardation and attenuation during transport for the 0.5–0.8- μm size classes of microspheres are depicted in Figure 5 and Table III. Peak abundance of uncharged latex microspheres came within 1 day of maximum chloride breakthrough. However, the maximum breakthrough of the polyacrolein

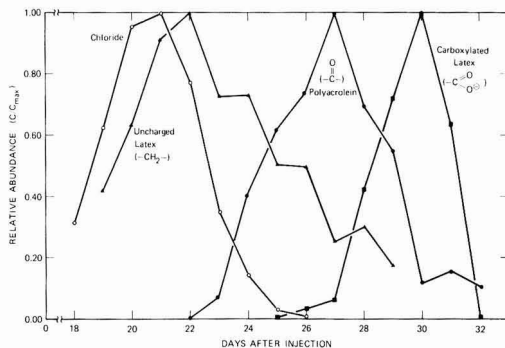


Figure 5. Concentration histories for chloride, uncharged latex (0.53- μm -diameter), polyacrolein (0.84- μm -diameter), and carboxylated latex (0.53- μm -diameter) microspheres in the natural-gradient test. Data have been normalized to maximum concentrations.

(carbonyl surface groups) and carboxylated latex microspheres was significantly retarded; peak abundances of the carboxylated latex and polyacrolein microspheres were retarded by 8 and 5 days, respectively, relative to the uncharged latex spheres. Little overlap in breakthrough of uncharged and carboxylated microspheres was observed. Retardation (relative to chloride) of peak breakthrough for the carboxylated microspheres was 9–10 days, with the exception of the 1.35- μm (diameter) spheres (2 days retardation). The difference in retardation between types of microspheres does not appear to result from size differences, because peak breakthrough of 0.23-, 0.53-, and 0.91- μm -diameter carboxylated microspheres occurred at approximately the same time.

Values of relative breakthrough, attenuation, and $(C/C_0)_{\text{max}}$ also varied among types of microspheres in the 0.5–0.8- μm size classes (Table III). Relative breakthroughs for carboxylated and uncharged latex microspheres were similar (0.04 vs 0.05, respectively), but were ~ 60 – 80 -fold lower than that for the polyacrolein microspheres. Attenuation of uncharged and carboxylated microspheres was $>99\%$, but $\sim 97\%$ for the polyacrolein microspheres.

Discussion

Bacteria. The appearance of DAPI-stained bacteria at sampler B in the forced-gradient experiment (Figure 3), in spite of the high degree of forced dispersion resulting from radially divergent flow, suggests that transport of bacterial populations through porous aquifers is possible. Earlier breakthrough of the DAPI-stained bacteria relative to bromide further suggests that this transport can be relatively rapid and that there may be some sort of chromatographic effect. Size exclusion chromatography involving preferential exclusion of bacteria from smaller, more tortuous pores between sediment particles would result in a more direct average path of travel for the unattenuated (nonadsorbed and unfiltered) bacteria. Hydrodynamic chromatography may also play a role, since bromide, on the basis of size, would be subjected to the effects of particle surface roughness to a greater degree than the stained bacteria.

Bacterial motility was not a factor in the transport and early breakthrough of DAPI-stained bacteria. This is because the short duration (10 h) of the forced-gradient test would not have allowed for chemotaxis to account for the differences in breakthrough relative to bromide. Also, bacterial motility would be expected to be random in the absence of chemical gradients. However, it has been demonstrated that in the presence of nutrient gradients

some bacteria can move by chemotaxis fairly quickly (up to 0.5 cm h^{-1}) through porous rock of low permeability (9). Therefore, motility may be an important process in long-term transport of bacteria in highly contaminated porous aquifers. Our results here indicate that even in the absence of strong chemical gradients unattenuated bacteria may be transported more quickly than a conservative tracer, simply on the basis of size.

Faster transport relative to a chemical tracer has also been observed in several tracer experiments involving microorganisms not indigenous to aquifers. For example, hydrogen sulfide producing strains of *Escherichia coli* were found to move through a New Zealand aquifer more quickly than rhodamine WT dye (10), and it has recently been observed that nonadsorbed viruses appear to travel through aquifer sediments about 1.5–1.9 times faster than halide tracers (C. Gerba, personal communication). Peak breakthrough of 2–3- μm -diameter yeast cells, *Saccharomyces cerevisiae*, injected into a sand and gravel aquifer in Florida, occurred before that of bromide and iodide (11), and it was believed that many of the yeast cells traveled through channels in the sand and gravel aquifer rather than through intergranular pores. The potential importance of secondary pore structure in the enhancement of microorganism transport through the subsurface can be inferred from results of column experiments, where up to 100-fold greater recovery of *E. coli* traveling through intact soil columns as compared with columns of repacked soil were observed (12).

The degree to which indigenous bacterial populations are transported through contaminated aquifers may be substantially greater than for nonindigenous populations. This is because growth of native bacteria during transport would, in part, compensate for their removal due to sorption/biological adhesion to particle surfaces, filtration (straining), predation by protozoa, and lysis. The effect of growth rate upon transport was not assessed in these experiments, since DAPI intercalates among the nucleic acid bases within the bacteria and thus impairs cell metabolism. However, measured in situ bacterial growth rates in the 5-km-long contaminant plume where the natural-gradient experiment was run range from $0.005 \pm 0.002 \text{ h}^{-1}$ in the more distal portion of the plume to $0.042 \pm 0.005 \text{ h}^{-1}$ near the source of contamination (13). At the higher growth rate, average generation time would be less than 17 h and would more than offset expected rates of attenuation occurring during transport. DAPI-stained bacteria were not employed in the natural-gradient experiment, since the stability of intracellular DAPI over the duration of the experiment was not known. However, if attenuation of bacteria relative to 1- μm -diameter carboxylated microspheres were the same in the natural-gradient experiment as in the forced-gradient experiment, total attenuation at 6.9 m downgradient in the former experiment would account for losses of $\sim 90\%$ of the bacteria injected. This estimate assumes no growth of the stained bacteria. Since this rate of attenuation would preclude a nongrowing bacterial population from being transported more than 100 m through aquifer sediments at Cape Cod, abundance of readily degradable dissolved organic carbon (DOC), which controls growth, may be one of the most important determinants of transport of the indigenous populations.

Abundance of DOC in highly contaminated aquifers may also affect bacterial size and propensity for solid surface attachment. Several studies suggest that, under severe nutrient limitation, a number of bacteria exhibit decreases in cell size and an increased adhesion to solid surfaces, where organic matter is more abundant (14–16). There-

fore, increased levels of utilizable organic matter should be accompanied by enhanced transport of bacteria in aquifer sediments. This is because larger, less surface-active bacteria would have a lesser tendency to contact and sorb onto particles. Transport of indigenous bacterial populations would appear to be greatest in heavily contaminated aquifers where growth rates are relatively high and attenuation in aquifer sediments relatively low.

Microspheres. The lower relative breakthrough and greater dispersion of the 0.2–1.2- μm (diameter) carboxylated microspheres relative to the fluorochrome-labeled bacteria of similar size in the forced-gradient injection experiment (Figure 2, Table II) suggest greater interaction between the microspheres and aquifer sediment particles. Interactions with sediment particles may also explain retardation in peak breakthrough, relative to chloride, for neutral latex and polyacrolein microspheres in the natural-gradient experiment (Table III). The greater dispersion of carboxylated microspheres relative to bacteria suggests carboxylated microspheres behave quite differently during transport through the aquifer than bacteria. However, since these microspheres are stable over time and for a given size class have a fairly tight size distribution and uniform and well-characterized surface characteristics, they can be used to obtain information involving abiotic transport processes.

The inverse relationship between size of the carboxylated microspheres and attenuation within permeable aquifer sediments in both natural and forced-gradient experiments can be predicted from colloid filtration theory (17). This model predicts that smaller microspheres within the bacterial size range should contact and therefore sorb to stationary surfaces in porous media with greater frequency because of their higher rates of diffusion or Brownian motion. Although there are a number of uncertainties in applying this model developed for wastewater-filter applications to bacteria removal in porous aquifers, there does appear to be an optimal size range for transport in the micron class. Our most recent natural-gradient tracer experiments (unpublished data) with neutral latex microspheres in the 1-, 3-, and 6- μm size classes suggest that optimal size for transport at our site may be as much as several microns. This has important implications for transport through aquifer sediments of at least the smaller protozoa (18) that prey upon groundwater bacteria.

Within the bacterial size range, microsphere size (0.2–1.4 μm) did not appear to be the primary determinant of retardation in these experiments. The only substantial difference in retardation among size classes of carboxylated microspheres occurred in the natural-gradient experiment (Figure 4) where peak breakthrough of 1.35- μm microspheres occurred first. However, there is evidence to suggest more rapid transport of larger microorganisms through aquifer sediment than smaller microorganisms. For example, it has been reported that *E. coli* injected simultaneously with coliphage f2 into an aquifer in a forced-gradient tracer test broke through at an observation well 150 m downgradient well in advance of the smaller virus (19), and a capsulated strain of *Klebsiella aerogenes* was observed to be transported through the aquifer more rapidly than a smaller noncapsulated strain (20). However, it cannot be assumed that differences in retardation of microbial transport through aquifer sediments can be explained totally on the basis of cell size, since the influence of surface characteristics was not known.

Surface characteristics of microspheres had a marked effect upon retardation during transport in the natural

gradient experiment (Table III, Figure 5). The relationship between microspheres' composition and retardation is complex, since microspheres can interact with both dissolved organic material (DOM) and aquifer sediment particles. That carboxylated latex microspheres were retarded the most and neutral latex microspheres the least may be attributed to differences in surface charge; carboxylated latex spheres have a stronger net negative surface charge at groundwater pH (6-7) and, consequently, should be influenced to a greater degree by surface charges (both positive and negative) on sediment particles. The neutral latex microspheres are likely to acquire a slight surface charge, due to adsorption of DOM. However, levels of DOC in groundwater at the test site are low (Table I). Surfaces of neutral spheres would be expected to be less reactive than those of the moderately retarded (RF = 1.3) polyacrolein spheres, which have carbonyl surface groups.

In general, there appeared to be no clear relationship between attenuation (immobilization within aquifer sediments) and retardation (slowing down of transport). In some cases, microspheres that were transported more slowly were subject to less attenuation (Table III). In the forced-gradient injection experiment with *E. coli* and f2 coliphage described by Gerba and Bitton (19), attenuation was substantially greater for the bacterium than for the virus even though the virus took longer to arrive at the sampling well downgradient. The reasons for this are unclear and the in situ decay rates for the two nonendemic microorganisms were likely quite different. However, it is clear that increased retardation does not necessarily lead to a greater removal of microorganisms. Although increased contact with aquifer sediments occurring as a result of increased retardation should allow for greater opportunities to sorb onto solid surfaces, our results with bacteria-sized microspheres suggest that attenuation and retardation can vary independently. It also appears that bacterial surface characteristics may play a bigger role in retardation in some highly porous aquifer sediments than the size of the microbe.

In summary, transport of bacteria through organically contaminated aquifers appears to be possible. Bacterial growth rate would appear to be an important factor in determining how far indigenous bacteria may be transported. At the higher in situ growth rates ($0.03-0.04 \text{ h}^{-1}$) reported for the contaminant plume at Cape Cod (13), some bacteria may be transported over 1000 m. None of the fluorescent, bacteria-sized microspheres that we tested appeared to be useful as tracers of bacteria in groundwater injection experiments. Although they are easy to detect, and reasonably well-defined, their transport behavior differed substantially from that of bacteria. Also, they do not account for bacterial growth, which can be substantial in highly contaminated aquifers. We are presently modifying the surfaces of selected microspheres so that the degrees of retardation, dispersion, and attenuation that occur during their transport through porous media will be closer to those observed for bacteria. The effects of nu-

trient and geohydrologic conditions upon transport of indigenous bacteria and how this transport affects degradation of organic compounds in contaminated aquifers have not been well studied and are subjects worthy of further study.

Acknowledgments

We thank C. Quadri, K. Hess, S. Garabedian, J. Duff, and M. Ceazan (U.S. Geological Survey) and B. Howes (Woods Hole Oceanographic Institute) for their assistance with the tracer tests and J. Rubin and T. Rees for their helpful comments on the manuscript. Discussion with P. Roberts (Stanford U.) and C. O'Melia (Johns Hopkins U.) concerning filtration theory is also gratefully acknowledged.

Literature Cited

- (1) Keswick, B. H. In *Groundwater Pollution Microbiology*; Bitton, G., Gerba, C. P., Eds.; Wiley: New York, 1984; pp 59-64.
- (2) Yavuz Corapcioglu, Y.; Haridas, A. J. *Hydrol. (Amsterdam)* 1984, 72, 149.
- (3) Yavuz Corapcioglu, Y.; Haridas, A. *Adv. Water Resour.* 1985, 8, 188.
- (4) McDowell-Boyer, L. M.; Hunt, J. R.; Sitar, N. *Water Resour. Res.* 1986, 22, 1901.
- (5) Harvey, R. W.; George, L. H.; Smith, R. L.; LeBlanc, D. R.; Garabedian, S. P.; Howes, B. L. In *Open-File Report 87-109*; U.S. Geological Survey: Reston, VA, 1987; pp B29-31.
- (6) LeBlanc, D. R. In *Open-File Report 84-475*; U.S. Geological Survey: Reston, VA, 1984; pp 1-46.
- (7) Garabedian, S. Ph.D. Dissertation, Massachusetts Institute of Technology, Cambridge, MA, 1987.
- (8) Harvey, R. W.; Smith, R. L.; George, L. *Appl. Environ. Microbiol.* 1984, 48, 1197.
- (9) Jenneman, G. E.; McInerney, M. J.; Knapp, R. M. *Appl. Environ. Microbiol.* 1985, 50, 383.
- (10) Pyle, B. H. *Lincoln College Department of Agricultural Microbiology Tech. Publ. No. 2*; Canterbury, New Zealand, 1979.
- (11) Wood, W. W.; Ehrlich, G. G. *Ground Water* 1978, 16, 398.
- (12) Smith, M. S.; Thomas, G. W.; Ritonga, D. *J. Environ. Qual.* 1985, 14, 87.
- (13) Harvey, R. W.; George, L. H. *Appl. Environ. Microbiol.* 1987, 53, 2992.
- (14) Fletcher, M.; Marshall, K. C. *Adv. Microb. Ecol.* 1982, 6, 199.
- (15) Dawson, M. P.; Humphrey, B. A.; Marshall, K. C. *Curr. Microbiol.* 1981, 6, 195.
- (16) Kjelleberg, S.; Humphrey, B. A.; Marshall, K. C. *Appl. Environ. Microbiol.* 1982, 43, 1166.
- (17) Yao, K. M.; Habibian, M. T.; O'Melia, C. R. *Environ. Sci. Technol.* 1971, 5, 1105.
- (18) Sinclair, J. T.; Ghiorse, W. C. *Appl. Environ. Microbiol.* 1987, 53, 1157.
- (19) Gerba, C. P.; Bitton, G. In *Groundwater Pollution Microbiology*; Bitton, G., Gerba, C. P., Eds.; Wiley: New York, 1984, pp 66-88.
- (20) Bitton, G.; Lahav, N.; Henis, Y. *Plant Soil* 1974, 40, 373.

Received for review December 29, 1987. Accepted June 28, 1988.

On the Distribution of Atmospheric Polychlorinated Biphenyl Congeners between Vapor Phase, Aerosols, and Rain

J. C. Duinker* and F. Bouchertal

Institute for Marine Science, University of Kiel, Düsternbrookerweg 20, 2300 Kiel, Federal Republic of Germany

■ Fourteen chromatographically well-separated PCB congeners were analyzed in filtered air, in particulates, and in rain collected simultaneously in an urban area. The PCB mixture was dominated by congeners with a low degree of chlorination in the filtered air and by congeners with a high degree of chlorination in the aerosols and in rain. The vapor phase represented up to 99% of total atmospheric concentrations for the most volatile congeners. Particle scavenging was the dominant source of PCBs in rain, despite the small contribution (only 1 or 2%) of particulate PCBs to the total atmospheric concentration.

Introduction

Atmospheric transport is an important pathway for the transfer of polychlorinated biphenyls (PCBs) from land to natural waters. For instance, 60-90% of the PCB burden in the Great Lakes system has been estimated to originate from the atmosphere (1, 2), and deposition from the atmosphere may be the main source of PCBs in remote oceanic regions (3-5).

Reliable information on the concentrations in the vapor phase, in aerosols, and in precipitation is essential for transport models and for estimates of wet and dry deposition rates. The acquisition of reliable field data is hampered by several technical and analytical problems. Doskey and Andren (6) have summarized these difficulties: (1) the operational distinction of vapor and particulate fractions with the use of a filter to retain particles and a backup adsorbent to collect vapor-phase constituents in high-volume sampling systems may result in desorption from particles collected on the filter; (2) the usual adsorbents are less effective for collecting the more volatile compounds from the vapor phase; and (3) common analytical chemical methods are inadequate to identify and quantitate the compounds present in the samples as well-defined chemical entities.

Recently, we described the properties of glass beads with strongly improved efficiency for adsorption of relatively volatile PCB fractions. This was established with the use of high-resolution gas chromatography (GC) on a single SE-54 column and electron capture detection (ECD) (7). The use of high-resolution multidimensional GC (MDGC-ECD) techniques (8) allows the identification of those congeners that can and of those that cannot be determined accurately by GC-ECD with the use of a single (SE-54) capillary column.

We have applied these techniques to determine several PCB congeners in atmospheric samples in order to get a better estimate of vapor-particulate partitioning of PCBs than has been possible before. In order to correlate the qualitative and quantitative aspects of the PCB mixtures in vapor, aerosols, and rain, these compartments were sampled simultaneously.

Experimental Section

The samples were taken on the roof of the building of the Institute for Marine Research in city of Kiel (western Baltic). Particulate matter was collected by filtering air (20-40 m³) through 7-cm-diameter glass-fiber filters (Whatman GF/F, 10 dm³ min⁻¹) during rainfall only.

Wind direction deviated not more than 20° from the main wind direction during that period (Table I). The filtered air was drawn through a stainless steel column filled with glass beads as adsorbent material, sampling PCB congeners of low as well as high degrees of chlorination (7, 9). An identical system was placed at 50-cm distance from the sampling system. Its content was analyzed along with the actual sample. It served as a procedural blank. Filters and glass beads were extracted with 100 cm³ of dichloromethane and treated further as described earlier (7).

Rain was sampled at the same time in glass vessels (30-cm opening). The vessel was open during rainfall only. The unfiltered rain samples were extracted three times with CH₂Cl₂ within 1 h after the rain had stopped.

All extracts were concentrated to ~100 μL under vacuum at <3 °C and separated into fractions by silica gel column chromatography. The first fraction (eluted with *n*-hexane) contained all PCB congeners. Compounds were identified and quantitated by temperature-programmed capillary column GC-ECD using a fused silica column (0.15 μm SE-54, 0.20 mm i.d.) and a ⁶³Ni ECD.

Practically all peaks in the sample chromatograms correspond to a peak in Clophen A30 and/or Clophen A60, with different relative heights, however (Figure 1).

Several peaks in commercial mixtures and environmental samples may consist of two or more congeners (10, 11). A newly developed technique was used to determine which congeners elute as well-resolved peaks from an SE-54 column and which ones have one or more coeluting congeners. On the basis of this information, those congeners were selected for analysis which elute from the column as well-separated peaks (for no. 153, a relatively small contribution from the coeluting congener 132 and a still smaller contribution from no. 105 was present; the numbering system was taken from ref 12). The method that we have applied involves the use of standards of about 170 individual congeners, the retention properties of all 209 congeners (11), and a MDGC technique (8). All 14 congeners analyzed (Table I) were available in sufficiently pure form to serve as reference compounds. This was established by MDGC-ECD. The congeners reported here contribute between 20 and 28% of total peak area in the various sample compartments. Neglecting the differences in response factors between congeners (11), the sum of the 14 congeners (ΣPCB) represent ~25% of the sum of concentrations of all congeners present in the samples (i.e., total PCBs). In order to facilitate comparisons between the samples, concentrations have also been expressed as percentage contributions to ΣPCB (13).

Results and Discussion

Data are presented here on four sets of PCB mixtures in vapor, particulates, and rain, collected simultaneously. Table I summarizes the quantitative data. Not enough precipitation was obtained in one occasion (sample 3). The concentrations of particulate PCB in sample 1 were below the detection limit (<0.1 pg/m³ for any congener). Figure 1 shows characteristic chromatograms of the PCB mixtures in the various sample compartments; those for the commercial mixtures Clophen A30 and A60 are given for

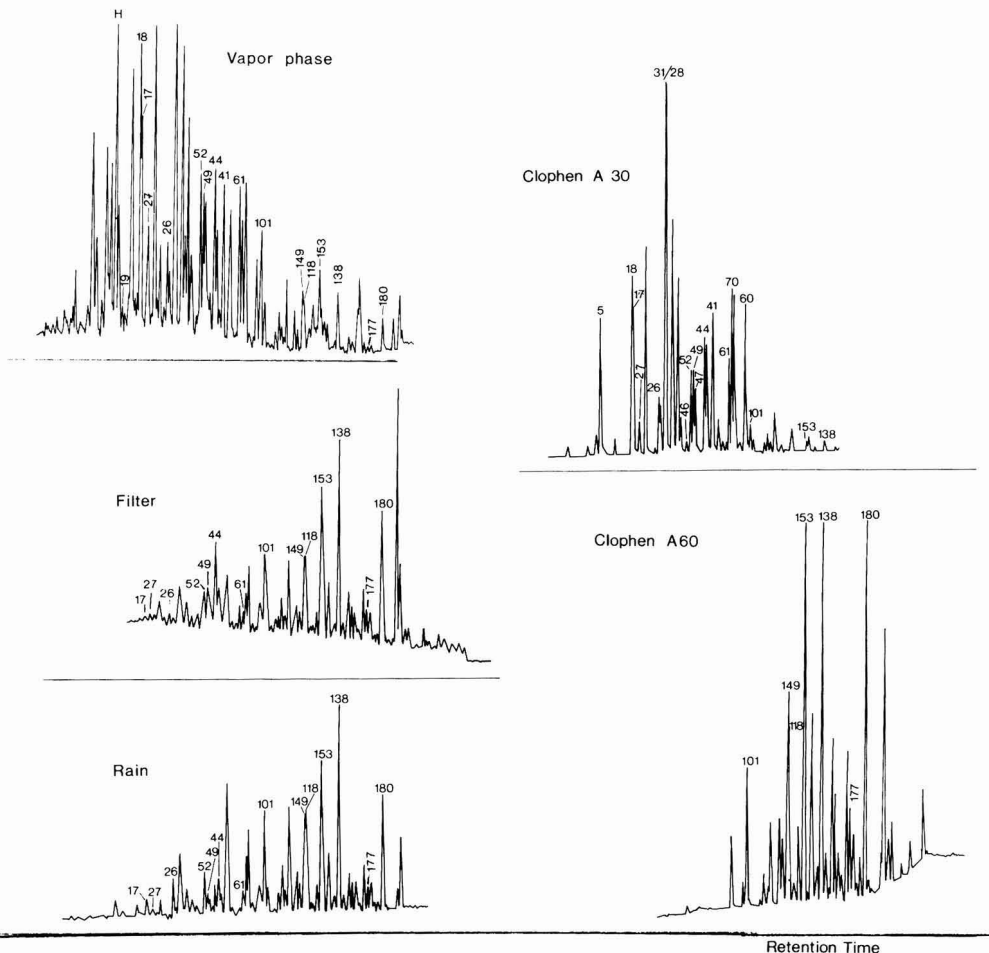


Figure 1. ECD chromatograms of *n*-hexane extracts of the vapor phase, filtered particulates, and rain of sample 2 (Table I) and of Clophen A30 and Clophen A60. Numbers (ref 12) identify PCB congeners that were separated and that were available as standards; H = hexachlorobenzene. Chromatographic conditions: 50-m fused silica column (0.22 mm i.d.), 0.15 μm SE-54; Gas chromatograph, Carlo-Erba (Model 4130) equipped with ^{63}Ni ECD, splitless injection mode; temperature program, 60–260 $^{\circ}\text{C}$ at 4 $^{\circ}\text{C min}^{-1}$; temperature detector, 310 $^{\circ}\text{C}$; temperature injector, 260 $^{\circ}\text{C}$.

comparison and reference purposes.

Vapor and Particulates. The vapor-phase PCB chromatograms are characterized by strong peaks of congeners with both low ($n_{\text{Cl}} = 3\text{--}4$) and higher ($n_{\text{Cl}} = 5\text{--}7$) degrees of chlorination. Their concentrations are in the 1–200 pg dm^{-3} range (Table I). The sum of their concentrations (ΣPCB) range between 75 and 830 pg dm^{-3} .

The strongest peaks in the chromatograms of the PCB mixtures in the aerosols originate from congeners with four and six chlorine atoms (Figure 1, Table I). The contributions of early eluting congeners (no. 18, 17, 27, 26) are considerably lower than in the corresponding vapor phase. Particulate concentrations of individual congeners were in the very low pg m^{-3} range and ΣPCB ranges between 7 and 18 pg m^{-3} .

The maximum ΣPCB values in the vapor phase (701–827 pg m^{-3} in samples 2 and 4) were obtained during periods with southwest as the main wind direction, and the minimum ΣPCB concentration (75 pg m^{-3} , sample 1) was obtained during a period of mainly northerly winds (Table I). The same relation exists for the aerosol data (Table I). A similar relation in this region has been established for volatile aliphatic and aromatic hydrocarbons

(14). Although the concentrations of each individual congener (as well as of ΣPCB in vapor-phase samples varied considerably (up to more than 1 order of magnitude), the compositional differences were only minor, as can be observed from the percentage contributions of each congener to ΣPCB in the various samples. For instance, the concentration of no. 17 varied more than 1 order of magnitude between vapor-phase samples, but its contribution to ΣPCB varied only between 16.0 and 17.5% (Figure 2). Similar small compositional differences were also found between the PCB mixtures in the particulate samples (Figure 2).

There are two important differences between PCBs in the vapor phase and the aerosols; these are related to quantitative as well as qualitative aspects. We shall consider these in succession. PCB values were considerable higher in the vapor phase than in the aerosols. The lower contribution of aerosols to the total concentration of PCBs in atmospheric samples has also been reported by others (1, 4, 7, 15, 16). For instance, the amount of PCBs on particulates was estimated as 27% of total atmospheric burden in the Great Lakes system (1) and less than 10% in remote marine atmosphere (17); see also the references

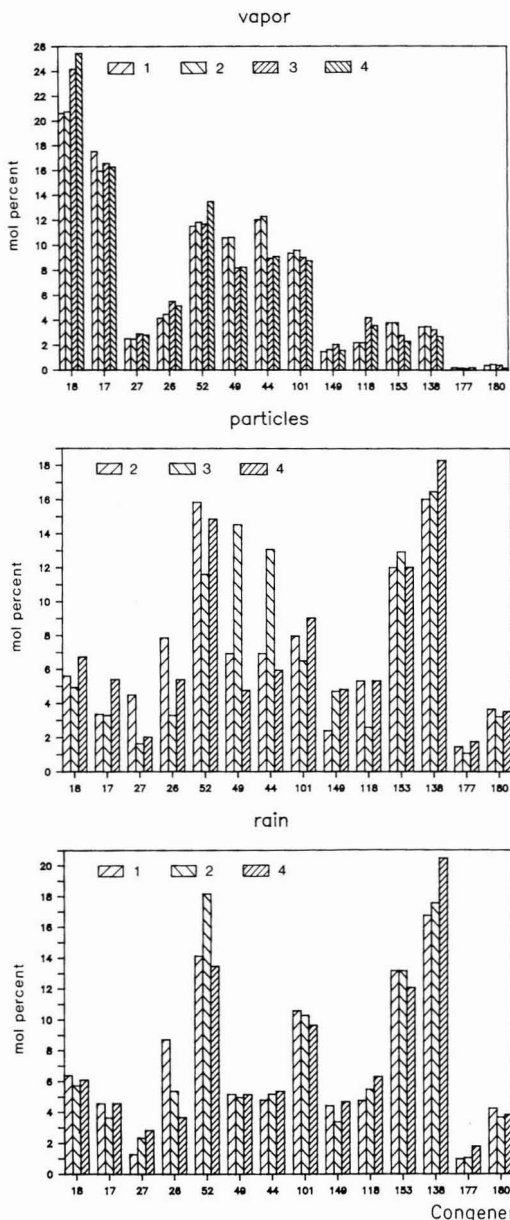


Figure 2. Percent contributions of the concentrations of PCB congeners (molar units) to \sum PCB (molar units) in vapor (top), particles (middle), and rain (bottom) in samples 1-4 (Table I). For numbering system of congeners see Table I.

in ref 2. In the present data, an even lower fraction is reported: the aerosol contribution was as low as <1-2% of total atmospheric concentrations for most of the volatile congeners. This reflects the increased efficiency of the glass beads for the more volatile fractions compared with other adsorbents (7).

The vapor-aerosol partitioning of an organic compound in the atmosphere depends on its vapor pressure and on the size, surface area, and organic carbon content of the particles. Theoretical considerations support the experimental findings on the dominance of the vapor phase (18).

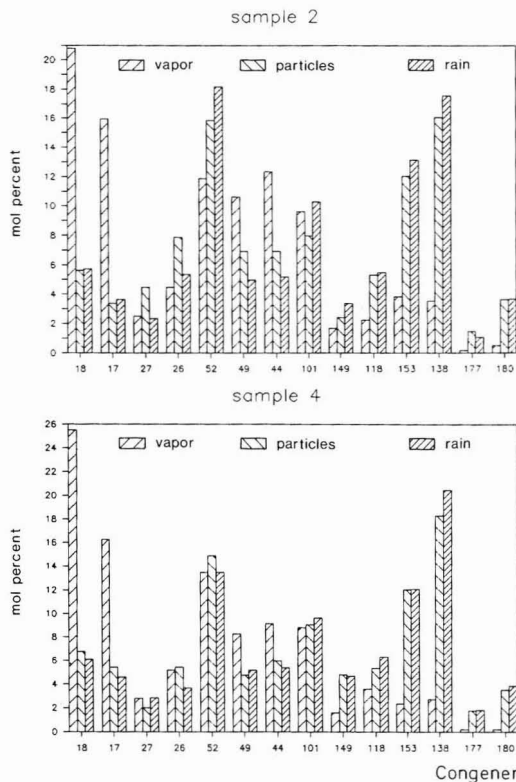


Figure 3. Percent contributions of the concentrations of PCB congeners (molar units) to \sum PCB (molar units) in vapor, particles, and rain of sample 2 (top) and sample 4 (bottom).

However, it should be taken into account that, generally, particle size distributions, the distribution of organics over the various size fractions, and total particulate concentrations are poorly known. Submicrometer particles may be the main sites for particulate PCBs (6).

The second aspect that needs attention when comparing PCBs in vapor phase and aerosols is the observation from the present data that vapor-particulate partitioning differs between individual congeners. Table I and Figure 3 show that particulates carry relatively more of the less volatile congeners, i.e., with the highest chlorine numbers. Although this is expected from first principles, Figure 3 shows this, to our knowledge for the first time, in quantitative form for several well-defined PCB congeners. Similar observations on the increasing importance of the particulates with increasing molecular weight have also been made for other organic compounds (19).

We have considered the possibility that the efficiency of the adsorbent material (glass beads) is affected by humidity. In the region where the samples were taken, relative humidity practically never exceeds 70% and temperatures are typically below 20 °C. The compositions of the PCB mixtures detected in the vapor phase in different seasons and under different atmospheric conditions covering 3 years in this region (more than 30 samples) are essentially identical with the data presented here. These observations suggest that these data are real.

Organic matter on the particulates may play an important role as sorption sites for organic compounds in the atmosphere. Similar to the findings for water-particulate partitioning of PCB congeners in natural water, octanol-

Table I. Concentrations of PCB Congeners [Identified by Structure and IUPAC Number (ref 12)] in the Vapor Phase, Aerosols, and Rain Collected in an Urban Area Simultaneously in Four Periods^a

PCB congener		sample 1			sample 2			sample 3		sample 4		
no.	structure	vapor, pg/m ³	aerosol, pg/m ³	rain, pg/dm ³	vapor, pg/m ³	aerosol, pg/m ³	rain, pg/dm ³	vapor, pg/m ³	aerosol, pg/m ³	vapor, pg/m ³	aerosol, pg/m ³	rain, pg/dm ³
18	2,2',5	13.9	<0.1	254.6	130.3	0.5	22.0	72.6	0.3	191.1	1.0	40.0
17	2,2',4	11.8	<0.1	182.3	100.1	0.3	14.0	49.7	0.2	122.0	0.8	30.0
27	2,3',6	1.7	<0.1	51.0	15.7	0.4	9.0	8.7	0.1	21.1	0.3	18.6
26	2,3',5	2.8	<0.1	348.1	28.1	0.7	20.6	16.5	0.2	38.7	0.8	24.1
52	2,2',5,5'	8.8	<0.1	639.0	84.3	1.6	79.1	39.8	0.8	114.6	2.5	100.0
49	2,2',4,5'	8.1	<0.1	234.5	75.6	0.7	21.7	27.9	1.1	70.3	0.8	38.4
44	2,2',3,5'	9.2	<0.1	218.0	87.6	0.7	22.6	30.5	0.9	77.5	1.0	40.0
101	2,2',4,5,5'	8.0	<0.1	535.1	76.4	0.9	50.0	34.4	0.5	83.5	1.7	80.0
149	2,2',3,4',5',6	1.4	<0.1	248.1	14.6	0.3	18.2	8.7	0.4	16.8	1.0	43.0
118	2,3',4,4',5	1.9	<0.1	241.4	17.7	0.6	26.7	16.1	0.2	34.2	1.0	52.3
153	2,2',4,4',5,5'	3.6	<0.1	736.6	33.7	1.5	70.8	11.8	1.1	24.6	2.5	110.8
138	2,2',3,4,4',5'	3.3	<0.1	936.7	31.0	2.0	94.5	13.7	1.4	28.6	3.8	187.9
177	2,2',3,3',4',5,6	0.2	<0.1	60.3	1.6	0.2	6.2	0.6	0.1	2.3	0.4	18.0
180	2,2',3,4,4',5,5'	0.4	<0.1	261.3	4.5	0.5	21.7	1.8	0.3	2.0	0.8	38.7
ΣPCB		75.1		4947.0	701.2	10.9	477.1	332.8	7.6	827.3	18.4	821.8
mean wind direction			N			SW		W			SW	
vol sampled		30.1 m ³	30.1 m ³	515 cm ³	32.7 m ³	32.7 m ³	1380 cm ³	21.3 m ³	21.3 m ³	45.7 m ³	45.7 m ³	517 cm ³

^a Only those congeners were analyzed that were separated well on a SE 54 column [a small contribution to no. 153 originates from no. 132 and a still smaller contribution from no. 105 (ref 8).] and were available as pure standards. The sum of their concentrations is given as ΣPCB. Concentrations in pg m⁻³ for vapor and aerosols and in pg dm⁻³ for rain. The volumes sampled and the main wind direction are indicated in the bottom rows.

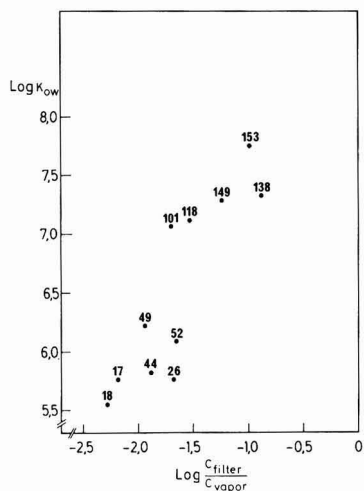


Figure 4. Plot of $\log k_{ow}$ ($\log C_{octanol}/C_{water}$) vs $\log C_{filter}/C_{vapor}$ for 12 of the PCB congeners [represented by numbers (ref 12)] analyzed in this paper. $\log k_{ow}$ data were taken from ref 20. Data for C_{filter} and C_{vapor} are in pg m^{-3} , for sample 4 (Table I).

water distribution coefficients (K_{ow}), as a measure for the tendency to associate with particulate organic fractions, might also be used for atmospheric samples as an estimate for vapor-particulate partitioning. Similarly, vapor pressure is expected to be a measure for concentrations in the vapor phase. Figure 4 relates the ratio of the concentrations of each congener in aerosols and in vapor with its octanol-water distribution coefficient (20) and Figure 5 relates the same ratio with the vapor pressure of the congener (21). The clear relationships suggest that the findings for the vapor-particulate partitioning are real or, alternatively, that evaporation losses and/or filter efficiency problems are equally important for congeners of high and low degrees of chlorination. The latter argument seems less probable (22).

Rain. The chromatograms of the PCB mixture in rain samples (Figure 1) show the presence of components with both low and high degrees of chlorination. The strongest

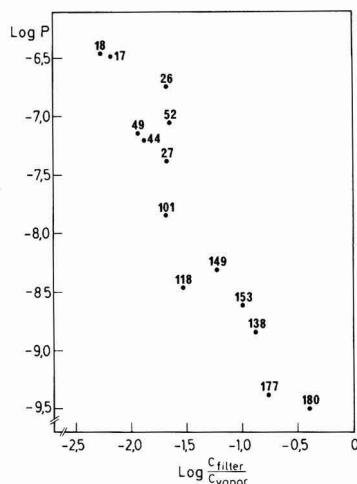


Figure 5. Plot of $\log p$ (vapor pressure in atm) vs $\log C_{filter}/C_{vapor}$ for 12 of the PCB congeners [represented by numbers (ref 12)] analyzed in this paper. Vapor pressure data were taken from ref 21. C_{filter} and C_{vapor} are in pg m^{-3} for sample 4 (Table I).

peaks correspond to hexa-, penta-, and tetrachloro congeners. The presence of PCBs in rain results from the dissolution of vapor-phase PCBs through gas-rain partition and from the scavenging of particles and their associated PCBs. The qualitative and quantitative distributions of PCBs in rain depend on vapor-particulate partitioning. In our samples, scavenging appears to be especially effective for penta- and hexachloro congeners. ΣPCB concentrations were in the range 477–4947 pg dm^{-3} (samples 2 and 1, respectively). Slightly higher variations in PCB concentrations are observed for rain than for vapor and aerosols. This may result from variations in wind direction and rain intensity during sampling. For instance, the amount of rain collected was 517 cm^3 at sample 4 and 1380 cm^3 at sample 2 (Table I). The main wind direction was southwest in both cases. The amount of PCB deposited was thus higher at lower rainfall during the precipitation event (sample 4), taking place over a longer period than

Table II. Difference between Measured (C_{expl}) and Calculated (C_{calcd}) Concentrations (in Molar Units) of PCB Congeners in Rain of Samples 2 and 4^a

congener no.	$(C_{\text{expl}} - C_{\text{calcd}})/C_{\text{expl}} \times 100$	
	sample 2	sample 4
18	8	10
17	15	-1
27	-106	30
26	-54	-46
52	9	-10
49	-40	-13
44	-34	-7
101	20	5
149	26	-6
118	-2	14
153	3	-4
138	3	6
177	-46	-6
180	-7	2
f_v/f_p	2.6×10^{-3}	2.5×10^{-3}

^aThe errors ($C_{\text{expl}} - C_{\text{calcd}}$) are expressed as percent of C_{expl} . Concentrations of PCB congeners in rain were calculated as linear combinations of concentrations in vapor and aerosol, minimizing the sum of squares of errors (eq 1). The ratio of the coefficients for the "best" solution to eq 1 is given in the last row.

for sample 2 (compare volumes of air sampled, Table I). Similar observations of variable scavenging efficiency during a precipitation event have been made for PAHs (23). The composition of the PCB mixtures in the rain samples was remarkably constant, similar to the findings for the vapor phase and aerosols (Figure 2). A final observation related to the qualitative aspects of the PCB mixtures in the different compartments is the inadequacy of commercial mixtures of both low and high overall chlorine content to mimic the composition in these compartments (Figure 1). An accurate fit is only obtained by the individual congener approach.

PCBs in Rain in Relation to Vapor-Rain Partitioning and Particle Scavenging. Several attempts have been made in the literature to evaluate the relative contributions of particle scavenging and vapor-rain partitioning to the observed levels of PCBs in rain. The comparison with experimental data has been hampered by the fact that sampling techniques as well as packed-column chromatograms have not given sufficient details between PCB compositions in vapor, aerosols, and rain.

The presently reported differences in compositions based on individual constituents may allow a better estimate. Calculations were carried out to mimic the composition in rain by a linear combination of the compositions in the corresponding vapor and aerosol samples according to a least squares of errors procedure. The proposed relation is represented by eq 1, where \bar{c}_r , \bar{c}_v , and \bar{c}_a represent

$$\bar{c}_r = f_v \bar{c}_v + f_a \bar{c}_a \quad (1)$$

vectors whose components are the concentrations of the 14 congeners in rain, vapor, and aerosol, respectively, and f_v and f_a are the coefficients minimizing the sum of squares of errors between the experimentally determined concentrations in rain ($\bar{c}_{r,\text{expl}}$) and those calculated from eq 1, i.e., $\bar{c}_{r,\text{calcd}}$.

The "best" solutions in the least-squares inverse matrix procedure are presented in Table II. The results show that, although only a very small fraction of Σ PCB was found in aerosols, the latter compartment accounted for more than 99% of the PCBs in rain. Particularly, congeners of higher degrees of chlorination are involved, those with lower degrees of chlorination remaining essentially

Table III. Theoretical Washout Ratios for Individual PCB congeners^a

congener no.	W_{calcd} ($\times 10^{-1}$)	W_{expl}		
		sample 1 ($\times 10^{-4}$)	sample 2 ($\times 10^{-2}$)	sample 3 ($\times 10^{-2}$)
18	8	2	2	2
17	8	2	1	2
27	9	3	6	9
26	7	12	7	6
52	11	7	9	9
49	9	3	3	5
44	13	2	3	5
101	14	7	7	9
149	17	18	12	24
118	29	13	15	15
153	25	20	20	41
138	33	28	29	58
177	76	30	34	67
180	78	65	43	138

^a W_{calcd} calculated from Henry's law constants (see text) and experimentally determined values [W_{expl} = concentration in rain (pg dm^{-3})/(concentration in vapor plus aerosol (pg dm^{-3}))] for samples 1, 2, and 4.

in the vapor phase. If this would be a general phenomenon in the atmosphere, wet precipitation would remove preferentially the less volatile fractions. The degree of agreement between calculated and experimental concentrations differs between the congeners. The differences are partly due to the simplicity of the model, involving the same behavior of all vapor-phase constituents in the vapor-rain partitioning process. A second reason for the discrepancies is the uncertainty associated with the extremely low concentration levels in the aerosols. Taking these facts into consideration, the fit in the least squares of errors procedure is promising, especially because the results for the two samples with different concentrations are very similar indeed. More research is needed to investigate this in detail in other atmospheric regimes.

The relative importance of particle scavenging and vapor-rain partitioning can also be estimated by comparing experimental and calculated washout ratios (W). A value for W can be calculated from Henry's law constant, $W = RT/H$ (2). The latter expression reflects the equilibrium vapor-rain partitioning. The experimental value for W is obtained as the ratio of the concentrations in rain and air. It reflects the washout of vapor plus particles. Increased contribution of particulates results in higher values of W_{expl} . Both theoretical and experimental values of W appear to increase with increasing chlorine number of the congeners (Table III), and the values of W_{expl} are in fact considerably larger than the calculated values for each congener. This can be considered as strong addition support for the dominant role of particles in determining the levels of individual PCB congeners in rain.

Registry No. 2,2',5'-PCB, 37680-65-2; 2,2',4'-PCB, 37680-66-3; 2,3',6'-PCB, 38444-76-7; 2,3',5'-PCB, 38444-81-4; 2,2',5',5'-PCB, 35693-99-3; 2,2',4,5'-PCB, 41464-40-8; 2,2',3,5'-PCB, 41464-39-5; 2,2',4,5,5'-PCB, 37680-73-2; 2,2',3,4',5',6'-PCB, 38380-04-0; 2,3',4,4',5'-PCB, 31508-00-6; 2,2',4,4',5,5'-PCB, 35065-27-1; 2,2',3,4,4',5'-PCB, 35065-28-2; 2,2',3,3',4',5,6'-PCB, 52663-70-4; 2,2',3,4,4',5,5'-PCB, 35065-29-3.

Literature Cited

- (1) Murphy, T. J.; Rzeszutko, C. P. *J. Great Lakes Res.* **1977**, *3*, 305-312.
- (2) Eisenreich, S. J.; Looney, B. B.; Thornton, J. D. *Environ. Sci. Technol.* **1981**, *15*, 30-38.
- (3) Bidleman, T. F.; Olney, C. E. *Bull. Environ. Contam. Toxicol.* **1974**, *11*, 442-450.

- (4) Harvey, G. R.; Steinhauer, W. G. *Atmos. Environ.* 1974, 8, 777-782.
- (5) Atlas, E.; Giam, C. S. *Science (Washington, D.C.)* 1981, 211, 163-165.
- (6) Doskey, P. V.; Andren, A. W. *Environ. Sci. Technol.* 1981, 15, 705-711.
- (7) Bouchertall, F.; Duinker, J. C. *Anal. Chim. Acta* 1986, 185, 369-375.
- (8) Duinker, J. C.; Schulz, D.; Petrick, G. *Anal. Chem.* 1988, 60, 478-482.
- (9) Billings, W. N.; Bidleman, T. F. *Environ. Sci. Technol.* 1980, 14, 679-683.
- (10) Duinker, J. C.; Hillebrand, M. T. J. *Environ. Sci. Technol.* 1983, 17, 449-456.
- (11) Mullin, M. D.; Pochini, C. M.; McCrindle, S.; Romkes, M.; Safe, S. H.; Safe, L. M. *Environ. Sci. Technol.* 1984, 18, 468-476.
- (12) Ballschmiter, K.; Zell, M. *Fresenius Z. Anal. Chem.* 1980, 302, 20-31.
- (13) Duinker, J. C.; Knap, A. H.; Binkley, K. C.; Van Dam, G. H.; Darrel-rew, A.; Hillebrand, M. T. J. *Mar. Pollut. Bull.* 1988, 19, 74-79.
- (14) Bouchertall, F. *Mar. Chem.* 1986, 19, 153-160.
- (15) Giam, C. S.; Atlas, E.; Chan, H. S.; Neff, G. *Atmos. Environ.* 1980, 14, 65-69.
- (16) Tanabe, S.; Hidaka, H.; Tatsukawa, R. *Chemosphere* 1983, 12, 277-288.
- (17) Bidleman, T. F.; Christensen, E. J.; Billings, W. N.; Leonard, R. J. *Mar. Res.* 1981, 39, 443-464.
- (18) Junge, C. E. In *Fate of Pollutants in the Air and Water Environment*; Suffet, I. H., Ed.; Wiley-Interscience, New York, 1977; pp 7-25.
- (19) Cautreels, W.; van Cauwenberghe, K. *Atmos. Environ.* 1978, 12, 1133-1141.
- (20) Rapaport, R. A.; Eisenreich, S. J. *Environ. Sci. Technol.* 1984, 18, 163-170.
- (21) Murphy, T. M.; Mullin, M. D.; Meyer, J. A. *Environ. Sci. Technol.* 1987, 21, 155-162.
- (22) Van Vaecck, L.; van Cauwenberghe, K.; Janssens, J. *J. Atmos. Environ.* 1984, 18, 417-430.
- (23) Van Noort, P. C. M.; Wongergem, E. *Environ. Sci. Technol.* 1985, 19, 1044-1048.

Received for review March 26, 1987. Revised manuscript received February 18, 1988. Accepted June 8, 1988.

Characterization of Chlorophenol and Chloromethoxybenzene Biodegradation during Anaerobic Treatment

Sandra L. Woods,*† John F. Ferguson,‡ and Mark M. Benjamin‡

Department of Civil Engineering, Oregon State University, Corvallis, Oregon 97331-2302, and Department of Civil Engineering, University of Washington, Seattle, Washington 98195

■ Chlorophenols, chloroguaiacols, chloroveratroles, and chlorocatechols were continuously treated in an upflow anaerobic sludge blanket reactor in the presence of high concentrations of readily biodegradable organic compounds. The chlorinated compounds were not completely mineralized, but were converted to lesser chlorinated compounds by biologically mediated reductive dechlorination reactions. Chlorinated veratroles were converted to chloroguaiacols and then to chlorocatechols before they were reductively dechlorinated. Reductive dechlorination reactions are dependent on chlorine position, with preference for the removal of chlorines from positions adjacent to hydroxyl groups. With acclimation, meta chlorines are also removed. There was no evidence for the removal of para chlorines during this study. There was also no evidence for dechlorination of monochlorophenols.

Introduction

Among the potential benefits of anaerobic waste water treatment is the ability of anaerobic microorganisms to participate in the biodegradation of halogenated organic compounds. This paper describes a study of the removal of chlorinated phenols, catechols, guaiacols, (*o*-methoxyphenols), and veratroles (*o*-dimethoxybenzenes) during continuous anaerobic treatment.

In batch studies with a single chloroaromatic compound as the sole source of carbon, many chlorophenols and chlorobenzoates can be degraded to methane and carbon dioxide. The initial step in the degradation of these compounds is a reductive dechlorination reaction in which

chlorine atoms are removed from the aromatic ring and replaced with hydrogen. Dechlorination is strongly dependent on the position of chlorine atoms on the aromatic ring and the acclimation of the microbial consortia. Unacclimated bacteria have been shown to preferentially remove chlorines from the position adjacent to the hydroxyl group for chlorophenols (1) and from the position meta to the carboxyl group in the dehalogenation of chlorobenzoates (2).

Chlorophenols also can be removed well in continuous anaerobic treatment processes. Guthrie et al. (3) examined the fate of pentachlorophenol (PCP) during the anaerobic digestion of sewage sludge in a semicontinuous flow, stirred tank reactor. Once the bacteria acclimated to pentachlorophenol, digesters receiving 19 $\mu\text{mol/L}$ (5.0 mg/L) PCP achieved greater than 99.9% PCP removal at retention times between 10 and 40 days.

The Enso-Fenox process (4, 5) has also been used to remove chlorinated phenolic compounds from pulp bleaching effluents. It is a two-stage process consisting of an anaerobic fluidized-bed reactor followed by a trickling filter. Although the first stage of this process is anaerobic, it does not yield methane. This process results in chlorophenol removal efficiencies between 65 and 100%.

The objective of this research was to characterize the removal of chlorinated phenols and chlorinated methoxybenzenes during continuous anaerobic treatment of a complex, concentrated waste water. Readily biodegradable organic compounds (4300 mg/L chemical oxygen demand) were present in the reactor influent, and several chlorinated aromatic compounds were treated concurrently. A continuous flow, upflow anaerobic sludge blanket reactor was operated at a moderately high volumetric organic loading rate (8.7-g COD/L day), and extensive dechlori-

*Oregon State University.

†University of Washington.

nation of chlorophenols and chlorocatechols was observed.

Experimental Program

The degradation studies were performed in a 6.6-L reactor operated as an upflow sludge blanket with recycle. The body of the reactor was constructed of Kimax beaded process pipe with Teflon flanged fittings (Ace Glass, Inc., Vineland, NJ) to minimize adsorption of chlorophenols to the reactor vessel. A 1-L glass separatory funnel served as the recycle flask. The reactor was housed in a constant temperature room held at 35 °C. Influent was pumped into the bottom of the reactor where it joined the recycle flow. The influent flow rate was 13.3 L/day, and the recycle ratio was 5.3 throughout these experiments.

Lithium was added to the reactor influent solution during experiments I and II to serve as a conservative tracer. Effluent lithium concentrations indicated that the reactor was completely mixed, and the hydraulic retention time was 13.2 h. This hydraulic retention time was maintained throughout the experiments.

The original source of inoculum was the municipal sludge digester at the West Point waste water treatment facility, Seattle, WA. These microorganisms were fed diluted caustic extraction effluent and sulfite evaporator condensate from the pulp and paper industry with additional carbon sources, inorganic nutrients, and vitamins for ~2 years. Prior to beginning this study, organisms were transferred to the upflow anaerobic sludge blanket reactor and fed a synthetic waste water (described below) for 3 months prior to the addition of chlorinated aromatic compounds.

The synthetic waste water contained three primary carbon sources: acetate (43.7 mmol/L), methanol (30.9 mmol/L), and glucose (0.278 mmol/L). Neutralization, inorganic nutrients, and vitamins were also provided. Concentrations of inorganic species were as follows (concentrations are expressed as mmol/L): NaOH, 35.6; NaHCO₃, 23.8; NH₄HCO₃, 6.07; NaH₂PO₄, 2.00; H₃PO₄, 3.68; FeS, 0.165; ZnS, 0.0014; CaHPO₄, 0.0537; CoCO₃, 0.0111; CuCO₃, 0.0016; MnCO₃, 0.0089; MgCO₃, 0.0062; KHCO₃, 1.57; H₃BO₃, 0.0081; NaMoO₄·2H₂O, 0.0009. The following vitamins were provided (concentrations are expressed as µg/L): biotin, 3.0; folic acid, 3.0; pyridoxine hydrochloride, 15.0; riboflavin, 7.5; thiamin, 7.5; nicotinic acid, 7.5; calcium pantothenate, 7.5; B₁₂, 0.15; *p*-amino-benzoic acid, 7.5; thioctic acid, 7.5.

The overall chemical oxygen demand (COD) of the synthetic waste water was 4.3 g/L, resulting in an organic loading rate to the reactor of 8.7-g COD/L day. The total mass of solids in the reactor varied between 5 and 20 g of volatile suspended solids (VSS) throughout the study. Therefore, organic loading rates varied between 3- and 11-g COD/(g VSS day). Chlorinated benzene derivatives added to the influent solution during each of the experiments are listed in Table I.

Samples of the reactor influent were collected from the influent reservoir and analyzed for acetate, methanol, glucose, and chlorinated benzene derivatives. No degradation of the organic compounds was observed in the influent container. Effluent samples were collected from a port on the recycle line. Effluent samples were filtered through Gelman (type A-E) glass-fiber filters.

Analytical Techniques. Chlorinated phenols, guaia-cols, catechols, and veratroles were measured by capillary gas chromatography with electron capture detection with a modification of the method described by Voss et al. (7) and the NCASI (8). Hexane extracts of acetylated samples (6) were analyzed with a Hewlett-Packard Model 5840A gas chromatograph equipped with a ⁶³Ni electron capture

Table I. Chlorinated Benzene Derivatives Added to Reactor Influent

compd	concn, µmol/L
experiment 1	
2,4,6-trichlorophenol	5.14
4,5-dichloroguaiacol	5.24
tetrachloroveratrole	3.44
experiment 2	
2,4,6-trichlorophenol	4.99
2,3,4,5-tetrachlorophenol	4.32
3,4,5-trichlorophenol	5.05
2,3-dichlorophenol	6.47
3,4-dichlorophenol	6.12
<i>p</i> -chlorophenol	7.75
4,5-dichloroguaiacol	5.27
tetrachloroguaiacol	3.64
4,5-dichloroveratrole	4.77
tetrachloroveratrole	3.55
4,5-dichlorocatechol	5.60
experiment 3	
pentachlorophenol	0.384
experiment 4	
2,4,6-trichlorophenol	varied
2,3,4,5-tetrachlorophenol	varied
3,4,5-trichlorophenol	varied
2,3-dichlorophenol	varied
3,4-dichlorophenol	varied
3,5-dichlorophenol	varied
2,4-dichlorophenol	varied
2,6-dichlorophenol	varied
pentachlorophenol	varied

detector (ECD) and a Hewlett-Packard Model 18835B capillary column inlet system operated in the splitless mode. Injections (1 µL) were made with a Hewlett-Packard 7671A autosampler. A 15 m × 0.25 mm i.d. DB-1 (durabonded SE-30) fused silica capillary column (J & W Scientific, Orangeville, CA) was used for the separation. The temperature program was as follows: the initial oven temperature was held at 45 °C for 1 min and then increased at a rate of 15 °C/min to 102 °C, followed by an increase at the rate of 2 °C/min to a final temperature of 200 °C. The detector was held at 320 °C, and the injection port was held at 210 °C. Helium (at 10 psig) was used as the carrier gas. The ECD auxiliary gas was 95% argon/5% methane. The inlet purge flow rate was 80 mL/min, and the inlet purge activation time was 0.6 min.

Results and Discussion

Evidence of Anaerobic Dechlorination Reactions. Chlorophenols. Chlorinated aromatic compounds were added singularly and in combination to evaluate their removal during anaerobic treatment. Influent concentrations of the chlorinated aromatic compounds were increased to a toxic level on two occasions to serve as a control by inhibiting biodegradation. Tracer experiments were also performed to characterize reactor mixing.

Three chlorinated benzene derivatives (Table I) were added with the lithium tracer to the reactor influent during the first experiment. In the absence of removal of the chlorinated compounds, their concentrations in the reactor would be expected to increase to their respective influent concentrations in the same manner as the lithium tracer (Figure 1A). 2,4,6-Trichlorophenol (246-TCP) concentrations closely follow the expected tracer curve during the first several (~12) hours of the experiment. However, 246-TCP removal began shortly thereafter, and its rate of removal increased until the effluent concentration reached a mean steady-state concentration of 0.035 µmol/L, corresponding to an average removal efficiency greater than 99%.

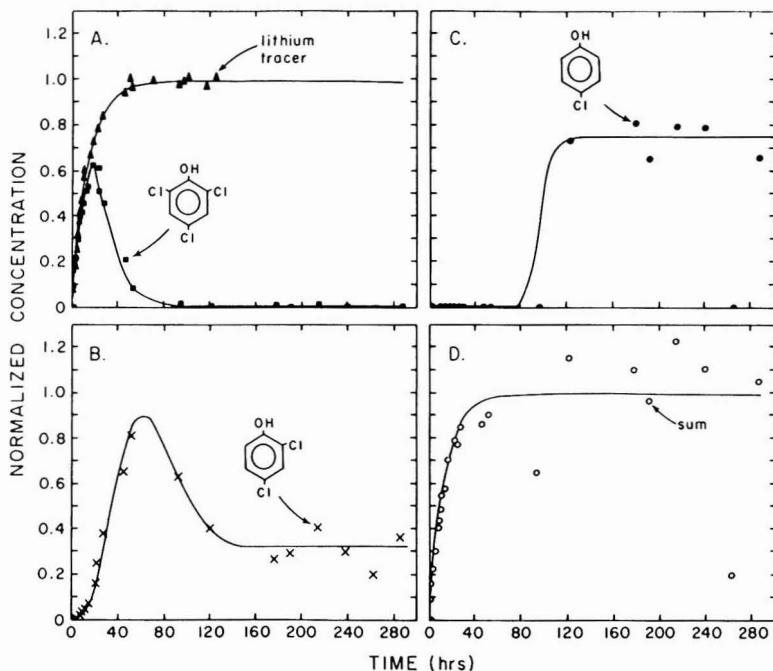


Figure 1. Normalized molar concentrations of lithium, 246-TCP, and its metabolites with time during experiment 1. (A) 246-TCP reactor concentrations normalized to the influent 246-TCP concentration of $5.14 \mu\text{mol/L}$ with lithium tracer data; (B) normalized molar 24-DCP soluble reactor concentrations; (C) normalized molar *p*-CP soluble reactor concentrations; (D) sum of the molar concentrations of 246-TCP, 24-DCP, and *p*-CP normalized to the influent 246-TCP concentration.

2,4-Dichlorophenol (24-DCP) appeared in the reactor for the first time after 6 h (Figure 1B) in amounts stoichiometric with the removal of 2,4,6-trichlorophenol. The appearance of 24-DCP suggests removal of one of the ortho chlorines from 246-TCP and replacement with a hydrogen. 2,6-Dichlorophenol, which could be formed by the removal of the para chlorine from 246-TCP, did not appear at detectable levels in any of the reactor samples throughout this experiment.

After 2 days, the reactor concentration of 2,4-dichlorophenol began to decrease with concomitant production of *p*-chlorophenol (Figure 1C). *o*-Chlorophenol, which would be produced by removal of the para chlorine from 2,4-dichlorophenol, did not appear at detectable levels in the reactor during this experiment. Thus, the second step in the degradation of 246-TCP is removal of the second ortho chlorine.

The mass balance for soluble concentrations of 246-TCP, 24-DCP, and *p*-CP is shown in Figure 1D. The influent mass of 246-TCP was recovered as the parent compound and its two metabolic products. The sum of the mean molar concentrations for 246-TCP, 24-DCP, and *p*-CP during the steady-state period after hour 120 was $5.11 \pm 1.59 \mu\text{mol/L}$, which is 99.4% of the influent 246-TCP concentration of $5.14 \mu\text{mol/L}$. Although the standard deviation was large, there was no evidence for dechlorination of *p*-chlorophenol during this 12-day experiment. During the experiment, the molar soluble concentration of total soluble chlorophenols (2,4,6-trichlorophenol and its two metabolic products) closely followed the dilution curve, indicating that removal by sorption or volatilization was not significant in the experiment.

During experiment 2, 11 chlorinated compounds were added to the reactor influent at an overall concentration of $57.5 \mu\text{mol/L}$ or 5.0 mg/L organically bound chlorine

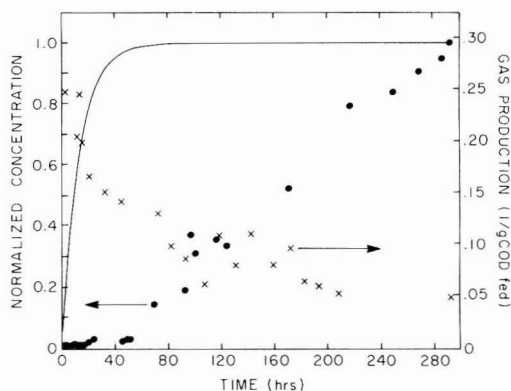


Figure 2. Gas production rates and normalized molar 246-TCP reactor concentrations during experiment 2 (X, 246-TCP; ●, gas production; —, theoretical tracer).

(Table I). This increase in the influent concentration of chlorinated aromatic compounds led to decreases in the removal of the chlorinated organic compounds as well as acetate, methanol, and glucose, which were also present in the influent. This reduction in biological activity was also characterized by a decrease in the gas production rate from 0.27 to 0.05 L of gas/g COD fed (Figure 2).

To verify that the conversion of 246-TCP to 24-DCP and *p*-CP was biologically mediated, concentrations of the chlorinated aromatic compounds continued to be monitored during the period when the reactor was failing. Concentrations of 246-TCP (normalized to its influent concentration) are shown in Figure 2. During the beginning of the experiment, 246-TCP was degraded to produce 24-DCP and *p*-CP. As the concentrations of the chlori-

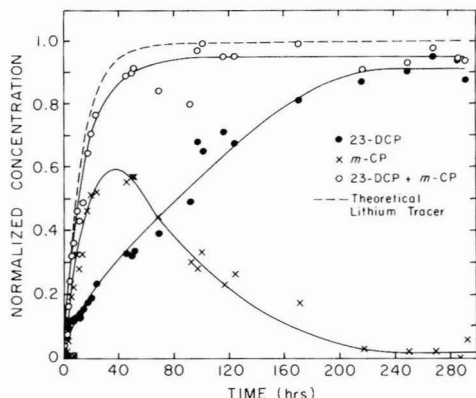


Figure 3. Normalized concentrations of 23-DCP and *m*-chlorophenol during experiment 2.

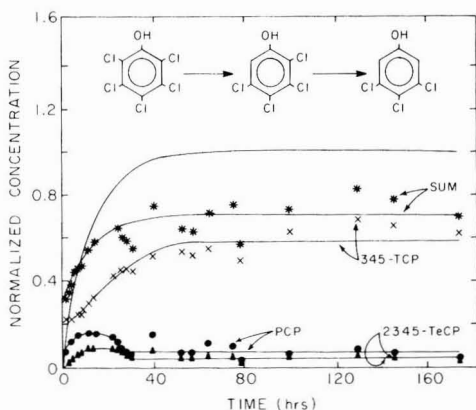


Figure 4. Normalized concentrations of PCP and its metabolites during experiment 3.

nated aromatic compounds in the reactor increased, the reactor concentration of 246-TCP in the reactor increased to its influent concentration. Although several chlorinated compounds were present in the influent, none could reasonably have produced 246-TCP. Therefore, this increase in the concentration of 246-TCP in the reactor was due to cessation of 246-TCP biodegradation, demonstrating the importance of biological removal processes.

During the first 60 h of experiment 2, while the chlorinated compounds were building up in the reactor to a toxic level, degradation of other chlorophenols was observed. 2,3-Dichlorophenol was dechlorinated at the ortho position to produce *m*-chlorophenol (Figure 3). However, its biodegradation also ceased as the chlorinated compounds diluted into the reactor and inhibited biodegradation.

A similar pattern of biodegradation was observed for pentachlorophenol (PCP). During experiment 3, pentachlorophenol was added to the reactor influent at 0.39 $\mu\text{mol/L}$ (100 $\mu\text{g/L}$). PCP was removed immediately (Figure 4) with the concomitant appearance of 2,3,4,5-tetrachlorophenol (2345-TeCP) and 3,4,5-trichlorophenol (345-TCP). No mono- or dichlorophenols were detected in the reactor, suggesting that 3,4,5-trichlorophenol, with no ortho chlorines, was not further dechlorinated during this 8-day experiment. PCP and 2345-TeCP were removed at efficiencies between 95 and 97% during the last 6 days of the experiment. Thus, the degradation pathway of

Table II. Steady-State Removal of Chlorophenols during Experiment 4

comps degraded by dechlorinatn at ortho positn	influent concn, $\mu\text{mol/L}$	removal effic, %
pentachlorophenol	0.32	94.9
	1.04	96.5
	1.92	94.9
2,3,4,5-tetrachlorophenol	0.37	94.9 ^a
	1.20	96.5 ^a
	2.21	64.9 ^a
	2,4,6-trichlorophenol	0.47
2,4-dichlorophenol	1.51	96.5
	2.79	95.5
	0.72	<i>b</i>
2,3-dichlorophenol	2.33	87.6 ^a
	4.29	80.9 ^a
2,6-dichlorophenol	0.62	74.6
	2.02	81.2
	3.73	80.3
	0.66	90.0
	2.15	92.3
	3.97	91.4

^aRemoval efficiency calculated on the basis of the influence concentration plus production by degradation of its parent compound (PCP is the parent compound for 2345-TeCP; 246-TCP is the parent compound for 24-DCP). ^bNon-steady-state period for 2,4-dichlorophenol.

polychlorinated phenols favors reductive dechlorination of chlorines in the ortho position, regardless of whether the meta positions are chlorinated.

During experiment 4, a suite of nine chlorophenols was added to the influent at increasing concentrations. This group included five dichlorophenols, chosen to include compounds with chlorines in several combinations of positions (2,6-, 2,4-, 2,3-, 3,4-, and 3,5-DCP). Pentachlorophenol, 2,3,4,5-tetrachlorophenol, 3,4,5-trichlorophenol, and 2,4,6-trichlorophenol were also present in the influent.

A comparison of the conversion of penta-, tetra-, tri-, and dichlorophenols to lower chlorinated phenols during experiment 4 indicates that the net efficiency of removal of a single ortho chlorine increases with the degree of chlorination of the parent compound (Table II). The removal efficiencies were calculated on the basis of the compound's influent concentration plus production by dechlorination of its parent compound. Although these proposed pathways and removal rates are specific to the microbial consortia in this group of experiments, the removal efficiencies at steady-state give an indication of the reaction rate. Steady-state removal efficiencies for the dechlorination of a single ortho chlorine ranged from 95% for the dechlorination of PCP, 2345-TeCP, and 245-TCP to between 75 and 81% for the removal of the ortho chlorine from 2,3-dichlorophenol. Of the three dichlorophenols dechlorinated at the ortho position (2,6-, 2,3-, and 2,4-dichlorophenol), the ortho chlorine was removed from 2,6-dichlorophenol more efficiently than from 2,3-dichlorophenol or 2,4-dichlorophenol.

Although each chlorophenol with two or more chlorines and containing ortho chlorines was immediately degraded by reductive dechlorination of an ortho chlorine throughout the study, compounds containing only meta and para chlorines were not immediately dechlorinated. During the first month of experiment 4, mass balances indicated that 3,4-dichlorophenol, 3,5-dichlorophenol, and 3,4,5-trichlorophenol were not dechlorinated. After the suite of nine chlorophenols was fed to the reactor at 100 and 325 $\mu\text{g/L}$ for 4 weeks, there was evidence of removal of meta

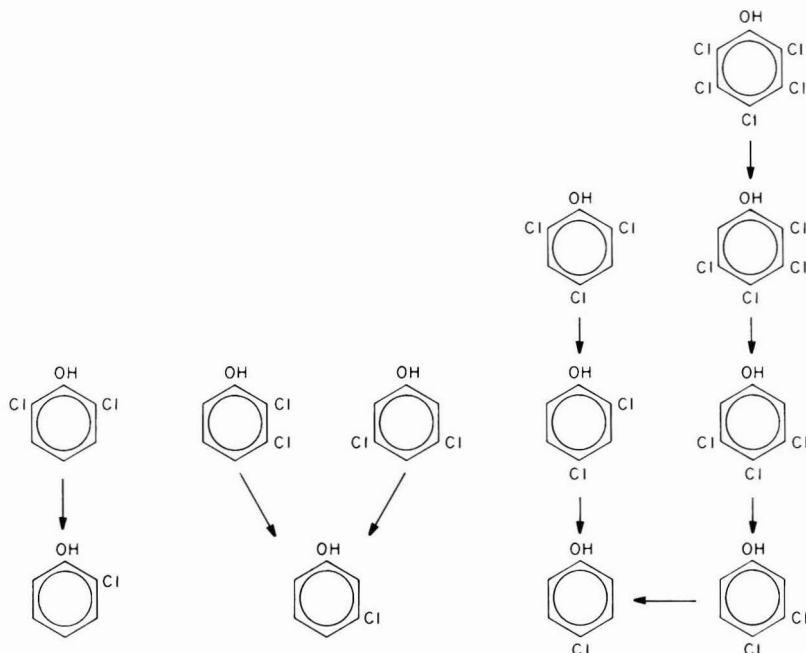


Figure 5. Summary of observed biodegradation pathways.

chlorines. Reductive dechlorination of the ortho chlorine from 2,3-dichlorophenol or either chlorine from 3,5-dichlorophenol would result in the production of *m*-chlorophenol, so these compounds must be considered in a mass balance on meta chlorines. The mass balance is shown in Table III.

During period 4a, only 2,3-dichlorophenol (23-DCP) was degraded to produce *m*-chlorophenol. Ninety-nine percent of the influent 2,3-dichlorophenol could be accounted for as 23-DCP or *m*-CP. 3,5-Dichlorophenol (35-DCP) was present in the reactor at 97.5% of its influent concentration, suggesting that it was not dechlorinated. During experimental period 4b, dechlorination of 35-DCP began. However, the reactor did not reach steady-state with respect to these compounds until period 4c. The steady-state reactor concentrations of 23-DCP, 35-DCP, and *m*-CP during period 4c indicated that 96.3% of the influent concentration of 23-DCP and 35-DCP could be recovered as the parent compounds or as their metabolite, *m*-CP. The reactor concentration of 35-DCP was 60.8% of its influent concentration. The loss of 35-DCP was accompanied by a stoichiometric increase in the concentration of *m*-CP, indicating that 35-DCP is degraded by reductive dechlorination of one of its meta chlorines. There was no evidence to suggest further reductive dechlorination of *m*-chlorophenol.

A summary of degradation pathways for the chlorophenols studied is shown in Figure 5. Bacteria readily removed ortho chlorines from 2,6-, 2,3-, and 2,4-dichlorophenol, 2,4,6-trichlorophenol, 2,3,4,5-tetrachlorophenol, and pentachlorophenol. With acclimation, meta chlorines were also removed from 3,5-dichlorophenol, 3,4-dichlorophenol, and 3,4,5-trichlorophenol. However, throughout 7 months of continuous treatment of the synthetic waste water, there was no evidence for dehalogenation of monochlorophenols or removal of chlorines from the position para to the hydroxyl group.

Although chlorines have been found to be removed from

Table III. Steady-State Concentrations of 2,3-Dichlorophenol, 3,5-Dichlorophenol, and *m*-Chlorophenol during Experiment 4

	exptl period		
	4a	4b	4c
steady-state period, days	7-21	31-49	51-63
2,3-dichlorophenol			
influence concn, $\mu\text{mol/L}$	0.623	2.02	3.73
steady-state reactor concn, $\mu\text{mol/L}$	0.158	0.380	0.735
removal effic, %	74.6	81.2	80.3
3,5-dichlorophenol			
influence concn, $\mu\text{mol/L}$	0.571	1.85	3.42
steady-state reactor concn, $\mu\text{mol/L}$	0.557	non-SS ^a	1.34
removal effic, %	2.5		60.8
<i>m</i> -chlorophenol			
influence concn, $\mu\text{mol/L}$	0.0	0.0	0.0
steady-state reactor concn, $\mu\text{mol/L}$	0.459	non-SS ^a	4.81
removal effic, %	0.0		0.0
sum			
influence concn, ^b $\mu\text{mol/L}$	1.19	3.87	7.15
steady-state reactor concn, ^b $\mu\text{mol/L}$	1.17	non-SS ^a	6.89
overall removal effic, %	1.3		3.7

^a Non-steady-state period with respect to this chlorinated compound. ^b Sum of the concentrations of 23-DCP, 35-DCP, and *m*-CP.

the para position of *p*-chlorophenol and 2,4- and 3,4-dichlorophenol during batch experiments (1), there was no evidence for removal of para chlorines during this study. Removal of monochlorophenols, ring cleavage, and complete degradation to methane and carbon dioxide could not be verified for any of the chlorinated organic compounds.

The lack of evidence for removal of chlorines from monochlorophenols may simply be due to kinetic limitations. The removal efficiency for each chlorophenol increased with increasing chlorination. Thus, if monochlorophenols were dechlorinated, the rate would be expected to be slower than for dichlorophenols. Therefore, treatment of these compounds at a longer retention time

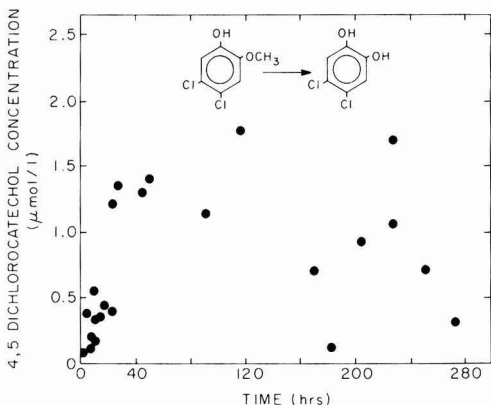


Figure 6. Emergence of 4,5-dichlorocatechol with the addition of 5.24 $\mu\text{mol/L}$ 4,5-dichloroguaiacol and 3.44 $\mu\text{mol/L}$ tetrachloroveratrole during experiment 1.

may have resulted in reductive dechlorination of the monochlorophenols.

Evidence for Demethylation Reactions. Chloroguaiacols and Chloroveratroles. During the first experiment, 4,5-dichloroguaiacol (a chlorinated methoxyphenol) and tetrachloroveratrole (a chlorinated dimethoxybenzene) were added to the reactor influent at 1 mg/L each (with 1 mg/L, 2,4,6-trichlorophenol). Throughout the experiment, 4,5-dichloroguaiacol and tetrachloroveratrole concentrations in the reactor were below the detection limit of the analytical procedure.

If 4,5-dichloroguaiacol was dechlorinated in a manner similar to the chlorophenols, a monochloroguaiacol should have been identified in the reactor. However, neither 4-chloro- nor 5-chloroguaiacol was detected in the reactor, suggesting that 4,5-dichloroguaiacol was not degraded by a reductive dehalogenation reaction, as the chlorophenols were. However, with the removal of 4,5-dichloroguaiacol and tetrachloroveratrole, there was the appearance of 4,5-dichlorocatechol (Figure 6) as well as other chlorinated catechols. Chlorocatechols are difficult to measure accurately, therefore the mass balance could not be closed. However, the absence of any 4,5-dichlorocatechol in the reactor prior to this experiment and its appearance upon the addition of the parent compounds is strong evidence that the chlorocatechol is a chemical or biological degradation product of one of these compounds.

Several other chlorinated compounds were identified in the reactor by GC/ECD and GC/MS during this experiment. Tetrachloroguaiacol and tetrachlorocatechol were identified, suggesting sequential demethylation of tetrachloroveratrole. Trichloroveratroles and trichloroguaiacols, which would be produced by reductive dechlorination of tetrachloroveratrole and tetrachloroguaiacol, were not detected. This is consistent with work by Boyd et al. (9) and Chen et al. (10), which showed similar demethylation reactions for unchlorinated methoxybenzenes.

3,4,5-Trichlorocatechol, 4,5-dichlorocatechol, and 4-chlorocatechol were also identified in the reactor. The proposed degradation pathway appearing in Figure 7 is consistent with the appearance of these compounds and the absence of other chlorinated aromatic compounds in the reactor. Since the mass balance could not be closed, alternative degradation pathways could not be disproved, and complete mineralization could not be verified. However, the appearance of the products suggests demethylation reactions followed by sequential dechlorination at the ortho positions, in a manner similar to the degradation

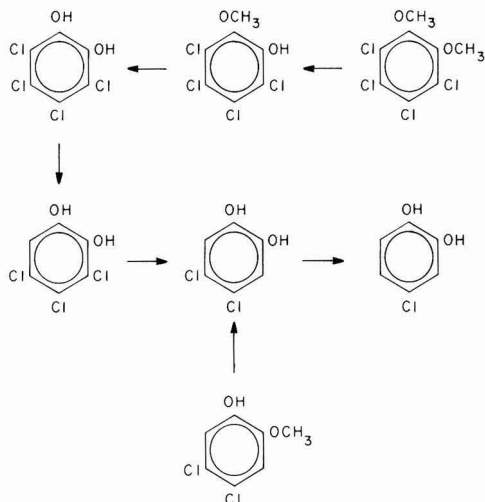


Figure 7. Proposed degradation pathways for tetrachloroveratrole and 4,5-dichloroguaiacol.

of the chlorophenols. The appearance of 4-chlorocatechol suggests removal of a meta chlorine from 4,5-dichlorocatechol. The compounds shown in Figure 7 were present in the reactor during this experiment and were measured by GC/ECD; their presence was confirmed by GC/MS, and no other chlorinated veratroles, guaiacols, or catechols were identified in the reactor.

Summary and Conclusions

Anaerobic treatment processes can lead to significant removal of chlorinated phenols, guaiacols, veratroles, and catechols. Degradation of polychlorinated phenols and catechols occurs readily at sequential dechlorination reactions at the positions adjacent to the hydroxyl groups. Removal of meta chlorines occurs with acclimation.

Chloromethoxybenzenes are converted to chlorohydroxybenzenes by demethylation reactions in the first step of their degradation. These reactions are extremely rapid and occur before reductive dechlorination reactions. Once chlorinated hydroxybenzenes are formed, dechlorination occurs in a manner similar to the conversion of chlorophenols. Chlorines are first removed from the positions adjacent to the hydroxyl group, followed by removal of meta chlorines.

Thus, anaerobic processes can be used to successfully biodegrade chlorinated hydroxy- and methoxybenzenes. Chlorophenols, chloroveratroles, chloroguaiacols, and chlorocatechols can be removed well during continuous treatment of a complex, concentrated waste water by an acclimated anaerobic microbial consortia. Although there was no evidence for the reductive dechlorination of monochlorophenols during this study, the rate of reductive dechlorination at the ortho position increased with increasing chlorination.

The ability of anaerobic consortia to reductively dechlorinate highly chlorinated compounds makes anaerobic processes attractive as a treatment alternative. Once dechlorinated, lesser chlorinated phenols may be readily degraded in aerobic treatment processes.

Acknowledgments

We express thanks to Risto Hakulinen for his comments and suggestions during this research and to Lawrence LaFleur of the National Council for Air and Stream Im-

provement (Corvallis, OR) for performing the GC/MS analyses.

Registry No. 2,4,6-Trichlorophenol, 88-06-2; 2,3,4,5-tetrachlorophenol, 4901-51-3; 3,4,5-trichlorophenol, 609-19-8; 2,3-dichlorophenol, 576-24-9; 3,4-dichlorophenol, 95-77-2; *p*-chlorophenol, 106-48-9; 4,5-dichloroguaiacol, 2460-49-3; tetrachloroguaiacol, 2539-17-5; 4,5-dichloroveratrole, 2772-46-5; tetrachloroveratrole, 944-61-6; pentachlorophenol, 87-86-5; 4,5-dichlorocatechol, 3428-24-8; 3,5-dichlorophenol, 591-35-5; 2,4-dichlorophenol, 120-83-2; 2,6-dichlorophenol, 87-65-0; *m*-chlorophenol, 108-43-0.

Literature Cited

- (1) Boyd, S. A.; Shelton, D. R. *Appl. Environ. Microbiol.* **1984**, *47*, 272-277.
- (2) Suflita, J. M.; Horowitz, A.; Shelton, D. R.; Tiedje, J. M. *Science (Washington, D.C.)* **1982**, *218*, 1115-1116.
- (3) Guthrie, M. A.; Kirsh, E. J.; Wukasz, R. F.; Grady, C. P. L. *Water Res.* **1984**, *18*, 451-461.
- (4) Hakulinen, R. *Pap. Puu* **1982**, *64*, May.
- (5) Salkinija-Salonen, M.; Paasivuori, R.; Koistinen, O.; Hakulinen, R. *DECHEMA-Monogr.* **1980**, *86*, 349-358.
- (6) Woods, S. L. The Fate of Chlorinated, Hydroxylated and Methoxylated Benzenes in Anaerobic Wastewater Treat-

ment. Dissertation, University of Washington, Seattle, WA, 1985.

- (7) Voss, R. H.; Wearing, J. T.; Wong, A. In *Advances in the Identification and Analysis of Organic Pollutants in Water*; Keith, L. H., Ed.; Ann Arbor Science: Ann Arbor, MI, 1981; Vol. 2, pp 1059-1095.
- (8) National Council of the Paper Industry for Air and Stream Improvement (NCASI). Experience with the Analysis of Pulp Mill Effluents for Chlorinated Phenols using an Acetic Anhydride Derivatization Procedure. Stream Improvement Technical Bulletin No. 347; June, 1981.
- (9) Boyd, S. A.; Shelton, D. R.; Berry, D.; Tiedje, J. *Appl. Environ. Microbiol.* **1983**, *46*, 50-54.
- (10) Chen, W.; Supanwong, K.; Ohmiya, K.; Shimizu, S.; Kawakami, H. *Appl. Environ. Microbiol.* **1985**, *50*, 1451-1456.

Received for review December 29, 1986. Revised manuscript received May 16, 1988. Accepted July 11, 1988. This work was funded by the Office of Exploratory Research, Environmental Protection Agency (Grant No. R-808675). We also acknowledge the financial support of Georgia Pacific Corp., Weyerhaeuser Co., ITT-Rayonier Inc., Scott Paper Co., Boise Cascade, and CH2M-Hill Inc.

Biodegradation of Trace Concentrations of Substituted Phenols in Granular Activated Carbon Columns

Gerald E. Spittel Jr.,*† Chih-Jen Lu, Mukesh Turakhia,‡ and Xian-Jin Zhu

University of Houston, Environmental Engineering Program, Houston, Texas 77004

■ Biodegradation of synthetic organic chemicals in granular activated carbon (GAC) columns may extend the GAC service life through in situ biological regeneration of sorption sites, by decreasing the chemical loading onto the GAC, or both. In addition, the combination of biodegradation and adsorption may provide more stable and reliable operation than with either process alone. Biodegradation of *p*-nitrophenol (PNP), 2,4-dichlorophenol (DCP), and pentachlorophenol (PCP) was investigated over the concentration range of 1-25 µg/L. GAC columns were equilibrated prior to the commencement of experiments. Biodegradation of both sorbed and liquid-phase substrate was measured. PNP and DCP were readily biodegraded; PCP also was biodegraded but at a slower rate. Significant biodegradation of sorbed substrate occurred only with PNP. Biodegradation of sorbed DCP was limited by slow desorption kinetics, while biodegradation of sorbed PCP was limited by slow microbial kinetics.

Introduction

Microbial activity in GAC columns is of interest because of the potential for extending service life through in situ biological regeneration of sorption sites. In addition, the presence of microbial activity may provide more stable and reliable operation of GAC columns during periods of fluctuating influent concentration. Much work has been done on the removal of total organic carbon (TOC) across biologically active GAC beds. To a very great extent TOC is composed of naturally occurring organic chemicals. Therefore, TOC measurements and carbon or dissolved

oxygen balances can establish the presence of biological activity, but cannot track the fate of synthetic organic chemicals (SOCs), which are just a small fraction of the TOC. Removal of SOC is of much interest because many of these chemicals are of health concern. Previous work (1) examined the removal of phenol and *p*-nitrophenol (PNP) in single-substrate systems over the concentration range of 20-100 µg/L. Significant biodegradation of the chemicals occurred in both the liquid and sorbed phases. This research extends the work to lower substrate concentrations (1-25 µg/L) and evaluates more highly substituted, chlorinated phenols.

Materials and Methods

Chemicals. Three substituted phenols were studied, *p*-nitrophenol, 2,4-dichlorophenol (DCP), and pentachlorophenol (PCP). PNP is moderately adsorbable and biodegradable, while PCP is highly adsorbable and very difficult to biodegrade. DCP is nearly as adsorbable as PCP, but is considerably more biodegradable. Thus, the three chemicals covered a broad range of adsorbability and biodegradability. ¹⁴C-Radiolabeled forms of the chemicals were used in many experiments; in all cases the chemicals were uniformly radiolabeled around the benzene ring. In several experiments acetate was used in addition to one of the phenols. Acetate is highly biodegradable, nonadsorbable chemical. It was added to stimulate overall microbial activity.

The adsorbability of the chemicals was measured to assist in experimental design and data interpretation. Adsorbability was characterized principally by equilibrium measurements. Experiments were carried out by the bottle point method (2). Equilibrium data, as measured by gas chromatography, were described by the Freundlich isotherm model. Desorption kinetics also were measured in

* Present address: University of Texas, Department of Civil Engineering, 8.6 ECJ, Austin, TX 78712.

† Present address: W. M. Kellogg Co., 3 Greenway Plaza, Houston, TX.

Table I. Buffer Salts and Nutrients

chemical	concn, mg/L		chemical	concn, mg/L	
	PNP	DCP, PCP		PNP	DCP, PCP
KH ₂ PO ₄	900	480	KNO ₃		13.3
K ₂ HPO ₄	29.5	490	CaCl ₂	23.2	23.2
NH ₄ Cl	3.5		MgSO ₄	8.6	8.6

several experiments. Equilibrated GAC (0.1 g) was placed in a differential column batch reactor (3), which had an initial liquid-phase concentration of zero in the 40-L reservoir. The increase in liquid-phase concentration was followed over time by both radiochemical techniques and gas chromatography.

The analysis of radiochemical data in the column experiments requires knowledge of the microbial yield coefficient and the endogenous decay coefficient. These were measured in batch experiments by using radiochemical techniques developed in previous work (4, 5).

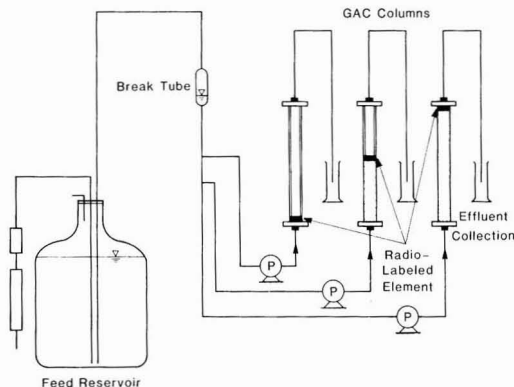
Buffer salts and nutrients were used in all experiments at the concentrations shown in Table I. Experiments with DCP and PCP were conducted at pH 7.2 and those with PNP at pH 5.5. The adsorbabilities of the dissociated and undissociated forms of PNP are quite different. At pH 5.5, PNP is almost entirely in its undissociated form. Because only one form of PNP is present, potential difficulties in data analysis and interpretation are avoided.

One or two phenols were intended to be the sole source of substrate in most experiments. To achieve this objective, experiments were conducted using water that had a very low concentration of other organic carbon sources. The water was treated by reverse osmosis, carbon adsorption, and ion exchange prior to exhaustive ozonation to destroy residual organic chemicals.

GAC. Calgon Filtrasorb 400 GAC was ground in an analytical mill and sieved to recover the 30 × 40 mesh fraction, which provided an average particle diameter of 0.5 mm. The small diameter prevented channeling in the laboratory-scale columns. After the GAC was sieved, it was rinsed with high-purity water to remove oil and fines and then was dried overnight in an oven at 103 °C. The GAC was stored in sealed containers until use. A portion of the 30 × 40 mesh fraction was completely pulverized for use in the adsorption isotherm experiments.

Column Experiments. The approach was very similar to that used in the past (1, 4). Experiments were initiated with the GAC and liquid phases in equilibrium, so that biodegradation in each phase could be quantified. GAC was pre-equilibrated for 2 weeks in bottles and then loaded into the columns. The water used to slurry the GAC for loading into the columns was seeded with microorganisms acclimated to the particular chemical being tested. The columns were fed the equilibrium substrate concentration throughout the experiment. A small portion of the GAC (0.5 g) in a specific location in each column had ¹⁴C substrate sorbed to its surface. The remainder of the GAC and liquid phase consisted of unlabeled substrate. The biodegradation rate of sorbed substrate was measured in the small element of GAC containing radiolabeled substrate. Biodegradation of sorbed substrate within this element led to the production of ¹⁴CO₂. The ¹⁴CO₂ diffused into the liquid phase and appeared in the column effluent, where it was easily measured. Biodegradation of substrate in the liquid phase was measured by gas chromatography.

A schematic of the experimental apparatus is shown in Figure 1. The GAC columns consisted of 1.5-cm diameter, glass chromatography columns, operated in upflow mode. Adjustable plungers were placed as needed in the columns

**Figure 1.** Schematic of experimental apparatus.

to minimize liquid volume above the GAC beds. The flow rate through each column was 2.5 mL/min, and all materials in contact with the liquid and GAC were glass, Teflon, stainless steel, or viton. Typically, three columns were tested in parallel, each of different length and each having the radiolabeled element at the effluent end of the column. Empty bed contact times (EBCT) varied from 0.4 min, for a column containing only a radiolabeled element, to 21 min. By using different column lengths, the variations in liquid-phase concentration and in sorbed substrate biodegradation (bioregeneration) were studied as a function of position in the column.

Samples for gas chromatography and radioactivity analyses were collected periodically throughout the experiments. The gas chromatography samples were immediately acidified to pH 2 and stored under refrigeration until subsequent analysis. Radioactivity samples were collected at high pH to minimize volatilization of ¹⁴CO₂; high pH was established in sampling vessels through the addition of Carbo-Sorb II, an organic base. The total radioactivity and as many as three fractions were measured for each sample. The three fractions were nonpurgeable ¹⁴C, filterable ¹⁴C, and particulate ¹⁴C. Nonpurgeable ¹⁴C includes all radioactivity except ¹⁴CO₂ when, as in this work, the substrates are nonvolatile. Filterable ¹⁴C includes all radioactivity except ¹⁴C biomass. Particulate ¹⁴C is a new measurement developed in this research. Samples were prepared by filtering 5 mL through a 0.2 μm filter, followed by a 20-mL wash with a 50% ethanol/water solution to remove residual ¹⁴C substrate and ¹⁴CO₂ from the filter. The filter was then assayed for radioactivity. The filtering material, cellulose triacetate for PNP and polycarbonate for DCP and PCP, exhibited a negligible uptake of substrate and ¹⁴CO₂ after washing; therefore, the particulate ¹⁴C concentration represents ¹⁴C biomass in the effluent. The filterable ¹⁴C and particulate ¹⁴C measurements are alternative approaches for gaining the same information. The particulate ¹⁴C measurement is attractive for chemicals, such as DCP and PCP, that show significant sorption to the filtering material in the absence of an ethanol/water washing step.

The radioactivity in the column effluent is comprised of three major components: substrate, CO₂, and biomass. The concentration of each component can be calculated from the four types of samples, as follows: ¹⁴CO₂ = total - nonpurgeable; ¹⁴C biomass = total - filterable = particulate; ¹⁴C substrate = filterable + nonpurgeable - total = nonpurgeable - particulate. The ¹⁴C substrate concentration also may include metabolic intermediates and end products, if these are not sorbed onto the GAC. Multi-

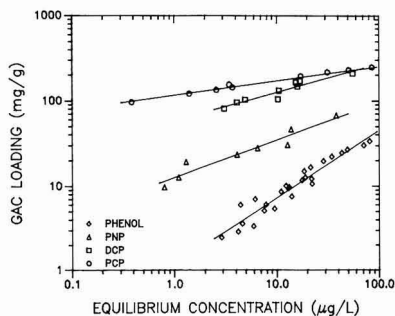


Figure 2. Adsorption isotherms.

plication of the concentrations by the associated flow rate gives the radioactivity production rate (dpm/min) for each constituent.

The $^{14}\text{CO}_2$ production rate is of principal interest because it allows calculation of the biodegradation rate of sorbed substrate originating from the radiolabeled element. Production of $^{14}\text{CO}_2$ occurs mainly from biodegradation of substrate; however, endogenous decay of ^{14}C biomass attached to the GAC is another potential source of $^{14}\text{CO}_2$. A mass balance on ^{14}C biomass in the GAC column allows the $^{14}\text{CO}_2$ production rate to be corrected for endogenous decay. The biodegradation rate of sorbed substrate, or the bioregeneration rate, is given by

$$J'_i = (r_c - bk_c X) / [(1 - Y)(SA)]$$

where J'_i is the biodegradation rate (μg substrate/min), r_c is the $^{14}\text{CO}_2$ production rate (dpm/min), b is the endogenous decay coefficient (min^{-1}), k_c is the fraction of biomass carbon converted to CO_2 as a result of endogenous decay, X is the mass (dpm) of ^{14}C biomass attached to the GAC, Y is the microbial yield coefficient (μg of cell carbon/ μg of substrate carbon), and SA is the specific activity (dpm/ μg). Specific activity is a known proportionality factor between total radioactivity and total substrate mass sorbed within the radiolabeled element at the start of the experiment. A detailed description of this calculation is presented elsewhere (1, 4).

Analytical Procedures. Radioactivity was assayed on a Beckman LS-3801 liquid scintillation counter. Quench correction was by the H -number with the instrument's cesium-137 standard. Samples also were corrected for background activity, which was approximately 30 disintegrations per minute (dpm). Glass scintillation vials were used in all analyses because radioactivity decreased over time in polypropylene vials, apparently from diffusion of $^{14}\text{CO}_2$ through the walls of the vials.

Liquid-phase concentrations of PNP, DCP, and PCP were measured by gas chromatography. PNP was measured by the direct aqueous acetylation and extraction procedure reported previously (1). One modification in this research was the use of a capillary column (J&W Scientific DB-5, 50 m, 0.24 mm i.d.), which permitted detection of much lower concentrations than the packed column used in the past. The temperature program was 3 min isothermal at 41 $^\circ\text{C}$, 5 $^\circ\text{C}/\text{min}$ to 90 $^\circ\text{C}$, hold for 7 min, 5 $^\circ\text{C}/\text{min}$ to 110 $^\circ\text{C}$, hold for 4 min, 20 $^\circ\text{C}/\text{min}$ to 170 $^\circ\text{C}$, hold for 5 min. The retention time for PNP was ~ 28 min. The internal standard was *m*-cresol. DCP and PCP samples were prepared by extracting 50 mL of sample with 2 mL of methylene chloride. The extract was concentrated by gentle purging with nitrogen gas. The concentrated extract was injected into a gas chromatograph equipped with the column noted above and an electron

Table II. Characteristics of Phenolics

chemical	Freundlich isotherm		biodegradation		
	K , (mg/g) (L/ μg) $^{1/n}$	$1/n$	Y , $\mu\text{gC}/\mu\text{gC}$	b , day $^{-1}$	k_c
phenol	1.09	0.816	0.48	0.15	0.5
<i>p</i> -nitrophenol	12.6	0.439	0.29	0.22	0.5
2,4-dichlorophenol	53.9	0.373	0.17		
pentachlorophenol	109	0.181	0.20		

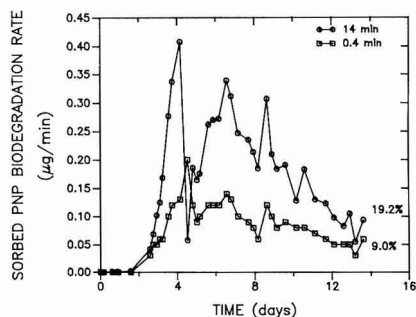


Figure 3. Biodegradation rates of sorbed PNP at an equilibrium concentration of 5 $\mu\text{g}/\text{L}$.

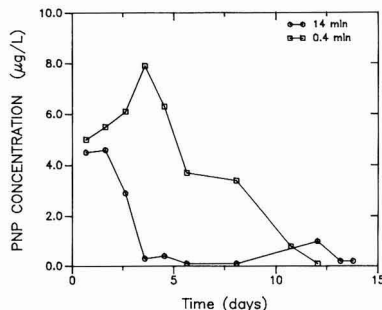


Figure 4. PNP effluent concentrations at an equilibrium concentration of 5 $\mu\text{g}/\text{L}$.

capture detector. The temperature program was 3 min isothermal at 80 $^\circ\text{C}$, 5 $^\circ\text{C}/\text{min}$ to 140 $^\circ\text{C}$, hold for 1 min, 5 $^\circ\text{C}/\text{min}$ to 170 $^\circ\text{C}$, hold for 7 min, 20 $^\circ\text{C}/\text{min}$ to 200 $^\circ\text{C}$. The retention times were 9 min for DCP and 26 min for PCP. The internal standard was 2,4,6-trichlorophenol.

Results and Discussion

The adsorption isotherms are shown in Figure 2. The isotherm for phenol also is included to provide a basis for comparison among the various phenols. The parameters that characterize adsorption and biodegradation are listed in Table II.

Figures 3 and 4 show the results of an experiment with PNP at an equilibrium concentration of 5 $\mu\text{g}/\text{L}$. Figure 3 presents the biodegradation rate of sorbed PNP in the radiolabeled element at the end of each column. Although not shown for the sake of clarity, the rate for a 7-min EBCT was essentially equal to that of the 14-min EBCT column. The rate of 0.4 min, however, was significantly smaller than the other two. Integration of each rate curve gives the mass of sorbed PNP biodegraded within the radiolabeled element. A percent bioregeneration is calculated by dividing the mass biodegraded by the mass of substrate initially sorbed in the radiolabeled element. These percentages are shown on Figure 3. Liquid-phase

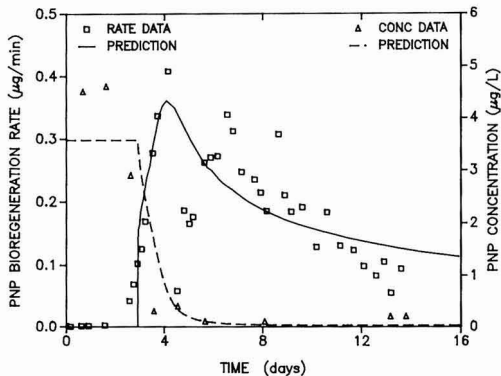


Figure 5. Predicted PNP bioregeneration rate and effluent concentration at an equilibrium concentration of 5 µg/L and 14-min EBCT.

concentrations are presented in Figure 4; again, the results at 7-min EBCT are not shown but were identical to those at 14-min EBCT. The effluent concentration at the 0.4-min EBCT was significantly higher than that at the 14-min EBCT throughout most of the experiment. This difference in effluent concentrations was expected, as the shorter EBCT provides less opportunity for biodegradation of liquid-phase PNP. The higher concentrations at the 0.4-min EBCT probably accounted for the smaller biodegradation rate of sorbed PNP. A smaller departure from phase equilibrium occurred; therefore, the diffusion rate of sorbed PNP from the GAC to the microorganisms was slower. A comparison of Figures 3 and 4 indicates the onset of microbial activity first results in a sharp decrease in liquid-phase concentration, closely followed by an increase in the biodegradation rate of sorbed PNP. The pattern is similar to that observed previously with phenol and PNP is higher equilibrium concentrations of 20–100 µg/L.

A computer model of biodegradation and adsorption in single-component systems was applied to the experimental data to determine if widely used mass transport and kinetic expressions were capable of describing the results. Adsorption was described by the homogeneous surface diffusion model, biodegradation by biofilm diffusion and Monod kinetics, and bulk liquid transport by advection with a liquid film transport resistance between the liquid and GAC phases (6, 7). Details of the model derivation, solution procedure, and input parameter estimation are provided elsewhere (7, 8). Figure 5 shows the best fit of the model to the 14-min EBCT data. The model fit the data from both the liquid and sorbed phases reasonably well and, thus, provides a means of extending these results to other systems.

A subsequent experiment examined a PNP equilibrium concentration of 2.5 µg/L. Sodium acetate at 2 mg/L also was added to the feed solution because of concern that the PNP concentration might be too low to support microbial growth. The results are presented in Figures 6 and 7. The bioregeneration rate varied significantly with position in the GAC column. Essentially no bioregeneration occurred at the 0.4-min EBCT. The largest extent of bioregeneration was at the 14-min EBCT. Both the rate and percent bioregeneration, however, were significantly smaller than in the previous experiment, and the shape of the rate curve was quite different, as well. Figure 7 suggests why this might be. The liquid-phase concentration did not decrease rapidly to a very low level; therefore, desorption and subsequent biodegradation of sorbed PNP could not proceed. For example, the concentration at the 14-min

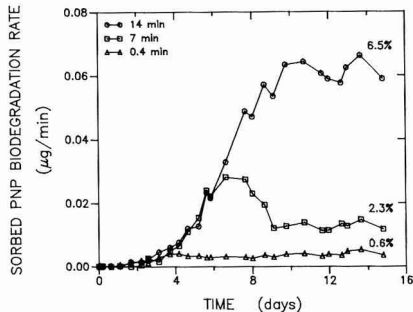


Figure 6. Biodegradation rates of sorbed PNP at an equilibrium concentration of 2.5 µg/L.

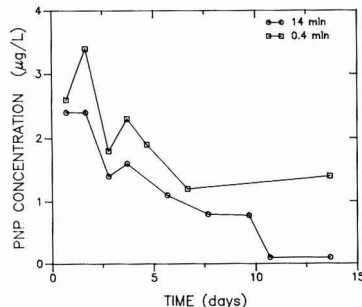


Figure 7. PNP effluent concentrations at an equilibrium concentration of 2.5 µg/L.

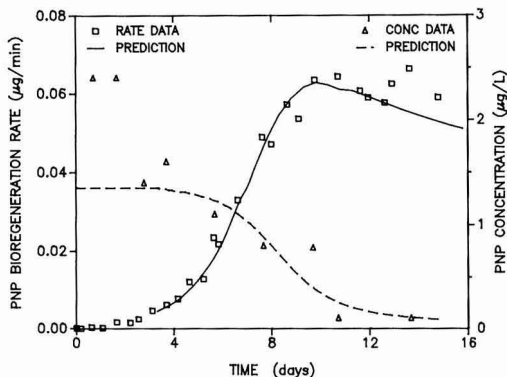


Figure 8. Predicted PNP bioregeneration rate and effluent concentration at an equilibrium concentration of 2.5 µg/L and 14-min EBCT.

EBCT was essentially zero in the previous experiment after 3.5 days (Figure 4), whereas in this experiment over 10 days were required to achieve the same result.

Two possibilities might account for the decreased biological activity relative to the previous experiment: the lower PNP concentration or preferential biodegradation of acetate. It seems unlikely, however, that a decrease in the equilibrium concentration from 5 to 2.5 µg/L would produce such a large effect by itself. A much more plausible explanation is preferential degradation of the highly biodegradable acetate. Either organisms capable only of metabolizing acetate dominated or many PNP degraders switched to acetate because of its higher concentration and biodegradability.

The biodegradation/adsorption computer model also was applied to the second PNP experiment. Of particular interest was the ability of the model to fit the unusually shaped bioregeneration rate curve. Figure 8 shows the best

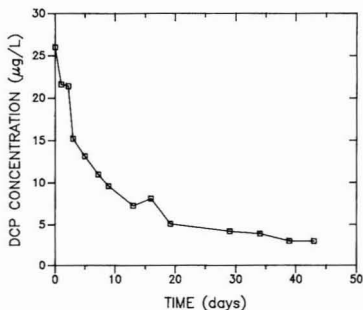


Figure 9. DCP effluent concentration at an equilibrium concentration of 26 $\mu\text{g/L}$.

fit of the model to the 14-min EBCT data. Two input parameters were different than those used in Figure 5. The initial amount of biomass was an order of magnitude smaller, and the Monod half-saturation coefficient was increased from 1 to 2.2 $\mu\text{g/L}$. The good fit with less biomass is consistent with the hypothesis of preferential acetate utilization; that is, the availability of acetate decreased the mass of cells degrading PNP, although increasing the total mass of cells in the column. The larger half-saturation coefficient caused a decreased biodegradation rate and likewise suggests a detrimental impact of acetate on PNP biodegradation.

The good fit of the model indicates that low levels of microbial activity are expected to change the characteristic shape of the bioregeneration rate curve. Rather than a sharp peak followed by a gradual decline, the rate rises to a plateau and remains at a constant, relatively low value for some time. Although not shown in Figure 8, the model eventually predicts a decline in the bioregeneration rate, as would be expected once a significant fraction of sorbed PNP is biodegraded.

The performance of GAC columns with DCP and PCP was substantially different than that observed with PNP. In a variety of experiments, negligible biodegradation of sorbed DCP and PCP occurred. Both chemicals, however, were biodegraded in the liquid phase, DCP much more readily than PCP. Figure 9 shows the effluent concentration from a 14-min EBCT column in an experiment with DCP at an equilibrium concentration of 26 $\mu\text{g/L}$. The effluent concentration decreased from 26 to 3 $\mu\text{g/L}$ over 30 days of operation. Despite the 90% decrease in liquid-phase concentration, the $^{14}\text{CO}_2$ and total radioactivity concentrations in the effluent were negligible. Virtually no biodegradation or desorption of sorbed DCP occurred. This contrasts sharply with expectations based on experience with PNP.

Similar results were obtained with PCP in two 14-min EBCT columns at an equilibrium concentration of 25 $\mu\text{g/L}$. One column was fed PCP alone, while the other received PCP and 1 mg of sodium acetate/L. After 1 month of operation, the effluent concentration from each column was $\sim 16 \mu\text{g/L}$ (32% removal), and no biodegradation of sorbed PCP had occurred. Acetate had no effect on the removal of PCP, as evidenced by the essentially identical performance of the columns. Obviously, the column receiving acetate developed more biomass, but these organisms were either incapable of degrading PCP or it was not advantageous for them to do so. Two factors might account for the absence of bioregeneration in this experiment. The modest decrease in liquid-phase concentration may have been inadequate to promote significant desorption from the GAC. Another possibility is that sorbed PCP is incapable of desorption, as apparently

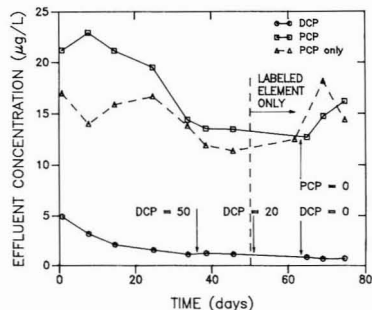


Figure 10. DCP and PCP effluent concentration at equilibrium concentrations of 6 and 15 $\mu\text{g/L}$, respectively.

happened in the DCP experiment.

A third experiment was carried out to explore PCP biodegradation in more detail. The EBCT was increased to 21 min and the PCP equilibrium concentration was reduced in an attempt to achieve a greater percent removal of PCP in the liquid phase. Also, a mixture of PCP and DCP was used in two columns. DCP was added to stimulate biodegradation of PCP; the structure of DCP is similar to that of PCP, yet it is more biodegradable. Because organisms probably use similar enzymes to degrade both DCP and PCP, DCP may be more effective than acetate in stimulating biodegradation of PCP. The entire experiment consisted of three columns. The first was in equilibrium with PCP at 15 $\mu\text{g/L}$. The second and third columns were in equilibrium with a mixture of PCP (15 $\mu\text{g/L}$) and DCP (6 $\mu\text{g/L}$). In one column the radiolabeled element contained labeled PCP, while in the other it contained labeled DCP. Because both PCP and DCP are biodegradable, two columns, identical except for the radiolabeling scheme, are required to measure biodegradation of sorbed substrate.

Figure 10 shows the effluent concentration from the column receiving PCP alone and the average effluent concentrations of DCP and PCP from the two columns receiving both. The effluent DCP concentration decreased from 5 to less than 1 $\mu\text{g/L}$ over the first 30 days of operation, indicating significant biodegradation of DCP in the liquid phase. In contrast, only a small fraction of the PCP was biodegraded, despite the aforementioned steps taken to increase biodegradation. The effluent PCP concentration in the columns receiving both PCP and DCP decreased from ~ 22 to 13 $\mu\text{g/L}$ over the first 45 days of operation, while a decrease from ~ 16 to 11 $\mu\text{g/L}$ occurred in the column receiving PCP only. A somewhat larger decrease in PCP concentration occurred in the presence of DCP, but the difference is not so large as to unequivocally demonstrate that DCP stimulated biodegradation of PCP. Perhaps a larger DCP concentration is required to produce a significant effect.

Biodegradation of sorbed PCP and DCP was negligible (1% or less) over the 80 days of operation. The negligible amount of bioregeneration supports the conclusion that removals of DCP and PCP observed in the liquid phase resulted from biodegradation. The GAC was initially exhausted, and in the absence of any bioregeneration the GAC had no capacity for further sorption.

The potential for bioregeneration of PCP adsorption sites was investigated by calculating the desorption rate corresponding to column conditions at 45 days of operation. The desorption rate represents the maximum possible biodegeneration rate, as microorganisms can biodegrade sorbed chemicals only as fast as the chemicals desorb

from the GAC. The homogeneous surface diffusion model for batch systems (3) was used as in the past (1) to perform the calculation. Based on the GAC loading at the start of the experiment and the average liquid-phase concentration after 45 days (12 $\mu\text{g/L}$), the desorption rate is quite small; only 2% of the PCP would desorb over 80 days under such conditions. The relatively high liquid-phase concentration in combination with the flat slope of the PCP isotherm (Figure 2 and Table II) results in a very small driving force for desorption. This illustrates that the promotion of significant bioregeneration requires a large decrease in the liquid-phase concentration, especially for strongly adsorbed chemicals.

Operating conditions were modified several times during the experiment in attempts to stimulate biodegradation of sorbed PCP and DCP. Influent concentrations were changed, and near the end of the experiment, the radiolabeled elements were isolated from the remainder of each column, effectively producing a column with a very short EBCT. In the columns receiving both PCP and DCP, the DCP concentration was increased from 6 to 50 $\mu\text{g/L}$ at 38 days to stimulate biodegradation. As shown in Figure 10, the increase in the influent DCP concentration had no effect on either the effluent PCP or DCP concentrations. Probably, the additional DCP was biodegraded or sorbed by the GAC near the influent region of the column and was then unavailable for promoting further microbial activity near the effluent end of the column. To assure that the increased DCP concentration reached the radiolabeled element at the end of the column, the columns were shortened at 51 days to approximately include only the radiolabeled element. This reduced the EBCT from 21 min to less than 1 min. An influent DCP concentration of 20 $\mu\text{g/L}$ was fed. Again, no impact on effluent concentrations or biodegradation of sorbed substrate was observed. The PCP and DCP influent concentrations were set to zero at 64 days to stimulate desorption from the GAC and subsequent biodegradation. Little change in the effluent PCP and DCP concentrations occurred. Because the influent concentrations were zero, PCP and DCP were desorbing from the GAC, but only a small amount of biodegradation resulted, as indicated by $^{14}\text{CO}_2$ production.

For an influent PCP concentration of zero, the desorption rate from the radiolabeled element can be calculated as the product of the effluent concentration (13 $\mu\text{g/L}$) and the flow rate (0.0025 L/min). This calculation is valid because all PCP in the effluent must originate from the GAC. The calculated desorption rate for PCP is 0.033 $\mu\text{g/min}$. The rate is near the lower end of the range of bioregeneration rates observed for PNP (see Figures 3 and 6). This suggests that PCP can desorb at reasonable rates and that the absence of bioregeneration is related to difficulties with biodegradation. Microbial activity was insufficient to keep up with the desorption rate; thus, rather than desorption with subsequent biodegradation, desorption followed by an increase in liquid-phase concentration was observed. Had the microorganisms been able to biodegrade the PCP and maintain a low liquid-phase concentration, the desorption rate probably would have been much greater. The low concentration would cause a larger departure from equilibrium between the two phases, and hence a greater desorption rate.

On the basis of Figures 9 and 10, the absence of bioregeneration with DCP and PCP appeared to be controlled by a different mechanism for each chemical. The rate-limiting steps seemed to be desorption for DCP and biodegradation for PCP. These conclusions were tested further in more controlled experiments that examined

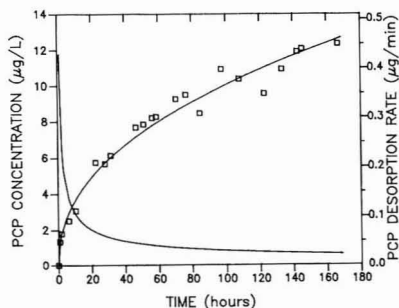


Figure 11. PCP batch desorption experiment.

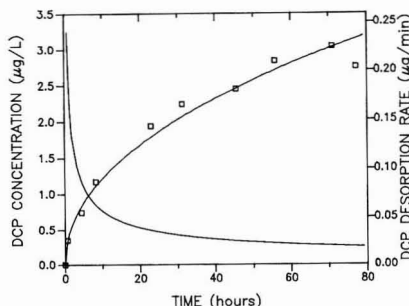


Figure 12. DCP batch desorption experiment—first reservoir.

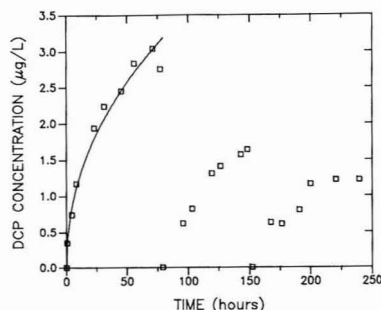


Figure 13. DCP batch desorption experiment—all three reservoirs.

desorption in the absence of microbial activity. Desorption rates were measured for PCP and DCP in a differential element batch reactor. Figure 11 shows the liquid-phase concentration of PCP over time. A power function (Concentration = $a\text{Time}^b$) was fitted to the data, and its derivative was used to estimate the desorption rate ($\mu\text{g/min}$), which also is shown in Figure 11. The desorption rate was quite large, especially considering that only 0.1 g of GAC was used in the experiment. A typical radiolabeled element contained 0.5 g, and its desorption rate at each corresponding liquid-phase concentration would be 5 times larger. The results corroborate the conclusions drawn from Figure 10: the absence of bioregeneration with PCP was a biodegradation, not a sorption, phenomenon.

Figure 12 shows desorption of DCP. The data suggest that DCP desorbs at reasonable rates; however, less than 1% of the sorbed DCP had moved into the liquid phase after 80 h. The fractional desorption was insufficient to confidently draw conclusions about desorbability. To stimulate additional desorption, the 40-L reservoirs were replaced twice with clean water, which caused a step change in the liquid-phase concentration. Figure 13 shows the results for all three reservoirs. After 240 h of operation,

only 1.6% of the DCP had desorbed. Furthermore, the amount of desorption decreased with each successive reservoir. For such a small fractional desorption, successive reservoirs should have nearly identical concentration patterns, if a chemical is readily desorbable. A substantial portion of the DCP appears to be irreversibly sorbed; perhaps only DCP on the outer surface of the GAC or in the macropores desorbs readily. The slow desorption rate of DCP explains the inability to biodegrade sorbed DCP, in that desorption must precede biodegradation.

Irreversible adsorption has been observed for chemicals other than DCP. Yonge et al. (9) demonstrated significant irreversible adsorption for phenols having methyl, ethyl, and methoxy substituents at the ortho position on the benzene ring. Pirbizar and Weber (10) found completely irreversible adsorption of polychlorinated biphenyls. Smith and Weber (11) in work with trichloroethylene and *p*-dichlorobenzene found that an adsorption model correctly predicted the effluent concentration during periods of adsorption, but overestimated the effluent concentration during periods of desorption. This suggests some degree of irreversible adsorption.

Conclusions

PNP and DCP were readily biodegradable in GAC columns, even at influent concentrations less than 10 µg/L. PCP also was biodegradable, but its rate was slower than those of PNP and DCP. Significant biodegradation of sorbed substrate occurred only with PNP. A substantial fraction of the DCP appeared to be irreversibly sorbed; therefore, negligible bioregeneration occurred, even though low concentrations in the liquid phase caused a significant departure from phase equilibrium. Bioregeneration might be possible with different types of GAC or other adsorbents. The absence of bioregeneration with PCP was linked to the slow biodegradation rate. Large decreases in liquid-phase concentration were not observed. Thus, only a small departure from phase equilibrium existed, resulting in a small driving force for desorption. Bioregeneration with PCP would be expected if the biodegradation rate can be stimulated through the use of better organisms or through the presence of more biodegradable chemicals. Attempts to implement the latter strategy showed that acetate had no effect on the PCP biodegra-

ation rate and that DCP may have marginally increased the PCP biodegradation rate.

Many contamination problems in practice involve mixtures of chemicals having a range of biodegradabilities and adsorbabilities. Most chemicals of concern compete for adsorption sites on GAC; therefore, biodegradation of some in the sorbed and liquid phases can increase the adsorption capacity for the less- or nonbiodegradable chemicals. Irreversibly adsorbed, yet biodegradable, chemicals also may contribute to this increase in adsorption capacity. Although bioregeneration is not possible, relatively rapid initiation of biodegradation in the liquid phase can prevent exposure of most of the GAC column to such chemicals, thus providing more adsorption sites for other chemicals.

Registry No. PCP, 87-86-5; PNP, 100-02-7; DCP, 120-83-2.

Literature Cited

- (1) Speitel, G. E., Jr.; DiGiano, F. A. *J.-Am. Water Works Assoc.* **1987**, *79*, 64-73.
- (2) Peel, R. G.; Benedek, A. *Environ. Sci. Technol.* **1980**, *14*, 66-71.
- (3) Hand, D. W.; Crittenden, J. C.; Thacker, W. E. *J. Environ. Eng. (N.Y.)* **1983**, *109*, 82-101.
- (4) Speitel, G. E., Jr. Ph.D. Dissertation, University of North Carolina, Chapel Hill, NC, 1985.
- (5) Speitel, G. E., Jr.; DiGiano, F. A. *Water Res.* **1988**, *22*, 829-835.
- (6) Speitel, G. E., Jr.; Dovantzis, K.; DiGiano, F. A. *J. Environ. Eng. (N.Y.)* **1987**, *113*, 32-48.
- (7) Zhu, X. J. M.S. Thesis, University of Houston, Houston, TX, 1987.
- (8) Speitel, G. E., Jr.; Zhu, X. J. submitted for publication in *J. Environ. Eng. (N.Y.)*.
- (9) Yonge, D. R.; Keintath, T. M.; Pozanska, K.; Jiang, Z. P. *Environ. Sci. Technol.* **1985**, *19*, 690-694.
- (10) Pirbizar, M.; Weber, W. J., Jr. *Adsorption of Polychlorinated Biphenyls from Water by Activated Carbon*; Cooper, W. J., Ed.; Ann Arbor Science: Ann Arbor, MI; *Chem. Water Reuse* **1981**, *2*, 309.
- (11) Smith, E. H.; Weber, W. J., Jr. *Environ. Sci. Technol.* **1988**, *22*, 313-321.

Received for review January 26, 1988. Accepted June 20, 1988. This research was supported by a grant to the University of Houston from the Texas Advanced Technology Research Program.

Measurements of the Gas/Particle Distributions of Atmospheric Organic Compounds

Mary P. Ligocki[†] and James F. Pankow*

Department of Environmental Science and Engineering, Oregon Graduate Center, 19600 N.W. Von Neumann Drive, Beaverton, Oregon 97006

■ The gas/particle distributions of polycyclic aromatic hydrocarbons (PAHs) and other organic compounds were measured at ground level in Portland, OR, and at the Oregon coast. Measured particulate-phase concentrations of most PAHs and oxo-PAHs were virtually the same whether glass fiber or Teflon membrane filters were used. Backup glass fiber filter concentrations were measured and found to be quite variable, averaging 30-70% of the primary filter values for alkanes, but less than 30% for all PAHs. At the coastal site, due to the lower concentrations of particulate matter there, the gas/particle distributions of PAHs were shifted toward the vapor phase relative to what was observed in Portland. At both sites, for the PAHs of low to intermediate volatility, the gas/particle distributions correlated with the supercooled liquid vapor pressures. However, acenaphthylene and fluorene showed more association with the particulate phase than predicted by those correlations. Possible explanations for the deviations include the presence of bound PAHs within particles and the presence of high energy adsorption sites on the surfaces of the particles.

Introduction

Atmospheric organic compounds are found in both the gas and particulate phases. Pankow (1) has recently reviewed the theories available for describing this distribution process. The manner in which a given compound partitions will influence that compound's atmospheric removal mechanisms and lifetime, as well as its health effects due to inhalation. The extent of association with particulate matter will depend upon the compound's vapor pressure, the amount and type of particulate matter present, and the temperature. The first equation developed to describe this partitioning process was derived by Junge (2) based on a linear Langmuir isotherm

$$\phi = c_p / (c_g + c_p) = c\theta / (p^\circ + c\theta) \quad (1)$$

where ϕ is the fraction of a compound that is associated with particles, c_g and c_p are the gas- and particulate-phase-associated atmospheric concentrations (ng/m^3), respectively, p° is the vapor pressure of the pure compound (Torr), and θ is the total suspended particulate surface area concentration (cm^2/cm^3). Eq 1 gives

$$\log \frac{c_g}{c_p} = \log \frac{1 - \phi}{\phi} = \log \frac{1}{c\theta} + \log p^\circ \quad (2)$$

Junge (2) used $c = 0.13$ to illustrate the dependence of ϕ on p° and θ .

Equation 1 is useful for demonstrating the general trend of increasing partitioning to particles with decreasing p° . However, the assumptions implicit in its derivation should be kept clearly in mind. First, it only describes adsorption that is *physical, nonspecific, and at equilibrium*, with

100% of any particulate-associated material assumed to be available for exchange (within the time frame of interest) with the gas phase. Second, one cannot expect that the value of c will be constant from compound class to compound class, or even necessarily within a given compound class. Indeed, as shown by Pankow (1) for physical adsorption, c will be a function of temperature T (K) and will only be constant for a given group of compounds when there is a compound-to-compound constancy in (1) the difference between the entropy of desorption from the specific particulate matter of interest and the entropy of vaporization of the pure compound and (2) the difference between the enthalpy of desorption from the particulate matter and the enthalpy of vaporization of the pure compound.

The measurement of c_g/c_p distributions is often accomplished by using a filter followed by an adsorbent such as polyurethane foam (PUF) or Tenax. In one of the first studies of this type, Cautreels and Van Cauwenbergh (3) provided measurements for polycyclic aromatic hydrocarbons (PAHs), alkanes, phthalate esters, and fatty acids. Yamasaki et al. (4) used a similar sampling approach and employed a linear Langmuir isotherm to examine the dependence of c_g/c_p distributions of PAHs in Tokyo upon T and the total suspended particulate matter concentration (TSP). They suggested that θ might be proportional to TSP and correlated their data using the equation

$$\log K = \log \frac{A(\text{TSP})}{F} = \log \frac{A}{F/\text{TSP}} = m/T + b \quad (3)$$

where A and F are the measured c_g and c_p values as determined on the adsorbent and filter, respectively, and m and b are compound-dependent constants. If there are no sampling artifacts, then $A = c_g$ and $F = c_p$. Under these conditions, one may view the expression for the constant K as the equilibrium ratio of A to F/TSP , i.e., as the equilibrium ratio of the concentration in the gas phase (ng/m^3) to that in/on the particulate matter ($\text{ng}/\mu\text{g}$). As $1/T$ decreases, the gas phase tends to be preferred over the particulate phase. As a result, the slope (m) is negative. The value of b will depend in part on the units selected for TSP. Yamasaki et al. (4) chose units of nanograms per cubic meter, but we will use units of micrograms per cubic meter.

As shown by Pankow (1), within a given class of compounds, the value of K may be expected to depend upon p° according to an equation of the type

$$\log K = \log C + \log p^\circ \quad (4)$$

where C is a temperature-dependent constant. For the PAHs at 20 °C, $\log C$ has been found to be ~ 7.5 . Assuming no sampling artifacts, eq 3 and 4 yield

$$\log c_g/c_p = \log C/\text{TSP} + \log p^\circ \quad (5)$$

A comparison of eq 2 and 5 leads to the conclusion that $C/\text{TSP} = 1/c\theta$.

There is often some uncertainty as to whether the quantities A and F provide good estimates of c_g and c_p .

[†]Present address: Environmental Quality Laboratory, California Institute of Technology, Pasadena, CA 91125.

Possible sources of artifacts during sampling include partial volatilization of collected particulate material (5), adsorption of gas-phase compounds onto filters (6-8), adsorption onto collected particles (9, 10), and chemical reactions with photochemically produced oxidants (11, 12). Despite these potential problems, Bidleman and co-workers (9, 10, 13, 14) have corroborated the results of Yamasaki et al. (4) and have been successful in applying eq 3 in parameterizing the dependence of A/F on TSP and $1/T$ for certain PAHs and organochlorines.

A significant observation (10, 13) is that although there is some scatter in the $\log K$ vs $1/T$ plots that are currently available for selected PAHs and organochlorines, there is also similarity in the sorption characteristics of the particulate matter of different cities. For example, for fluoranthene and pyrene, the values of m and b obtained in Columbia, SC, (13) are similar to those obtained in Tokyo (4). In terms of eq 5, these results can be interpreted in terms of a rough constancy in the temperature-dependent functionality of C for these compounds (1).

In the studies cited above, either glass or quartz fiber filters were used. Recently, some researchers have advocated the use of Teflon membrane filters (TMFs) instead of fiber filters. The Teflon surface, often considered to be less reactive than glass or quartz, has been expected to reduce the amount of "filter-catalyzed" oxidation of PAHs. An early study (15) indicated that the concentration of total PAHs in ambient and exhaust samples was higher when measured on TMFs than when measured on glass fiber filters (GFFs). Subsequent studies have differed in the extent to which this effect was observed for specific PAHs. One study found GFF/TMF concentration ratios for pyrene and benzo[*a*]pyrene of 0.25 and 0.76, respectively (16). Another study found both of these ratios to be ~ 0.85 and also found no difference in the mutagenicities of the samples collected on the different filter media (17). As part of a continuing study of atmospheric organic compounds (1, 18-23), this work was conducted to investigate the gas/particle distribution process with both GFFs and TMFs. The contributions to the measured particulate-phase concentrations made by gas adsorption to the GFFs were determined.

Experimental Section

The GFFs (102-mm diameter) were obtained from Gelman (Ann Arbor, MI). The TMFs (20 \times 25 cm sheets, Zefluor, 2- μ m pore size) were obtained from Membrana (Pleasanton, CA). The latter were cut into 102-mm circles. PUF of density 0.022 g/cm³ was obtained in 7.6-cm thick sheets and was cut into 5.1-cm diameter plugs (PUFPs). Tenax-GC and -TA were obtained from Alltech Associates (Deerfield, IL). Solvents were distilled-in-glass grade (B&J, Muskegon, MI). Perdeuteriated PAHs were obtained from KOR Isotopes (Cambridge, MA) and MSD Isotopes (Los Angeles, CA). GFFs were cleaned prior to sampling by baking at 400 °C for 2 h. TMFs were cleaned by two successive 10-min sonic extractions in 60:40 acetone/hexane, followed by air drying. Filters were transported to and from the field wrapped in prebaked aluminum foil. PUFPs were cleaned by Soxhlet extraction for 24 h in 60:40 acetone/hexane and dried under a stream of prepurified nitrogen. They were stored and transported in clean screw-capped glass jars with Teflon cap liners. Teflon tape was wrapped around the threads of each jar to provide an airtight seal. Tenax cartridges were cleaned as described elsewhere (24).

Sampling took place in an urban residential section of Portland, OR (20, 21), and at a nonurban Oregon coastal site [Ft. Stevens State Park (23)]. In some cases, both

front and backup filters were used. In every case, a front and a backup PUF followed the filter(s). A branch of the sampler carried a small fraction of the flow from the filter(s) through a set of Tenax cartridges. The maximum/minimum temperature range during all sampling was generally less than 6 °C. The sampling periods were 5-30 h. The face velocities (30-60 cm/s) were comparable to high-volume face velocities. Six sets of samples were obtained in Portland, OR, in February and April 1984 by using GFFs with backup filters. The range of the mean sampling temperatures for the six sets was 5-9 °C. The overall mean temperature was 8 °C. A portion of the data from these samples has been discussed elsewhere (20, 21, 24). Four sets of samples were also collected in Portland with duplicate samplers during February and March, 1985; one sampler was equipped with GFFs and the other with TMFs. The range of the mean sampling temperatures for the four sets of samples was 3-9 °C; the overall mean temperature was 5 °C. The flow rates remained constant throughout each sampling period, but ranged from 100 to 190 L/min over the four events. The flow rates were always within 10 L/min on the two samplers. Pressure drops across the filters were ~ 1 psi for both types of filters. Three sets of samples were obtained with TMFs at the coastal site during April 1985. The range of those mean sampling temperatures was 8-10 °C; the overall mean temperature was 9 °C.

After sampling, portions of most of the GFFs were first analyzed for particulate organic carbon, particulate elemental carbon, and total particulate carbon (TPC) (\approx organic + elemental) with a thermal/optical carbon analyzer (25, 26). [Inorganic particulate carbon in Portland is low (26).] The GFFs and TMFs were extracted and analyzed as described previously for GFFs (20, 21), except that the acid/neutral separation step was omitted for the 1985 samples. Briefly, several deuteriated PAHs in acetone were added directly to the filters as internal standards. The filters were Soxhlet extracted in 25 mL of 1:1 acetone/methylene chloride, and the solvent volume was reduced to 2 mL in a miniature Kuderna-Danish concentrator. The extracts were cleaned up on 5 mL of 15% deactivated silica gel and then reconcentrated to 200 μ L by N₂ blowdown. The extracts were analyzed on an HP 5790A gas chromatograph equipped with a capillary column (30 m long, 0.32 mm i.d., 0.25- μ m DB-5 film, J&W Scientific, Folsom, CA) that was interfaced to a Finnigan 4000 mass spectrometer/data system (GC/MS/DS). The PUFPs were analyzed similarly, except that 500 mL of 60:40 acetone/hexane was the initial solvent. The Tenax cartridges were analyzed by thermal desorption and GC/MS/DS as described previously (24).

Results and Discussion

Filter Blanks. Table I gives the mean blank levels of the alkanes, phthalates, and PAHs on the GFFs and TMFs. The GFF blanks were low for the PAHs in agreement with other work (16, 27), but nonnegligible for bis(2-ethylhexyl) phthalate. The blanks were nearly uniformly higher on the TMFs. In addition to physical adsorption, absorption of background contaminants into the Teflon polymer matrix (28, 29) might be a possible cause for the high TMF blank levels. For example, Hult (28) has found that using syringes with TFE Teflon seals to analyze gas samples containing low molecular weight hydrocarbons can lead to prolonged cross-contamination problems. For TMFs, McDow (8) has suggested that the blank levels might be lowered by baking them out at a high temperature, e.g., at 300 °C, which is just below the melting point of Teflon.

Table I. Comparison of per Filter Blank Levels for GFFs and TMFs for Sampling in Portland, OR, during February and April 1985, Including the TMF Blank Data for the April 1985 Sampling at the Coast^a

compound	TMF (n = 9), ng	GFF (n = 4), ng
eicosane	91 ± 60	3.5 ± 4.4
heneicosane	121 ± 122	2.0 ± 4.0
docosane	162 ± 268	2.9 ± 3.5
tricosane	213 ± 422	ND ^b
tetracosane	291 ± 515	11 ± 16
pentacosane	241 ± 453	ND
hexacosane	214 ± 436	6.2 ± 12.5
octacosane	170 ± 353	7.2 ± 14.3
diethyl phthalate	104 ± 77	30 ± 14
dibutyl phthalate	271 ± 113	51 ± 43
butyl benzyl phthalate	59 ± 36	20 ± 20
bis(2-ethylhexyl) phthalate	944 ± 918	1876 ± 1467
dioctyl phthalate	25 ± 46	2.6 ± 5.2
phenanthrene	1.1 ± 1.3	ND
fluoranthene	0.3 ± 0.7	ND
pyrene	0.2 ± 0.5	
chrysene	0.6 ± 0.8	

^aData values are means ± 1σ. ^bND, not detected.

Front and backup filter sample mass amounts were considered nonzero only when they exceeded the mean blank mass amounts at the 95% confidence level. Because of the high TMF blanks for alkanes and phthalates, these compounds generally did not exhibit ambient levels that passed the significance test as determined on the TMFs. Normalized blanks were calculated by dividing the blank mass amounts by the corresponding sample volumes. When the significance test was passed, the normalized blank was subtracted from the calculated ambient concentration.

Filter Detection Limits. With the GC/MS/DS operated in the scanning mode, the instrument mass detection limits for the PAHs, alkanes, and phthalates were all ~0.1 ng. Depending upon the volume of air sampled, this translated into concentration detection limits of 0.03–0.2 ng/m³. No compound more volatile than acenaphthylene was ever found on the filters. For those volatile compounds that were found, the levels were close to the detection limits. When the April 1985 Portland filter samples were reanalyzed for PAHs with the GC/MS/DS in the multiple ion detection (MID) mode, the resulting enhanced sensitivity produced concentration detection limits of 0.002–0.01 ng/m³; the most volatile PAH found on the filters remained acenaphthylene.

Adsorption of Organic Glass by GFFs. Since the GFFs used exhibit >99% collection efficiency for all particle sizes (30, 31), any material found on a GFF backup filter in a blank-corrected quantity greater than ~1% of the front filter amount probably represented sorbed gas. Figure 1 shows typical front, backup, and blank GFF chromatograms obtained during 1984 in Portland. As in Figure 1, the backup filters occasionally exhibited a small hump of compounds that occurred earlier in the chromatogram than the hump in the front filter chromatogram. The determinations of total carbon on the filters generally gave backup filter amounts that were ~15% of the front filter values, in good agreement with results of others (7) for quartz fiber and silver membrane filters. In this context, it may also be noted that Fitz et al. (17) observed that GFFs produced an average of 48% more solvent-extractable mass for the same volume of air sampled than did Teflon-impregnated GFFs. They concluded that this was due primarily to filter-mediated gas-to-solid conversion of inorganic gases on the GFFs. (The solvent mix they

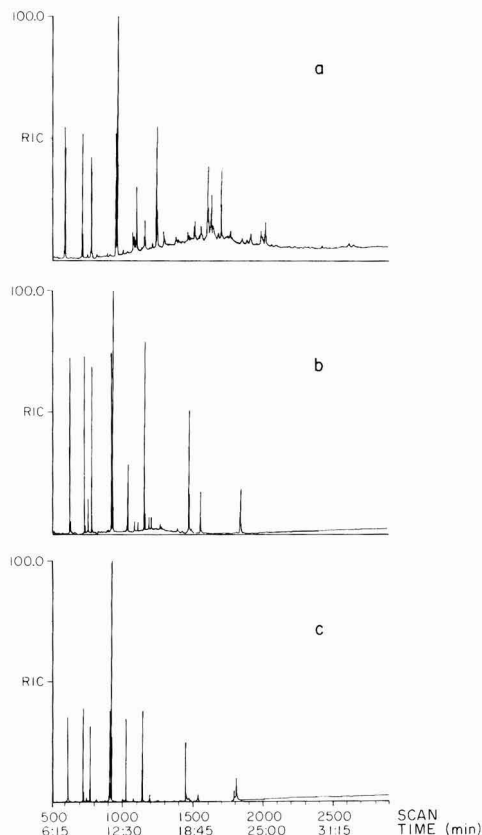


Figure 1. Typical primary (a), backup (b), and blank (c) glass fiber filter chromatograms obtained from sampling in Portland, OR. Several of the large peaks in each of the chromatograms are internal standard compounds.

used contained methanol, which is capable of extracting some inorganic salts.) Since total "particulate" organic carbon on filters in Portland is usually ~20–30% of TSP, and since the GFF gas adsorption effect observed here corresponded to only 15% of total carbon on the front filters, that conclusion is consistent with our results.

All of the target compounds found on the backup filters had vapor pressures in the range 10⁻⁸–10⁻⁴ Torr. No target compounds more volatile than phenanthrene were found on any backup filter, though due to the extremely low particulate-phase concentrations of the most volatile compounds, backup concentrations even as high as 30% of their front filter concentrations would not have been detected. The backup filter values were quite variable. For one sampling event, no target compounds except chrysene were detected. For another event, 16–39% of the front filter amounts were found on the backup filter for PAHs in the 10⁻⁸–10⁻⁴ Torr vapor pressure range. The other events generally fell between these two extremes. Table II gives the average values for the backup filters in GC elution order in terms of the (1) mass amounts, (2) equivalent concentrations, and (3) percentages of the front filter amounts. (It may be noted that phenanthrene has a higher solid vapor pressure than does 9-fluorenone, though it does elute after 9-fluorenone on the GC column used here.) For the methylphenanthrenes and fluoranthene, the mean amounts were 29 and 19%, respectively. For the alkanes and phthalates with vapor pressures in the

Table II. GFF Backup Filter Levels in Terms of Mass Amounts, Equivalent Concentrations (Mass/Sample Volume), and Percentages of Primary Filter Values (Means $\pm 1\sigma$) for Sampling in Portland, OR, during February and April 1984

compound	mass amt, ng	equiv concn, ng/m ³	% of F_{primary}
9-fluorenone	1.6 \pm 1.9	0.02 \pm 0.02	21 \pm 32
phenanthrene	1.4 \pm 3.5	0.03 \pm 0.07	5.5 \pm 13
methylphenanthrenes	6.6 \pm 4.3	0.06 \pm 0.05	29 \pm 30
9,10-anthracenedione	8.8 \pm 9.9	0.08 \pm 0.12	9.7 \pm 13
fluoranthene	14 \pm 23	0.10 \pm 0.14	19 \pm 27
pyrene	12 \pm 24	0.09 \pm 0.13	12 \pm 18
benz[a]anthracene	3.5 \pm 6.3	0.06 \pm 0.12	4.0 \pm 6.7
chrysene	14 \pm 8.7	0.15 \pm 0.21	9.5 \pm 8.6
eicosane	37 \pm 38	0.49 \pm 0.85	71 \pm 87
heneicosane	64 \pm 73	0.89 \pm 1.63	52 \pm 54
docosane	37 \pm 36	0.37 \pm 0.54	24 \pm 24
butyl benzyl phthalate	110 \pm 120	0.71 \pm 0.58	28 \pm 28

critical range, the adsorption was fairly large, with backup filter amounts for eicosane averaging 71% of the front filter values. Because alkanes were not measurable on the TMFs due to blank problems, their adsorption on GFF backup filters could not be compared to that on TMFs.

Losses of adsorbed organic material due to volatilization from collected particles were not measured in this study, though conditions that helped to minimize volatilization included (1) low (~ 1 psi) pressure drops across the filters and (2) small temperature fluctuations during sampling. Van Vaeck et al. (5) recently concluded that volatilization losses can be very problematic in high-volume sampling for compounds of intermediate volatility. However, they did not consider the effects of gas adsorption. The special sampler that they used to minimize volatilization, and therefore standardize against in their studies, employed fresh filter portions for each of a series of short sampling intervals. Minimizing the (sample volume)/(filter area) ratio will, however, tend to maximize gas adsorption effects since filter sorption capacities are limited. Indeed, it may be noted that Fitz et al. (17) collected 33% more solvent-extractable mass with four sequential 3-h Teflon-impregnated GFFs than they collected with a single, concurrent, 12-h filter. Also, Cadle et al. (7) have concluded that at high filter loadings, the amount of organic material adsorbed on quartz fiber filters is no longer linearly dependent on the total organic carbon filter loading. If a gas adsorption effect similar in magnitude to that found in the present study occurred during the sampling of Van Vaeck et al. (5), then gas adsorption could have been responsible for a significant portion of the artifact that they ascribed to volatilization. This is a definite possibility since the sample volumes per square centimeter of filter in the work of Van Vaeck et al. (5) (~ 0.8 m³/cm²) were similar to those used in the present study (~ 0.8 to ~ 4 m³/cm²).

Corrections for gas adsorption on filters were not made in two of our previous papers (20, 21) concerning precipitation scavenging of organic compounds, since the potentially compensatory effects of volatilization losses were not measured. For the sake of completeness, corrections for gas adsorption alone were calculated here. The corrections are fairly small when compared to other uncertainties. Moreover, the general distinctions between the relative importances of gas and particle scavenging made in those papers remain unchanged for all compounds. Since gas adsorption leads to an overestimation of the particulate-phase concentration, it causes an underestimation of particle scavenging ratio (W_p) values. As expected, the alkanes required the largest correction factors. For the mean W_p values cited earlier (21), the mean cor-

rection factors are as follows: eicosane, 1.6; heneicosane, 1.4; docosane, 1.5.

GFF/TMF Comparison. Since sampling artifacts can obviously affect the accuracy of measured c_p and c_g values, an examination of collection on both GFFs and TMFs was included in this study. Prior investigations of filter artifacts (12, 15-17, 32) have included examinations of (1) the effects of different types of filters on measured levels of ambient atmospheric PAHs, as well as (2) the recoveries of PAHs spiked onto different filter surfaces. In studies involving the collection of ambient PAHs on GFFs, quartz fiber filters (QFFs), and TMFs, the amounts of PAHs found on TMFs have often exceeded the amounts found on GFFs or QFFs, leading to GFF/TMF and/or QFF/TMF ratios that are less than 1.0 (16, 17). The mechanism usually proposed as the cause is catalytic degradation on the glass or quartz surface. This degradation might take place at the interface between a collected particle and the filter surface, or simply on the filter surface alone. The latter might occur following volatilization from a particle than readsorption onto the filter surface. When compounds are spiked directly onto blank filters, reactions at particle/filter interfaces will clearly not be involved. However, in studies involving the spiking of compounds onto filters also holding precollected particulate matter, both filter and particle/filter catalysis could be occurring.

In addition to filter-catalyzed degradation, a second possible mechanism for higher TMF levels is an enhanced adsorption of gas-phase compounds on the TMF surface (16). Also, using radioactive benzo[a]pyrene (BaP), Lee et al. (15) have obtained evidence that suggests that either GFF material itself or species sorbed onto it during sampling can lead to BaP degradation during the filter extraction step. Finally, although it has not yet been suggested, it seems possible that the different profiles of the pressure drops through GFFs and TMFs could cause different volatilization losses of the "blow-off" type discussed by Van Vaeck et al. (5). That is, although the overall pressure drop across a TMF will tend to be greater than that across a GFF, the type of bed filtration that takes place with a GFF could lead to comparatively more exposure of collected particles to reduced pressure than would occur with a TMF. With the latter, the bulk of the pressure drop occurs in the interior of the porous membrane where there are few collected particles.

The results of the GFF/TMF comparison in the 1985 Portland sampling revealed few significant differences in the concentrations of most PAHs and oxo-PAHs. The mean GFF/TMF ratios and the significance levels for their deviations from 1.0 with a two-tailed test are presented in Table III. Only phenanthrene was collected in significantly ($\geq 95\%$ confidence level) lower quantities on the GFFs, and only 7,12-benz[a]anthracenedione and acenaphthylene were significantly higher on the GFFs. The mean GFF/TMF ratios for the remaining compounds fell between 0.58 and 1.16. These results differ somewhat from those of Grosjean (16), who obtained average GFF/TMF ratios of 0.25-0.77 for some of the same compounds in Los Angeles, but are comparable to those of Fitz et al. (17), who obtained ratios of 0.48-1.03 in the same general area (El Monte). In agreement with our work, it was for phenanthrene in one sampling event that Fitz et al. (17) obtained one of the lowest GFF/TMF ratios (0.58). It should be pointed out here that for compounds subject to deviations from 1.0 in the GFF/TMF ratio, there will very likely be no single, typical GFF/TMF ratio. That is, variabilities due to differences in the sampling conditions during different studies are to be expected.

Table III. Mean GFF/TMF Ratios ($\pm 1\sigma$) for PAH and Oxo-PAH Compounds for Sampling in Portland, OR, during February and March 1985

compound	GFF/TMF ratio	p^a
acenaphthylene	1.43 \pm 0.27	0.05
dibenzofuran	0.83 \pm 0.76	0.68
fluorene	0.61 \pm 0.59	0.28
phenanthrene	0.55 \pm 0.24	0.03
methylphenanthrenes	0.58 \pm 0.35	0.09
fluoranthene	0.97 \pm 0.28	0.86
pyrene	1.06 \pm 0.24	0.70
benzo[a]fluorene	0.90 \pm 0.24	0.47
benzo[b]fluorene	0.93 \pm 0.23	0.63
benz[a]anthracene	1.06 \pm 0.24	0.66
chrysene	1.11 \pm 0.28	0.48
benzo[b+j+k]fluoranthene	1.10 \pm 0.24	0.47
benzo[e]pyrene	1.12 \pm 0.23	0.39
benzo[a]pyrene	0.89 \pm 0.27	0.48
perylene	1.05 \pm 0.26	0.76
indeno[1,2,3-cd]pyrene	0.99 \pm 0.21	0.90
dibenz[a,c]- + dibenz[a,h]anthracene	0.91 \pm 0.23	0.48
benzo[ghi]perylene	1.05 \pm 0.20	0.64
coronene	0.91 \pm 0.36	0.65
9-fluorenone	0.81 \pm 0.19	0.14
9,10-anthracenedione	1.16 \pm 0.19	0.19
7-benz[de]anthracenone	1.09 \pm 0.19	0.40
7,12-benz[a]anthracenedione	1.27 \pm 0.10	0.01

^a p , probability that GFF/TMF ratio is the same as 1.0. $p \leq 0.05$ indicates a significant (95% confidence level) difference between GFF and TMF values.

BaP is of particular interest in a GFF/TMF comparison because several studies have been carried out on its reactivity. Pitts et al. (11) found some conversion of BaP to various oxygenated and nitrated compounds when milligram quantities were spiked onto blank filters and exposed to a flow of ambient air. Brorstrom et al. (12) found losses of up to 40% for ambient BaP on GFFs when 1 ppm NO₂ was added to the airstream. Grosjean et al. (33) found no degradation when BaP was placed onto GFFs and TMFs and exposed to ambient air as well as purified air spiked with low levels of oxidants, i.e., 100 ppb NO₂, SO₂, or O₃. Blank filters as well as filters loaded with ambient, diesel, and fly ash particles were studied by Grosjean (33). Degradation was only observed when HNO₃ was present.

Although no significant differences in the concentrations of BaP measured on the two types of filters are apparent in Table III, a close examination of the BaP levels in conjunction with the levels of benzo[e]pyrene (BeP), a less reactive isomer (34, 35), is warranted. The BaP/BeP ratios were therefore computed for the four events sampled in 1985 in Portland. The mean ratios ($\pm 1\sigma$) were found to be 1.20 \pm 0.19 and 1.55 \pm 0.06 for the GFFs and TMFs, respectively. Thus, the ratio was found to be significantly higher ($p = 0.05$) as well as more consistent on the TMFs, and so it is possible that some slight losses of BaP did occur on the GFFs. Those losses may have been kept low by virtue of the fact that the oxidant levels were also low in Portland during the sampling.

The fact that particulate concentrations of most PAHs were largely the same whether measured on GFFs or TMFs indicates that for this investigation, within the uncertainties of the sampling and analytical methods [± 15 and $\pm 18\%$, respectively (23)], filter-catalyzed degradation of most PAHs was not a large problem. It also indicates that gas adsorption of PAHs was not appreciably greater on GFFs than on TMFs. Since measurements of total organic carbon on TMFs have been found to be affected in only a small way by gas adsorption (8), the general comparability of the GFF/TMF results supports the conclusion

Table IV. Mean Gas- and Particulate-Phase Concentrations ($\pm 1\sigma$) and Resulting ϕ Values in Portland, OR, during February and April 1984 and February and April 1985^a

compound	gas, ng/m ³	particulate, ng/m ³	ϕ
acenaphthylene	32 \pm 24	0.021 \pm 0.011	0.0010 \pm 0.0005
dibenzofuran	19 \pm 9	0.10 \pm 0.11	0.0024 \pm 0.0025
1- + 2-naphthol	6.8 \pm 5.6	0.25 \pm 0.20	0.055 \pm 0.054
fluorene	11 \pm 7	0.067 \pm 0.076	0.0062 \pm 0.0075
9-fluorenone	7.0 \pm 2.5 (7.0 \pm 2.5)	0.14 \pm 0.14 (0.12 \pm 0.14)	0.018 \pm 0.014 (0.016 \pm 0.013)
dibenzothiophene	1.8 \pm 1.0	0.039 \pm 0.041	0.023 \pm 0.025
phenanthrene	26 \pm 10 (26 \pm 10)	0.28 \pm 0.25 (0.27 \pm 0.23)	0.010 \pm 0.007 (0.010 \pm 0.006)
anthracene	3.4 \pm 2.2	0.035 \pm 0.020	0.009 \pm 0.004
xanthone	1.5 \pm 0.7	0.060 \pm 0.035	0.039 \pm 0.021
2- + 3-methyl-phenanthrene	7.2 \pm 3.8 (7.2 \pm 3.8)	0.19 \pm 0.13 (0.15 \pm 0.09)	0.025 \pm 0.013 (0.020 \pm 0.009)
1- + 4- + 9-methyl-phenanthrene	5.7 \pm 2.8 (5.8 \pm 2.8)	0.16 \pm 0.10 (0.12 \pm 0.08)	0.027 \pm 0.013 (0.020 \pm 0.011)
9,10-anthracenedione	2.5 \pm 1.0 (2.5 \pm 1.0)	0.59 \pm 0.22 (0.52 \pm 0.18)	0.19 \pm 0.04 (0.17 \pm 0.04)
eicosane	4.8 \pm 2.6 (5.4 \pm 3.0)	0.88 \pm 0.63 (0.30 \pm 0.17)	0.15 \pm 0.07 (0.059 \pm 0.025)
fluoranthene	7.9 \pm 3.1 (8.0 \pm 3.1)	0.53 \pm 0.31 (0.42 \pm 0.25)	0.061 \pm 0.027 (0.049 \pm 0.023)
heneicosane	2.6 \pm 1.3 (3.4 \pm 2.5)	1.1 \pm 1.1 (0.69 \pm 0.53)	0.33 \pm 0.14 (0.19 \pm 0.09)
pyrene	6.7 \pm 2.7 (6.8 \pm 2.7)	0.62 \pm 0.37 (0.53 \pm 0.31)	0.083 \pm 0.038 (0.071 \pm 0.032)
benzo[a]fluorene	1.6 \pm 0.8	0.43 \pm 0.30	0.19 \pm 0.09
benzo[b]fluorene	1.5 \pm 0.7	0.45 \pm 0.32	0.22 \pm 0.10
docosane	1.4 \pm 0.4 (1.9 \pm 1.0)	2.9 \pm 2.6 (2.1 \pm 1.8)	0.47 \pm 0.21 (0.31 \pm 0.17)
butyl benzyl phthalate	5.0 \pm 0.8	4.1 \pm 3.1	0.42 \pm 0.25
benz[a]-anthracene	0.32 \pm 0.14 (0.37 \pm 0.21)	1.2 \pm 0.8 (1.2 \pm 0.8)	0.76 \pm 0.10 (0.73 \pm 0.11)
chrysene	0.49 \pm 0.17 (0.66 \pm 0.30)	1.5 \pm 0.9 (1.4 \pm 0.9)	0.72 \pm 0.11 (0.65 \pm 0.12)
7-benz[de]-anthracenone	0.067 \pm 0.029	1.7 \pm 1.2	0.97 \pm 0.02
dioctylphthalate	0.39 \pm 0.39	0.48 \pm 0.25	0.56 \pm 0.30
benzo[b+j+k]-fluoranthene	0.11 \pm 0.12	3.6 \pm 1.9	0.96 \pm 0.04

^a Values in parentheses are corrected for gas absorption with backup filter data.

that gas adsorption did not cause major errors in the thermal/optical measurements of total particulate carbon (TPC) on the GFFs.

Gas/Particle Distributions. The mean blank-corrected gas and particulate phase concentrations in Portland in 1984-1985 are given in Table IV together with the resulting ϕ values. The values are based directly on the data from the front filters and the sorbents. For those compounds found on the backup filters, the values were also corrected for gas adsorption with the backup filter data and

$$A_{\text{corr}} = A + 2F_{\text{backup}} \quad (6)$$

$$F_{\text{corr}} = F_{\text{front}} - F_{\text{backup}} \quad (7)$$

Equations 4 and 5 incorporate the assumption that gas adsorption occurred to the front and backup filters to an equal extent. The corrected data are given in parentheses in Table IV. The factor of 2 in eq 4 arises from the fact that both the backup filter concentration and an equal amount due to the assumed sorption on the front filter must be added to the gas concentration. Since backup filters were not used in the 1985 samplings, the corrections of the 1985 data utilized the average backup filter percentage for each compound from the 1984 samples. Because contributions of the volatilization artifact were not measured in this study, the corrected values may not necessarily be more correct than the measured values.

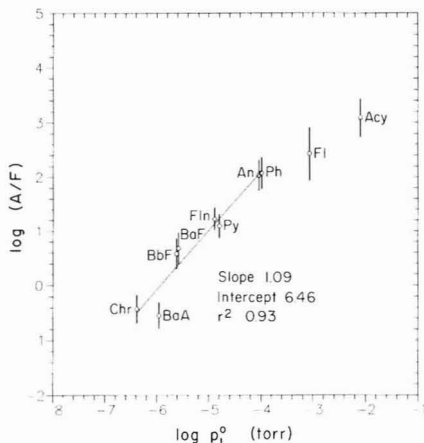


Figure 2. Log A/F for PAH compounds vs $\log p_L^0$ (Torr) at 7 °C for samples obtained in Portland, OR, in 1984 and 1985. Acy, acenaphthylene; Fl, fluorene; Ph, phenanthrene; An, anthracene; Fin, fluoranthene; Py, pyrene; BaF, benzo[*a*]fluorene; BaA, benzo[*a*]anthracene; Chr, chrysene. The bars represent $\pm 1\sigma$ for the multiple samplings.

Nevertheless, the former are useful as indicators of the uncertainties in A and F_{front} . It is reassuring that only the alkanes required significant corrections.

In agreement with other studies conducted in urban areas (3-5, 36, 37), the ϕ values for the unsubstituted PAHs at the Portland site were <0.1 for three rings, 0.05-0.8 for four rings, and ~ 1.0 for five rings. Since the mean temperatures at the Portland and coastal sampling sites (7 and 9 °C, respectively) were fairly close, it may be assumed that the compound-dependent p^0 values were nearly the same for the two sets of samplings. If, in addition, the particulate matter in Portland and at the coast were similar in both size distribution and sorption characteristics, it might be assumed that the compound-dependent values of c and C were also approximately constant between the two sites. For each compound, then, eq 1 and 5 yield $\theta_{\text{Portland}}/\theta_{\text{coast}} = \text{TSP}_{\text{Portland}}/\text{TSP}_{\text{coast}} = (1 - \phi_{\text{coast}})\phi_{\text{Portland}}/(1 - \phi_{\text{Portland}})\phi_{\text{coast}}$. The values obtained varied between 0.7 (anthracene) and 8.6 (7-benz[*de*]anthracene). The mean value was 2.5. Since the mean TSP level in Portland is only $\sim 30 \mu\text{g}/\text{m}^3$ (38), $\theta_{\text{Portland}}/\theta_{\text{coast}}$ and $\text{TSP}_{\text{Portland}}/\text{TSP}_{\text{coast}}$ might indeed be only ~ 3 .

To the extent that (1) artifacts are not problematic, (2) θ is indeed proportional to TSP, and (3) the values of c and C are constant within a compound class, then for a given sampling for that compound class, both eq 2 and 5 predict that a plot of $\log A/F$ vs $\log p^0$ will be linear with slope +1 and intercept $-\log c\theta = \log C/\text{TSP}$. Different samplings carried out at similar temperatures but different θ (TSP) values will lead to different, but parallel lines. Therefore, under these assumptions, when mean data for those multiple samplings are averaged and plotted, then the slope will still be $+1.0$ and the intercept will be the mean value of $-\log c\theta$, which will in turn be equal to the mean value of $\log C/\text{TSP}$.

Figure 2 is a plot of $\log A/F$ vs $\log p_L^0$ (vapor pressure for the subcooled liquid) (i.e., vs $\log p_L^0$) for the Portland PAH data. (The p_L^0 values used for Figure 2 were corrected to 7 °C.) In this case as well as those discussed below, the values of $\log A_{\text{corr}}/F_{\text{corr}}$ are quite similar to the $\log A/F$ values, and so the former are not plotted. The bars on each of the points represents $\pm 1\sigma$ for the data from the multiple samplings. The values of p_L^0 used were from the literature (39-41). When the data in Figure 2 are plotted vs the

vapor pressures of the solid compounds, the plot is significantly less regular (23). [The worst outliers in that context are anthracene and benz[*a*]anthracene (23).] The points in Figure 2 for acenaphthylene and fluorene deviate from the rough linearity defined by the other data. When the latter are subjected to a linear fit, a slope of 1.09 and intercept of 6.46 are obtained ($r^2 = 0.93$). As expected, the slope is near 1.0. When the data are assumed to have a slope of +1.00, the best fit intercept is 5.99. When the whole data set is subjected to a linear fit, the best fit slope is 0.86 and the intercept is 5.20 ($r^2 = 0.93$).

It is useful to examine the intercept value (5.99) found for the less volatile compounds in Figure 2 when the data is assumed to have a slope of +1.00. As discussed above, according to Junge's (2) model, this intercept should equal $-\log c\theta$. A value for θ of $\sim 4 \times 10^{-6} \text{ cm}^2/\text{cm}^3$ can be calculated by assuming the particle size distribution reported for Los Angeles (42) and the average Portland TSP level of $\sim 30 \mu\text{g m}^{-3}$. This gives an average c value of ~ 0.3 for phenanthrene through chrysene at 7 °C. This is somewhat smaller than the c value of 1.3 discussed by Pankow (1) for PAHs at ~ 20 °C. Since increasing the temperature will tend to reduce c [Pankow (1)], the difference in temperature cannot account for the difference in c values. However, $\sim 4 \times 10^{-6} \text{ cm}^2/\text{cm}^3$ is likely to be an overestimation for θ for particulate matter in Portland. Indeed, the specific surface area for Portland particulate matter (A_{TSP} , $\text{cm}^2/\mu\text{g}$) is likely to be significantly smaller than for Los Angeles where gas-to-particle reactions can lead to significant numbers of particles in the submicron size range.

Although the degree of correlation for the Figure 2 data is the same ($r^2 = 0.93$) regardless of whether or not the points for acenaphthylene and fluorene are included, these two compounds may have been behaving differently than the others. The fact that the correlation line for phenanthrene through chrysene alone gives a slope very close to the theoretical value of 1.0 is further evidence in support of that conclusion. It is not immediately clear why acenaphthylene and fluorene may have behaved differently. Even if a 30% filter adsorption effect is assumed for them (i.e., just below the filter detection limit), their points would still not fall near the best fit line for the other compounds. Also, since volatilization losses for them would have caused the measured A/F values to be too high, such losses would have tended to alleviate any nonlinearity and not be its cause.

On the basis of the above, we conclude that the nonlinearity in Figure 2 is substantially real and not due to artifacts. More than one explanation can be invoked for this result. In terms of Junge's (2) model, the values of c for acenaphthylene and fluorene might have been comparatively greater than for the other compounds. Alternatively, portions of all of the PAHs might have been trapped within particles where rapid exchange with the gas phase could not occur. In the case of the lower volatility PAHs, this would have comparatively small effects on the measured A/F values since significant fractions of the nontrapped portions of those compounds would be adsorbed to the particles anyway. This would leave their $\log A/F$ values similar to what would be expected for full equilibrium and leave the expected linearity for $\log A/F$ vs $\log p_L^0$ largely intact. In the case of the most volatile compounds, however, at full equilibrium, extremely low values of ϕ would be expected. Therefore, for such compounds, even very small amounts of nonexchangeable material in the particulate phase would significantly diminish their measured $\log A/F$ values. As shown by

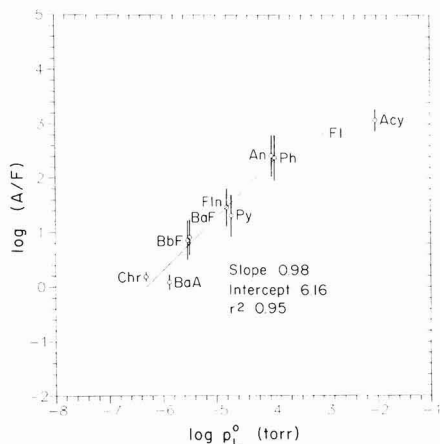


Figure 3. Log A/F for PAH compounds vs $\log p_L^0$ (Torr) at 9 °C for samples obtained at the Oregon coast in 1985. The bars represent $\pm 1\sigma$ for the multiple samplings.

Pankow (43), only $\sim 0.02\%$ of nonlabile material could cause the downward shift from the linear correlation line observed here. This second explanation is not inconsistent with the repartitioning hypothesis identified elsewhere (21) as a possible reason for the relatively larger particle precipitation scavenging ratios (W_p) observed for the lower molecular weight PAHs. That hypothesis involved the supposition that the exchangeable fraction is larger for the lower molecular weight PAHs than it is for the higher molecular weight PAHs, thus allowing them to repartition more extensively onto larger, more easily scavenged particles. Certainly the presence of a relatively larger fraction of exchangeable material is still possible for a given compound if only $\sim 0.02\%$ of it is restricted as being nonexchangeable.

As a third explanation for the nonlinearity at high $\log p_L^0$, it might be possible that 100% of the compounds are exchangeable, but that the sorptive surfaces of the aerosol are not uniform with respect to the energetics of sorption. In this case, even a relatively small percentage of strong sites could result in the same effects described above for the exchangeable/nonexchangeable case. For the high energy site explanation to be valid, however, there would have to be sufficient numbers of those sites available for sorption of the less strongly bound compounds, and the extent to which that would occur would depend upon the amounts of the more strongly bound compounds present. Indeed, the latter would tend to displace the former. At the present time, the general result of nonlinearity for PAHs with high p_L^0 values remains unconfirmed; the similar, linear correlation of $\log A(\text{TSP})/F$ vs $\log p_L^0$ carried out by Bidleman and Foreman (9) only extended to PAHs with p_L^0 values up to about -3 .

Figure 3 is analogous to Figure 2, but presents data for the Oregon coast. Corrections for gas adsorption were not made since backup filters were not used during those samplings. The p_L^0 were corrected to the mean temperature of 9 °C. The points for acenaphthylene and fluorene again seem to deviate from the linearity exhibited by the other data. When those two compounds are excluded, the remaining points give a best fit line with a slope of 0.98 and an intercept of 6.16 ($r^2 = 0.95$). When the slope is assumed to be 1.00, the best fit intercept is 6.28. When acenaphthylene and fluorene are included, the best fit parameters are 0.76 and 5.04, respectively ($r^2 = 0.93$). Compared to Figure 2 data, the Figure 3 data are shifted

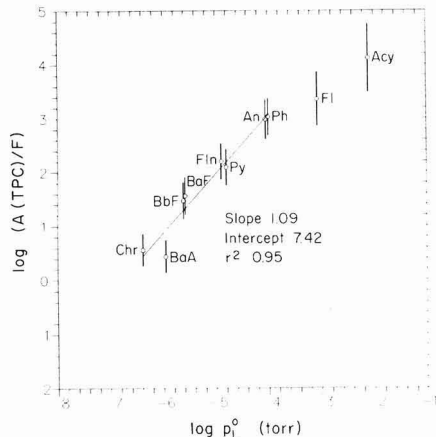


Figure 4. Log $A(\text{TPC})/F$ for PAH compounds vs $\log p_L^0$ (Torr) at 7 °C for selected samples obtained in Portland, OR in 1984 and 1985. The bars represent $\pm 1\sigma$ for the multiple samplings.

Table V. Average Values ($\pm 1\sigma$) for $\log A(\text{TPC})/F$ for PAHs in Portland, OR, for February and April 1984 and February and March 1985^a

compound	$\log A(\text{TPC})/F$	$\log A(\text{TSP})/F$	$\log p_L^0$
acenaphthylene	4.12 ± 0.63	4.60 ± 0.63	-2.10
fluorene	3.36 ± 0.50	3.84 ± 0.50	-3.07
phenanthrene	3.03 ± 0.34 (3.06 \pm 0.35)	3.51 ± 0.34 (3.54 \pm 0.35)	-4.00
anthracene	2.98 ± 0.37	2.46 ± 0.37	-4.05
fluoranthene	2.20 ± 0.33 (2.28 \pm 0.34)	2.68 ± 0.33 (2.76 \pm 0.34)	-4.89
pyrene	2.09 ± 0.34 (2.14 \pm 0.34)	2.57 ± 0.34 (2.62 \pm 0.34)	-4.80
benzo[a]fluorene	1.56 ± 0.34	2.04 ± 0.34	-5.59
benzo[b]fluorene	1.47 ± 0.34	1.95 ± 0.34	-5.62
benz[a]anthracene	0.44 ± 0.30 (0.53 \pm 0.32)	0.92 ± 0.30 (1.01 \pm 0.32)	-5.96
chrysene	0.56 ± 0.30 (0.75 \pm 0.33)	1.04 ± 0.30 (1.23 \pm 0.33)	-6.39

^a $\log A(\text{TSP})/F$ values are also given assuming $\text{TPC} \approx \text{TSP}/3$ for the events sampled. The overall mean temperature was 7 °C. Gas adsorption corrected values are given in parentheses.

up somewhat as expected based on the value calculated above for the average computed $\theta_{\text{Port}}/\theta_{\text{coast}}$ ratio. (Since the best fit slopes are not 1.00, the corresponding best fit intercepts are not consistent with an upwards shift at $\log p_L^0 = 0$.) This shift toward the gaseous phase has also been found by Marty et al. (44) for PAHs in gas and particulate samples taken during a cruise in the east Atlantic off the coast of southwest Africa, specifically Gabon.

Although TSP levels were not measured in this work, TPC values were obtained for several of the samplings in Portland. Since organic compounds might associate most strongly with the carbonaceous portion of the TSP, it seems possible that TPC might be a better choice than TSP for correlating gas/particle distributions with p_L^0 . For the sampling conducted in this work, TPC levels in Portland ranged from 7 to 27 $\mu\text{g}/\text{m}^3$, or $\sim 1/3$ of the TSP values that have been measured at the same site (38). The quantity $\log A(\text{TPC})/F$ is therefore plotted vs $\log p_L^0$ (7 °C) for the Portland PAH data in Figure 4. (The data for Figure 4 are presented in Table V.) Since each sampling event was characterized by a single TPC value for all compounds, the data exhibit the same trends present in Figures 2 and 3. The best fit slope and intercept for phenanthrene through chrysene are 1.09 and 7.42, re-

spectively ($r^2 = 0.95$). When the slope is assumed to be 1.00, the best fit intercept is 6.95.

It is interesting to note that the $\pm 1\sigma$ bars in Figure 4 are not narrower than in Figure 2. This indicates that including TPC in the parameterization did not significantly improve the correlatability of $\log A/F$ with $\log p_L^*$. As a result, it is unclear at the present time whether TPC plays a special role in sorption in the urban atmosphere. Nevertheless, it can be pointed out that the phenanthrene through chrysene portion of Figure 4 bears much similarity to plots of $A(\text{TSP})/F$ for PAHs at 20 °C reported by other workers. If TPC is assumed to have been equal to $\sim \text{TSP}/3$ for the winter/spring events sampled in Portland, then the slope 1.00 intercept of 6.95 (7 °C) is equivalent to a $\log C$ value of 7.55 at the sampling temperature of 7 °C. This is very close to the value of ~ 7.5 found for eq 4 for PAHs by Pankow (1) for 20 °C. Table V gives the $A(\text{TSP})/F$ values for 7 °C computed by assuming $\text{TSP} = \text{TPC}/3$.

Summary and Conclusions

The extent of the adsorption of gas-phase PAHs and oxo-PAHs on GFFs was variable, but averaged $<30\%$ of the measured particulate concentrations for the compounds in the vapor pressure range 10^{-8} – 10^{-4} Torr. Alkanes and phthalates were adsorbed to a greater extent, up to an average of 71% for eicosane. Within the experimental uncertainties, particulate-phase concentrations for most PAHs were the same whether measured on GFFs or TMFs. This indicates that the measured gas/particle distributions of PAHs were reasonably close to the actual atmospheric distributions during sampling. The ϕ values of PAHs ranged from 0.01 for phenanthrene, to 0.7 for benz[a]anthracene and chrysene, to 1.0 for benzo[a]pyrene. A comparison of Portland ϕ values with those at the Oregon coast using Junge's (2) model indicated that θ was lower by ~ 3 at the coast. The trend in the plot of corrected $\log A/F$ values vs $\log p_L^*$ followed Junge's (2) model for PAHs with $p_L^* < 10^{-4}$ Torr, but the more volatile PAHs seem to show greater association with the particulate phase than would be obtained on the basis of an extrapolation of the behavior of compounds with lower p_L^* values. The most likely reason for this increased association was the presence of a certain portion of nonexchangeable material. Plots of $\log A(\text{TPC})/F$ vs $\log p_L^*$ at 7 °C were found to be very similar to previously reported plots of $\log A(\text{TSP})/F$ vs $\log p_L^*$.

Acknowledgments

We express our appreciation to James J. Huntzicker for the use of the carbon analyzer and the Oregon Department of Environmental Quality and Ft. Stevens State Park for the use of the sampling sites. The donation of the Tenax-TA used in this study by Alltech Associates, Deerfield, IL, is gratefully acknowledged. We also wish to thank Kenneth M. Hart for valuable assistance in eliminating errors.

Registry No. Acenaphthylene, 208-96-8; dibenzofuran, 132-64-9; fluorene, 86-73-7; phenanthrene, 85-01-8; methylphenanthrene, 31711-53-2; fluoranthene, 206-44-0; pyrene, 129-00-0; benzo[a]fluorene, 30777-18-5; benzo[b]fluorene, 30777-19-6; benz[a]anthracene, 56-55-3; benzo[b]fluoranthene, 205-99-2; benzo[e]pyrene, 192-97-2; benzo[a]pyrene, 50-32-8; perylene, 198-55-0; indeno[1,2,3-*cd*]pyrene, 193-39-5; dibenz[a,c]anthracene, 215-58-7; dibenz[a,h]anthracene, 53-70-3; benzo[ghi]perylene, 191-24-2; coronene, 191-07-1; 9-fluorenone, 486-25-9; chrysene, 218-01-9; 9,10-anthracenedione, 84-65-1; 7-benz[de]anthracenone, 82-05-3; 7,12-benz[a]anthracenedione, 2498-66-0; benzo[*f*]fluoranthene, 205-82-3; benzo[*k*]fluoranthene, 207-08-9; 1-

naphthol, 90-15-3; 2-naphthol, 135-19-3; dibenzothiophene, 132-65-0; anthracene, 120-12-7; xanthone, 90-47-1; 2-methylphenanthrene, 2531-84-2; 3-methylphenanthrene, 832-71-3; 1-methylphenanthrene, 832-69-9; 4-methylphenanthrene, 832-64-4; 9-methylphenanthrene, 883-20-5; eicosane, 112-95-8; heneicosane, 629-94-7; docosane, 629-97-0; butyl benzyl phthalate, 85-68-7; dioctyl phthalate, 117-81-7; zefluor, 9002-84-0.

Literature Cited

- (1) Pankow, J. F. *Atmos. Environ.* **1987**, *21*, 2275–2283.
- (2) Junge, C. E. *Fate of Pollutants in the Air and Water Environments*; Suffet, I. H., Ed.; Wiley: New York, 1977.
- (3) Cautreels, W.; Van Cauwenbergh, K. *Atmos. Environ.* **1977**, *12*, 1133–1141.
- (4) Yamasaki, H.; Kuwata, K.; Miyamoto, H. *Environ. Sci. Technol.* **1982**, *16*, 189–194.
- (5) Van Vaecck, L.; Van Cauwenbergh, K.; Janssens, J. *Atmos. Environ.* **1984**, *18*, 417–430.
- (6) Eichmann, R.; Neuling, P.; Ketseridis, G.; Jaenicke, R.; Junge, C. *Atmos. Environ.* **1979**, *13*, 587–599.
- (7) Cadle, S. H.; Groblicki, P. J.; Mulawa, P. A. *Atmos. Environ.* **1983**, *17*, 593–600.
- (8) McDow, S.; Ph.D. Thesis, Oregon Graduate Center, 1986.
- (9) Bidleman, T. F.; Foreman, W. T. In *The Chemistry of Aquatic Pollutants*; Hites, R. A., Eisenreich, S. J., Eds.; Advances in Chemistry 216; American Chemical Society: Washington, DC, 1987; p 27.
- (10) Bidleman, T. F.; Billings, W. N.; Foreman, W. T. *Environ. Sci. Technol.* **1986**, *20*, 1038–1043.
- (11) Pitts, J. N.; Var. Cauwenbergh, K. A.; Grosjean, D.; Schmid, J. P.; Fitz, D. R.; Belsler, W. L.; Knudson, G. B.; Hynds, P. M. *Science (Washington, D.C.)* **1978**, *202*, 515–519.
- (12) Brostrom, E.; Grennfelt, P.; Lindskog, A. *Atmos. Environ.* **1983**, *17*, 601–605.
- (13) Keller, C. D.; Bidleman, T. F. *Atmos. Environ.* **1984**, *18*, 837–845.
- (14) Bidleman, T. F.; Keller, C. D. In *Synthetic Fossil Fuel Technologies, Results of Health and Environmental Studies*; Cowser, K. E., Ed.; Ann Arbor Science: Ann Arbor, MI, 1984; p 417.
- (15) Lee, F. S. C.; Pierson, W. R.; Ezike, J. In *Polynuclear Aromatic Hydrocarbons: The Fourth International Symposium*; Battelle: Columbus, OH, 1980; p 543.
- (16) Grosjean, D. *Atmos. Environ.* **1983**, *17*, 2565–2573.
- (17) Fitz, D. R.; Lokensgard, D. M.; Doyle, G. J. *Atmos. Environ.* **1984**, *18*, 205–213.
- (18) Pankow, J. F.; Isabelle, L. M.; Asher, W. E.; Kristensen, T. J.; Peterson, M. E. In *Precipitation Scavenging, Dry Deposition, and Resuspension*; Pruppacher, H. R., Semonin, R. G., Slinn, W. G. N., Eds.; Elsevier: New York, 1983; p 403.
- (19) Pankow, J. F.; Isabelle, L. M.; Asher, W. E. *Environ. Sci. Technol.* **1984**, *18*, 310–318.
- (20) Ligocki, M. P.; Leuenberger, C.; Pankow, J. F. *Atmos. Environ.* **1985**, *19*, 1609–1618.
- (21) Ligocki, M. P.; Leuenberger, C.; Pankow, J. F. *Atmos. Environ.* **1985**, *19*, 1619–1626.
- (22) Leuenberger, C.; Ligocki, M. P.; Pankow, J. F. *Environ. Sci. Technol.* **1985**, *19*, 1053–1058.
- (23) Ligocki, M. P. Ph.D. Thesis, Oregon Graduate Center, 1986.
- (24) Ligocki, M. P.; Pankow, J. F. *Anal. Chem.* **1985**, *57*, 1138–1144.
- (25) Johnson, R. L.; Shah, J. J.; Huntzicker, J. J. *ASTM Spec. Tech. Publ.* **1980**, *721*, 111.
- (26) Shah, J. J.; Johnson, R. L.; Heyerdahl, E. K.; Huntzicker, J. J. *Air Pollut. Control Assoc.* **1986**, *36*, 254–257.
- (27) Robertson, D. J.; Groth, R. H.; Gardner, D. G.; Glastir, E. G. *Air Pollut. Control Assoc.* **1979**, *29*, 143–146.
- (28) Hult, M., personal communication, 1987.
- (29) Josefson, C. M.; Johnston, J. B.; Trubey, R. *Anal. Chem.* **1984**, *56*, 764–768.
- (30) Lockhart, L. B.; Patterson, R. L.; Anderson, W. L. U.S. Naval Research Laboratory Report 6054, 1964.
- (31) John, W.; Reischl, G. *Atmos. Environ.* **1978**, *12*, 2015–2019.
- (32) Pitts, J. N.; Zielinska, B.; Sweetman, J. A.; Atkinson, R.; Winer, A. M. *Atmos. Environ.* **1985**, *19*, 911–915.

- (33) Grosjean, D.; Fung, K.; Harrison, J. *Environ. Sci. Technol.* 1983, 17, 673-679.
- (34) Nielsen, T. *Environ. Sci. Technol.* 1984, 18, 157-163.
- (35) Greenberg, A.; Darack, F.; Harkov, R.; Lioy, P.; Daisey, J. *Atmos. Environ.* 1985, 19, 1325-1339.
- (36) Thrane, K. E.; Mikalson, A. *Atmos. Environ.* 1981, 15, 909-918.
- (37) Pyysalo, H.; Tuominen, J.; Wickström, K.; Skyttä, E.; Tikannen, L.; Salomaa, S.; Sorsa, M.; Nurmela, T.; Mattila, T.; Pohjola, V. *Atmos. Environ.* 1987, 21, 1167-1180.
- (38) Oregon Department of Environmental Quality, Portland Air Quality Data, 1985, 1986.
- (39) Macknick, A. B.; Prausnitz, J. M. *J. Chem. Eng. Data* 1979, 24, 175-178.
- (40) Sonnefeld, W. J.; Zoller, W. H.; May, W. E. *Anal. Chem.* 1983, 55, 275-280.
- (41) Yamasaki, H.; Kuwata, K.; Kuge, Y. *Nippon Kagaku Kaishi* 1984, 8, 1324-1329.
- (42) Whitby, K. T.; Husar, R. B.; Liu, B. Y. H. *J. Colloid Interface Sci.* 1972, 39, 177-204.
- (43) Pankow, J. F. *Atmos. Environ.* 1988, 22, 1405-1409.
- (44) Marty, J. C.; Tissier, M. J.; Saliot, A. *Atmos. Environ.* 1984, 18, 2183-2190.

Received for review September 17, 1987. Accepted July 11, 1988. This work was made possible in part with federal funds from the United States Environmental Protection Agency under Grant No. R8113380 and with the continued support of the Northwest Environmental Research Center. The contents do not necessarily reflect the view or policies of the U.S. EPA, nor does mention of any trade names or commercial products constitute an endorsement or recommendation for use.

Distribution of Polychlorinated Biphenyl Congeners and Other Halocarbons in Whole Fish and Muscle among Lake Ontario Salmonids

Arthur J. Niimi* and Barry G. Oliver†

Department of Fisheries and Oceans, Canada Centre for Inland Waters, Burlington, Ontario, Canada L7R 4A6, and Environment Canada, Canada Centre for Inland Waters, Burlington, Ontario, Canada L7R 4A6

■ A total of 92 monochloro- to decachlorobiphenyl congeners were monitored in brown and lake trout, small and large rainbow trout, and small and large coho salmon from Lake Ontario. Highest concentrations were among the pentachloro- and hexachlorobiphenyl homologues, with 2,2',4,4',5,5'-hexachlorobiphenyl (IUPAC no. 153) the most common. Total congener concentrations ranged from 1 to 10 mg/kg in whole fish and from 0.3 to 4 mg/kg in muscle. Consistent values of congener composition were shown when individual congener levels were expressed as percent of total composition. The 10 most common congeners represented ~52% of the total content; this value does not appear to be influenced by species or by total concentration. The homologues observed averaged ~56% chlorine by weight in fish and muscle.

Introduction

Polychlorinated biphenyls (PCBs) have been used in different industrial applications since the 1930s, but were not recognized as environmental contaminants until 1966 (1). Nearly all quantitative analyses for PCBs are still based on chemical standards composed of mixtures and reported as total PCB concentrations, although some recent studies have reported congener-specific analyses (2-7). Analyses of PCB mixtures indicate measurable levels of 45-118 of the possible 209 congeners are present in some Aroclors (8-11). Studies that examined the composition of PCBs in environmental samples have reported the presence of up to 78 congeners in fish, but no consistent relationships have been established among congeners or with total PCB content (3, 6). Laboratory studies have shown differences in elimination rates among congeners in fish (12), and comparative studies on mammalian systems indicate some congeners are more toxic than others (13). Additional studies of specific congeners are required before such information can be effectively applied to issues such as PCB kinetics in aquatic ecosystems and the human

health implications of PCBs in consumable fish products.

In this study, 92 monochloro- to decachlorobiphenyl congeners, and 12 other organochlorine chemicals, were monitored in whole fish and muscle of four species of Lake Ontario salmonids. The objectives were to examine the quantitative composition of the more common congeners present in fish, compare their composition in fish with that reported in PCB mixtures, and examine the relationship between congener distribution in fish and muscle.

Experimental Section

Fish. Ten brown trout (*Salmo trutta*) averaging 1430 ± 360 g (mean ± SD), 8 "small" rainbow trout (*Salmo gairdneri*) of 1140 ± 120 g, and 10 "small" coho salmon (*Oncorhynchus kisutch*) of 1190 ± 190 g were collected off Vineland, Ontario. Ten lake trout (*Salvelinus namaycush*) weighing 2410 ± 770 g were taken off Port Credit, and 12 "large" rainbow trout of 3380 ± 870 g and 9 "large" coho salmon of 3330 ± 520 g were taken from the Credit River. Eggs from gravid females in the last three groups were removed, and all fish were frozen at -20 °C until analyses. Fish were prepared for analyses according to procedures described previously (12). Tissue samples were taken that would be representative of chemical levels in whole fish and muscle.

Chemicals Examined. All samples were analyzed for 92 monochloro- to decachlorobiphenyl congeners that are identified according to the International Union of Pure and Applied Chemistry (IUPAC) system (14) and are listed as follows: monochlorobiphenyls 1 and 3; dichlorobiphenyls 4-8, 10, 12, and 13; trichlorobiphenyls 16-19, 22, 24-28, and 31-33; tetrachlorobiphenyls 40-42, 44-49, 52, 53, 56, 60, 64, 66, 70, 71, 74, 76, 77, and 81; pentachlorobiphenyls 82, 84, 85, 87, 91, 92, 95, 97, 99, 101, 105, 110, 118, and 126; hexachlorobiphenyls 128, 129, 132, 136, 138, 141, 146, 149, 151, 153, 156, and 169; heptachlorobiphenyls 170, 171, 173, 174, 177, 178, 180, 182, 183, 185, 187, and 190; octachlorobiphenyls 194-196, 198, 201, 203, and 205; nonachlorobiphenyls 206 and 207; and decachlorobiphenyl 209. Samples were also analyzed for *p,p'*-DDT, *p,p'*-DDD, *p,p'*-DDE, mirex, photomirex, 1,2,3,4-tetrachlorobenzene (TECB), pentachlorobenzene (QCB), hexachlorobenzene

* Department of Fisheries and Oceans.

† Environment Canada. Present address: ELI Eco Laboratories, 143 Dennis Street, Rockwood, Ontario, Canada NOB 2K0.

Table I. Number of Congeners in Lake Ontario Salmonids and Total and Individual Concentrations ($\mu\text{g}/\text{kg}$) of the More Common Congeners in Fish and Muscle^a

congener	brown trout (n = 10)		lake trout (n = 10)		rainbow trout				coho salmon			
	fish	muscle	fish	muscle	small (n = 8)		large (n = 12)		small (n = 10)		large (n = 9)	
					fish	muscle	fish	muscle	fish	muscle	fish	muscle
no.	57 ± 4	51 ± 3	65 ± 2	59 ± 4	52 ± 5	33 ± 9	60 ± 2	55 ± 2	54 ± 2	50 ± 2	57 ± 2	54 ± 1
(28 + 31)	36 ± 15	15 ± 7	72 ± 20	27 ± 12	15 ± 5	1 ± 1	42 ± 13	14 ± 3	22 ± 4	8 ± 2	30 ± 10	15 ± 3
66	95 ± 51	43 ± 30	353 ± 141	138 ± 77	64 ± 26	12 ± 7	191 ± 52	73 ± 19	84 ± 21	34 ± 12	174 ± 53	87 ± 24
(70 + 76)	96 ± 48	43 ± 30	320 ± 108	124 ± 63	56 ± 23	11 ± 7	149 ± 49	63 ± 18	82 ± 22	32 ± 12	164 ± 56	78 ± 18
(56 + 60)	50 ± 22	21 ± 11	184 ± 56	69 ± 32	24 ± 11	1 ± 1	80 ± 19	27 ± 7	35 ± 8	13 ± 4	69 ± 24	33 ± 7
52	43 ± 18	18 ± 10	148 ± 57	61 ± 33	24 ± 9	5 ± 3	72 ± 17	26 ± 5	31 ± 7	13 ± 5	54 ± 15	28 ± 6
47	30 ± 11	16 ± 11	140 ± 50	56 ± 26	22 ± 10	1 ± 1	60 ± 15	24 ± 6	28 ± 8	11 ± 5	54 ± 16	30 ± 6
81	24	10	90	38	13	ND	30	9	26	8	2	14
77	5	2	18	8	6	ND	11	4	8	3	10	5
101	144 ± 67	62 ± 31	609 ± 228	237 ± 130	101 ± 31	21 ± 8	366 ± 103	133 ± 37	128 ± 35	52 ± 20	271 ± 69	136 ± 30
84	127 ± 81	60 ± 43	636 ± 294	254 ± 153	84 ± 34	19 ± 9	323 ± 99	129 ± 42	108 ± 32	46 ± 18	276 ± 84	142 ± 34
118	133 ± 77	60 ± 41	634 ± 230	242 ± 133	80 ± 35	16 ± 8	310 ± 105	115 ± 40	100 ± 30	39 ± 13	271 ± 89	136 ± 24
110	135 ± 80	61 ± 45	475 ± 185	183 ± 99	85 ± 33	18 ± 7	309 ± 88	113 ± 33	114 ± 32	45 ± 17	256 ± 79	125 ± 25
(87 + 97)	111 ± 63	36 ± 54	390 ± 117	156 ± 70	76 ± 30	15 ± 9	245 ± 92	94 ± 32	135 ± 46	54 ± 25	258 ± 93	117 ± 35
105	55 ± 38	24 ± 19	253 ± 101	101 ± 60	34 ± 16	6 ± 4	138 ± 44	50 ± 15	48 ± 15	19 ± 7	121 ± 40	56 ± 13
95	50 ± 24	22 ± 13	170 ± 58	68 ± 38	32 ± 11	8 ± 3	112 ± 27	41 ± 10	42 ± 9	17 ± 5	75 ± 20	38 ± 11
153	182 ± 125	92 ± 66	1080 ± 405	419 ± 214	129 ± 46	33 ± 14	556 ± 200	217 ± 73	153 ± 42	72 ± 28	462 ± 148	242 ± 37
138	131 ± 79	60 ± 43	601 ± 270	237 ± 140	81 ± 27	18 ± 8	336 ± 107	129 ± 42	108 ± 29	44 ± 16	284 ± 85	140 ± 31
149	129 ± 71	53 ± 37	327 ± 123	124 ± 64	67 ± 21	16 ± 6	290 ± 91	109 ± 35	97 ± 26	39 ± 13	233 ± 66	117 ± 26
246	52 ± 31	22 ± 15	184 ± 71	70 ± 41	29 ± 10	5 ± 3	122 ± 36	44 ± 14	39 ± 12	15 ± 6	104 ± 33	49 ± 12
141	44 ± 26	18 ± 14	196 ± 66	79 ± 44	26 ± 8	7 ± 2	115 ± 39	43 ± 14	33 ± 8	14 ± 4	84 ± 25	42 ± 7
128	37 ± 24	16 ± 12	173 ± 77	66 ± 43	24 ± 9	4 ± 3	93 ± 30	32 ± 10	30 ± 9	12 ± 5	76 ± 22	36 ± 8
180	104 ± 67	49 ± 32	471 ± 237	195 ± 122	62 ± 20	17 ± 7	272 ± 94	111 ± 37	78 ± 20	35 ± 13	218 ± 64	118 ± 29
(182 + 187)	70 ± 37	31 ± 20	285 ± 83	110 ± 51	41 ± 15	16 ± 4	167 ± 50	67 ± 22	52 ± 13	29 ± 13	143 ± 44	73 ± 13
(170 + 190)	42 ± 26	20 ± 15	206 ± 106	82 ± 57	26 ± 7	7 ± 3	111 ± 40	46 ± 16	32 ± 10	14 ± 5	87 ± 26	46 ± 14
183	42 ± 26	18 ± 12	164 ± 65	67 ± 39	21 ± 8	5 ± 3	93 ± 39	36 ± 14	28 ± 9	13 ± 5	75 ± 22	37 ± 8
(196 + 203)	23 ± 18	14 ± 8	125 ± 53	53 ± 31	16 ± 5	3 ± 4	72 ± 23	33 ± 11	20 ± 6	11 ± 4	57 ± 16	31 ± 6
201	20 ± 16	12 ± 8	110 ± 40	46 ± 24	7 ± 8	2 ± 3	64 ± 22	29 ± 9	18 ± 5	9 ± 3	48 ± 14	27 ± 5
194	10 ± 8	6 ± 3	56 ± 35	25 ± 16	8 ± 3	3 ± 2	33 ± 11	15 ± 4	9 ± 2	5 ± 2	24 ± 6	14 ± 3
206	5 ± 4	2 ± 3	24 ± 16	11 ± 8	2 ± 3	ND	13 ± 4	7 ± 3	1 ± 2	1 ± 2	10 ± 5	6 ± 3
209	2 ± 4	ND	16 ± 10	7 ± 6	1 ± 1	ND	8 ± 4	2 ± 3	ND	ND	4 ± 4	1 ± 1
total congeners	2379	1066	9866	3881	1449	288	5656	2132	1968	794	4646	2310
mean	1303	716	3570	2069	524	149	1692	642	541	292	1380	484

^aValues shown represent the mean ± SD for each group.

Table II. Percent of Total Concentration of the 10 Most Common Congeners Observed in Lake Ontario Fish (Total Percent Contribution of All Congeners in Each Homologue Group Is Also Shown)

congener	brown trout	lake trout	rainbow trout		coho salmon	
			small	large	small	large
			trichlorobiphenyls			
total	2.0 ± 1.3	1.0 ± 0.3	1.0 ± 0.2	1.0 ± 0.4	1.1 ± 0.2	0.6 ± 0.1
			tetrachlorobiphenyls			
total	18.4 ± 2.9	15.4 ± 1.4	17.0 ± 3.9	13.9 ± 2.0	17.9 ± 0.8	14.2 ± 1.0
			pentachlorobiphenyls			
101	6.3 ± 0.7	6.1 ± 0.6	7.2 ± 0.8	6.5 ± 0.4	6.5 ± 0.7	5.9 ± 0.4
84	5.1 ± 0.7	6.3 ± 0.7	5.6 ± 1.0	5.7 ± 0.3	5.4 ± 0.4	5.9 ± 0.5
118	5.5 ± 0.6	6.3 ± 0.4	5.3 ± 0.8	5.4 ± 0.5	5.0 ± 0.3	5.8 ± 0.4
110	5.6 ± 0.3	4.8 ± 0.9	5.8 ± 0.3	5.5 ± 0.2	5.8 ± 0.2	5.5 ± 0.4
(87 + 97)	4.6 ± 0.5	4.1 ± 1.0	5.3 ± 0.8	4.3 ± 0.5	6.8 ± 0.6	5.4 ± 0.7
total	35.5 ± 1.8	36.5 ± 1.2	37.5 ± 3.2	36.4 ± 0.8	38.7 ± 1.2	36.9 ± 1.1
			hexachlorobiphenyls			
153	7.3 ± 0.9	10.8 ± 1.3	9.1 ± 1.3	9.7 ± 1.0	7.8 ± 0.4	9.9 ± 1.1
138	5.4 ± 0.4	5.9 ± 0.7	5.7 ± 0.5	5.9 ± 0.2	5.5 ± 0.2	6.1 ± 0.2
149	5.1 ± 0.4	3.4 ± 1.0	4.8 ± 0.6	5.1 ± 0.2	4.9 ± 0.2	5.0 ± 0.2
total	27.7 ± 2.0	29.2 ± 1.4	28.0 ± 2.9	30.4 ± 1.4	27.6 ± 0.8	30.5 ± 1.2
			heptachlorobiphenyls			
180	4.2 ± 0.4	4.6 ± 0.7	4.5 ± 0.9	4.7 ± 0.4	4.0 ± 0.1	4.7 ± 0.3
total	13.9 ± 1.0	14.1 ± 0.9	14.0 ± 3.3	14.6 ± 1.0	12.3 ± 0.6	14.4 ± 0.8
			octachlorobiphenyls			
total	2.2 ± 0.7	3.3 ± 0.5	2.4 ± 1.1	3.3 ± 0.3	2.4 ± 0.2	3.0 ± 0.2
			nonachlorobiphenyls			
total	0.2 ± 0.1	0.3 ± 0.1	0.1 ± 0.1	0.3 ± 0.1	0.1 ± 0.1	0.2 ± 0.1
			decachlorobiphenyl			
total	0.1 ± 0.1	0.2 ± 0.1	0	0.1 ± 0.1	0	0.1 ± 0.1

(HCB), α -hexachlorocyclohexane (α -BHC), γ -hexachlorocyclohexane (lindane), γ -chlordane, and octachlorostyrene (OCS). In addition, the 1,2-, 1,3-, and 1,4-dichloro-, 1,2,3-, 1,2,4-, and 1,3,5-trichloro-, and 1,2,3,5- and 1,2,4,5-tetrachlorobenzenes, the 2,3,6- and 2,4,5-trichloro- and 2,3,4,5,6-pentachlorotoluenes, and hexachlorobutadiene were analyzed, but were not detected in any of the samples.

Chemical Analyses. Sample cleanup procedures for chromatographic analyses has been described (15). Chemical analyses were done by gas chromatography using dual fused silica capillary columns (30 m \times 0.22 mm i.d. Durabond-5 and Durabond-17 with 0.25- μ m film thickness) and electron capture detectors. Detector temperature was 350 °C. Carrier gas was helium with a linear velocity flow of 20 cm/s. Temperature program was 50–250 °C at a rate of 1 °C/min. Some congeners coeluted even with this slow temperature program. These included (24 + 27), (28 + 31), (40 + 71), (70 + 76), (56 + 60), (87 + 97), (170 + 190), (182 + 187), and (196 + 203). Detection limits for most chemicals were in the 1–10 μ g/kg range, except for the monochlorobiphenyls with detection limits of 50 μ g/kg.

The procedure described above was not suitable to monitor the levels of many nonortho chloro substituted congeners because of their low concentrations and potential coelution with more common congeners of higher chlorine content (16). This problem was resolved by combining equal volumes of sample extracts from each fish within each group and reducing the volume to increase instrument sensitivity. The composite sample for each group was analyzed by a Hewlett-Packard mass selective detector (MSD) set in the selected ion-monitoring mode. Detection limit was \sim 2 μ g/kg.

Congener identification and quantitation were based on a mixture of Aroclors 1221, 1016, 1254, and 1262 in a ratio of 10:5:3.5:3. These Aroclors were obtained from the U.S. EPA Repository for Toxic and Hazardous Materials (Research Triangle Park, NC). Composition of this mixture

was determined from congener-specific analyses (11, 16). Confirmation of peak identification and quantitative analyses were made from 50 standards that were obtained from commercial sources and 51 congeners from the National Research Council of Canada (Atlantic Research Laboratory, Halifax, NS). Some samples were also analyzed by gas chromatography/mass spectrometry for further confirmation. OCS was obtained as a gift from Dow Chemical Co., Walnut Creek, CA. Photomirex was synthesized according to Chau and Thomson (17). Standards for the other organochlorine chemicals were obtained from commercial sources. Lipid content was determined by chloroform/methanol extraction (18). Chemical and lipid concentrations are reported on a wet-weight basis.

Data Analyses. Chemical concentrations in micrograms per kilogram were reported for all individual congeners observed in fish; total congener concentration was also determined. Percent chlorine content of total congener concentration was estimated by multiplying the total concentration of each homologue group by the percent molecular weight represented by chlorine for each homologue. Results shown for most of the variables measured represent the mean \pm standard deviation for each group of 8–12 values, depending on species. Paired *t* tests were used to compare differences between fish and corresponding muscle values within each group. Analysis of variance (ANOVA) was used to test for statistically significant differences among groups.

Results and Discussion

Principal Congener Analyses. PCB analyses on four salmonid species indicated an average of 54–68 congeners were present in whole fish and 33–62 in muscle, including the nonortho chloro substituted congeners which were analyzed as a composite sample, among the 92 congeners monitored. Total congener concentrations ranged from 1450 μ g/kg in small rainbow trout to 9970 μ g/kg in lake

trout, and 288 to 3880 $\mu\text{g}/\text{kg}$ in muscle for the respective species. There was a large range in mean congener concentrations in fish and muscle among species. Concentrations of the more common congeners observed are shown in Table I.

Congeners 1, 3-8, 10, 12, 13, 19, 25, 45, 169 were not detected in any species, while congeners 16-19, 22, 24, 26, 27, 32, 33, 40-42, 46, 48, 53, 126, 129, 169, 173, 185, 195, 198, 205, and 207 were present at mean levels below 10 $\mu\text{g}/\text{kg}$ in most species except lake trout which were slightly higher. Levels of the other congeners observed were in the 10-100 $\mu\text{g}/\text{kg}$ range.

Congener levels reported in decreasing concentrations in Table I demonstrated a trend of decreasing values that is consistent for fish and muscle, within homologue groups, as well as among species. When levels of individual congeners were expressed as a percent of total concentration, their mean percent contribution were similar for fish (Table II) and muscle among different species even though total concentrations vary widely. The most common congener was 153 (2,2',4,4',5,5'-hexachlorobiphenyl), averaging 9.5% of total congener content in fish and muscle. The same response was also demonstrated when total percent contribution by each homologue group is calculated. The pentachloro-, hexachloro-, tetrachloro-, and heptachlorohomologues represented about 37, 29, 16, and 13% of the total congener concentrations, respectively. The other homologues cumulatively represented less than 5% of total concentration among all species.

Consistency among congener contribution is further demonstrated by the cumulative percentages of the more common congeners. The ten most common congeners, 84, (87 + 97), 101, 110, 118, 138, 149, 153, and 180, accounted for 49.3 ± 3.2 , 52.2 ± 0.9 , 53.0 ± 1.7 , 52.8 ± 1.8 , 51.7 ± 1.0 , and $54.4 \pm 0.6\%$ of the total in brown, lake, small and large rainbow trout, and small and large coho salmon, respectively. Corresponding values in muscle were 52.3 ± 2.4 , 52.8 ± 0.7 , 60.3 ± 5.5 , 53.7 ± 1.2 , 53.7 ± 1.2 , and $55.1 \pm 0.6\%$ for the respective species. The ten next most common congeners were 66, (70 + 76), 95, 105, 146, (182 + 187), and (170 + 190) whose individual contributions ranged from 1.8 to 3.9% in fish. Cumulative contributions for these 20 congeners were 68.5 ± 3.4 , 70.1 ± 1.3 , 72.4 ± 0.9 , 71.0 ± 0.9 , 70.9 ± 1.5 , and $73.0 \pm 1.0\%$ in fish and 71.5 ± 2.4 , 70.8 ± 1.3 , 81.0 ± 5.8 , 72.0 ± 1.1 , 73.0 ± 1.3 , and $73.5 \pm 0.7\%$ in muscle for the respective species.

The relationship between homologue frequency and total congener concentration was examined by using percent chlorine content. Chlorine composition were 55.74 ± 0.51 , 56.28 ± 0.26 , 55.97 ± 0.77 , 56.48 ± 0.37 , 55.74 ± 0.14 , and $56.42 \pm 0.21\%$ for brown, lake, small and large rainbow trout, and small and large coho salmon, respectively. Values in muscle were 55.87 ± 0.42 , 56.33 ± 0.28 , 56.75 ± 0.82 , 56.65 ± 0.34 , 55.95 ± 0.17 , and $56.51 \pm 0.19\%$ for the respective species. ANOVA indicated no significant differences among the chlorine percentages of lake, large rainbow trout, and large coho salmon and the chlorine percentages of brown and small rainbow trout and small coho salmon, but the percentages between these groups were significantly different ($P < 0.01$). Paired *t* tests between fish and muscle for each sample within each group showed significantly higher chlorine percentages ($P < 0.05$) in muscle than fish in all species, except lake trout.

Analyses for 12 other chemicals observed in fish indicated DDE was present at the highest concentrations among those monitored, with lake trout again containing the highest concentrations (Table III). A listing of chemicals by concentrations also demonstrated the con-

Table III. Concentrations ($\mu\text{g}/\text{kg}$) of Other Chemicals Monitored in Lake Ontario Salmonids

chemical	brown trout		lake trout		rainbow trout		coho salmon					
	fish	muscle	fish	muscle	small fish	small muscle	large fish	large muscle	small fish	small muscle	large fish	large muscle
DDE	486 ± 448	203 ± 203	1982 ± 1203	618 ± 486	257 ± 114	52 ± 34	1073 ± 504	372 ± 107	391 ± 124	154 ± 58	964 ± 315	456 ± 125
DDD	31 ± 16	15 ± 12	218 ± 114	83 ± 56	31 ± 17	8 ± 6	125 ± 44	42 ± 11	25 ± 6	12 ± 4	70 ± 32	27 ± 14
DDT	59 ± 24	26 ± 12	160 ± 94	64 ± 49	35 ± 11	8 ± 2	87 ± 33	38 ± 8	58 ± 14	24 ± 9	79 ± 25	36 ± 10
mirex	77 ± 61	41 ± 33	430 ± 241	183 ± 131	51 ± 27	16 ± 3	246 ± 82	112 ± 36	45 ± 35	33 ± 15	203 ± 63	110 ± 31
phocomirex	38 ± 22	16 ± 12	196 ± 110	78 ± 52	25 ± 15	6 ± 4	129 ± 58	52 ± 19	26 ± 8	12 ± 5	108 ± 31	54 ± 15
HCB	25 ± 7	10 ± 4	90 ± 43	37 ± 25	20 ± 8	5 ± 2	42 ± 7	16 ± 3	26 ± 6	10 ± 5	24 ± 7	13 ± 3
OCS	18 ± 10	7 ± 5	130 ± 101	52 ± 45	14 ± 7	4 ± 3	52 ± 13	18 ± 4	16 ± 6	7 ± 3	36 ± 9	16 ± 7
γ -chlordane	3 ± 1	1 ± 1	48 ± 30	19 ± 15	10 ± 2	2 ± 1	24 ± 3	8 ± 2	13 ± 3	5 ± 2	15 ± 4	8 ± 2
α -BHC	25 ± 5	11 ± 2	22 ± 7	8 ± 5	11 ± 5	3 ± 2	12 ± 4	5 ± 1	16 ± 2	6 ± 2	4 ± 1	1 ± 1
lindane	5 ± 1	2 ± 1	4 ± 1	2 ± 1	2 ± 1	ND	2 ± 1	1 ± 1	4 ± 1	2 ± 1	ND	ND
QCB	7 ± 5	3 ± 2	10 ± 4	4 ± 2	2 ± 1	ND	5 ± 1	2 ± 1	4 ± 1	2 ± 1	2 ± 1	ND
TECB	5 ± 7	2 ± 3	4 ± 2	2 ± 3	1 ± 1	ND	ND	ND	1 ± 1	ND	ND	ND

Table IV Percent Composition of 10 Congeners in Aroclors 1254 (Clophen A50) and 1260 (Clophen A60), Reported by Zell et al. (2), Albro et al. (9), Capel et al. (10), and Mullin (11), and Their Mean Composition Observed in Lake Ontario Fish^a

congener	Zell			Albro			Capel			Mullin			present study
	A50	A60	56%	1254	1260	56%	1254	1260	56%	1254	1260	56%	
153	3.3	10.4	5.7	3.3	8.2	5.0	3.1	1.3	2.5	6.2	10.6	7.7	9.0
101	8.1	6.6	7.6	7.0	5.0	6.3	8.4	4.0	7.0	7.1	2.5	5.6	6.4
138	4.8	12.4	7.3	—	—	—	9.1	1.3	6.5	5.9	5.2	5.7	5.8
118	0.5	0.6	0.5	8.1	2.0	6.1	—	—	—	6.1	0.6	4.3	5.6
149	5.8	—	—	3.6	9.5	5.6	—	—	—	5.9	8.7	6.8	4.7
84	2.5	0.4	1.8	1.7	0.7	1.4	—	—	—	4.2	0.2	2.9	5.6
110	1.1	0.1	0.8	8.6	3.6	6.9	10.3	1.6	7.4	9.6	1.4	6.9	5.5
180	0.4	6.2	2.3	0.8	7.2	2.9	0.5	6.5	2.5	1.2	12.1	4.8	4.4
(87 + 97)	7.0	1.5	5.2	6.4	1.7	4.8	6.4	0.5	4.4	5.5	0.4	3.8	5.2

^aThe "56%" equivalents were estimated from the compositions reported for Aroclors 1254 and 1260.

sistent trend of corresponding decreasing levels among species, similar to that observed for PCB congeners.

Lipid levels varied widely among species. Values in fish were 14.3 ± 1.6 , 17.4 ± 3.0 , 6.0 ± 2.4 , 13.0 ± 1.7 , 8.4 ± 1.8 , and $4.5 \pm 0.8\%$ for brown, lake, small and large rainbow trout, and small and large coho salmon, respectively. Corresponding values in muscle were 4.8 ± 1.1 , 7.3 ± 2.2 , 1.3 ± 0.5 , 4.9 ± 1.1 , 3.4 ± 0.7 , $2.3 \pm 0.4\%$ for the respective species. Regression analyses among samples indicated percent lipid in fish increased significantly ($P < 0.05$) with weight in lake trout and small coho salmon, but not the other groups. Lipid levels in muscle increased significantly ($P < 0.01$) with weight only in lake trout.

Behavior of PCB Congeners. The bioaccumulation of PCBs in aquatic ecosystems is well established (7, 19). Studies using mass fragmentation techniques have indicated percentages of higher chlorinated biphenyls increase at higher trophic levels in the marine ecosystem (20). Congener-specific analyses could allow a more detailed examination of these processes if the measurements are representative of most of the principal PCB congeners. This criterion is met in this study, as shown by comparisons between the congeners observed and those reported in PCB mixtures. The 92 congeners monitored in this study accounted for about 82, 80, 97, and 93% of total congener composition of Aroclor 1254 (Clophen A50) reported by Zell et al. (8), Albro et al. (9), Capel et al. (10), and Mullin (11), respectively. Similar comparisons with Aroclors 1242 and 1248 indicated slightly higher percentages, while those with Aroclor 1260 (Clophen A60) were slightly lower.

A hypothesis on PCB kinetics in Lake Ontario salmonids could be developed by comparing the congener composition monitored in fish with that reported in PCB mixtures. Congener composition of Lake Ontario salmonids was compared with Aroclor 1254 which has been used as a reference standard for PCB analysis although Aroclor mixtures are now commonly used (21). Comparisons among the percentage contribution of the more common congeners observed in fish and those reported in Aroclor 1254 mixtures generally indicate higher frequencies of 153 and 180 and lower frequency of 110 (Table IV). This analysis could suggest some congeners are selectively retained and others eliminated, and the kinetics of PCBs in fish would be determined by the net response of individual congeners. It was previously reported that most pentachlorinated and higher chlorinated congeners have biological half-lives in excess of several hundred days in trout; therefore, this apparent difference in composition could not be attributed to their clearance rates (12).

PCB congeners in Lake Ontario salmonids averaged 56% chlorine. A PCB mixture containing 56% chlorine by weight can be obtained by mixing Aroclors 1254 and

1260 in a 2:1 ratio (Table IV). Percent frequency comparisons among the more common congeners with the 56% chlorine Aroclor mixture indicate similarities among most values, although some differences are suggested. The frequencies of congeners 153, 84, and perhaps 110 may be higher in fish, while 110 and possibly 149 may be lower than the 56% chlorine mixture (Table IV). Nevertheless, this analysis would suggest the more persistent congeners tend to behave as a homogeneous mixture rather than as individual congeners.

It could also be difficult to establish a basis for this distribution pattern based on structure-activity relationship (SAR) analysis because these species represent a high trophic status in the Lake Ontario ecosystem, and most fish lack the capacity to metabolize the higher chlorinated congeners. For example, the enriched congeners 153 and 180 have two para chloro substituted positions and no vacant vicinal positions, although 84 has no para chloro substituted and two vacant vicinal positions. Congeners 110 and 149, with lower relative frequencies, have one para chloro substituted position and at least one vacant vicinal position. Congeners 101, 138, and 118, whose frequencies were similar to the 56% chlorine mixture, have at least one para chloro substituted and one vacant vicinal position. Therefore, the frequency distribution among the more common congeners cannot be consistently explained on the basis of SAR. It is probable that if SAR criteria could be applied to PCB kinetics in aquatic ecosystems, it would most likely be demonstrated at lower trophic levels and most evident among the lower chlorinated congeners (7, 22).

Environmental Monitoring and Toxicological Implications. On the basis of current information, it is difficult to propose which congeners could be routinely monitored for environmental assessment. Most congener-specific studies indicate 101, 138, 153, and 180 are present at the highest concentrations in fish, although other congeners should be monitored to provide a more comprehensive assessment. Use of congener-specific analyses to assess health risks associated with consumable products presents an even more difficult task. At least 16 congeners, including 77, 81, 105, 114, 118, 126, 128, 138, 156, 169, and 170, have been identified as aryl hydrocarbon hydroxylase (AHH) inducers (23). The 10 monitored in this study accounted for ~18.5% of total congener composition. Other studies indicate eight of these AHH inducers were reported in pomfret (3) and seven in salmon eggs (6). Mullin (11) reported 12 of these congeners in Aroclor 1254.

Nonortho chloro substituted congeners with substitutions at both para and at least two meta positions are the most toxic although their environmental concentrations are low (24). Congener 169 was not detected, and 126 was

detected only in lake trout and large rainbow trout at 19 and 10 $\mu\text{g}/\text{kg}$, respectively. Congeners 77 and 81 were present in Lake Ontario salmonids at concentrations in the low microgram per kilogram range (Table I). These levels represent about 0.2% and 0.8% of total concentration, respectively.

Use of congener-specific analyses for regulatory purposes of PCBs in consumable products would be desirable, but further studies are required before its application would be feasible. Nonortho chloro substituted congeners occur at concentrations that approach or are below detection limits of most current routine analytical procedures. Analysis for congener 77 using electron capture gas chromatography is difficult because of coelution with congener 110 on most capillary columns (16, 25). Coelution problems could be minimized by using a secondary cleanup procedure with a carbon/glass fiber packed column (26). Also, quantitation could be made more reliable by use of a mass selective detector.

Studies of the sublethal effects of PCBs on fishes in contaminated ecosystems could be more definitive if specific congeners rather than total PCBs were monitored. Emphasis should focus on the relation of the concentration of a congener and its toxicity. The concentration of congener 153 is ~45-fold higher than 77 in Lake Ontario salmonids. Data from other studies indicate congener 153 is 38-fold higher than 77 in pomfret (3) and 18-fold higher in salmon eggs (6). Comparative enzyme induction studies on mammalian systems suggest congener 77 could be over 10–41-fold more toxic than 153 (22, 27). Thus, the concentrations of congener 77 in Lake Ontario salmonids could be as important as 153 from a toxicological perspective. This factor is more obvious among the chlorinated dioxins, where 2,3,7,8-TCDD is many orders of magnitude more toxic than most other dioxins (28). Therefore, chemical toxicity, in addition to concentration, is an important consideration for chemical groups with many homologues when issues such as human health and sublethal effects on fishes are being examined. This assessment was done in a recent study using toxic equivalent factors (TEF) based on a composite index, AHH induction, and thymic atrophy responses in mammalian systems (29). The results indicated TEF values for PCB levels in Lake Ontario salmonids were several fold higher than TEF values for dioxin and furan levels in the same fish.

Acknowledgments

We thank R. Lewies of the Ontario Ministry of Natural Resources, L. Durham and K. D. Nicol of Environment Canada, and G. Dookhran, J. D. Fitzsimons, M. J. Keir, P. L. Luxon, and D. M. Whittle of the Department of Fisheries and Oceans for their technical assistance. Comment on the manuscript by R. E. Reinert, University of Georgia, is also acknowledged.

Registry No. PCB 28, 7012-37-5; PCB 31, 16606-02-3; PCB 66, 32598-10-0; PCB 70, 32598-11-1; PCB 76, 70362-48-0; PCB 56, 41464-43-1; PCB 60, 33025-41-1; PCB 52, 35693-99-3; PCB 47, 2437-79-8; PCB 81, 70362-50-4; PCB 101, 37680-73-2; PCB 84, 52663-60-2; PCB 118, 31508-00-6; PCB 110, 38380-03-9; PCB 87, 38380-02-8; PCB 97, 41464-51-1; PCB 105, 32598-14-4; PCB 95, 38379-99-6; PCB 153, 35065-27-1; PCB 138, 35065-28-2; PCB 149, 38380-04-0; PCB 146, 51908-16-8; PCB 141, 52712-04-6; PCB 128, 38380-07-3; PCB 182, 60145-23-5; PCB 187, 52663-68-0; PCB 170, 35065-30-6; PCB 190, 41411-64-7; PCB 193, 69782-91-8; PCB

196, 33091-17-7; PCB 203, 52663-76-0; PCB 201, 52663-75-9; PCB 194, 35694-08-7; PCB 206, 40186-72-9; PCB 209, 2051-24-3; DDE, 72-55-9; DDD, 72-54-8; DDT, 50-29-3; HCB, 118-74-1; OCS, 29082-74-4; α -BHC, 319-84-6; QCB, 608-93-5; TECB, 634-66-2; mirex, 2385-85-5; photomirex, 39801-14-4; γ -chlordane, 5566-34-7; lindane, 58-89-9.

Literature Cited

- (1) Jensen, S. *Ambio* 1972, 1, 123.
- (2) Zell, M.; Neu, H. J.; Ballschmiter, K. *Fresenius' Z. Anal. Chem.* 1978, 292, 97.
- (3) Tanabe, S.; Tanaka, H.; Tatsukawa, R.; Nakamura, I. *Bull. Jpn. Soc. Sci. Fish.* 1980, 46, 763.
- (4) Tuinstra, L. G. M.; Driessen, J. J. M.; Keukens, H. J.; van Munsteren, T. G.; Roos, A. H.; Traag, W. A. *Int. J. Environ. Anal. Chem.* 1983, 14, 147.
- (5) Boon, J. P.; Duinker, J. C. *Environ. Monit. Assess.* 1986, 7, 189.
- (6) Giesy, J. P.; Newsted, J.; Garling, D. L. *J. Great Lakes Res.* 1986, 12, 82.
- (7) Oliver, B. G.; Niimi, A. J. *Environ. Sci. Technol.* 1988, 22, 388.
- (8) Zell, M.; Neu, H. J.; Ballschmiter, K. *Chemosphere* 1977, 2/3, 69.
- (9) Albro, P. W.; Corbett, J. T.; Schroder, J. L. *J. Chromatogr.* 1981, 205, 103.
- (10) Capel, P. W.; Rapaport, R. A.; Eisenreich, S. J.; Looney, B. B. *Chemosphere* 1985, 14, 439.
- (11) Mullin, M. D. Congener Specific PCB Workshop, U.S. EPA, Grosse Ile, MI, 1985.
- (12) Niimi, A. J.; Oliver, B. G. *Can. J. Fish. Aquat. Sci.* 1983, 40, 1388.
- (13) Safe, S. *CRC Crit. Rev. Toxicol.* 1984, 13, 319.
- (14) Ballschmiter, K.; Zell, M. *Fresenius' Z. Anal. Chem.* 1980, 302, 20.
- (15) Oliver, B. G.; Nicol, K. D. *Chromatographia* 1982, 16, 336.
- (16) Mullin, M. D.; Pochini, C. M.; McCrindle, S.; Romkes, M.; Safe, S. H.; Safe, L. M. *Environ. Sci. Technol.* 1984, 18, 468.
- (17) Chau, A. S. Y.; Thomson, R. T. *J. Assoc. Off. Anal. Chem.* 1979, 62, 1302.
- (18) Bligh, H. G.; Dyer, W. J. *Can. J. Biochem. Physiol.* 1959, 37, 911.
- (19) Thomann, R. V. *Can. J. Fish. Aquat. Sci.* 1981, 38, 280.
- (20) Tanabe, S.; Tanaka, H.; Tatsukawa, R. *Arch. Environ. Contam. Toxicol.* 1984, 13, 731.
- (21) Bache, C. A.; Serum, J. W.; Youngs, W. D.; Lisk, D. J. *Science (Washington, D.C.)* 1972, 177, 1191.
- (22) Furukawa, K. In *Biodegradation and Detoxification of Environmental Pollutants*; Chakrabarty, A. M., Ed.; CRC: Boca Raton, FL, 1982; pp 37–57.
- (23) Safe, S.; Mullin, M.; Safe, L.; Pochini, C.; McCrindle, S.; Romkes, M. In *Physical Behavior of PCBs in the Great Lakes*; Mackay, D., Paterson, S., Eisenreich, S. J., Simmons, M. S., Eds.; Ann Arbor Science: Ann Arbor, MI, 1983; pp 1–13.
- (24) Safe, S.; Bandiera, S.; Sawyer, T.; Robertson, L.; Safe, L.; Parkinson, A.; Thomas, P. E.; Ryan, D. E.; Reik, L. M.; Levin, W.; Denomme, M. A.; Fujita, T. *EHP, Environ. Health Perspect.* 1985, 60, 47.
- (25) Schwartz, T. R.; Stalling, D. L.; Rice, C. L. *Environ. Sci. Technol.* 1987, 21, 72.
- (26) Smith, L. M. *Anal. Chem.* 1981, 53, 2152.
- (27) McKinney, J. D.; Chae, K.; McConnell, E. E.; Birnbaum, L. S. *EHP, Environ. Health Perspect.* 1985, 60, 57.
- (28) Kociba, R. J.; Cabey, O. *Chemosphere* 1985, 14, 649.
- (29) Niimi, A. J.; Oliver, B. G. *Chemosphere*, in press.

Received for review August 4, 1987. Revised manuscript received March 4, 1988. Accepted August 15, 1988.

Characteristics of Radioactive Particles Released from the Chernobyl Nuclear Reactor

R. G. Cuddihy,* G. L. Finch, G. J. Newton, F. F. Hahn, J. A. Mewhinney, S. J. Rothenberg, and D. A. Powers†

Lovelace Biomedical and Environmental Research Institute, Inhalation Toxicology Research Institute, P.O. Box 5890, Albuquerque, New Mexico 87185

■ Particles from the Chernobyl nuclear reactor accident that deposited on a nearby surface were analyzed to determine their radioactive and chemical compositions. They were mainly composed of uranium, carbon, cerium, and lanthanum, or zirconium. The latter two types of particles also contained aluminum, silicon, calcium, phosphorus, and chlorine that probably derived from high-temperature interactions between fuel and the reactor structures or soil that was deposited on the core. The major γ -emitting radionuclides associated with the particles were ^{95}Zr – ^{95}Nb , ^{103}Ru , ^{106}Ru – ^{106}Rh , ^{134}Cs , ^{137}Cs – ^{137}Ba , ^{141}Ce and ^{144}Ce – ^{144}Pr . They did not include ^{131}I or ^{140}Ba – ^{140}La , radionuclides that were frequently reported as being abundant in samples collected at more distant locations throughout Europe. When selected particle samples were placed in aqueous media similar in ionic composition to lung fluids, all of the radionuclides were slow to dissolve; the average dissolution half-time was 160 days. We concluded that if similar particles were inhaled by people near the reactor site, the largest portion of the related radiation doses would be delivered to lung tissue.

Introduction

The nuclear reactor accident at Chernobyl Unit 4 led to the release of a large quantity of radioactive material to the environment between April 26 and June 1, 1986 (1, 2). The reactor accident first became apparent to outside observers when two explosions occurred at 1:24 a.m. on April 26.

Four phases of radionuclide discharges were described. The first phase resulted from the explosions which caused mechanical discharges of fuel material, vapors, and gases. The second phase, April 26 through May 2, resulted from high fuel temperatures caused by the initial reactivity excursion, radioactive decay energy, and burning graphite. Daily releases of radioactivity decreased during this phase because the core was smothered with soil, lead, and boron carbide in efforts to contain the accident. However, finely dispersed fuel particles and volatile fission products still escaped in the flow of hot combustion products. During the third phase, May 3 through May 6, fuel temperatures increased again due to the release of residual heat. This caused more fission products to migrate through the covering material and into the atmosphere. The fourth phase, after May 6, was characterized by a rapid decline in radionuclide releases (1).

Although ^{238}U was the major constituent of the core, it constituted a negligible fraction of the total radioactivity because of its very low specific activity. Amounts of other radionuclides present depended upon their fission yields, the yields of radioactive precursors in their decay chains, and their radioactive half-lives. Estimated discharges are highest for the most volatile radionuclides and lowest for the most refractory materials. Virtually all of the core contents of inert radioactive gases, xenon and krypton,

were released and dispersed widely in the atmosphere. Approximately 10–20% of the more volatile elements (iodine, tellurium, and cesium) and 2–5% of the fuel material were also released (1). Most of these were in particulate form or became associated with particles that have now settled back to earth, mainly in the northern hemisphere. The highest concentrations of radioactivity deposited in eastern Europe; probably 30% of the deposited radioactivity stayed within 50 km of the Chernobyl plant.

This report is based upon analyses of particles that deposited on a wood surface soon after the reactor accident. The wood was part of a shipping crate that was on a railroad car probably within 80 km of Chernobyl at the time of the reactor accident, but a precise exposure history of the shipping crate is not known. The railroad car arrived in Munich, Germany, toward the end of May where the radioactive crate was removed. In June, a sample of the wood was provided for the analyses we describe. We studied particle characteristics that (1) indicate how the radionuclides were released during the accident and (2) influence the deposition, retention, and long-term radiation doses to body organs if the particles are inhaled or ingested by people. These include particle size, shape, chemical composition, and rate of dissolution in aqueous media. This information is important for evaluating the long-term exposure risks to people who live near the Chernobyl reactor and to others who may be exposed to similar material in the event that serious nuclear reactor accidents occur in the future. Because our analyses began in July 1986, no information was gained related to very short-lived radionuclides.

Experimental Section

Methods. A lithium-drifted germanium detector was used to obtain a γ -ray spectrum of the wood sample to identify radionuclides present. Autoradiographs of the intact wood surface were done using Kodak standard X-ray film to locate radioactive particles. Small areas of the wood surface were then microdissected under a stereo light microscope to obtain individual particle samples. Some of these were embedded in paraffin and cut with a microtome into 7- μm -thick sections to produce microautoradiographs. Sections were dipped in Kodak NTB-3 emulsion, exposed for 20 min, and developed.

Other particle samples were mounted on carbon stubs and coated with carbon or gold for scanning electron microscopy (SEM; JEOL Model JSM-35, operated at 20–25 keV) and energy dispersive X-ray analysis (EDXA; Kevex Model 5100 spectrometer). Particles that were imaged by standard secondary mode SEM were first located by using backscattered electron images of large areas of the samples (Figure 1). Those composed of elements with high atomic numbers, such as uranium or fission products, appeared bright against the darker background. These were individually analyzed by placing the electron beam on the particle in reduced raster mode (typically <10 μm^2) and acquiring a spectrum for 100 s. Selected spectra were quantitatively analyzed for elemental content

*D.A.P. is in the Department of Reactor Safety Research of Sandia National Laboratories in Albuquerque, NM.

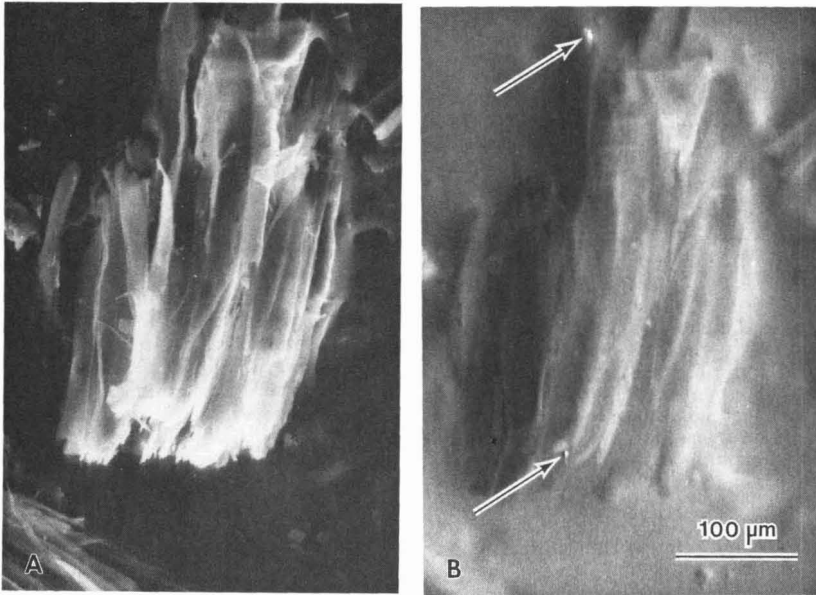


Figure 1. Scanning electron micrograph of a microdissected wood sample in conventional secondary electron imaging mode (A), and in backscattered electron imaging mode (B), showing bright spots indicating the presence of particles composed of heavy elements.

(Quantex Software, KeveX, Foster City, CA; concentration detection limit of ~1% by mass). The EDXA could identify chemical elements having higher atomic numbers than sodium that were present in individual particles. Particles that contained detectable amounts of uranium or fission products and were correlated with radioactive "hot spots" were assumed to be derived from the Chernobyl reactor fuel. Also, particles that were identified as radioactive by microautoradiography, but did not produce a unique spectrum with EDXA, were assumed to be composed of carbon derived from the graphite used as the neutron moderator in the reactor.

The rates of solubilization of radionuclides from two particle samples were determined for 60 days in an aqueous solvent similar in ionic composition to lung fluids (3). The rate of particle solubilization can be used to predict the amounts of inhaled and deposited radionuclides that may leave the lung and accumulate in other body organs. Because large particles deposited in the lung normally do not pass through the tissue and into the blood circulation, the associated radionuclides must first dissolve in lung fluids to be absorbed. These are important factors in determining the internal radiation dose distribution.

Results

A γ -ray spectrum of the intact radioactive sample of wood is shown in Figure 2. The most apparent radionuclides are ^{141}Ce , ^{144}Ce - ^{144}Pr , ^{103}Ru , ^{106}Ru - ^{106}Rh , ^{134}Cs , ^{137}Cs - ^{137}Ba , and ^{95}Zr - ^{95}Nb . Notably absent from this spectrum are ^{131}I and ^{140}Ba - ^{140}La ; this could have resulted if (a) only a small portion of these radionuclides were in particulate form or (b) they solubilized and washed off in rain water while the shipping crate was in transit to Munich. The autoradiograph of the intact wood sample indicated that ~30 individual sources of radioactivity were present over 125 cm² of its surface. A microautoradiograph of one source after removal from the block is shown in Figure 3. Radioactivity was observed at adjacent locations on several consecutive microtome sections and indicated the presence of one large radioactive particle ~50 μm in

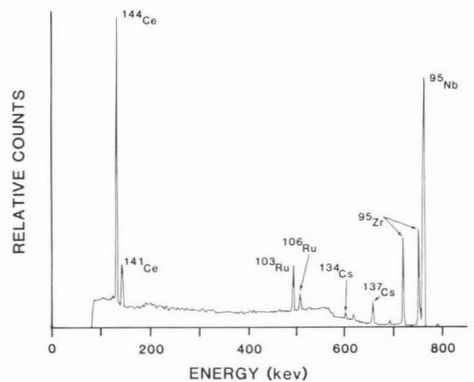


Figure 2. γ -Ray spectrum obtained from radioactive particles on the intact wood surface with a lithium-drifted germanium detector on July 1, 1986.

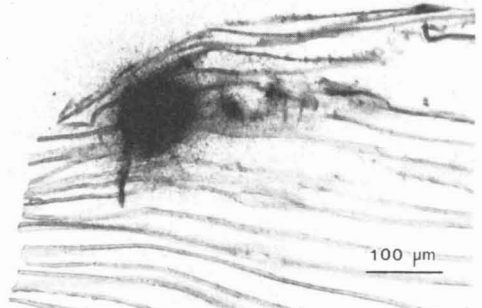


Figure 3. Microautoradiograph of radioactive particles on a wood fragment that was embedded in paraffin and sectioned with a microtome.

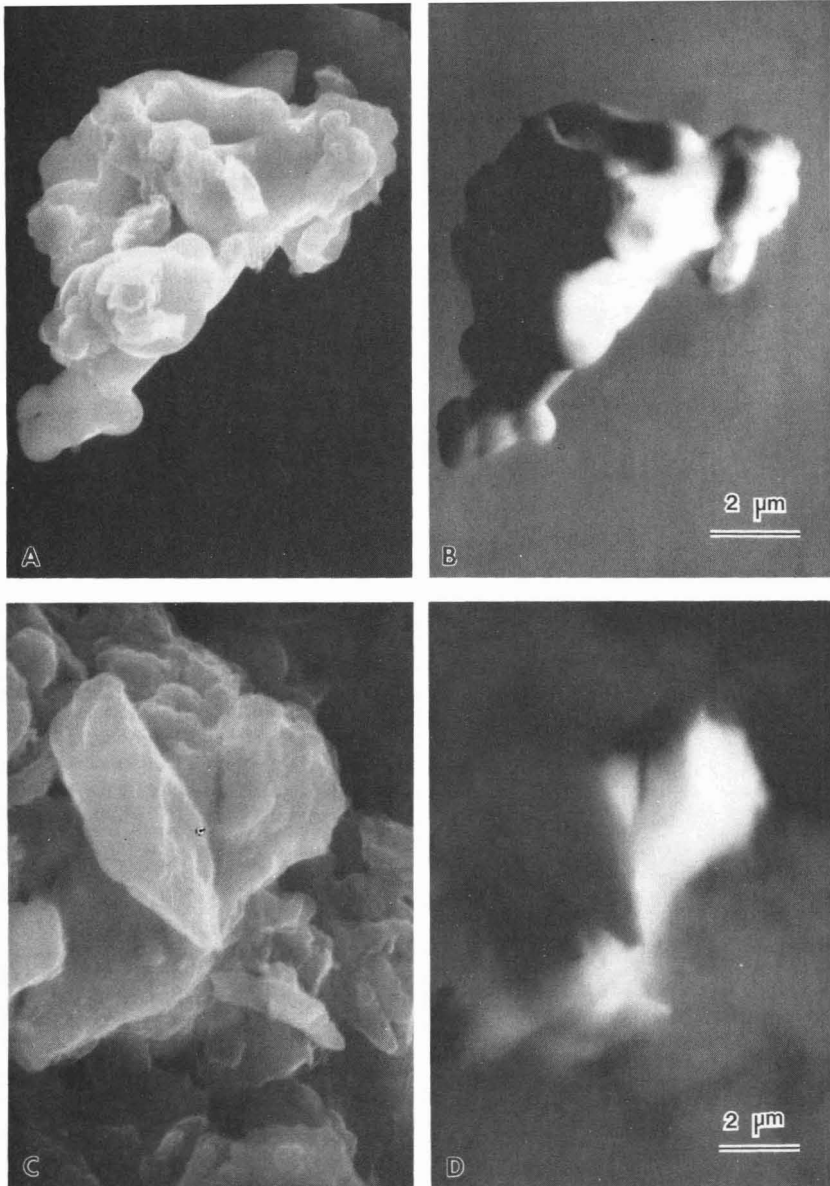


Figure 4. Secondary electron scanning electron micrographs (A, C) and corresponding backscattered electron images (B, D) of particles composed almost totally of uranium.

diameter that was easily cut by the microtome along with two adjacent small particles. All of these particles contained β -emitting radionuclides.

Particles composed almost totally of uranium are shown in Figure 4. Several similar particles were observed, and all such particles had average diameters between 2 and 10 μm . Many particles appeared to be agglomerates of smaller fragments, including spheres. Other particles evaluated by EDXA were composed of fission products, cerium and lanthanum, or zirconium (Figure 5). These particles also contained small amounts of silicon, calcium, aluminum, phosphorus, and chlorine. Particle characteristics are summarized in Table I.

When the particles shown in Figure 3 were analyzed by EDXA, the two small particles were found to be primarily composed of uranium, but no concentrated fission product elements were found at the location of the large particle. Furthermore, no contrast at the location of the particle was observed in the backscattered electron imaging mode, indicating that the mean atomic number of elements comprising the particle was similar to that of the wood matrix. Therefore, likely possibilities for the composition of the large particle are carbon and boron. Carbon is most likely because the Chernobyl reactor was moderated with ~ 1700 tons of graphite; boron carbide is also possible because a few tons of this material were dumped on the reactor core

Table I. Summary of EDXA and γ Spectral Analyses of Individual Particles

particle no.	composition ^a	general description
1	uranium	~6 μm in diameter with few fission products
2-7	uranium	2-6 μm in diameter with significant quantities of adsorbed fission products
8	carbon	~50 μm in diameter with significant quantities of adsorbed fission products
9	Ce (60%), La (30%), Al, Si, Ca, P, and Cl as minor components	~5 μm in diameter with significant quantities of adsorbed fission products (bulk of particle is probably carbon)
10	Zr (20%), Al (20%), and Cl (60%)	<5 μm in diameter with significant radioactivity present

^a EDXA used for these analyses does not detect elements having atomic numbers lower than sodium. Therefore, particle 8 is assumed to be mainly carbon and particles 9 and 10 may also be mainly composed of carbon. Percentages listed are of the total detected elements present.

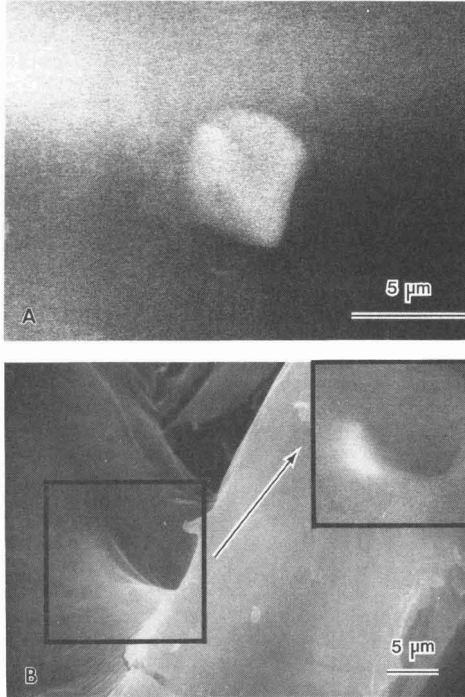


Figure 5. Scanning electron micrographs of particles composed of (A) cerium and lanthanum adsorbed onto carbon and (B) zirconium on a wood surface (inset shows the backscattered electron image).

during the week following the accident as a containment measure. However, because of the relatively larger amount of carbon present and the association of the large particle with smaller uranium particles, it was probably composed of carbon released during the initial explosion (long before boron carbide was used).

γ -Ray spectral analyses (Figure 2) and autoradiographs indicated that the uranium particles probably contained a mixture of fission products. In samples of particles composed of zirconium or cerium and lanthanum, only ^{141}Ce , ^{144}Ce - ^{144}Pr , and ^{95}Zr - ^{95}Nb were detected (Figure 6). This suggests that simple comminution of the fuel was not the mechanism for formation of these particles and that cerium and zirconium radionuclides were likely associated with the same particles.

Two types of particle samples were used to determine the dissolution rates of the associated radionuclides in an aqueous media. One type of sample included ^{141}Ce , ^{144}Ce - ^{144}Pr , ^{103}Ru , ^{106}Ru - ^{106}Rh , ^{134}Cs , ^{137}Cs - ^{137}Ba , and ^{95}Zr - ^{95}Nb while the other contained only ^{141}Ce , ^{144}Ce - ^{144}Pr , and ^{95}Zr - ^{95}Nb . Dissolution data were described by two-

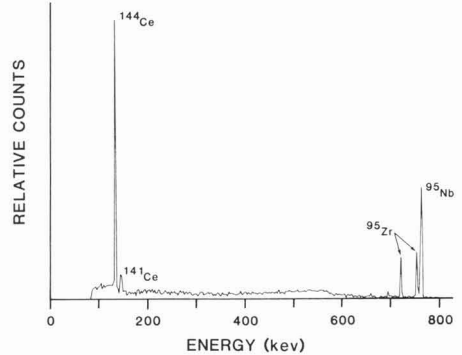


Figure 6. γ -Ray spectra of particle sample obtained with a lithium-drifted germanium detector on December 4, 1986. The major difference between this spectrum and that shown in Figure 2 is the absence of Ru and Cs radionuclides.

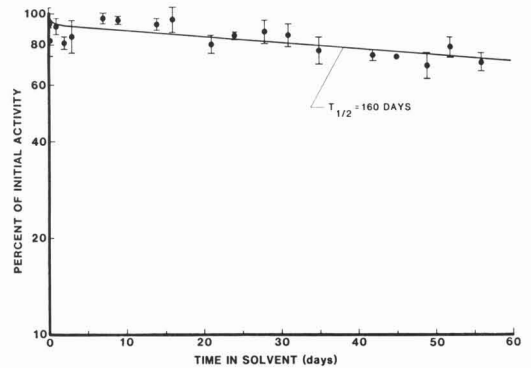


Figure 7. Dissolution of ^{95}Zr - ^{95}Nb from a particle sample immersed in an aqueous solvent. The long-term component of a two-component negative exponential function fit to the data accounted for ~90% of the radioactivity which dissolved with a half-time of 160 days.

component negative exponential functions. In each case, ~10% of the initial radioactivity went into solution within a few hours (Figure 7). The remaining 90% of the radioactivity dissolved slowly with a half-time of ~160 days. This pattern was observed for each radionuclide in both particle samples.

Discussion

Formation and Release of Radioactive Particles. Uranium-containing particles that were analyzed included differing amounts of fission products. Those associated with the particle shown in Figure 4A were barely detectable by ordinary γ spectroscopy techniques. This is expected for particles composed only of fuel material without additional adsorbed fission products. For example, a particle

of Chernobyl reactor fuel 5 μm in diameter would only contain 10 Bq of ^{144}Ce and 20 Bq of ^{95}Zr at the time of release. Other uranium particles analyzed apparently contained several hundred becquerels of γ -emitting fission products and activation products, although we cannot exclude the possibility that other types of particles were also present in these same wood samples (e.g., particles having less than 1% fission products by mass would not have been identified as Chernobyl fuel particles even though they would contain significant amounts of fission product radioactivity). However, spectra accumulated by using the EDXA system to detect X-rays produced only by the radiations emitted from within the particles (i.e., without electron beam excitation) clearly showed uranium lines. Thus, significant amounts of fission products must have been intimately associated with the uranium particles, probably condensed on the particle surfaces.

Van der Veen et al. (4) analyzed a single radioactive particle from Chernobyl that was 125 μm in diameter. It contained 0.07 Bq of $^{239,240}\text{Pu}$ and other α -emitting radionuclides; this led the authors to conclude that it was composed of uranium fuel. However, a Chernobyl fuel particle of that size should contain ~ 230 Bq of $^{239,240}\text{Pu}$, assuming uniform distribution of the plutonium in the irradiated fuel. If the particle was derived from the uranium fuel, plutonium isotopes must have migrated out of the uranium before or during particle formation.

All observations regarding uranium particles suggest that they were likely released by fuel comminution. Most of the particles had sharp edges. Occasionally, rounded particle fragments were observed, suggesting that some fuel melting had occurred. Many uranium particles contained measurable amounts of fission products, whereas others did not. Fission products were mainly refractory radionuclides that probably condensed on surfaces of uranium particles at the time of their release. Thus, interior volumes of particles may be depleted of fission products, perhaps even plutonium, due to their migration in the uranium fuel under high temperatures.

Samples of airborne radioactivity collected at different locations throughout Europe varied in radionuclide composition (5-9). Radioisotopes of iodine, tellurium, ruthenium, cesium, and barium were commonly found. In many cases, more than half of the radioiodine was in vapor form. Some individual particles were found to contain only one or two predominant radioactive elements. These were ^{103}Ru and ^{106}Ru - ^{106}Rh , ^{140}Ba - ^{140}La , ^{134}Cs and ^{137}Cs - ^{137}Ba , ^{141}Ce and ^{144}Ce - ^{144}Pr , or U and U plus Zr (1, 2, 5, 10, 11).

The particle described above (Figure 5a) as being mainly composed of Ce and La was ~ 5 μm in diameter and contained 40 Bq of ^{144}Ce - ^{144}Pr at the time of its release. Because we estimate that the specific activity of ^{144}Ce - ^{144}Pr in the reactor core was $\sim 1.6 \times 10^{13}$ Bq/g of cerium, the total mass of cerium in the particle could be no more than 2.5×10^{-12} g. Also, if the particle density was between 2 and 7 g/cm³, then the masses of cerium and lanthanum identified by EDXA could only account for 1-4% of the total particle mass. Therefore, the bulk of the particle must have been composed of another material, such as carbon, not detected by EDXA analysis.

The observation in this and other studies that individual particles may contain only one or a few radioactive elements is of interest with respect to the mechanisms for their formation. Some aspects of particle formation in high-temperature processes have been studied in experiments with molten reactor fuel and coal combustion aerosols (12-14). Temperatures in excess of 1500 $^{\circ}\text{C}$ were used. The more volatile chemical elements were generally found

to be enriched among small particles, suggesting that vaporization and condensation were important mechanisms for their release and particle formation. With aerosols resulting from combustion of pulverized coal, the volatile elements mainly condensed onto particles of aluminosilicate which constitute a major portion of the ash in the effluent stream.

After the initial explosion, the most likely processes that led to formation of particles containing only a few radionuclides are vaporization and condensation. Highly volatile radionuclides were probably released first and may have dispersed widely in the environment before condensing onto ambient particles. These particles may have come from any source and were small enough to disperse worldwide. The more refractory radionuclides would have volatilized at higher temperatures and condensed onto particles in the immediate vicinity of the reactor core. These particles were most likely the products of high-temperature reactions with the reactor structures, carbon, soil, and uranium. Because vaporization and condensation of individual radionuclides depend highly upon temperature, only radionuclides that have similar vapor pressures were likely to be associated with the same particles.

Radiation Dose to Exposed People. The above information on radioactive aerosols released from the Chernobyl nuclear reactor can be used to estimate radiation doses to people who were nearby during and after the accident. The dose estimates that follow are based on data obtained in this study and data from published reports.

Relative amounts of selected fission products in the Chernobyl reactor core, in the air above the reactor (an average over the period of April 26 to May 5) and on soil (collected on May 17) at 30 km from Chernobyl are shown in Figure 8. Fission products present in the environmental samples, but absent from the particles analyzed in this study, are ^{131}I and ^{140}Ba - ^{140}La . These radionuclides were abundant in irradiated reactor fuel and in the environmental release; they also have sufficiently long half-lives to be detected in our samples. Therefore, most of the released ^{131}I and ^{140}Ba could not have been incorporated into large insoluble particles. In fact, a large portion of the radioiodine was reported to be in vapor form (5, 6) and was absent from other analyses of radioactive particles (10, 11). Highly radioactive particles containing the more refractory radionuclides (^{95}Zr - ^{95}Nb , ^{103}Ru , ^{106}Ru - ^{106}Rh , ^{141}Ce , and ^{144}Ce - ^{144}Pr) still persist on the ground near Chernobyl. Such particles were rarely observed in significant amounts outside of the USSR. Most of these particles are large, between 1 and 10 μm in diameter. If inhaled, particles in this size range would mainly deposit in the upper respiratory tract. However, the number of particles characterized in this study is not adequate to define the size distribution of aerosols that was inhaled by people.

Very limited information is currently available on the amounts of radionuclides that were actually inhaled by workers at the reactor site (1). Also, it is uncertain if all of the emergency workers wore respiratory protection. However, it appears that ^{131}I and ^{137}Cs - ^{137}Ba were the main contributors to doses from internally deposited radionuclides. These must have been in vapor form or in very soluble forms associated with particles that deposited in the upper respiratory tract. Other less soluble radionuclides that were in the same atmosphere were not found in large quantities in the lung or other internal body organs. Further information on these exposures would be very useful.

Several estimates of the magnitudes of radiation doses to people at different geographic locations have been re-

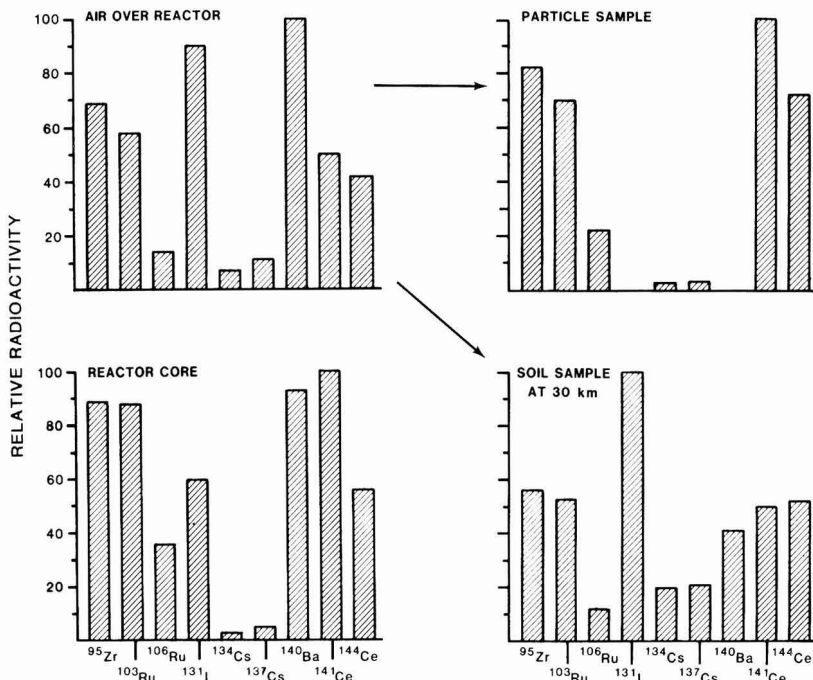


Figure 8. Histograms of selected fission product radioactivity in the Chernobyl reactor core and in samples of nearby air and soil (compiled from ref 1 and this report).

ported (1, 2, 6, 8, 9). In general, estimates suggest that the lifetime whole-body effective radiation doses from internally deposited radionuclides were about equal to the doses derived from external irradiation due to radioactivity deposited on ground surfaces. However, such calculations depend heavily on the dosimetry model assumptions, for example, pathways for ingestion, inhaled particle characteristics, shielding factors used in external dose calculations, and the related steps taken to reduce exposures. Average whole-body doses estimated for people in western Europe are less than 1 cGy; those to people who were within 30 km of Chernobyl were estimated to be about 3–50 cGy. Thus, except for a few people who were very close to the reactor (many actively engaged in controlling the accident), the radiation exposures were small and not likely to add significantly to an individual's total health risk. Taken collectively, the total radiation dose to the population of the northern hemisphere was significant, and it has been estimated that 0–30 000 additional cases of cancer may result (2). However, the high end of this range only represents a 0.4% increase over the current spontaneous cancer rate and this is never likely to be detected. About 40% of the added cancers were predicted to occur in people who were in the European part of the USSR at the time of the Chernobyl reactor accident.

Conclusions

The major γ -emitting radionuclides associated with particles released from the Chernobyl nuclear reactor accident and deposited on a nearby wood surface were ⁹⁵Zr–⁹⁵Nb, ¹⁰³Ru, ¹⁰⁶Ru–¹⁰⁶Rh, ¹³⁴Cs, ¹³⁷Cs–¹³⁷Ba, ¹⁴¹Ce, and ¹⁴⁴Ce–¹⁴⁴Pr. Scanning electron microscopic and X-ray analyses revealed a variety of particle morphologies and the presence of uranium, carbon, cerium and lanthanum, or zirconium. An in vitro dissolution assay demonstrated that particles were relatively insoluble. If similar particles were inhaled by people near the accident site, we concluded

that the major portion of the radiation dose would be to lung.

Acknowledgments

We gratefully acknowledge the assistance of W. Jacobi of the GSF in Munich, FRG, for providing the sample of radioactive particles analyzed in this study and the helpful comments of R. O. McClellan, B. B. Boecker, F. A. Seiler, and M. D. Hoover of the Inhalation Toxicology Research Institute in the preparation and review of this manuscript. Also, M. F. Conrad, S. A. Likens, P. C. Lawson, R. A. Smith, and R. W. Norgan provided valuable assistance in the preparation of samples for autoradiography, electron microscopy, γ spectroscopy, and particle dissolution measurements.

Registry No. U, 7440-61-1; C, 7440-44-0; Ce, 7440-45-1; La, 7439-91-0; Al, 7429-90-5; Si, 7440-21-3; Ca, 7440-70-2; P, 7723-14-0; Cl, 7782-50-5; Zr, 7440-67-7; ¹⁴¹Ce, 13967-74-3; ¹⁴⁴Ce, 14762-78-8; ¹⁴⁴Pr, 14119-05-2; ¹⁰³Ru, 13968-53-1; ¹⁰⁶Ru, 13967-48-1; ¹⁰⁶Rh, 14234-34-5; ¹³⁴Cs, 13967-70-9; ¹³⁷Cs, 10045-97-3; ¹³⁷Ba, 13981-97-0; ⁹⁵Zr, 13967-71-0; ⁹⁵Nb, 13967-76-5.

Literature Cited

- (1) USSR State Committee on the Utilization of Atomic Energy. The Accident at the Chernobyl Nuclear Power Plant and Its Consequences. Information compiled for the IAEA Experts Meeting in Vienna, Austria, August 25–29, 1986.
- (2) Committee for the Assessment of Health Consequences in Exposed Populations. Health and Environmental Consequences of the Chernobyl Nuclear Power Plant Accident. Report to the U.S. Department of Energy Office of Health and Environmental Research from the Interlaboratory Task Group on Health and Environmental Aspects of the Soviet Nuclear Accident, June 1987.
- (3) Kanapilly, G. M.; Raabe, O. G.; Boyd, H. A. In *Proceedings of the Third International Congress of the Radiation Protection Association*, CONF-730907, Washington, DC, September 9–14, 1973; p 1237.

- (4) Van Der Veen, J.; Van Der Wijk, A.; Mook, W. G.; De Meijer, R. J. *Nature (London)* 1986, 323, 399.
- (5) Devell, L.; Tovedal, H.; Bergstrom, U.; Appelgren, A.; Chyssi, J.; Andersson, L. *Nature (London)* 1986, 321, 192.
- (6) Fry, F. A.; Clarke, R. H.; O'Riordan, M. C. *Nature (London)* 1986, 321, 193.
- (7) Hohenemser, C.; Deicher, M.; Ernst, A.; Hofsass, H.; Lindner, G.; Recknagel, E. *Environment* 1986, 28, 7.
- (8) Institut für Strahlenschutz der Gesellschaft für Strahlen- und Umweltforschung. Umweltradioaktivität und Strahlenexposition in Südbayern durch den Tschernobyl-Unfall. München-Neuherberg, West Germany, 1986.
- (9) Commissariat à l'Énergie Atomique, Institut de Protection et de Sureté Nucleaire. The Tschernobyl Accident. IPSN Report No. 2/86, 1986.
- (10) Raunemaa, T.; Lehtinen, S.; Saari, H.; Kulmala, M. *J. Aerosol Sci.* 1987, 18, 693.
- (11) Balashazy, I.; Szabadine-Szende, G.; Lörinc, M.; Zombori, P. Gamma-Spectrometric Examination of Hot Particles Emitted During the Chernobyl Accident. Hungarian Academy of Sciences, Central Research Institute for Physics, KFKI-1987-24/K, 1987.
- (12) Powers, D. A. Aerosol Generation During Core Debris/Concrete Interactions. Seventh International Light Water Safety Research Information Exchange Meeting, Gaithersburg, MD, 1978.
- (13) Powers, D. A. Phenomena of the Ex-vessel Source Term. Proceedings of an International Symposium on Source Term Evaluation for Accident Conditions, International Atomic Energy Agency, Vienna, 1986.
- (14) Damle, A. S.; Ensor, D. S.; Ranade, M. B. *Aerosol Sci. Technol.* 1982, 1, 119.

Received for review January 14, 1988. Revised manuscript received July 7, 1988. Accepted July 29, 1988. This work was supported by the U.S. Department of Energy's Office of Health and Environmental Research under Contract DE-AC04-76EV01013.

Increases in the Polynuclear Aromatic Hydrocarbon Content of an Agricultural Soil over the Last Century

Kevin C. Jones,^{*†} Jennifer A. Stratford,[†] Keith S. Waterhouse,[†] Edward T. Furlong,[‡] Walter Giger,[§] Ronald A. Hites,[‡] Christian Schaffner,[§] and A. E. Johnston^{||}

Institute of Environmental and Biological Sciences, University of Lancaster, Bailrigg, Lancaster LA1 4YQ, UK, School of Public and Environmental Affairs and Department of Chemistry, Indiana University, Bloomington, Indiana 47405, Swiss Federal Institute for Water Resources and Water Pollution Control (EAWAG), Swiss Federal Institute of Technology, CH-8600 Dubendorf, Switzerland, and Department of Soils and Plant Nutrition, Rothamsted Experimental Station, Harpenden, Hertfordshire AL5 2JQ, UK

■ Soil samples collected from Rothamsted Experimental Station in southeast England at various times since the mid-1800s and up to the present have been analyzed recently for polynuclear aromatic hydrocarbons (PAHs). All the soils were collected from the plough layer (0-23 cm) of an experimental plot for which atmospheric deposition will have been the only source of PAH input. The total PAH burden of the plough layer has increased approximately 4-fold since the 1880/1890s, with some compounds (notably, benzo[b]fluoranthene, benzo[k]fluoranthene, benzo[a]pyrene, benzo[e]pyrene, pyrene, benzo[a]anthracene, and indeno[1,2,3-cd]pyrene) showing substantially greater increases. Average rates of increase for individual PAHs in the Rothamsted plots over the century since 1880/1890 are similar to contemporary atmospheric deposition rates to semirural locations. Regional fallout of anthropogenically generated PAHs derived from the combustion of fossil fuels will be the principal source of PAHs to the Rothamsted soils. It is suggested that the increases in soil PAHs observed this century at Rothamsted are representative of those likely for agricultural soils in many industrialized countries or regions.

Introduction

Previous studies have examined the temporal trends in environmental PAHs, but these have used dated marine and freshwater sediment cores as the sampling medium, with the majority of work undertaken in the United States and mainland Europe (1-11). In general, these studies

have found (i) an increasing sediment PAH burden since the mid-1800s, with a peak in the 1950/1960s, and (ii) a constant qualitative PAH pattern for most of the locations studied, with an increase in PAH abundance near urban centers. These observations, and other studies, have pointed to anthropogenic combustion of fossil fuels as the major source of environmental PAHs and to the significance of long-range atmospheric processes in dispersing PAHs through the environment (12, 13).

This paper describes changes in the polynuclear aromatic hydrocarbon (PAH) content of soils collected from the same experimental plot between the mid-1800s and the present day. All the samples analyzed here originate from the Broadbalk Experiment, which has been under continuous arable cultivation since 1843 at the Rothamsted Experimental Station, a semirural location in southeast England. The experiment was initiated to measure the effects of N, P, K, Na, and Mg, applied singly and in various combinations, on yields of winter wheat. However, one plot (i.e., the "control") has not received any additions of soil fertilizers or amendments. Therefore, by comparing the chemical composition of archived soils from this plot with that of recent samples the significance of atmospheric inputs can be determined. Previous publications have reported temporal trends in the elemental composition of this and other soils at Rothamsted, due to both atmospheric and treatment inputs (14-17).

This is the first study to investigate long-term changes in the atmospheric fallout of PAHs by using archived soils as the sampling medium. There are several advantages to this approach as opposed to using sediment cores. First, the sampling dates are known with certainty and the samples have been undisturbed since collection and preparation for storage. Second, the control plots at Ro-

[†]University of Lancaster.

[‡]Indiana University.

[§]Swiss Federal Institute of Technology.

^{||}Rothamsted Experimental Station.

thamsted will *only* have received inputs via the atmosphere, whereas the interpretation of some sediment cores may be confused by additional inputs of runoff from the surrounding catchment (1, 6, 8, 18). Third, the soils will have received inputs *directly* from the atmosphere, while material deposited in sediments may have undergone chemical/physical changes during passage through the water column and received additional inputs of biogenic PAHs (7, 19, 21). Two further differences should be realized—the potential for direct atmosphere–soil exchange of PAHs via the vapor phase prior to sampling, and photolysis of PAHs adsorbed to particulates at the soil surface. Once in storage, however, photolytic and microbial degradation is likely to have been minimal, as the samples were kept air-dried in the dark at room temperature in sealed glass containers.

In addition to using these samples as an historical monitoring tool, there is another purpose to the investigation of PAHs in soils. Dietary intake has been identified as the principal route of human exposure to PAHs for nonsmokers (22), with plant-based foodstuffs constituting roughly 50% of the total PAH intake in a typical United Kingdom diet (23). While it is likely that the majority of PAHs associated with crop plants result from direct atmospheric deposition and soil splash onto the leaves and shoots (24) or are introduced in the preparation and cooking of foods, uptake of PAHs via the root system has been reported (25–27). Adsorption of PAHs from the vapor phase may also be important.

Materials and Methods

Sampling and Sample Storage. Rothamsted (grid reference TL 120137) is a “semirural” location in western Europe. It lies 42 km north of central London and within 2 km of the major A5, A6, and M1 trunk roads, although the surrounding area is primarily agricultural. All the soils sampled for this study were from the control of “nil treatment” plot of the Broadbalk Experiment, which has been under continuous winter wheat since 1843 (28). These soils are neutral or slightly calcareous silty clay loams (Batcombe series), containing about 20–30% clay and 0.9–1.1% C, composed primarily of quartz and calcite with smaller amounts of illite, kaolinite, chlorite, and sanidine. All the samples analyzed relate to the 0–23-cm layer, which is the cultivated plough layer for this arable experiment.

All soils had been air-dried and ground in the same iron pestle and mortar after collection and passed through <2-mm sieves. This procedure is unlikely to contaminate the soils during processing. The samples were subsequently stored in glass jars with cork lids to the present day in a dark room at ambient temperatures. For this study samples from the years 1846, 1881, 1893, 1914, 1944, 1956, 1966, 1980, and 1986 were taken from the archive, transferred to acetone/hexane-rinsed glass jars sealed with similarly rinsed aluminum foil, and then ground in an agate tema mill to produce a fine powder.

Analytical Methods. For comparative purposes, and to improve the reliability of the data, two different laboratories analyzed samples for PAHs. Both used established procedures to analyze a selection of the soils. Method I was a capillary gas chromatography–mass spectrometry technique and was applied to two separate soil subsamples (extractions I and II). Method II used a capillary GC separation and detection by flame ionization. Both methods were used on the 1846 sample; samples from 1881, 1914, 1956, and 1980 were analyzed by method I. Method II was used for the 1893, 1944, 1966, and 1986 samples. The compounds analyzed are listed in Table I. All PAHs

measured have previously been identified as combustion-derived atmospheric particulate components, although perylene is more commonly considered a natural diagenetic product in special environmental contexts, i.e., recent sediments.

Method I. The samples were analyzed by a procedure similar to that described by Gschwend and Hites (10). Dry soil (12–16 g) was loaded into solvent-rinsed, glass wool lined glass thimbles (all glassware used in the procedure was prerinsed with redistilled solvents—which were also used throughout the analyses). Prior to extraction, the soils were spiked with an eight-component mixture of deuteriated PAHs. The soils were sequentially Soxhlet extracted, first with 2-propanol for 24 h; then a second flask containing dichloromethane was switched with the 2-propanol flask and extraction continued for a second 24 h. After being cooled, extracts were reduced with a rotary evaporator and combined. Combined extracts were desulfured on an activated copper column and then reduced in volume and charged to a 20-g column of 5% deactivated silica gel. A 40-mL aliquot of hexane was passed through the column and discarded. PAHs were then eluted in two fractions, the first fraction 50 mL of 15% dichloromethane in hexane, the second fraction 50 mL of pure dichloromethane. These two fractions were collected, combined, reduced, and stored below freezing in amber glass vials with Teflon-lined caps. Samples were held no longer than 2 weeks prior to analysis.

PAH analysis was performed by selective ion monitoring with a Hewlett-Packard 5995 GC/MS system. Separation was achieved with a Hewlett-Packard HP-5 fused silica capillary column (liquid phase cross-linked 5% phenyl methyl silicone; column dimensions, 25 m × 0.32 mm i.d. × 17 μm film thickness). Temperature programming used to achieve separation was 40 °C for 4 min, then temperature increasing at 4 °C min⁻¹, and ending at 280 °C and holding for 30 min. The mass spectrometer was operated in the EI mode, with selected ion monitoring for expected PAH and their deuteriated analogues.

PAH concentrations were calculated from measured amounts of added internal standard deuteriated PAH and response factors calculated for a wide range of PAH to deuteriated PAH ratios (100:1 PAH to DPAH to 1:100 PAH to DPAH).

Duplicate analyses of PAHs were performed on two subsamples. This method has been previously used on replicate sediment samples, and the 95% confidence limit for all PAH averages 12% around the mean (29). The confidence limit is slightly higher for higher molecular weight compounds (at worst, 30% for benzo[e]pyrene). This method was also tested by analyzing a United States National Bureau of Standards (NBS) urban air particulate reference material (NBS standard reference material no. 1649). Concentrations for phenanthrene, fluoranthene, pyrene, chrysene, benzo[a]pyrene, and benzo[ghi]perylene were within the certified NBS limits.

Method II. Samples were analyzed by a procedure similar to that described by Giger and Schaffner (30). Dry soils (26–40 g) were Soxhlet extracted with dichloromethane. The extracts were concentrated in a rotary evaporator at room temperature, after which elemental sulfur was removed by percolation through a column of activated copper. This eluate was evaporated, dissolved in a minimum quantity of benzene/methanol (1:1), and subjected to gel permeation chromatography (Sephadex LH-20). The same solvent mixture was used to elute two 50-mL fractions. Another 50 mL was then used to flush the column before applying the next sample. Both frac-

Table I. List of Abbreviations Used in Broadbalk PAH Analyses

abbrev	full name
Phenan	phenanthrene
Anthrac	anthracene
Fluoran	fluoranthene
Pyrene	pyrene
B[a]anth	benzo[a]anthracene
Chrysene	chrysene (plus coeluting triphenylene)
B[e]P	benzo[e]pyrene
B[a]P	benzo[a]pyrene
Pery	perylene
Anthan	anthanthrene
B[ghi]Py	benzo[ghi]perylene
B[b]Fln	benzo[b]fluoranthene
B[k]Fln	benzo[k]fluoranthene
Napth	naphthalene
Acenaphthyl	acenaphthylene
Acenaphth	acenaphthene
Fluor	fluorene
Dibenzo	dibenzothiophene
4H-Cyclo	4H-cyclopenta[def]phenanthrene
Indeno	indeno[1,2,3-cd]pyrene
Coro	coronene
B.fln	benzfluoranthenes

tions were cautiously evaporated to dryness (rotary evaporator, reduced pressure, ~30 °C), taken up in 1 mL of *n*-pentane, and applied to silica gel columns. A 25-mL volume of pentane and 25 mL of dichloromethane yielded two eluates of low and medium polarity, respectively, the latter containing the PAH fraction. For GC analyses, the samples were concentrated at room temperature in a stream of nitrogen to volumes of 0.1–0.2 mL. The internal standard (1-chlorotetradecane) was added as a hexane solution yielding a concentration of 1–10 µg of internal standard per sample.

Gas chromatography was performed on a Carlo Erba apparatus (Model 2101 AC) with a flame-ionization detector. A 20 m × 0.3 mm glass capillary column with an SE-52 stationary phase was used for the separations. Aliquot samples of 1–2 µL were injected without stream splitting. The injector temperature was held at 270 °C. Hydrogen was used for carrier gas. The GC procedures

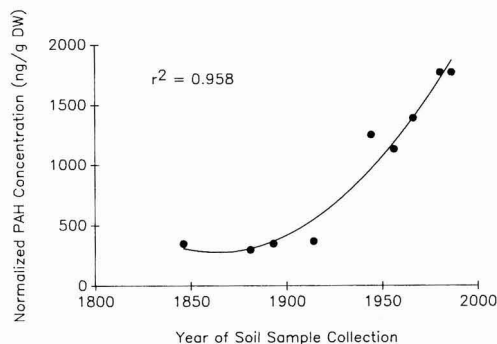


Figure 1. Temporal trends in soil plough layer PAH content at Broadbalk, Rothamsted. Two methods of analysis were used. Each data set normalized against the most recent sample analyzed in each batch. Σ PAHs (7) from Table III are plotted.

followed those described by Grob and Grob (31). Electronic integration of the gas chromatographic peak areas was performed by a digital integrator (Minigrator, Spectra-Physics). A Finnigan GC/MS system (Model 1015D) combined with an on-line computer (Model 6000) was used for mass spectrometric identification and mass chromatography.

Results and Discussion

Comments on the Comparability of Data between Methods. The compounds analyzed by methods I and II (or both) are detailed in Table I. Data for all the soils analyzed by both procedures are given in Table II. The data are presented to show all the compounds analyzed by both techniques and the “total PAH” content of each soil. This allows a direct comparison between both data sets. Both methods were applied to the 1846 sample and indicate good general agreement between the procedures. Although the *absolute* values for individual PAHs differed, the temporal trends for the five samples analyzed by method I and the five analyzed by method II show excellent agreement. This is most clearly illustrated in Figure 1, where both data sets for Σ PAHs have been normalized

Table II. Summary of Broadbalk PAH Values (ng g⁻¹ Dry Weight)

	1846 ^{a,b}	1881 ^a	1893 ^b	1914 ^a	1944 ^b	1956 ^a	1966 ^b	1980 ^a	1986 ^b
Phenan	46	68	45	89	110	120	160	140	48
Anthrac	4.5	13	9		4	10	9	13	11
Fluoran	39	45	43	37	120	190	120	210	120
Pyrene	19	14	7	11	50	120	75	150	99
B[a]anth	22	9.4	3	5.9	25	69	26	110	56
Chrysene	24	16	11	18	50	87	41	120	78
B[e]P	24	13	7	11	35	65	27	130	53
B[a]P	18	6.7		12	23	73	28	120	72
Pery	2.2	0.86			<3	15	9	18	14
Anthan	1.2	0.12				1.2		2.9	
B[ghi]Py	22	8.3		6.1		55		66	
B[b]Fln	18	12	9	86	35	76	30	220	58
B[k]Fln	17	8.4	9	6.2	35	73	30	250	58
Napth	39	38		53		28		23	
Acenaphthyl	1.6	0.73				3.4		5.0	
Acenaphth	2.0	0.9		2.0		4.2		6.0	
Fluor	0.78					3.7		9.7	
Dibenzo	6.2	6.8		6.6		11		32	
4H-Cyclo	14	19		4.9		15		22	
Indeno	23	14	5	12	31	92	29	100	63
Coro	7.1	5.4	3	5.4	9	18	9	22	17
total	350	300	150	370	530	1130	590	1770	750
normalized total	350	300	(350)	370	(1250)	1130	(1390)	1770	(1770)

^a Measured in duplicate by method I. ^b Measured by method II.

(Table II) with respect to the most recent sample analyzed by each method (i.e., method I, 1980; method II, 1986). Absolute values and trends for individual PAHs can also be compared in Table II. Both methods give similar concentration rankings for the compounds analyzed. For example, in the 1846 sample phenanthrene, fluoranthene, and benzofluoranthenes are the most abundant. For the later (1980, 1986) samples, of the compounds analyzed by both methods, the trends were as follows.

Method I: B[b]fln Fluoran B[e]P B[a]P Pyrene Chrysene Phenanthranth Pery Anthrac.

Method II: Fluoran B.Fln Pyrene Chrysene B[a]P B[a]anth B[e]P Phenanthranth Pery Anthrac.

Temporal Trends in Soil PAH. The soil plough layer PAH burden at Broadbalk has increased roughly 4–5-fold between 1880 and 1890 and the present (Table II, Figure 1). It should be stressed that the Broadbalk control plot will *only* have received PAH inputs via the atmosphere (i.e., not through the deliberate or accidental addition of amendments to the soil) and that the plot is not near to a local point source of PAHs. In fact, Rothamsted is situated in a semirural location surrounded by agricultural land, but with the small town of Harpenden ~2 km away and industrial conurbations approximately 40 km to the south (London) and 100 km to the north (Birmingham). Winds are predominantly from the southwest.

Samples collected prior to 1865 at Rothamsted were not processed and stored in the same way as those taken subsequently; pre-1865 samples were not air-dried and sieved, thereby allowing microbial activity to continue during sample storage. Consequently, samples taken earlier than this date have often yielded anomalous results in previous studies on the macronutrient (principally N) content of the Broadbalk soils (32), despite the pre-1865 samples being reprocessed (i.e., dried and sieved) in the late 1860s. Our data also yield rather surprising results for the 1846 sample, in that its total PAH content is higher than that measured in later samples from 1881 and 1893. On the basis of the evidence of dated lake sediment cores collected in mainland Europe and the United States, (3, 9) one would expect an increase in the atmospheric deposition of PAHs through the late 1800s, following increases in the level of industrialization and therefore in anthropogenically derived combustion products emitted to the atmosphere. For the remainder of this discussion we will therefore treat the 1846 data as anomalous and consider the trends revealed in the century since the 1880/1890s.

The total PAH data (Figure 1) indicate a continued steady increase in the soil plough layer PAH burden at Broadbalk, with a slight reduction in the rate of increase suggested by the values from method II between 1966 and 1986. This is of interest, in that the marked post-1950s' decreases in the deposition flux of PAHs to both lacustrine and marine sediments that have been observed in North America (9, 10) and mainland Europe (1, 2) are not observed in this soil time series. However, without corroborating evidence, this should not be interpreted as indicative of a significantly different atmospheric PAH history for the United Kingdom. This is especially true when the variability in PAH deposition and other uncertainties are considered.

Other studies have pointed to anthropogenic combustion of fossil fuels as the major source of environmental PAHs and to the significance of long-range processes in dispersing PAHs through the environment (12, 13). It is therefore of interest to compare the rate of increase in soil PAHs at Rothamsted since 1880/1890 with the known history

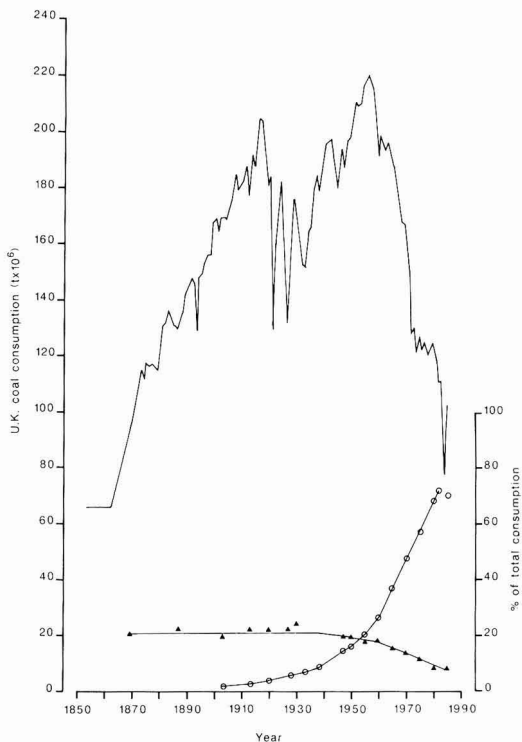


Figure 2. United Kingdom coal consumption between the mid-1800s and the present day. Also shown are the percentage of total consumption used domestically (▲) and for electricity generation (O).

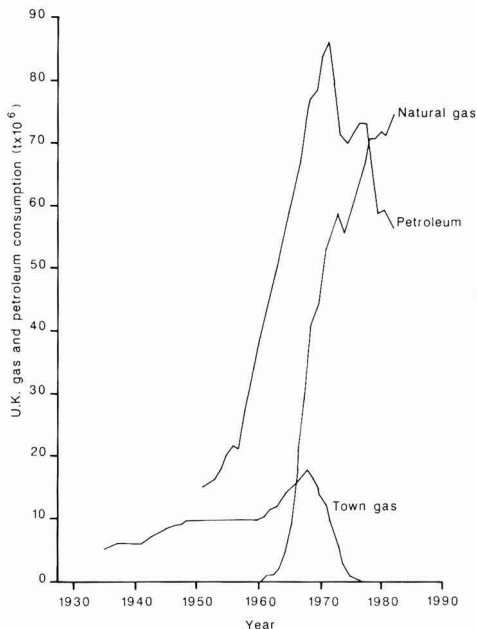


Figure 3. United Kingdom gas and petroleum consumption since the early to mid-1900s to the present day.

of fossil fuel consumption in the United Kingdom. Figure 2 shows United Kingdom coal consumption between the mid-1800s and the present with data collated from several

Table III. Calculated Fluxes of PAHs to Broadbalk Soils. Data between 1881 and 1980 (Method I)

compd	flux rate, mg m ⁻² year ⁻¹	compd	flux rate, mg m ⁻² year ⁻¹
Phenan	0.20	B[b]Fln	0.67
Anthrac	0	B[k]Fln	0.68
Fluoran	0.46	Napth	
Pyrene	0.40	Acenaphthyl	0.12
B[a]anth	0.29	Acenaphth	0.01
Chrysene	0.30	Fluor	
B[e]P	0.38	Dibenzo	0.07
B[a]P	0.36	4H-Cyclo	0.01
Pery	0.05	Indeno	0.25
Anthan	0.10	Coro	0.05
B[ghi]py	0.16	Total PAH flux	4.56

Table IV. General Classification of 1980-1986:1880-1890 Ratios for Individual PAH Compounds in Broadbalk Soils

ratio	compd
>15	B[b]fln, B[k]fln, B[a]P
10-15	Pyrene, B[a]anth, B[e]P, Indeno
5-10	Chrysene, B[ghi]py, Acenaphthyl, Acenaphth
<5	Phenan, Anthrac, Fluoran, Napth, Dibenzo, 4H-Cyclo, Coro

sources (33-35) and distinguishes between the percentage of total consumption used domestically (i.e., many small PAH sources) and for electricity generation (few large-scale PAH emissions). Figure 3 presents data on the consumption of petrol and gas (36).

Data from Table II have been used to calculate annual rates of increase in soil PAHs at Broadbalk. The plough layer at Broadbalk contains 2870 t of soil ha⁻¹, so the changes in soil PAH concentration with time can readily be converted to a flux (mg of PAH m⁻² year⁻¹). The data are presented in Table III and are the average rates of change over the hundred or so years since 1880/1890. It should be noted, however, that deposition fluxes to the soil are likely to have altered during this time. Fluxes for individual PAH compounds vary between 0.01 and 0.67 (mean 0.21) mg m⁻² year⁻¹, the most abundant of which are benzo[b]fluoranthene, benzo[k]fluoranthene, fluoranthene, pyrene, benzo[e]pyrene, benzo[a]pyrene, benzo[a]anthracene, and phenanthrene. These fluxes are within the range observed in lacustrine sediments from rural United States sites (29, 37).

Losses of PAHs from the soil system are possible through microbial breakdown, photooxidation, volatilization, crop uptake, and leaching. The rates of increase in soil PAH at Broadbalk are therefore not necessarily equivalent to deposition fluxes to the soil. However, it is worth comparing the rates of increase with deposition flux data reported for other locations. Remote sites in the United States consistently have present-day deposition rates for individual PAHs of ~0.1 mg m⁻² year⁻¹; sites located nearer to urban centers have much greater current inputs (average of 0.35 mg m⁻² year⁻¹) (10). This further suggests that Rothamsted now receives substantial inputs of anthropogenically derived ΣPAHs as fallout from the increased number of urban/industrial conurbations that have started or been expanded since the 1950s. This may explain the continued, post-1950s' increase in soil PAH shown in Figure 1. Another possible source of PAHs to Rothamsted soils is localized fallout from stubble burning, a practice that is commonly adopted in the United Kingdom, but not on the Station's experimental plots. The importance of PAH inputs to soils from this source is unknown (38).

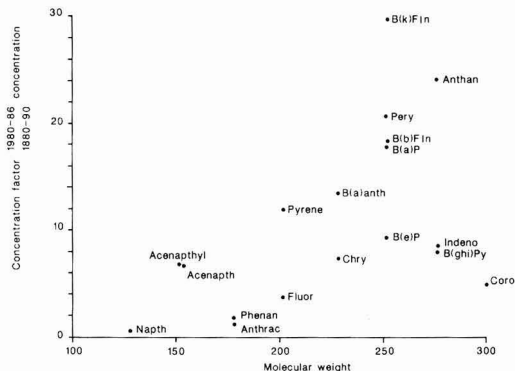


Figure 4. Concentration factor versus molecular weight for the Broadbalk PAH data.

Table V. Selected PAH Ratios for the Broadbalk Soils

soil sample year	Phenan/Anthrac	Fluoran/Pyrene	B[a]anth/Chrysene	B[e]P/B[a]P
(a) Method I				
1846	15	1.5	1.0	1.5
1881	5.3	3.1	0.60	1.9
1914	NA	3.4	0.33	0.61
1956	12	1.5	0.79	0.88
1980	11	1.3	0.93	1.1
(b) Method II				
1846	5	3.9	0.68	1.2
1893	5	6.1	0.27	NA
1944	27	2.4	0.5	1.5
1966	18	1.6	0.63	0.96
1986	4.4	1.2	0.72	0.74

Trends in Individual PAHs. Although the total PAH soil plough layer burden has increased approximately 4-5-fold since 1880/1890, some individual PAH compounds have shown substantially greater increases (Table IV). Most notable in this regard are some of the more abundant PAHs—benzo[b]fluoranthene, benzo[k]fluoranthene, benzo[a]pyrene, benzo[e]pyrene, pyrene, and benzo[a]anthracene. Others have shown virtually no change with time. Naphthalene, the compound with the lowest boiling point, has shown a decline with time; this most probably reflects losses via the vapor phase during sample processing and storage. Molecular weight (among other factors) is important in influencing the size of the soil concentration increase shown by each PAH compound (i.e., 1980/1986 compound concentration:1880/1890 compound concentration) (Figure 4). Microbial breakdown and soil retention of PAHs are both known to depend on the compound's structure, while volatilization losses will be greater for low molecular weight compounds (39).

Some workers have suggested that individual PAH compounds can be used as "indicators" of particular combustion processes or fuels. Coronene emissions are relatively high from vehicle emissions, while benzo[a]pyrene and benzo[e]pyrene are often associated with coal combustion. Another approach has been to use the ratio of selected individual PAHs to reflect fractionation between compounds with relatively similar physical and chemical properties. This minimizes artificial ratio variations due to differences between individual analyses, and the data thus produced have previously been used to distinguish between routes of PAH transport to sediments, i.e., atmospheric or via catchment runoff. Table V presents data on PAH compound ratios based on the approach of Gschwend and Hites (10). With the exception of one ratio

(Table Vb, 1893, fluoranthene to pyrene ratio of 6:1), fluoranthene to pyrene and benzo[e]pyrene to benzo[a]pyrene ratios observed in Broadbalk soil samples all fall within the range observed in lake sediments, remote from PAH sources (29, 40). Isomer ratios were examined to minimize differences due to volatility or analytical variation (10). Elevated phenanthrene to anthracene and benzo[e]pyrene to benzo[a]pyrene are probably due to the greater photochemical reactivities of anthracene and benzo[a]pyrene on air particulates or fly ash (13). All ratios observed in Broadbalk soils suggest PAH sources that are dominated by coal combustion (10). It should be borne in mind, however, that PAH compound ratios can only be used to give general indications as to the predominance of certain combustion processes. They are probably insufficiently sensitive to be used to monitor changes in the types of fossil fuel combustion and usage pattern in this data set.

Conclusions

The total PAH burden at Broadbalk in 1880/1890 was similar to that observed in contemporary remote locations in the United Kingdom (39). Data on the PAH content of contemporary soils for numerous locations varying between "remote" and "urban" have been published elsewhere (6, 25, 39, 41-44). On this basis, the contemporary total PAH content at Rothamsted lies well within the range between the two, indicating the semirural character of the Broadbalk plot. Other evidence for the applicability of this description to Rothamsted comes from the estimated PAH deposition fluxes (Table III) compared with current rates (10) and the calculated deposition fluxes of Cd at Broadbalk in relation to those reported for the United Kingdom and Europe as a whole (17). It therefore seems reasonable to postulate that the increases in plough layer PAH observed at Rothamsted can be generally extrapolated to many other areas. Indeed, agricultural soils in many parts of the industrialized world will have been subject to similar dramatic increases over the last century (39). Soils nearer to major conurbations may be expected to contain levels considerably above those at Rothamsted (39), as will soils near to point sources and those receiving PAH inputs in other forms (e.g., sewage sludge). Furthermore, atmospheric inputs are likely to remain fixed in the top few centimeters of undisturbed (i.e., unploughed) soils (43, 45), as opposed to the situation at Broadbalk where surface layer increases have been "diluted" through the 0-23-cm depth.

The rates of PAH input (i.e., atmospheric deposition) clearly exceed rates of output (microbial breakdown, photooxidation, vaporization, crop offtake, and leaching) at Broadbalk. The similarities between the average annual rates of increase in the soil PAH burden and the likely average atmospheric deposition flux at Rothamsted suggest that losses via these five possible mechanisms probably effectively remove only a relatively small proportion of the total annual input. This implies long residence times for PAHs in soils. It would clearly be useful to quantify inputs to and outputs from experimental plots to obtain data on present annual net changes in the soil PAH burden, thereby enabling predictions of future trends to be made. Biodegradative losses will be particularly important in this regard.

Intake of plant-based foodstuffs constitute a substantial proportion of ingested PAHs in the human diet. It is therefore also of importance to establish the significance of increases in soil PAHs on the composition of major foodstuffs. In this connection we will subsequently be presenting data on PAHs in grain samples harvested over

the last century from the Broadbalk plots (46).

Registry No. Phenanthrene, 85-01-8; anthracene, 120-12-7; fluoranthene, 206-44-0; pyrene, 129-00-0; benzo[a]anthracene, 56-55-3; chrysene, 218-01-9; triphenylene, 217-59-4; benzo[e]pyrene, 192-97-2; benzo[a]pyrene, 50-32-8; perylene, 198-55-0; anthanthrene, 191-26-4; benzo[ghi]perylene, 191-24-2; benzo[b]fluoranthene, 205-99-2; benzo[k]fluoranthene, 207-08-9; naphthalene, 91-20-3; acenaphthylene, 208-96-8; acenaphthene, 83-32-9; fluorene, 86-73-7; dibenzothiophene, 132-65-0; 4H-cyclopenta[def]phenanthrene, 203-64-5; indeno[1,2,3-cd]pyrene, 193-39-5; coronene, 191-07-1.

Literature Cited

- (1) Grimmer, G.; Bohnke, H. *Cancer Lett. (Shannon, Irel.)* 1975, 1, 75-84.
- (2) Grimmer, G.; Bohnke, H. Z. *Naturforsch., C: Biosci.* 1977, 32C, 703-711.
- (3) Hites, R. A.; Laflamme, R. E.; Farrington, J. W. *Science (Washington, D.C.)* 1977, 198, 829-831.
- (4) Muller, G.; Grimmer, G.; Bohnke, H. *Naturwissenschaften* 1977, 64, 427-431.
- (5) Laflamme, R. E.; Hites, R. A. *Geochim. Cosmochim. Acta* 1979, 42, 427-431.
- (6) Windsor, J. G.; Hites, R. A. *Geochim. Cosmochim. Acta* 1979, 43, 27-33.
- (7) Giger, W.; Schaffner, C.; Wakeham, S. G. *Geochim. Cosmochim. Acta* 1980, 44, 119-129.
- (8) Wakeham, S. G.; Schaffner, C.; Giger, W. *Geochim. Cosmochim. Acta* 1980, 44, 403-413.
- (9) Hites, R. A.; Laflamme, R. E.; Windsor, J. G.; Farrington, J. W.; Deuser, W. G. *Geochim. Cosmochim. Acta* 1980, 44, 873-878.
- (10) Gschwend, P. M.; Hites, R. A. *Geochim. Cosmochim. Acta* 1981, 45, 2359-2367.
- (11) Tan, Y. L.; Heit, M. *Geochim. Cosmochim. Acta* 1981, 45, 2267-2279.
- (12) Bjorseth, A.; Lunde, G.; Lindskog, A. *Atmos. Environ.* 1979, 13, 45-53.
- (13) Behymer, T. D.; Hites, R. A. *Environ. Sci. Technol.* 1985, 19, 1004-1006.
- (14) Rothbaum, H. P.; McGaveston, D. A.; Wall, T.; Johnston, A. E.; Mattingly, G. E. G. *J. Soil. Sci.* 1979, 30, 147-153.
- (15) Rothbaum, H. P.; Goguel, R. L.; Johnston, A. E.; Mattingly, G. E. G. *J. Soil Sci.* 1986, 37, 99-107.
- (16) Jones, K. C.; Symon, C. J.; Johnston, A. E. *Sci. Total Environ.* 1987, 61, 131-144.
- (17) Jones, K. C.; Symon, C. J.; Johnston, A. E. *Sci. Total Environ.* 1987, 67, 75-89.
- (18) Prahl, F. G.; Creelius, E.; Carpenter, R. *Environ. Sci. Technol.* 1984, 18, 687-693.
- (19) Wakeham, S. G.; Schaffner, C.; Giger, W. *Geochim. Cosmochim. Acta* 1980, 44, 415-429.
- (20) Varanasi, U.; Reichert, W. L.; Stein, J. E.; Brown, D. W.; Sanborn, H. R. *Environ. Sci. Technol.* 1985, 19, 836-841.
- (21) Whitehouse, B. *Estuarine, Coastal Shelf Sci.* 1985, 20, 393-402.
- (22) Shuker, L.; Bennett, B. G. Exposure Commitment Assessments of Environmental Pollutants Volume 6 PAHs. Monitoring and Assessment Research Centre, University of London. Technical Report, 1988.
- (23) Dennis, J. M.; Massey, R. C.; McWeeny, D. J.; Watson, D. H. In *Polynuclear Aromatic Hydrocarbons*; Cooke, M. W., Dennis, A. J., Eds.; Battelle: Columbus, OH, 1982; pp 405-412.
- (24) Chaney, R. L. In Proceedings, Pan American Health Organization Workshop on the International Transportation, Utilization or Disposal of Sewage Sludge, Washington DC, 1984. Jacobs, L. W.; O'Connor, G. A.; Overcash, M. A.; Zabik, M. J.; Ruggiewicz, P. In *Land Application of Sludge: Food Chain Implication*; Page, A. L., Logan, T. J., Ryan, J. A., Eds.; Lewis Publishers, Inc.: Chelsea, MI, 1987; pp 101-143.
- (25) Edwards, N. T. *J. Environ. Qual.* 1983, 12, 427-441.
- (26) Harms, H.; Sauerbeck, D. R. In *Environmental Effects of Organic and Inorganic Contaminants in Sewage Sludge*;

- Davis, R. D., Hucker, G., L'Hermite, P., Eds.; D. Reidel: Dordrecht, Holland, 1983; pp 38-51.
- (27) Weber, J. B.; Dorney, J. R.; Overcash, M. R. In Proceedings, Triangle Conference on Environmental Technology, Duke University, Paper No. 17, 1984.
- (28) Johnston, A. E.; Garner, J. V. Report of the Rothamsted Experimental Station for 1968, Part 2, pp 12-25.
- (29) Roll, L. A. Polycyclic Aromatic Hydrocarbons in Sediments from Lakes Receiving Acidic Atmospheric Deposition. MS Thesis, Indiana University, 1986.
- (30) Giger, W.; Schaffner, C. *Anal. Chem.* 1978, 50, 243-249.
- (31) Grob, K., Grob, K., Jr. *High Resolut. Chromatogr. Capill. Chromatogr.* 1978, 1, 57-64.
- (32) Rothamsted Experimental Station, Report for 1968 Part 2. Lawes Agricultural Trust, Harpenden, Hertfordshire, UK.
- (33) *Colliery Year Book and Coal Trades Directory*; The Louis Cassier Co. Ltd.: London, 1955.
- (34) Department of Energy, 1986. Energy trends: a statistical bulletin. HMSO, London.
- (35) National Coal Board, 1985. Report and Accounts 1984/5, NCB, London.
- (36) Annual Abstracts of Statistics. Central Office of Statistics, HMSO, London.
- (37) McVeety, B. D. Atmospheric deposition of polycyclic aromatic hydrocarbons to water surfaces: a mass balance approach. Ph.D. Thesis, Indiana University, 1986.
- (38) Crosby, N. T.; Hunt, D. C.; Philip, L. A.; Patel, I. *Analyst (London)* 1981, 106, 135-145.
- (39) Jones, K. C.; Stratford, J. A.; Waterhouse, K. S.; Vogt, N. B., submitted for publication in *Environ. Sci. Technol.*
- (40) Furlong, E. T.; Cessar, L. R.; Hites, R. A. *Geochim. Cosmochim. Acta.*, in press.
- (41) Youngblood, W. W.; Blumer, M. *Geochim. Cosmochim. Acta* 1975, 39, 1303-1314.
- (42) Blumer, K.; Blumer, W.; Reich, T. *Environ. Sci. Technol.* 1977, 11, 1082-1084.
- (43) Butler, J. D.; Butterworth, V.; Kellow, S. C.; Robinson, H. G.; *Sci. Total Environ.* 1984, 33, 75-85.
- (44) Vogt, N. B.; Brakstad, F.; Thrane, K.; Nordenson, S.; Krane, J.; Aamot, E.; Kolset, K.; Esbensen, K.; Steinnes, E. *Environ. Sci. Technol.* 1987, 21, 35-44.
- (45) Jones, K. C.; Stratford, J. A.; Tidridge, P.; Waterhouse, K. S.; Johnston, A. E. *Environ. Pollut.*, in press.
- (46) Jones, K. C.; Grimmer, G. A.; Jacob, J.; Johnston, A. E. *Sci. Total Environ.*, in press.

Received for review January 28, 1988. Accepted July 5, 1988.

Evaporation Times and Rates of Specific Hydrocarbons in Oil Spills

Warren Stiver, Wan Ying Shlu, and Donald Mackay*

Department of Chemical Engineering and Applied Chemistry, University of Toronto, Toronto, Ontario M5S 1A4, Canada

■ A theoretical treatment is presented for the evaporation rate of specific hydrocarbons from crude oil spills. The fraction remaining of a specific hydrocarbon at any given evaporative exposure (directly related to time) can be calculated from the hydrocarbon's vapor pressure. Experimental data from four crude oils support the theory and define the one unknown parameter. In addition, a technique is developed to predict fresh oil composition based on a weathered oil's composition and the weathered oil's initial boiling point. The initial boiling point is used to calculate the exposure to which the oil has been subjected based on a correlation developed from nine crude oils. This exposure is then used to predict the fraction remaining of each component that in combination with the weathered oil's composition can be used to deduce the fresh oil's composition.

Introduction

When crude oil or a petroleum product is spilled it becomes subject to a number of transport and transformation processes collectively termed weathering. The dominant initial process is usually evaporation with other processes such as dissolution into water, permeation into soil, photolysis, oxidation, and biodegradation becoming significant later as reviewed by NAS (1), McAuliffe (2), Lee (3), and Stiver and Mackay (4). Oils are usually complex mixtures of hydrocarbons; however, normally only the more volatile or structurally simple compounds are fully characterized. Analysis usually focuses on the normal alkanes, the simple monoaromatics, the polynuclear aromatic hydrocarbons, and certain terpenes. As the oil weathers its composition changes as hydrocarbons are lost, each at a rate specific to its physical, chemical, and reaction properties. In principle, if the composition of an oil is known, it should be possible to predict future oil composition as a function of time. Such a predictive capability could also be used

to calculate the composition of the original unweathered oil from a knowledge of the composition of a weathered sample.

There are two primary incentives for developing such a composition prediction tool. First, in assessing the toxicology of oil spills it is useful to know the residence time of specific hydrocarbons such as benzene or naphthalene. In bioassays aimed at obtaining toxicity information relevant to environmental conditions, it is important that the exposures (in terms of concentration and time) be realistic. There is little merit in studying the toxicity of a hydrocarbon such as benzene over 96 h in the laboratory if its residence time in an oil slick is only 1 h.

Second, there is the forensic incentive to demonstrate that a sample of spilled oil originated from a particular source or cargo. Considerable effort has been devoted to devising methods of identifying such samples by gas and liquid chromatography, spectroscopy, and metal and sulfur analyses, a comprehensive review having been given by Bentz (5). Complicating the forensic process is the alteration in composition due to weathering. Currently, methods are used in which the source and sample oil are analyzed for parameters (such as metal content) that are subject to minimal change on weathering. The capability of calculating the compositional change during weathering would provide an additional link between the sample and the alleged source.

In this work two issues are addressed. The first is the calculation of the residence time of specific hydrocarbons in oil slicks or pools that are subject to loss by evaporation. The second is to establish the exposure to which a sample of weathered oil has been subjected. The specific hydrocarbon residence time issue has been previously addressed by several workers. Regnier and Scott (6) evaporated samples of a No. 2 fuel oil in Petri dishes under wind speeds of 21 km/h. Residual samples were analyzed by capillary column gas chromatography, and the percent

remaining of the *n*-alkanes was determined. Plots of the logarithm of this percent remaining versus the exposure time resulted in straight lines. They also showed that the slope of this line was directly proportional to the component's vapor pressure.

Butler (7) developed a model to predict the percent remaining as a function of the carbon number. The coefficients in Butler's equations were based on experimental results of Krieder (8) on an unspecified crude oil. The agreement between the expected results and the actual data indicates the form of their equations is probably correct. There has been no comparison with other crude oils and weathering conditions; therefore, the generality of the coefficients is uncertain.

Drivas (9) has developed a model to predict the percent remaining as a function of time. The model was compared with experimental results from Johnson et al. (10). Unfortunately, the evaporating conditions were not well-defined such that average mass-transfer coefficients were used to fit a range of data. Thus, only a tentative validation was accomplished.

The approach taken here is first to relate the dimensionless evaporative exposure (θ), introduced by Stiver and Mackay (4), to the fraction remaining of a specific hydrocarbon. This evaporative exposure (θ) is a function of time, slick area, volume and thickness, and wind speed. The relationship between the evaporative exposure and the fraction remaining proves to be a function of the hydrocarbon's vapor pressure and one unknown parameter, the mean effective oil molar volume. On the basis of experimental results obtained for four crude oils, the mean effective oil molar volume is estimated. This leads to a procedure to predict composition as a function of evaporative exposure which can be applied to both past and future behavior.

The difficulty in "back-calculating" oil compositions is then in establishing the exposure to which the oil has been subjected. A direct approach is to estimate θ on the basis of knowledge of the time and conditions of exposure. This information is often not readily available; therefore, an alternative approach is developed here. The approach will be to relate the initial boiling point of a weathered oil to the evaporative exposure based on experimental results.

Theory

(i) **Pure Liquids.** It has been shown (4) that the evaporation rate of a pool of pure liquid is given by

$$N = KaP/RT \quad (1)$$

where N is the evaporation rate (mol/s), K is the mass-transfer coefficient (m/s), a is the spill area (m²), P is the liquid's vapor pressure (Pa), R is the gas law constant (8.314 Pa·m³/mol·K), and T is the liquid's temperature (K).

Combining eq 1 with a relationship between N and the volume fraction evaporated gives

$$(V_0/v) dF_v/dt = KaP/RT \quad (2)$$

or

$$dF_v = (Pv/RT)(Ka dt/V_0) \quad (3)$$

or

$$dF_v = H d\theta \quad (4)$$

or for constant H , F_v equal to zero when θ is zero,

$$F_v = H\theta \quad (5)$$

where F_v is the volume fraction evaporated, t is the time (s), V_0 is the initial volume (m³), v is the liquid's molar

volume (m³/mol), H is Pv/RT , and θ is the evaporative exposure.

The volume fraction evaporated is the product of two dimensionless groups. The first, Pv/RT , is the ratio of the equilibrium concentration in the air (P/RT) and in the liquid ($1/v$) and is denoted as H since it is a form of Henry's law constant. It is a thermodynamic function and thus dependent only on the liquid and its temperature. The second group, $Kadt/V_0$, is termed the evaporative exposure and is denoted as $d\theta$. The evaporative exposure accounts for the variables that are a function of the spill dimensions and conditions only. It is analogous to the ratio of the vapor volume leaving the oil during evaporation to the liquid volume.

For a pure liquid H is constant; therefore, eq 4 can be integrated to give eq 5 which shows that evaporation is complete when θ is $1/H$. Obviously, the liquid boiling point remains constant during this period. If the spill area increases as a function of time and is $a(t)$, this can be taken into account if θ is calculated as

$$\theta = \int [Ka(t)/V_0] dt \quad (6)$$

Variation in K with time can also be included. The essential point is that as evaporation proceeds, θ increases until no liquid is left when θ (as some integrated function of K , a , and t) equals $1/H$.

A convenient experimental approach is to use gas stripping in which air is bubbled into a liquid and leaves the liquid in a saturated condition. This avoids mass-transfer limitations. In this case, eq 1 does not apply. However, if the Ka is replaced by G , the air flow rate (m³/s), the development is the same and eq 4 applies. In this case, the evaporative exposure, θ , is defined as Gt/V_0 instead of Kat/V_0 . θ becomes the actual ratio of the vapor volume leaving the liquid to the initial liquid volume. Evaporation is complete when θ is $1/H$ or when Gt equals V_0/H .

(ii) **Mixtures.** For mixtures the behavior is more complex because H decreases as evaporation proceeds and the lighter hydrocarbons evaporate. The liquid's boiling point also increases. Whereas the plot of fraction evaporated F_v versus θ is a straight line for a pure liquid (eq 5), it is curved for a mixture displaying a reduced slope H as evaporation proceeds. As has been discussed by Stiver and Mackay (4), a plot of F_v versus θ is thermodynamic in nature and does not depend on how θ is achieved (e.g., by tray evaporation or by gas stripping). It is a function only of the oil composition and temperature.

It is interesting to explore how the evaporation rates of the various components of the oil mixture differ. Their specific evaporation rate is dependent on their individual vapor pressures and mole fractions. Applying eq 1 and Raoult's law (but corrected by using an activity coefficient), on an individual component basis we have

$$N_i = Kax_i\gamma_i P_i/RT \quad (7)$$

where N_i is the evaporation rate of component i (mol/s), x_i is the mole fraction of component i , P_i is the equilibrium vapor pressure of component i (Pa), and γ_i is the activity coefficient of component i .

Equation 7 is equivalent to

$$dn_i/dt = -Ka(n_i/n_T)\gamma_i P_i/RT \quad (8)$$

where n_i is the number of moles of component i (mol) and n_T is the total number of moles present (mol).

By introducing the identity

$$n_T = [(1 - F_v)V_0/v_0] \quad (9)$$

where F_x is fraction moles evaporated and v_c^0 is the initial oil molar volume (m^3/mol), eq 8 becomes

$$dn_i/n_i = -[v_c^0/(1 - F_x)](\gamma_i P_i/RT)(Kadt/V_0) \quad (10)$$

$$d \ln n_i = -[v_c^0 \gamma_i / (1 - F_x)] (P_i/RT) d\theta = -v_c (P_i/RT) d\theta \quad (11)$$

For simplicity the term $v_c^0 \gamma_i / (1 - F_x)$ is replaced by a single term v_c which is termed the mean effective oil molar volume. The value of v_c will vary from component to component and will vary while an individual component is evaporating. These changes in v_c reflect the changes in mole fraction of component i as a result of the evaporation of other components as well as any changes in activity coefficients. This variability will be evident experimentally in two ways. First, a plot of the natural logarithm of fraction remaining of component i versus the evaporative exposure will be nonlinear. Second, there will be increases in the value of v_c for lower volatility hydrocarbons for which F_x is large. Analysis of the terms in eq 11 demonstrates that while the component-to-component variation in θ and (P_i/RT) can be orders of magnitude, the term v_c is relatively constant. By assuming v_c constant for component i , eq 10 can be integrated to give

$$\ln n_i/n_i^0 = -v_c (P_i/RT) \theta \quad (12)$$

A plot of the natural logarithm of fraction component i remaining versus the evaporative exposure should result in a straight line. The slope of this line divided by P_i/RT will be v_c .

(iii) **Weathered Oil Exposure.** To estimate the exposure of a weathered oil a relationship between evaporative exposure and boiling temperature can be developed. Stiver and Mackay (4) showed that the volume fraction evaporated could be related to the evaporative exposure by eq 13 if a linear relationship between F_v and boiling temperature (T_B) was assumed, as in eq 14.

$$F_v = (1/Q) \ln(1 + H_0 Q \theta) \quad (13)$$

$$T_B = T_0 + T_G F_v \quad (14)$$

where $\ln H_0 = A - BT_0/T$, $Q = BT_G/T$, A is a dimensionless constant (≈ 6.3), B is a dimensionless constant (≈ 10.3), T is the environmental temperature (K), T_0 is the initial boiling temperature (K), and T_G is the gradient of the temperature versus fraction distilled curve (K).

It is noteworthy that if Q is small (i.e., T_G is small), and the distillation curve is shallow, expansion of the series in $\ln(1 + H_0 Q \theta)$ gives F_v equal to $H_0 \theta$, which is eq 5.

Rearrangement of eq 13 and 14 to eliminate F_v gives

$$\theta = [T/[BT_G \exp(A)]] [\exp(BT_B/T) - \exp(BT_0/T)] \quad (15)$$

This equation has the correct property that when T_B equals T_0 , θ is zero. But as T_B greatly exceeds T_0 the term in T_0 becomes negligible and

$$\theta \approx [T/[BT_G \exp(A)]] [\exp(BT_B/T)] \quad (16)$$

The exposure thus becomes dependent only on T_B and the "memory" of the original boiling point T_0 is gradually lost. Oils of differing initial boiling points thus approach a similar exposure-boiling point curve when $T_B \gg T_0$. Intuitively this is reasonable, since a light oil rapidly loses its volatile components and after prolonged weathering becomes similar in properties to an oil that was initially less volatile.

A plot of the natural logarithm of evaporative exposure versus boiling temperature will give a straight line with slope of B/T and intercept of $\ln [T/[BT_G \exp(A)]]$.

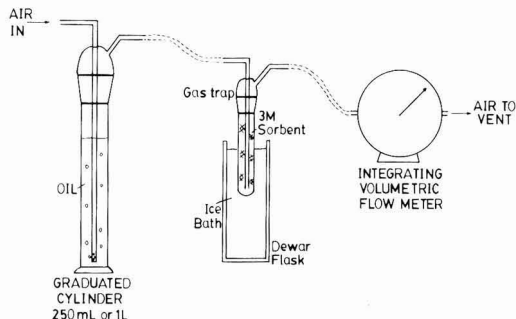


Figure 1. Gas stripping apparatus.

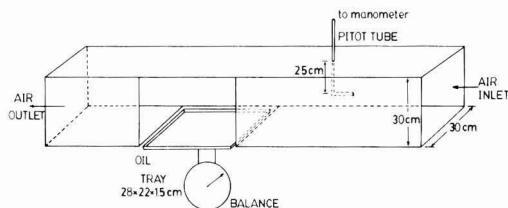


Figure 2. Tray evaporation apparatus.

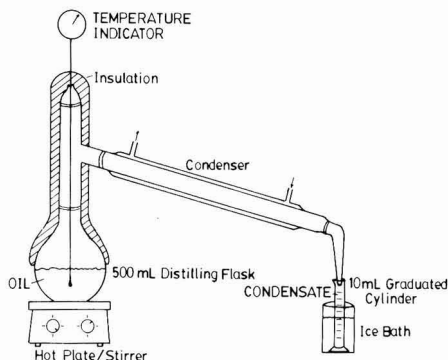


Figure 3. Distillation apparatus.

Experimental Section

Experimental configurations and procedures have been described in detail in Stiver and Mackay (4). Only a brief outline is given here.

The evaporated crude oil samples were prepared by two techniques. The initial evaporation was done by gas stripping as shown in Figure 1. Gas stripping involved the slow bubbling of air at 1 L/min through a column of the crude oil in a 250-mL graduated cylinder. The mass and volume of the oil were measured as a function of time and of the air volume passed through the oil. Samples were taken at various times during the run. The residue from this gas stripping run was then tray evaporated in a wind tunnel. For tray evaporation, a volume of oil was weighed and placed on a tray (area, 0.082 m^2) to obtain a slick thickness of 1–5 mm. The tray was then placed in a wind tunnel, as shown in Figure 2, and subjected to wind speeds between 4 and 12 m/s. The mass-transfer coefficients for the various wind speeds were measured separately by toluene evaporation. The mass of the toluene or oil was measured as a function of time with an in situ top-loading balance. The duration of the experiments varied from 6 h to 2 weeks. Samples were taken during the run for both GC and density analyses.

Table I. Fraction Remaining versus Evaporative Exposure

n-alkane	crude oil ^a				P _i /RT, mol/m ³	v _c , m ³ /mol
	Kuwait	Prudhoe Bay	Norman Wells	La Rosa		
heptane	8.3E-04				8.3E-04	2.14
octane	2.6E-04	2.7E-04	2.3E-04	3.3E-04	2.7E-04	0.647
nonane	7.0E-05	9.0E-05	8.2E-05	7.4E-05	7.9E-05	0.191
decane	1.9E-05	1.5E-05	2.5E-05	2.6E-05	2.1E-05	0.0573
hendecane	5.9E-06	4.7E-06	9.5E-06	4.6E-06	6.2E-06	0.0167
dodecane	2.1E-06	1.3E-06	3.3E-06	1.3E-06	2.0E-06	0.00491
tridecane	6.8E-07	5.2E-07	1.8E-06		1.0E-06	0.00134
tetradecane		1.2E-07	7.3E-07		4.3E-07	0.000489

^aSlopes = -(P_i/RT)(v_c).

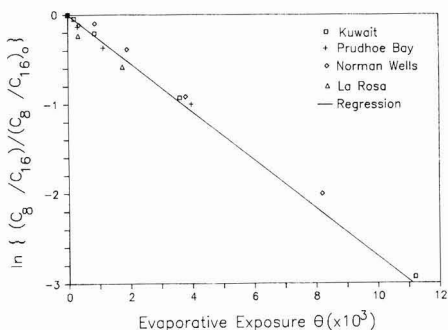


Figure 4. Fraction octane remaining versus evaporative exposure.

The distillation apparatus is depicted in Figure 3. The oil was added to a 500-mL flat-bottom distilling flask with glass beads and a magnetic stirring bar. Condensate was collected, and the liquid boiling temperature was recorded as a function of volume distilled.

Compositional analysis of all samples was performed by direct-injection gas chromatography (GC), with very weathered viscous samples being diluted in pentane to facilitate injection. The gas chromatograph was a Hewlett-Packard Model 5700A equipped with a flame-ionization detector. The column was a 50 m long by 0.5 mm i.d. glass capillary (GSOT) column coated with OV101. The GC oven was temperature programmed from 50 to 220 °C at a rate of 4 °C/min with an 8-min postinjection time; the final temperature was held for 32 min. The injection port and detector temperature were set at 250 and 300 °C, respectively.

The residence time results are presented as graphs of natural logarithm of fraction remaining [ln [(C_i/C₁₆)/(C_i/C₁₆)₀]] versus the evaporative exposure (θ). Normalization to C₁₆ (which is assumed not to evaporate) was done to eliminate the effects of GC variability. Figures 4 and 5 illustrate the results for n-octane and n-dodecane. The line represents the average slopes for the oils. Table I summarizes the results. Included are the slopes for each n-alkane from heptane through to tetradecane for the four oils. From the slope of each oil an average slope is obtained, and by dividing by P_i/RT for each component a value for v_c is obtained.

The evaporative exposure versus boiling point results are presented in Figure 6.

Discussion

From the data in Table I, the average v_c value for the alkanes heptane to dodecane is 4.0 × 10⁻⁴ m³/mol (SD 0.2 × 10⁻⁴). The values for tridecane and tetradecane are 7.5 × 10⁻⁴ and 8.7 × 10⁻⁴, respectively. As expected, the term v_c is fairly constant during the evaporation of an individual

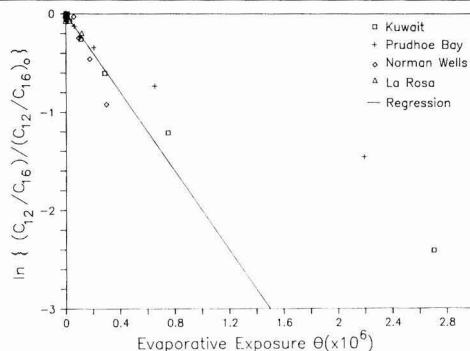


Figure 5. Fraction dodecane remaining versus evaporative exposure.

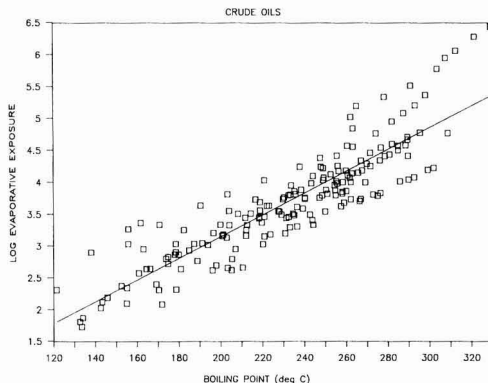


Figure 6. Evaporative exposure versus boiling temperature.

component as evidenced by the linearity of Figures 4 and 5. However, the changes in the value of F_x and possibly γ_i are sufficient to increase the value of v_c for tridecane and tetradecane. It is unclear why the effect of (1 - F_x) is not apparent until tridecane. On the basis of these results, a value for v_c of 4.0 × 10⁻⁴ m³/mol is recommended for most crude oils. For relatively nonvolatile components, correction of the value of v_c will lead to greater accuracy in the estimation of the fraction of moles evaporated. The value of 4.0 × 10⁻⁴ is consistent with a crude oil of density 800 kg/m³ and an average initial molecular mass of 320 g/mol. This result does not represent a direct measurement of either the molar volume or the molecular weight since this quantity also incorporates nonidealities or deviations from Raoult's Law.

In summary, to establish the half-life evaporative exposure for a specific hydrocarbon the following method may be used:

(i) Calculate P_i/RT for the component of interest at the desired temperature.

Table II. Illustrative Example^a

n-alkane	A ^b	B ^c	C ^d
7	<0.04	0.000003	0.004
8	<0.04	0.022	0.19
9	0.26	0.32	0.61
10	0.72	0.71	0.86
11	0.90	0.91	0.96
12	0.99	0.97	0.99
13	0.94		
14	1.08		
15	1.00		
16	1.00		

^a Actual evaporative exposure, 14800; initial boiling point, 239 °C. ^b Measured fraction remaining by gas chromatography. ^c Predicted fraction remaining based on $\theta = 14800$ and eq 11. ^d Predicted fraction remaining based on $T_B = 239$ °C which, by using eq 16, gives $\theta = 6500$.

(ii) The rate constant for evaporation is then 4.0×10^{-4} (P_i/RT); thus, the exposure at which half of the component has evaporated will be given by

$$0.693 / [(4 \times 10^{-4})(P_i/RT)]$$

(iii) The exposure can then be related to real time based on the prevailing mass-transfer conditions. As a rule of thumb, under typical environmental conditions an evaporative exposure of 1 million per day could be expected [K of 0.01 m/s, V_0/a of 1 mm; see Mackay and Matsugu (11) for a relationship between the mass-transfer coefficient K and the air wind speed].

As discussed earlier, to back-calculate oil compositions it is necessary to establish the evaporative exposure. Equation 15 presents a relationship between the initial boiling point of a weathered oil and the evaporative exposure. Figure 6 illustrates the results for nine oils after both gas stripping and tray evaporation. A linear correlation gives

$$\ln \theta = 0.0393T_B - 11.37 \quad r^2 = 0.8 \quad (17)$$

where T_B is the boiling temperature (K).

To estimate the exposure to which a weathered crude oil has been subjected and ultimately the fraction remaining of a specific hydrocarbon in that weathered oil the following procedure is recommended:

(i) Measure the initial boiling point of the weathered oil. (ii) By use of eq 17, calculate the evaporative exposure. From this evaporative exposure real time can be estimated knowing the mass-transfer conditions.

(iii) By use of eq 12, the specific hydrocarbon's vapor pressure, and 4.0×10^{-4} m³/mol for v_c , calculate fraction of the hydrocarbon remaining.

Equation 17 is a correlation and should only be applied to oils of a similar nature of the conventional crude oils used in the development of eq 17. The correlation should not be used with petroleum products.

Inherent in the development of this work is the understanding that the evaporation is controlled by the gas-phase mass transfer and that there is no liquid-phase resistance. In most cases this will be true; however, when the oil is very viscous or waxy, the oil depth is large, and the oil's turbulence is diminished, the liquid-phase resistance may become appreciable. Under these conditions the above equations will not hold, as evaporation will not only be slower (in a real time sense) but the relative evaporation rate of each component will be altered.

Illustration

Table II summarizes the results of a test oil which had not been used in developing any of the above correlations

or relationships and was weathered to an evaporative exposure of 14800. Both the fresh and weathered oil were analyzed by GC. The measured fraction remaining is shown in column A of Table II. The predicted fraction remaining based on an evaporative exposure of 14800 and eq 12 is shown in Column B. The agreement is excellent. The weathered oil was distilled, and the initial boiling point of 239 °C was used to predict the evaporative exposure of 6500 using eq 17. Based on this evaporative exposure the fraction remaining was predicted and is shown in column C. The agreement is satisfactory. Clearly the errors in back-calculating compositions are due to the exposure prediction. The reason for the discrepancy is due to a difference between the composition of an oil that is 26% evaporated as compared to the same oil that is 26% distilled.

Conclusions

The capability has been developed to predict the component specific residence time in an evaporating oil spill. By using eq 12 and a value of 4.0×10^{-4} m³/mol for v_c , the fraction remaining of a particular component can be readily calculated for a particular exposure. This evaporative exposure is directly related to time through the prevailing mass-transfer conditions.

In addition, the capability to estimate the evaporative exposure to which a weathered oil has been exposed has also been established. On the basis of the weathered oil's initial boiling point and by use of eq 17, the evaporative exposure can be calculated. From this evaporative exposure the fraction remaining of any component and thus the composition of the fresh oil can be determined.

The principles and approach demonstrated can be applied to predictions of the fate of specific chemicals in other spilled chemical mixtures.

Registry No. Heptane, 142-82-5; octane, 111-65-9; nonane, 111-84-2; decane, 124-18-5; hendecane, 1120-21-4; dodecane, 112-40-3; tridecane, 629-50-5; tetradecane, 629-59-4; pentadecane, 629-62-9; hexadecane, 544-76-3.

Literature Cited

- (1) NAS Oil in the Sea: Inputs, Fates and Effects; National Academy Press: Washington, DC, 1985.
- (2) McAuliffe, C. D. *Fate and Effects of Petroleum Hydrocarbons in Marine Ecosystems and Organisms*; Proceedings of a Symposium, Seattle, WA, November 10-12, 1976; Permagon: New York, 1977.
- (3) Lee, R. F. *Marine Environmental Pollution, 1. Hydrocarbons*; Geyer, R. A., Ed.; Elsevier: Amsterdam, 1980; Chapter 12.
- (4) Stiver, W.; Mackay, D. *Environ. Sci. Technol.* **1984**, *18*, 834-840.
- (5) Bentz, A. P. *Anal. Chem.* **1978**, *50*, 655A-658A.
- (6) Regnier, Z. R.; Scott, B. F. *Environ. Sci. Technol.* **1975**, *9*, 469-472.
- (7) Butler, N. J. *Transfer of Petroleum Residues from Sea to Air: Evaporative Weathering, Marine Pollutant Transfer*; Windom, H. L., Duce, R. A., Eds.; Lexington Books: Lexington, MA, 1976; pp 201-211.
- (8) Krieder, R. I. *Proceedings, Joint Conference on Prevention and Control of Oil Spills*; American Petroleum Institute; 1971; pp 119-124.
- (9) Drivas, P. J. *Environ. Sci. Technol.* **1982**, *16*, 726-728.
- (10) Johnson, J. C.; McAuliffe, C. D.; Brown, R. A. *ASTM Spec. Tech. Publ.* **1978**, No. 659, 141-158.
- (11) Mackay, D.; Matsugu, R. S. *Can. J. Chem. Eng.* **1973**, *53*, 434-439.

Received for review December 15, 1987. Accepted June 27, 1988. We are grateful to the Natural Sciences and Engineering Research Council for financial support.

A New Gas-Phase Nitric Acid Calibration System

Linda J. Nunnermacker,* Russell R. Dickerson,[†] Alan Fried,[‡] and Robert Sams[§]

Department of Chemistry, University of Maryland, College Park, Maryland 20742

■ A new calibration source of gaseous nitric acid has been developed, based on the conversion of gaseous hydrogen chloride, HCl(g), to HNO₃ on solid silver nitrate, AgNO₃(s). The concentration of HNO₃ produced by the system has been determined by three independent techniques: tunable diode laser absorption spectroscopy (TDLAS), chemiluminescence detection (CD), and ion chromatography (IC). The three techniques agreed to within 9%. At 20 °C, the system converts HCl to HNO₃ with an efficiency of >90%. Production of HNO₃ is relatively insensitive to changes in HCl flow and in temperature. A dynamic dilution calibration system has been used to produce HNO₃ concentrations as low as 10 ppbv.

Introduction

Nitric acid, HNO₃, is a very important trace constituent of the atmosphere in both the gas and particulate phases. It comprises approximately one-third of total acid deposition and its contribution appears to be increasing (1-3). Nitric acid also plays an important role in the atmospheric nitrogen cycle, as it is the primary sink for reactive nitrogen species in the troposphere (4, 5).

Thus, tropospheric measurements of HNO₃ are important (6). There are many different techniques (7-11) for measuring ambient concentrations of HNO₃, which range from less than 0.05 ppbv (parts per billion by volume) to many ppbv. However, these techniques require accurate HNO₃ calibration standards. Carrying out such a calibration with high accuracy is a particularly difficult task. HNO₃ is both polar and highly reactive, and thus surface absorption, adsorption, decomposition, and artifact formation (12, 13) make it very difficult to generate and measure trace nitric acid concentrations accurately.

A nitrous/nitric acid source based on oxalic acid-potassium nitrite/nitrate sublimation has recently been reported (14). However, the sublimation rate varies widely with time, making this source unsuitable as a calibration standard. Diffusion tubes have also been used to generate HNO₃ (15). These devices, however, are very susceptible to changes in temperature, pressure, and diluent flow and require long periods of equilibration.

The most popular method for generating trace HNO₃ concentrations is a permeation device (8), in which a nitric acid liquid/vapor-phase equilibrium is maintained in a sealed Teflon vial kept at a constant temperature. The HNO₃ permeates through the Teflon into a controlled flow of air, and the concentration of HNO₃ is determined from periodic weight loss measurements of the permeation device and measurements of the diluent flow rate (8).

Impurities such as NO₂ and water are almost always present in nitric acid permeation devices. If not taken into account, one may erroneously deduce systematically high nitric acid calibration concentrations. The presence of NO₂ can cause systematic errors as high as 12% (8). In the case

of H₂O, an azeotropic mixture may be formed resulting in erroneously high emission rates of ~30%. Observations from our laboratory further indicate that slight perturbations in the temperature of, or air flow rate over, the HNO₃ permeation tubes can cause dramatic changes in the weight loss, by as much as 40%. This is in contrast to NO₂ permeation tubes which are quite stable in the same environment.

Although permeation devices can generate accurately known concentrations of HNO₃, an alternative source of HNO₃ is highly desirable. We have developed and characterized a calibration source that can be used to generate HNO₃ concentrations in the parts-per-million by volume (ppmv) and sub-ppmv range with verifiable accuracy. A hydrogen chloride gas mixture is used to produce HNO₃ through the following reaction:



$$\Delta G^\circ = -13.3 \text{ kcal mol}^{-1} (16)$$

Experimental Section

Nitric Acid Generation. Nitric acid is generated by passing a gaseous mixture of HCl in N₂ (Matheson, certified standard, nominally 93 ppmv) through a 145-mm length of 4.0-mm-i.d. Teflon tubing containing 6.21 g (~6-8 mesh) of crystalline silver nitrate (Merck, reagent grade) (Figure 1). The flow of HCl was maintained by a 0.5 L min⁻¹ mass flow controller (MFC) with Kalrez O-rings to minimize potential corrosion. A low flow of nitrogen was continuously passed through the flow controller whenever the HCl was not in use in order to keep the flow controller dry and prevent corrosion. Lower HNO₃ concentrations (<87 ppmv) were obtained by dynamically diluting the flow from the column with nitrogen or "zero air". Background concentrations of HNO₃ were determined by replacing the HCl flow with an equivalent flow of nitrogen or zero air over the AgNO₃ column. All connections, solenoid valves, and tubing in the system were TFE Teflon unless otherwise specified.

The temperature dependence of the column conversion efficiency was investigated by using a temperature-controlled water bath (MGW Lauda, RM6) to circulate water around the AgNO₃ column, as shown in Figure 1. The temperature could then be controlled to ±0.01 °C.

Ion Chromatography (IC). Ion chromatographic analysis (8) was employed to measure the concentration of HCl in the cylinder, the residual unconverted HCl passing through the column, and the HNO₃ generated by the column. To prepare samples, a known gas volume, as measured by a calibrated wet test meter, was bubbled through 50 mL of deionized water contained in a sealed 250-mL Teflon beaker (first flow path, Figure 1). A single beaker collection efficiency of 99.6 ± 2% (±1σ) was determined for both Cl⁻ and NO₃⁻. Samples were then transferred into 60-mL Nalgene bottles and immediately analyzed or placed in frozen storage. Samples were analyzed for both ions with a Dionex 2020i ion chromatograph employing an AG4A precolumn and an AS4A column.

Chemiluminescence Detection (CD). In the second flow path of Figure 1, a NO chemiluminescence detector

*Permanent address: Department of Meteorology, University of Maryland, College Park, MD 20742.

[†]Permanent address: National Center for Atmospheric Research, 1850 Table Mesa Dr., Boulder, CO 80303.

[‡]Permanent address: National Bureau of Standards, Gas Metrology Group, CAC, Gaithersburg, MD 20899.

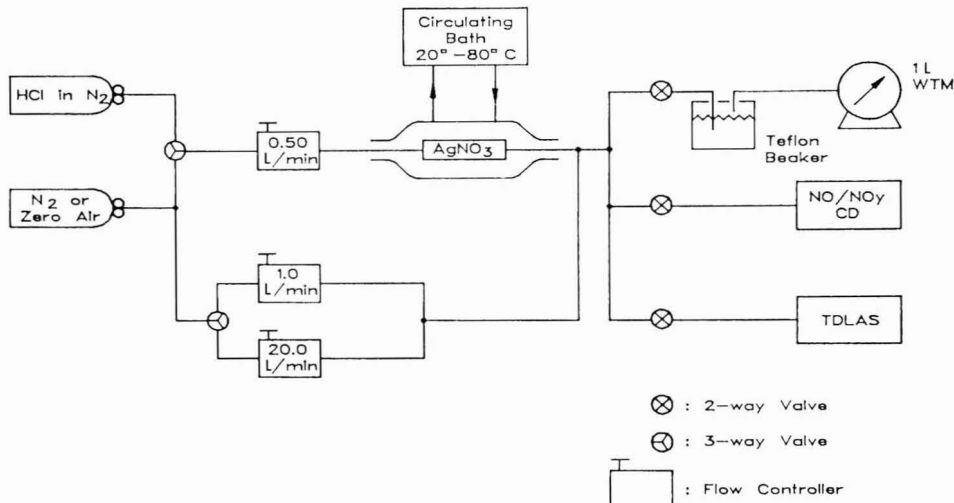


Figure 1. Schematic diagram of the HNO₃ calibration system. WTM, wet test meter; CD, chemiluminescence detection; TDLAS, tunable diode laser absorption spectroscopy.

(CD) (Model 10, Thermo Electron Corp., Hopkinton, MA) was used to measure the total concentration of reactive nitrogen compounds emanating from the calibration system. Our CD employed a hot stainless steel (SS) converter operating at 660 °C; at this temperature NO₂ and HNO₃ are converted to NO with high efficiency (17). The sum of all oxides of nitrogen is typically denoted as [NO_y] (18). For our CD/SS measurements, the [NO_y] term includes compounds such as HCN, RCN, and NH₃, which are converted to NO on stainless steel at 660 °C. For some measurements, the calibration system output was first passed through a 47-mm nylon filter (Membrana) and through a 2.7-m length of nylon tubing. Nylon quantitatively removes HNO₃, HONO, and various other acidic gases (19–21). The CD response in this case is then a measure of the nonacidic or weakly acidic reactive nitrogen compounds remaining in the flow path, [NO_y*]. The difference in CD measurements without and with the nylon in the flow path, [NO_y] - [NO_y*], is thus a measure of the concentration of HNO₃ (we assume other acidic nitrogen compounds are negligible). The CD instrument was calibrated with 93 ppmv NO/N₂ standard reference material (SRM) gas mixtures.

A modified 14 B/E Thermo Electron chemiluminescent NO analyzer (22, 23) was used to measure the sub-ppmv reactive nitrogen concentrations. This CD employed a Mo converter operating at 375 °C, which will not convert compounds such as NH₃, HCN, and organocyanides to NO.

The NO_y detection limits (3σ) for the Model 10 and modified Model 14 B/E were 0.125 ppmv and 0.0003 ppmv, respectively. The NO detection limit (3σ) for the Model 14 B/E was 0.00005 ppmv.

Tunable Diode Laser Absorption Spectroscopy (TDLAS). TDLAS was used to spectroscopically identify HNO₃ vapor as the main component of the calibration system output; IC and CD are not specific for gas-phase HNO₃. In addition, TDLAS provided an independent means of HNO₃ quantitation and was important in determining the upper bounds for concentrations of other reactive nitrogen species such as NO₂ and HONO in the calibration system output.

The tunable diode laser spectrometer and data reduction procedures have previously been described in detail (17, 24, 25) and will not be discussed here. For this experiment,

one diode laser covered the 1603-cm⁻¹ region and was used to detect NO₂ by sweep integration second harmonic detection (17). The calibration system effluent was passed into a White cell (81-m total path length) at a total pressure of 9.85 Torr and compared with a 5.19 ppmv calibration mixture of NO₂ in air. The second diode laser covered the 1720–1830-cm⁻¹ spectral region and was used to measure HNO₃, HONO, and NO. The HNO₃ concentration was determined by direct absorption using the vibration-rotation line at 1722.4390 cm⁻¹, employing the technique of sweep integration. Absorption coefficients recently calculated by Maki (26) based upon the ν₂ band strength measurements of Giver et al. (27) were used in this analysis. Absorption coefficients recently determined by May et al. (28) for other HNO₃ lines in this band are in general agreement with those determined by Maki (~3%), suggesting an uncertainty of this order.

The integrated absorbance for the vibration-rotation line was fit by a nonlinear least-squares routine (24, 25) and a Voigt line profile using the Humlicek algorithm (29). The following line parameters were employed in this calculation: an integrated absorption coefficient of 0.5609 cm⁻² atm⁻¹; a calculated Doppler-broadened halfwidth-at-half-maximum of 0.00134 cm⁻¹; and N₂-broadening and self-broadening coefficients of 0.13 and 0.74 cm⁻¹ atm⁻¹, respectively. The integrated absorbance calculated was substituted into the Beer-Lambert expression together with values for the sample pressure, path length, and integrated absorption coefficient to determine the HNO₃ concentration.

Results and Discussion

Analysis of the HCl Cylinder. The concentration of nitric acid generated by the calibration system depends directly on the concentration of the HCl employed. We performed a thorough analysis of our HCl cylinder to verify the manufacturer's concentration (93 ppmv ± 5%, as determined by acid-base titration) and to identify any potential contaminants. IC analyses of the HCl cylinder revealed an average gas-phase [HCl] = 94.3 ± 2.1 ppmv and a gas-phase [HNO₃] < 3 ppmv. On the basis of the measurement precision and estimates of various measurement uncertainties, we estimate a total uncertainty of ±5.6 ppmv (all uncertainties are 2σ, unless stated other-

wise). These results also indicate that the cylinder contents have been stable for over 2½ years. Such stability is an important prerequisite for the successful long-term operation of the HNO₃ calibration system in the field.

Potential contaminants in the HCl cylinder were examined by the two CDs and TDLAS. The NO concentration in the HCl cylinder was ≤0.0005 ppmv. The concentration of nonacidic or weakly acidic reactive nitrogen compounds in the HCl cylinder ([NO_y*]) as measured by CD was found to be 1.77 and 0.019 ppmv using the SS and Mo converters, respectively. The CD/Mo result suggests a moderately low concentration of NO₂ in the HCl cylinder, as verified by TDLAS. The much larger response obtained with the SS converter suggests that small amounts of HCN, RCN, NH₄Cl, or other nitrogen species are present in the HCl cylinder at concentrations of ≥1.75 ppmv. However, at HNO₃ concentrations of 79 ppmv such impurities would only cause an error of 2%. Thus, they are not considered to be major interferences.

Determination of HNO₃ Produced. Nitric acid was first generated at a column temperature of 20 °C. Ion chromatography was employed to measure both the [HCl] and [HNO₃] emanating from the column. An average [HNO₃] of 79.6 ± 4.2 ppmv was determined. The total uncertainty of this measurement is ±6.1 ppmv. No detectable chloride ion was found.

The output of the AgNO₃ column was also examined for HNO₃ by use of CD with the SS converter. This method was used routinely to determine the [HNO₃] because of its fast response and ease of operation. Nitric acid was measured by difference ([NO_y] - [NO_y*]). The concentration of nonacidic or weakly acidic reactive nitrogen compounds (NO_y*) emanating from the column was measured with the SS converter and averaged 4.97 ppmv (5.5% of [NO_y]). This (together with the NO_y* concentration of 1.77 ppmv emanating directly from the HCl cylinder) indicates that the AgNO₃ column generates 3.20 ppmv NO_y*. This value remained constant throughout the study. In subsequent experiments, we measured only the total NO_y concentration and subtracted out the constant 4.97 ppmv NO_y* contribution.

The 3.20 ppmv (NO_y*) produced by the column was analyzed by CD/Mo and TDLAS. The CD measurements indicated that the column produces an insignificant amount of NO (≤0.0045 ppmv). An NO₂ concentration of 1.02 ± 0.033 ppmv was measured at the output of the column by TDLAS. This measurement was confirmed by CD/Mo ([NO₂] = 0.84 ppmv). The remaining 2.2 ppmv (3.20 - 1.02) of the [NO_y*] cannot be accounted for and may be due to an unknown compound generated by the column. The increase in NO₂ at the output of the column over that measured directly from the HCl cylinder is probably due to a small amount of HNO₃ decomposing to NO₂ on the column.

The HNO₃ concentration was remarkably stable. Measurements by CD averaged 85.2 ppmv and resulted in a standard deviation of 2.6 ppmv over a 3-month period. Based on the precision of the measurements, uncertainty in the NO standard, and the efficiency of the SS converter, an absolute accuracy of 3% was estimated. The column efficiency, defined as [HNO₃]_{CD}/[HCl]_{IC} × 100, was 90.3% at 20 °C. Efficiency is reduced by loss of either HCl upstream or HNO₃ downstream of the column. Measurements of HCl at both the inlet and outlet of the calibration system with the AgNO₃ column removed, however, were equivalent within the measurement precision. Reduced conversion efficiency may be due to loss of HNO₃ or HCl on the AgNO₃ column, or decomposition of HNO₃ to NO₂.

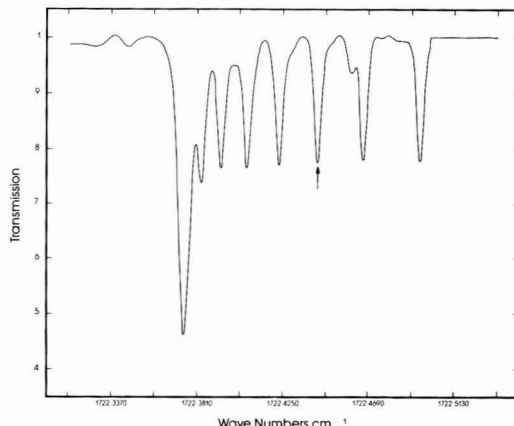


Figure 2. TDL scan of the calibration output in the 1722.4-cm⁻¹ region. The arrow marks the absorption feature at 1722.4390 cm⁻¹ used for quantitative analysis.

CD and TDLAS measurements indicate that decomposition only contributes ≤1.1% to the reduced conversion efficiency.

In Figure 2 we show a high-resolution tunable diode laser absorption scan of the calibration system output in the 1722.4-cm⁻¹ region. All of the absorption features evident are characteristic of HNO₃, confirming that the calibration system does in fact generate HNO₃ in the gas phase. Quantitative analysis, using the procedures previously outlined, was carried out on the absorption feature at 1722.4390 cm⁻¹ (marked by the arrow shown in Figure 2). An average HNO₃ concentration of 76.9 ± 2.4 ppmv (1σ precision) was thus determined from four laser scans. On the basis of this precision and the uncertainties in the measurement of pressure and path length as well as those of the spectroscopic parameters, we estimate an overall accuracy of ±6.7 ppmv.

With the column operating at 20 °C, the three distinctly different methods for HNO₃ analysis ([HNO₃]_{CD} = 85.20 ± 2.6 ppmv, [HNO₃]_{IC} = 79.6 ± 6.1 ppmv, [HNO₃]_{TDLAS} = 76.9 ± 6.7 ppmv) agree within the estimated accuracies of each technique. The TDLAS yields the most selective results and this may in part be responsible for the lowest determined HNO₃ concentration. The IC analysis agrees remarkably well with the TDLAS value (to within 3.5%). The CD measurements are the least selective; a higher [HNO₃] would result if HONO or HO₂NO₂ were present in the column effluent. However, HONO was not detected by TDLAS (2.0 ppmv detection limit), and HO₂NO₂ should not exist under the experimental conditions of temperature and pressure employed in this study. Nevertheless, the agreement among all three techniques is quite good and results in an unweighted average [HNO₃] value of 80.6 ppmv.

Temperature and Flow Dependence of the [HNO₃]. The [HNO₃] ultimately depends on the [HCl] and the efficiency of the reaction; therefore, the flow rate of the HCl and the residence time on the AgNO₃ could be important. As shown in Figure 3, the calibration system demonstrates very little HCl flow dependence; the HNO₃ concentration produced at the lower flow rate of 0.170 L min⁻¹ was 3.6% less than at 0.548 L min⁻¹.

The data in Figure 3 also show that this HNO₃ generation system is relatively insensitive to column temperature, a distinct advantage over permeation devices. The efficiency approaches 100% at the higher temperature (70

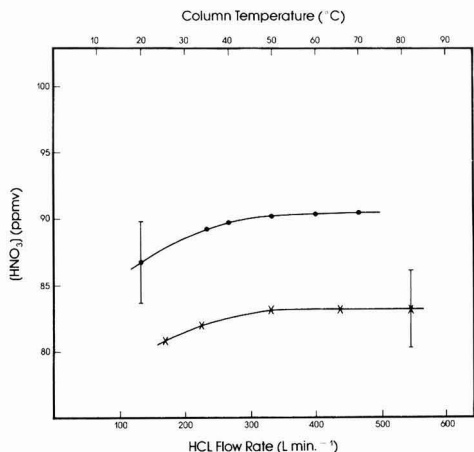


Figure 3. HNO_3 concentration (measured with CD) vs. the HCl flow rate (X) from 0.170 to 0.548 L min^{-1} and the HNO_3 concentration vs the column temperature (●) from 20 to 70 °C. Bars indicate the uncertainty in the chemiluminescent measurement.

°C). This is an increase of 4%, which may be due to HNO_3 being driven off the Teflon walls of the system.

Dynamic Dilution of the Generator Output. A dynamic dilution system, consisting of two MFCs, was used to produce low concentrations of HNO_3 . One MFC controlled the flow of the HCl/N_2 mixture, while a second MFC controlled the flow of diluent zero air. Mixtures were produced by dynamically diluting 0.17 L min^{-1} of the AgNO_3 column effluent with zero air (from 0.1 to 11 L min^{-1}) in a quartz mixing chamber. Shown in Figure 4 (column at 40 °C) is a least-squares linear regression plot of the HNO_3 concentration as determined by CD as a function of the flow dilution ratio concentration. The calibration system is linear from 0.01 to 87.4 ppmv. Concentrations of HNO_3 below 1.0 ppmv were obtained by using a 39.8 ppmv HCl cylinder, an HCl flow of 0.003 L min^{-1} , and diluent flows up to 11 L min^{-1} . The linearity indicates good mixing and negligible surface adsorption of nitric acid after sufficient time is allowed for equilibration (~1–2 h).

Conclusions

This HNO_3 generation system represents a dependable new way to provide stable low-level gaseous HNO_3 mixtures. The system is $\geq 90.3\%$ efficient at 20 °C and $\geq 92.7\%$ efficient at 40 °C in converting HCl to HNO_3 on a AgNO_3 column. With a dynamic dilution calibration system, the HNO_3 source can be used for instrument calibration at concentrations ranging from ~0.01 to 87 ppmv, almost 4 orders of magnitude. The HNO_3 produced at 20 °C over a 3-month period was remarkably stable, with an average concentration of 85.2 ± 2.6 ppmv. After 3 months of use, no change in the efficiency was observed. A decrease in efficiency would indicate the need to replace the AgNO_3 crystals. The generation system has a distinct advantage for field use in that the HNO_3 concentration is relatively independent of column flow and temperature. With these attributes, the system could be used in the field without electrical power. This source also provides an alternate and independent means of calibrating HNO_3 permeation devices.

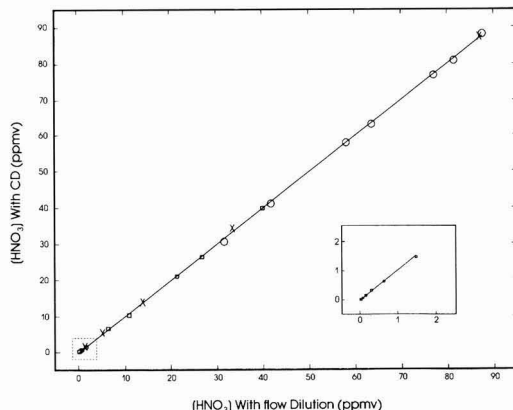


Figure 4. Overall HNO_3 calibration curve at 40 °C (employing the 94.3 ppmv HCl cylinder and AgNO_3 column) based upon flow dilution and an average $[\text{HNO}_3] = 87.4$ ppmv (as determined by CD): data obtained on 2/2/87 (X), data obtained on 2/20/87 (O), data obtained on 4/29/87 (□). The data obtained on 4/29/87 used a 39.8 ppmv HCl cylinder (as a source for HNO_3) calibrated by IC and with the same NO/SRM used for all previous measurements. Inset expands the low-level portion of the curve from 10 ppbv to 2 ppmv. The correlation coefficient, r^2 , is 0.99991, the slope is 0.996 and the y intercept is 0.013 ppmv.

Acknowledgments

We thank W. D. Dorko, D. H. Stedman, N. Yates, W. T. Luke, and B. C. Cadoff for their assistance in developing this method. We also thank W. F. Koch and K. A. Brletic for performing the IC analyses reported in this paper. Thanks go to G. Helz and P. Kijak for use of the UMD-IC instrument for preliminary testing. Thanks also to C. A. Murphy for her drafting help. This study was from a dissertation to be submitted to the Graduate School, University of Maryland, by L.J.N. in partial fulfillment of the requirements for the Ph.D. degree in chemistry. L.J.N. also thanks the National Bureau of Standards for her 1040 student appointment.

Registry No. HNO_3 , 7697-37-2; HCl, 7647-01-0; AgNO_3 , 7761-88-8.

Literature Cited

- Calvert, J. G., Ed. *Acid Deposition: Atmospheric Processes in Eastern North America*, reviewed by the Committee on Atmospheric Transport and Chemical Transformation of Acid Deposition; National Academy Press: Washington DC, 1983; 365 pages.
- Galloway, J. N.; Likens, G. E. *Atmos. Environ.* **1981**, *15*, 1081–1085.
- Likens, G. E.; Bormann, F. H.; Pierce, R. S.; Eaton, J. S.; Munn, R. E. *Atmos. Environ.* **1984**, *18*, 2641–2647.
- Logan, J. A. *J. Geophys. Res., C: Oceans Atmos.* **1983**, *88*, 10785–10807.
- Stedman, D. H.; Shetter, R. E. *Trace Atmospheric Constituents: Properties, Transformations and Fates*; Schwartz, S. E., Ed.; Wiley: New York, 1983; p 443.
- National Research Council *Global Tropospheric Chemistry: A Plan For Action*; National Academy Press: Washington DC, 1984.
- Spicer, C. W.; Howes, J. E., Jr.; Bishop, T. A.; Arnold, L. H.; Stevens, R. K. *Atmos. Environ.* **1982**, *16*, 1487–1500.
- Goldan, P. D.; Kuster, W. C.; Albritton, D. L.; Fehsenfeld, F. C.; Connell, P. S.; Norton, R. D.; Huebert, B. J. *Atmos. Environ.* **1983**, *17*, 1355–1364.
- Kelly, T. J.; Stedman, D. H.; Kok, G. L. *Geophys. Res. Lett.* **1979**, *6*, 375–378.
- Huebert, B. J.; Lazarus, A. L. *J. Geophys. Res., C: Oceans Atmos.* **1980**, *85*, 7322–7328.

- (11) Schiff, H. I.; Hastie, D. R.; Mackay, G. I.; Iguchi, T.; Ridley, B. A. *Environ. Sci. Technol.* **1983**, *17*, 352A-364A.
- (12) Appel, B. R.; Wall, S. M.; Tokiwa, Y.; Haik, M. *Atmos. Environ.* **1980**, *14*, 549-554.
- (13) Appel, B. R.; Tokiwa, Y.; Haik, M. *Atmos. Environ.* **1981**, *15*, 283-289.
- (14) Braman, R. S.; de la Cantera, M. A. *Anal. Chem.* **1986**, *58*, 1533-1537.
- (15) Kelly, T. J.; Stedman, D. H.; Ritter, R. A.; Harvey, R. B. *J. Geophys. Res.* **1980**, *85*, 7417-7425.
- (16) Weast, R. C.; Ed. *CRC Handbook of Chemistry and Physics*, 67th ed.; CRC: Boca Raton, FL, 1986.
- (17) Fried, A.; Sams, R. L.; Dorko, W.; Elkins, J.; Cai, Z.-T. *Anal. Chem.* **1988**, *60*, 394-403.
- (18) Fehsenfeld, F. C.; Dickerson, R. R.; Huebler, G.; Luke, W. T.; Nunnermacker, L. J.; Williams, E. J.; Roberts, J. M.; Calvert, J. G.; Curran, C. M.; Delany, A. C.; Eubank, C. S.; Fahey, D. W.; Fried, A.; Gandrud, B. W.; Langford, A. O.; Murphy, P. C.; Norton, R. B.; Pickering, K. E.; Ridley, B. A. *J. Geophys. Res.*, *D: Atmos.* **1987**, *92*, 14710-14822.
- (19) Joseph, D. W.; Spicer, C. W. *Anal. Chem.* **1978**, *50*, 1400-1403.
- (20) Eatough, D. J.; White, V. F.; Hensen, L. D.; Eatough, N. L.; Ellis, E. C. *Anal. Chem.* **1985**, *57*, 743-748.
- (21) Sanhueza, E.; Plum, C. N.; Pitts, J. N., Jr. *Atmos. Environ.* **1984**, *18*, 1029-1031.
- (22) Delany, A. C.; Dickerson, R. R.; Melchior, F. L.; Jr.; Wartburg, A. F. *Rev. Sci. Instrum.* **1982**, *53*, 1899-1902.
- (23) Dickerson, R. R.; Delany, A. C.; Wartburg, A. F. *Rev. Sci. Instrum.* **1984**, *55*, 1995-1998.
- (24) Sams, R. L.; Fried, A. *J. Mol. Spectrosc.* **1987**, *126*, 129-139.
- (25) Sams, R. L.; Fried, A. *Appl. Opt.* **1987**, *26*, 3552-3558.
- (26) Maki, A. G. *J. Mol. Spectrosc.* **1988**, *127*, 104-111.
- (27) Giver, L. P.; Valero, F. P. J.; Goorvitch, D.; Bonomo, F. S. *J. Opt. Soc. Am. B: Opt. Phys.* **1984**, *1*, 715.
- (28) May, R. D.; Webster, C. R.; Molina, L. T. *J. Quant. Spectrosc. Radiat. Transfer* **1987**, *38*, 381-388.
- (29) Humlicek, J. *J. Quant. Spectrosc. Radiat. Transfer* **1979**, *21*, 309-313.

Received for review April 1, 1988. Accepted July 13, 1988. This work was supported in part by the Research Corp. (Grant 10242), NSF Grants ATM-83-05843 and ATM-86-8619491, and EPA/NBS IAG DW13931661-01-0. Mention of trade names or commercial products is for information only and does not constitute endorsement or recommendations for use.

Paleolimnological Evidence for Trace-Metal Sensitivity in Scaled Chrysophytes

Sushil S. Dixit,^{*†} Aruna S. Dixit,[†] and R. Douglas Evans[†]

Department of Biology, Queen's University, Kingston, Ontario K7L 3N6, Canada, and Trent Aquatic Research Centre, Trent University, Peterborough, Ontario K9J 7B8, Canada

■ A stratigraphic study of scaled chrysophyte microfossils (golden-brown algae) in the sediments of three Sudbury, Ontario, lakes was initiated to examine their sensitivity to increased trace-metal pollution. Corresponding to an increase in metal input at the beginning of this century, the chrysophyte abundance declined greatly in Lohi and Clearwater Lakes. In Hannah Lake the deposition of scales has increased significantly since 1975 when the lake was limed. The changes correspond closely with changes in the metal concentrations within the lakes. The study provides paleolimnological evidence for sensitivity of chrysophytes to trace metals and suggests that in soft-water lakes increases in metal concentrations can cause major changes in the chrysophyte community.

Introduction

Algal microfossils deposited in lake sediments have been used widely to reconstruct changes in lake water chemistry (1-5). Whereas most of the recent work has centered on the prediction of lake water pH from shifts in diatom species composition (2, 4), scaled chrysophytes (Mallomonadaceae, Chrysophyceae) also have been suggested as possible pH indicators (5, 6). One problem with interpreting reconstruction of a particular chemical parameter is that environmental changes are often accompanied by simultaneous changes in other water-column constituents. For example, it has been found that a decline in lake water pH often leads to a concomitant increase in trace-metal concentrations (7, 8).

Field enclosure and laboratory studies have found that specific trace-metal concentrations are toxic to green algae

(9, 10), but no such comparable studies exist for the chrysophytes. It is possible that this group, like the green algae, is affected adversely by increased concentrations of certain metals. If chrysophyte species are affected by changes in trace-metal concentrations, the influence of metals needs to be known in order to enhance their use in paleoenvironmental reconstructions.

The objective of our study is to investigate trace-metal sensitivity of chrysophytes by utilizing sites where metal concentrations have increased due to human activity. Sediment metal profiles indicate that there have been large increases in concentrations of many trace metals in many North American lakes in recent years (2, 7, 11). The Sudbury area of Ontario, Canada, offers a unique situation because many lakes in this area have undergone large additions of trace metals due to extensive metal smelting and mining activities (7). The lakes also underwent large increases in acidity, with lake pHs in the area commonly falling in the range of 4.5-5.0 (12). Three lakes from this area, Lohi (46°21' N 81°01' W), Clearwater (46°22' N 81°03' W), and Hannah (46°21' N 81°02' W), were selected for this study.

Methods

In July 1984, a sediment core (ca. 20 cm long) from the deepest site of each of the study lakes was obtained by using a modified Kajak-Brinkhurst (K-B) gravity corer (13). The cores were sliced into 0.25-cm sections to a depth of 2.5 cm, 0.5-cm sections from 2.5 to 5.0 cm, 1-cm segments from 5 to 15 cm, and thereafter in segments of 2 cm. Chrysophyte scales were isolated from the sediment subsamples with concentrated sulfuric acid and potassium dichromate. Cleaned quantitative subsamples were placed in evaporation plates (14) and microfossil-coated cover slips

^{*}Queen's University.

[†]Trent University.

were mounted by using Hyrax mounting media. For each sample an average of 400 scales was identified and counted in random fields at 1000 \times magnification. Accumulation rates of scales to the sediments were computed [accumulation rate (scales \cdot cm $^{-2}\cdot$ year $^{-1}$) = (scales-dry sediment mass g $^{-1}$) \times sedimentation rate (g of dry sediment \cdot cm $^{-2}\cdot$ year $^{-1}$)].

Sediment cores were analyzed for Ni, Cu, Pb, Zn, Fe, and Al concentrations. Sediment samples from various levels were dried for 24 h at 90 $^{\circ}$ C and then digested overnight at 70 $^{\circ}$ C with a 2:1 mixture of HCl and HNO $_3$. The metal concentrations were determined at appropriate wavelengths with a Varian flame atomic absorption spectrophotometer. The cores were dated by the 210 Pb technique. The 210 Pb activity in sediment samples was measured following the method of Eakins and Morrison (15), and the constant rate of supply model (16) was used for calculating the dates. The unsupported 210 Pb activity in cores indicated typical log-linear relationship with depth (17). The absence of mixing zones suggested that the sediment cores were undisturbed.

Results and Discussion

In Lohi and Clearwater Lakes, the concentrations of Cu and Ni, prior to anthropogenic activity (Figure 1), are comparable to background concentrations in lakes from several regions of North America (2, 11, 18). However, at the beginning of this century, Cu and Ni inputs increased in both lakes causing the observed changes in sediment concentrations. The increase in Cu and Ni occurred somewhat earlier in Hannah Lake, and the pre-anthropogenic concentrations were higher in comparison to Lohi and Clearwater Lakes (Figure 1). This is most likely due to metal input from Cu- and Ni-rich sulfide deposits in the drainage basin and from open-pit roasting of ore in the latter part of the last century. By the end of the 1920s, the metal input had increased significantly in the sediments of all three lakes, but in Clearwater and Lohi Lakes the largest increase occurred after the installation of the 155-m stack at Copper Cliff in 1923. Highest concentrations of Cu and Ni were observed in the sediments of Hannah Lake—a result of its proximity to the Copper Cliff Smelter (4 km). Lohi and Clearwater Lakes, located 12 km downwind from the smelter, received less input.

In all three lakes the increase in anthropogenic Pb and Zn occurred about 80–100 years ago (Figure 2), and the concentrations are typical of lakes in southern Ontario (18, 19). This suggests that the increase in Pb and Zn is not mainly due to metal-smelting activity in the Sudbury area, but is significantly influenced by the long-range transport of atmospheric pollutants. Moreover, the fact that there is no increase in concentration of these metals with decreasing distance from Sudbury, as seen for Cu and Ni (20), also suggests that there is little influence of localized activity on the concentrations of Zn and Pb. The small local effect is expected because the metal ores of the Sudbury area contain low amounts of Pb and Zn (7).

Although Fe concentrations are higher in the recent sediments of all three lakes (Figure 2), the profiles may not necessarily indicate a real increase in input because of the mobility of Fe in anoxic sediments. The aluminum sediment metal profiles of the study lakes are deceptive (Figure 2). They indicate that in Hannah and Clearwater Lakes the Al levels have increased slightly in the past, whereas in Lohi Lake first there was an increase in Al, but later the levels declined to the background level. Although the lack of any definite pattern in Al is most likely due to its mobilization from the sediments to the water column as a result of recent lake acidification (21), variation in the

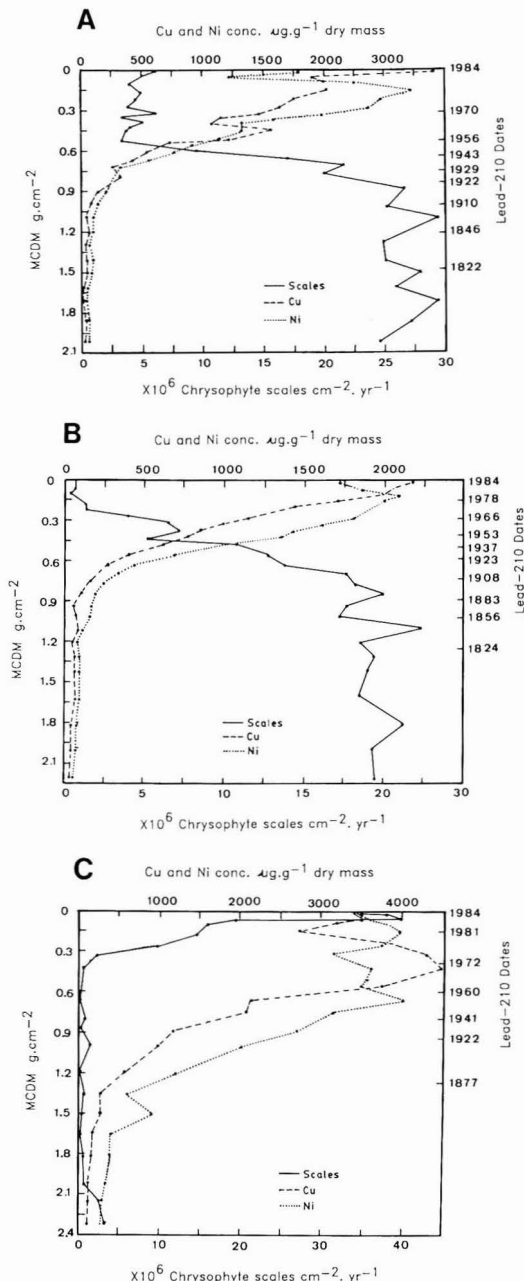


Figure 1. Cu and Ni concentrations and the accumulation of chrysophyte scales in (A) Lohi, (B) Clearwater, and (C) Hannah Lakes. Core depth is expressed as MCDM (midpoint cumulative dry mass of sediment per unit area) to take into account sediment compaction (39).

rate of sedimentation or composition of the matrix (organic matter, non-Al-bearing minerals) may have also played an important role.

Sulfur deposition must have increased about the same time that metal input increased in the study lakes. However, the inferred pH reconstruction study indicates that in Clearwater and Lohi Lakes acidification occurred since \sim 1930, whereas in Hannah Lake acidification occurred

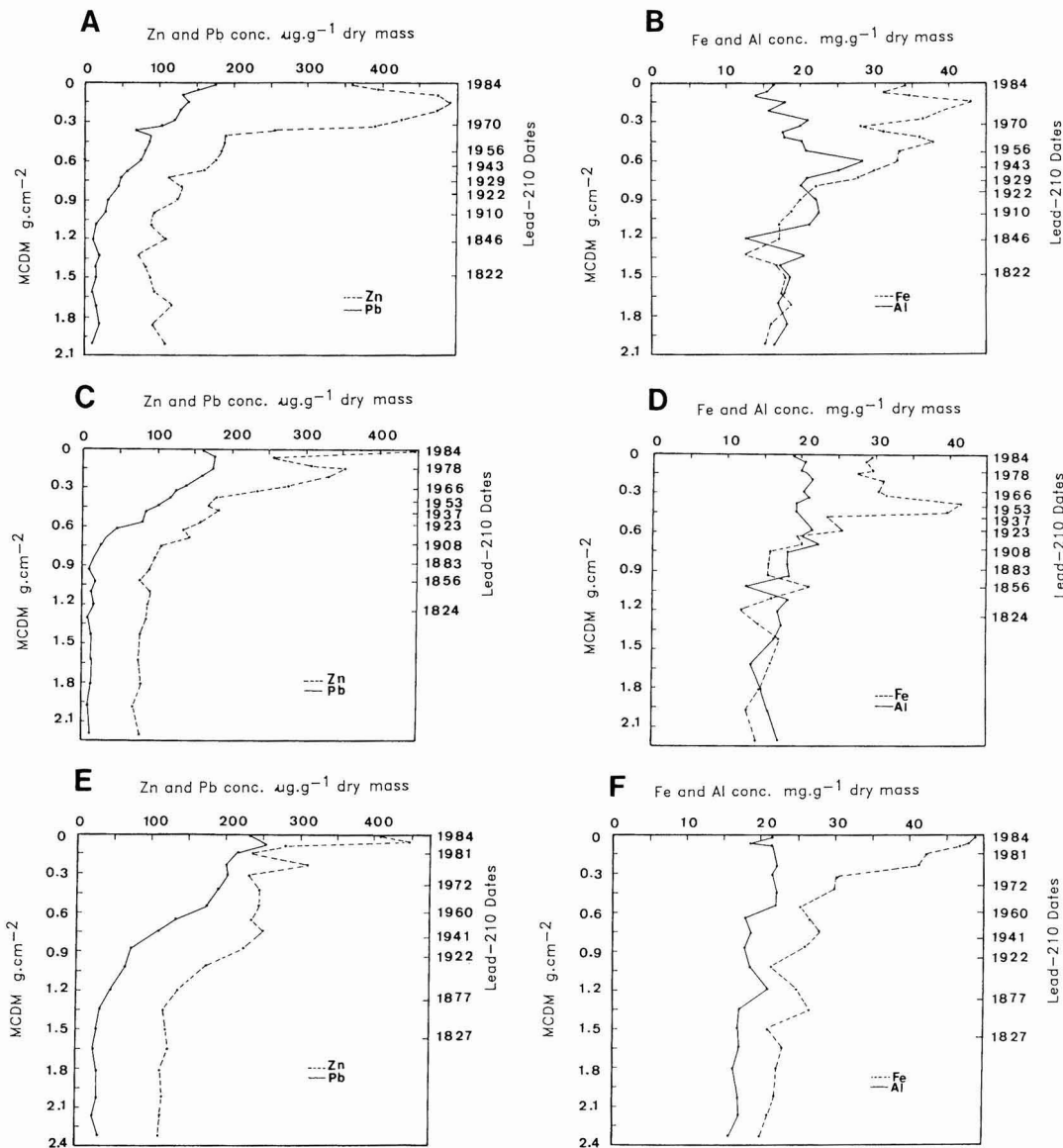


Figure 2. Zn, Pb, Fe, and Al concentrations in Lohi (A, B), Clearwater (C, D), and Hannah (E, F) Lakes.

after 1880 (17, 22). Although a complex of factors may be responsible for the ~30-year delay in acidification from the time when metal input increased in Clearwater and Lohi Lakes, the existing buffering ability of lakes and their watersheds may have played the lead role, especially at a time when tall stacks were not installed (pre-1920). In soft-water lakes, bicarbonates provide most of the buffering and the pH of these waters declines slowly to the pH value 5.6, but when pH declines below 5.6 the bicarbonates are lost and then rapid acidification occurs (23, 24). Dillon et al. (8) and Seip (25) indicated that calcareous soils or carbonate-rich material in the watershed of a lake assimilate hydrogen ions and continue to provide a buffering system until the buffering ability is completely exhausted. Recently it has been also demonstrated that both hypolimnetic and epilimnetic sediments can generate significant amounts of alkalinity in lakes to neutralize input of acidic

precipitation (26, 27). In situ alkalinity production can be the most important source of alkalinity in lakes that have low water-column alkalinity (28). Because the background (pre-1930) pH of Clearwater and Lohi Lakes was about 6.5, this mechanism would have provided resistance against the rapid decline in lake water pH.

In Hannah Lake, no marked delay was noticed between the timing of acidification and trace-metal input. Massive emissions of SO₂ from the open-pit roasting of ore near Hannah Lake were likely to have consumed the lake's buffering capacity in a short time. Moreover, Hannah Lake would have acidified rapidly because its background inferred pH (~5.8) was about 1 pH unit lower than Clearwater and Lohi Lakes. Hannah Lake's pH was very close to the pH value (pH 5.6) at which the primary buffering components, bicarbonates, are replaced by sulfate. This shift in ionic balance was most likely accom-

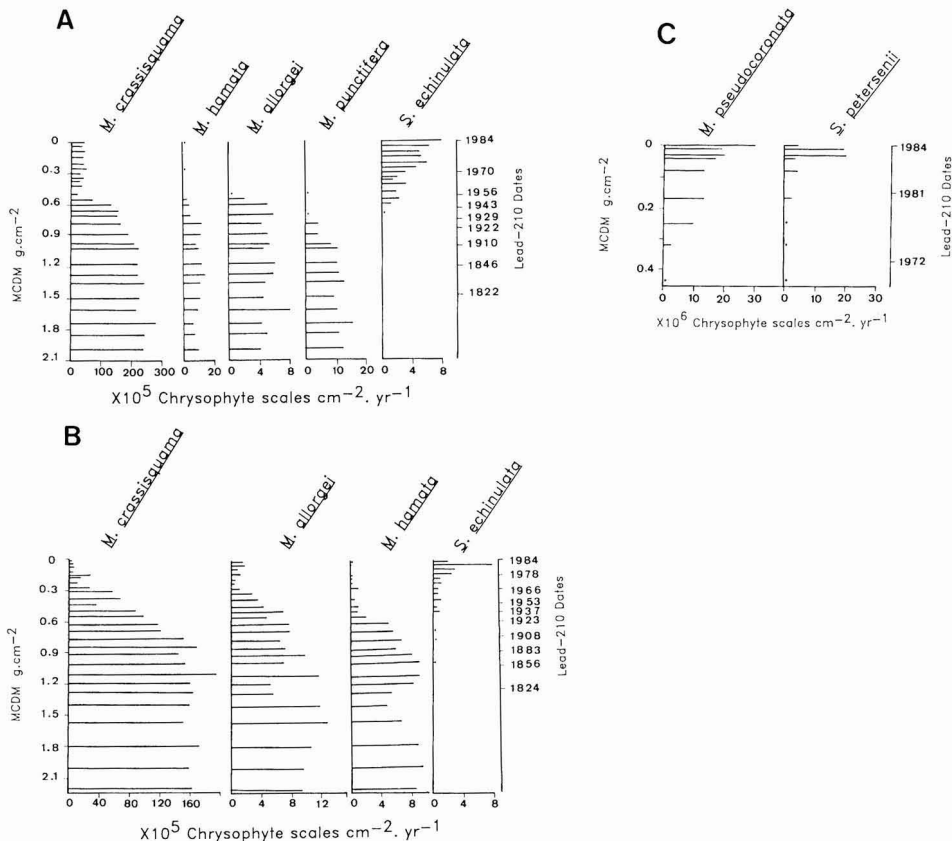


Figure 3. Accumulation rates of scales of common chrysophyte taxa in (A) Lohi, (B) Clearwater, and (C) Hannah Lakes.

panied by a rapid decline in lake water pH.

In addition to factors mentioned above, the increase in sediment metal concentrations may precede increases in inferred acidity because in acidic lakes metals may diffuse into the sediments and be retained several centimeters below the mud-water interface (29, 30). Moreover, it is valid to hypothesize that before acidification, the metal inputs to lake sediments were proportional to the atmospheric input, because under natural conditions sediment retention of metals is quite high (18, 19). Once acidification occurred, the same proportion of metal would not have reached the sediment because a significant amount of the total metal input would have remained in solution at the reduced pH of the lake waters. The loading of metals may have been much higher after acidification than indicated by the sediment metal profiles. Thus, as with any other paleolimnological study, we can not provide absolute inferences of past lake water metal concentrations, but can estimate trends of increasing metal concentrations in lake water with confidence.

In the sediments of Lohi and Clearwater Lakes, the accumulation rate of chrysophycean scales remained relatively stable until about 1920 (Figure 1), but then declined dramatically. The decline mirrors closely the increase in metal inputs and acidification, within 10–15 years. While it is impossible from these data to attribute specific sensitivity to either Cu or Ni, or one of the other trace metals that was increasing in concentration at this time, literature for other algal groups (9, 10) suggests that metal toxicity may be the likely cause of the decline in chrysophyte

populations. A close evaluation of the time scale indicates that the decline occurred at a time of modest metal increase. The changes in scale deposition cannot be explained by the lake water pH because of the lack of similar declines in the deposition of chrysophyte scales in lakes that have recently acidified (5, 31, 32).

In addition to examining the decline in chrysophycean assemblages of Clearwater and Lohi Lakes (Figure 1), the accumulation rates of common chrysophyte taxa were computed to investigate (a) the interspecies differences in metal sensitivity in chrysophytes and (b) the possibility of using chrysophytes as pH indicators when their assemblages are influenced by metals.

In Clearwater and Lohi Lakes, *Mallomonas crassisquama* was the most abundant taxon (Figure 3), and in both lakes, its population has declined greatly since the beginning of this century. In earlier studies (31–34) *M. crassisquama* was identified as a pH generalist, but one that avoided very acidic waters (pH < 5). Because the decline of this taxon was concurrent with the increase in metal inputs, it may be that *M. crassisquama* is sensitive to high metal concentration and this may be a reason why declines were observed in earlier studies, at pH values where metals have high desorption. The declines in *Mallomonas hamata* started about 1920, and only trace levels remained in the recent sediments (Figure 3). Because this taxon is usually most competitive in acidic (pH < 5) waters (6, 31), theoretically the abundance of *M. hamata* should increase as lakes acidified. However, its decline probably reflects its sensitivity to metals. The poor

Table I. Pre- and Postneutralization Values for Lake Water pH, Cu, and Ni in Hannah Lake (17, 35)

year	pH	Cu, $\mu\text{g/L}$	Ni, $\mu\text{g/L}$
1973	4.31	1090	1620
1974	4.29	1110	1870
1975	7.02	58	346
1976	6.67	52	427
1977	6.59	41	393
1978	6.96	45	307
1979	7.07	25	233
1984	6.81	22	19

representation of this taxon in the surface sediment samples of acidic lakes with high metal concentrations near Sudbury (6) also indicates that *M. hamata* is a metal-sensitive species. It is likely that in acidic lakes of low metal concentrations, *M. hamata* is a pH indicator species, but when metal concentrations increase it also responds to metals.

The increase of *Synura echinulata* and the decline in *Mallomonas allorgei* coincided with acidification (~1930) in Lohi and Clearwater Lakes. *S. echinulata* is an acidic species (17, 31, 33), whereas *M. allorgei* is a circumneutral taxon (34). The close correspondence between the timing of increase in *S. echinulata* and acidification (as inferred by diatoms) not only substantiates that in Clearwater and Lohi Lakes acidification commenced about 1930 but also suggests that in lakes of high metal concentrations *S. echinulata* can be a valuable indicator of lake acidification. For unknown reasons, *S. echinulata* appears to be unaffected by metals.

Unlike Lohi and Clearwater Lakes, chrysophyte populations in Hannah Lake remained relatively unchanged but at a very low level until 1975 (Figure 1). In 1975 the lake was artificially neutralized and the lake water pH increased from 4.3 to 7.0 (35). Initially, these results may seem at odds with those from the other two study lakes. However, the results do in fact support the hypothesis of metal sensitivity in the chrysophytes. In comparison to Lohi and Clearwater Lakes, very few scales were deposited in Hannah Lake's sediments prior to 1930. As noted earlier, pre-1930 metal concentrations in this lake appear to have been much higher than in the other two lakes, presumably for the geologic reasons discussed earlier. For example, the background Cu concentrations in the sediment of this lake (Figure 1) were significantly higher (122–192 $\mu\text{g-g dm}^{-1}$) than those observed in Lohi and Clearwater (48–91 and 44–84 $\mu\text{g-g dm}^{-1}$, respectively). The sediment metal concentrations in both these lakes at the time of the decline of chrysophytes are below the concentrations found in Hannah as early as 1880. A close correspondence between the sediment metal concentrations at which chrysophytes declined in Clearwater and Lohi Lakes and background metal concentrations of Hannah Lake at which chrysophyte populations remained low supports our conclusions.

Since 1975 there has been an ~40-fold increase in the deposition of scales in Hannah Lake (Figure 1). The change was due exclusively to increases in *Mallomonas pseudocoronata* and *Synura peterseii* (Figure 3). While it is tempting to hypothesize that this increase is a result of decreased acidity, there is evidence to suggest that the changes may be also metal-related. Measurements of water-column concentrations of Cu and Ni prior to and after neutralization indicate a 10–20-fold reduction in metals (Table I). Scaled chrysophytes are exclusively planktonic and thus will be affected by lake water metal concentrations. The increase in pH from 4.3 to 7.0 resulted

in removal and precipitation of a significant portion of the labile metal pool (35). This appears to be a reason why the sediment concentrations of Cu and Ni have not dropped as precipitously as the water concentrations. At a pH of 7.0, the existing metal concentrations in the water column of Hannah Lake appear to be acceptable for the chrysophytes. We expect these concentrations to be higher than tolerable in low-pH lakes where the major portion of the metals will be in labile form.

The increase of free metal ions in low-pH waters is associated with the dissociation of metal complexes from organic and inorganic ligands. It has been suggested that only a small fraction of free metal ions are major toxic forms (36). Although hydrogen ions regulate chemical speciation of the dissolved metal pool, they also compete with free metal cations for cellular binding sites in algae (37, 38). It is possible that these two responses may be antagonistic. However, in the complex natural environment, the ecological significance of declines in metal uptake at low pH requires careful assessment. The effect of metals on chrysophytes is likely to vary with the ambient water chemistry.

Summary

This study provides paleolimnological evidence that chrysophytes are sensitive to trace-metal contamination. Although the threshold level for sensitivity of various metals and interspecies variability in sensitivity of the chrysophytes require further investigation, the changes in common chrysophyte taxa in study lakes provide an indication that interspecies variability in metal tolerance exists in chrysophytes. For example, *M. crassiquama* and *M. hamata* appear to be metal-sensitive, whereas *S. echinulata* is a metal-tolerant taxon. We suggest that in lakes where metal levels are not high, chrysophytes are useful indicators of pH, but in lakes where metal levels are high, they additionally may be sensitive indicators of excess metal input. Although many questions concerning metal-chrysophyte interactions remain unanswered, there is a strong possibility that continued metal input to soft-water lakes may adversely affect chrysophyte communities.

Acknowledgments

Many thanks to J. P. Smol and J. C. Kingston for providing constructive comments on this manuscript.

Registry No. Co, 7440-50-8; Ni, 7440-02-0; Zn, 7440-66-6; Pb, 7439-92-1; Fe, 7439-89-6; Al, 7429-90-5.

Literature Cited

- (1) Brugam, R. B. *Ecology* 1978, 59, 19–36.
- (2) Charles, D. F.; Norton, S. A. In *Acid Deposition: Long Term Trends*; National Academy Press: Washington, DC, 1986; pp 335–506.
- (3) Davis, R. B.; Anderson, D. S.; Berge, F. *Nature (London)* 1985, 316, 436–438.
- (4) Smol, J. P.; Battarbee, R. W.; Davis, R. B.; Meriläinen, J., Eds. *Diatoms and Lake Acidity*; W. Junk: Dordrecht, The Netherlands, 1986.
- (5) Smol, J. P.; Charles, D. F.; Whitehead, D. R. *Nature (London)* 1984, 307, 628–630.
- (6) Dixit, S. S.; Dixit, A. S.; Evans, R. D. *Can. J. Fish. Aquat. Sci.* 1988, 45, 1411–1421.
- (7) Nriagu, J. O.; Wong, H. K. T.; Coker, R. D. *Environ. Sci. Technol.* 1982, 16, 551–560.
- (8) Dillon, P. J.; Jeffries, D. S.; Snyder, W.; Reid, R.; Yan, N. D.; Evans, R. D.; Moss, J. J. *Fish. Res. Board Canada* 1978, 35, 809–815.
- (9) Gachter, R.; Mares, A. *Schweiz. Z. Hydrol.* 1979, 41, 228–246.
- (10) Petersen, R. *Environ. Sci. Technol.* 1982, 16, 443–447.

- (11) Galloway, G. N.; Likens, G. E. *Limnol. Oceanogr.* **1979**, *24*, 427-433.
- (12) Keller, W.; Gunn, J.; Conroy, N. In *Ecological Impact of Acid Precipitation*; Drablos, D., Tollan, A., Eds.; SNSF Project: Oslo, 1980; pp 228-229.
- (13) Brinkhurst, R. O.; Chua, K. E.; Batoosingh, E. *J. Fish. Res. Board Canada* **26**, 2581-2593.
- (14) Battarbee, R. W. *Limnol. Oceanogr.* **1973**, *18*, 647-656.
- (15) Eakins, J. D.; Morrison, R. I. *Int. J. Appl. Radiat. Isot.* **1978**, *29*, 531-536.
- (16) Appleby, P. G.; Oldfield, F. *Catena (Cremlingen-Destedt, Ger.)* **1978**, *5*, 1-8.
- (17) Dixit, S. S. Ph.D. Thesis, Queen's University, Kingston, 1986.
- (18) Evans, H.; Smith, P. J.; Dillon, P. J. *Can. J. Fish. Aquat. Sci.* **1982**, *40*, 570-579.
- (19) Evans, R. D.; Dillon, P. J. *Hydrobiologia* **1982**, *91*, 131-137.
- (20) Ontario Ministry of Environment, "Studies of Lakes and Watersheds Near Sudbury, Ontario: Final Limnological Report"; No. SES 009/82, Ontario, 1982.
- (21) Cronan, C. S.; Schofield, C. L. *Science (Washington, D.C.)* **1979**, *204*, 304-306.
- (22) Dixit, S. S.; Dixit, A. S.; Evans, R. D. *Sci. Total Environ.* **1987**, *67*, 53-67.
- (23) Wright, R. F.; Gjessing, E. T. *Ambio* **1976**, *5*, 219-223.
- (24) Henriksen, A. In *Ecological Impact of Acidification*; Drablos, D., Tollan, A., Eds.; SNSF Project: Oslo, 1980; pp 68-74.
- (25) Seip, H. M. In *Ecological Impact of Acidification*; Drablos, D., Tollan, A., Eds.; SNSF Project: Oslo, 1980; pp 358-366.
- (26) Kelly, C.; Rudd, J.; Schindler, D.; Cook, R. *Limnol. Oceanogr.* **1982**, *27*, 868-882.
- (27) Kelly, C.; Rudd, J. *Biogeochemistry* **1984**, *1*, 63-74.
- (28) Schindler, D.; Turner, M.; Staiton, M.; Linsey, G. *Science (Washington, D.C.)* **1986**, *232*, 844-847.
- (29) Carignan, R.; Tessier, A. *Science (Washington, D.C.)* **1985**, *228*, 1524-1526.
- (30) Carignan, R.; Nriagu, J. *Geochim. Cosmochim. Acta* **1985**, *49*, 1753-1764.
- (31) Smol, J. P. In *Diatoms and Lake Acidity*; Smol, J. P., Battarbee, R. W., Davis, R. B., Meriläinen, J., Eds.; W. Junk: Dordrecht, The Netherlands, 1986; pp 257-287.
- (32) Christie, C.; Smol, J. P. *Hydrobiologia* **1986**, *143*, 355-360.
- (33) Steinberg, C.; Hartmann, H. *Naturwissenschaften* **1986**, *73*, 137-139.
- (34) Smol, J. P.; Charles, D. F.; Whitehead, D. R. *Can. J. Bot.* **1984**, *62*, 611-630.
- (35) Yan, N. D.; Lafrance, C. In *Environmental Impacts of Smelters*; Nriagu, J. O., Ed.; Wiley: New York, 1984; pp 457-521.
- (36) Sunda, W.; Guillard, R. R. *J. Mar. Res.* **1976**, *34*, 511-529.
- (37) Campbell, P. G. C.; Stokes, P. M. *Can. J. Fish. Aquat. Sci.* **1985**, *42*, 2034-2049.
- (38) Peterson, H. G.; Healey, F. P.; Wagemann, R. *Can. J. Fish. Aquat. Sci.* **1984**, *41*, 974-979.
- (39) Robbin, J. A. In *The Biogeochemistry of Lead in the Environment*; Nriagu, J. O., Ed.; Elsevier: Amsterdam, 1978; pp 285-408.

Received for review March 6, 1987. Revised manuscript received December 9, 1987. Accepted August 2, 1988. This paper is a part of the Ph.D. Thesis of S.S.D. submitted to Queen's University. Financial support was made available in the form of a Queen's Graduate Fellowship to S.S.D. and a NSERC grant to R.D.E.

Oxidative Co-Oligomerization of Guaiacol and 4-Chloroaniline

Kathleen E. Simmons, Robert D. Minard, and Jean-Marc Bollag*

Department of Agronomy and Department of Chemistry, The Pennsylvania State University, University Park, Pennsylvania 16802

■ The polymerization of guaiacol, a humus constituent, and 4-chloroaniline, a pesticide derivative, was catalyzed by oxidoreductases in aqueous solution. The first stages of the polymerization reactions produced five co-oligomeric compounds and six guaiacol-derived oligomers. The oligomers were found to have aminoquinone, carbazole, and iminodiphenoquinone structures. The formation of aminoquinone and nitrogen heterocyclic trimers occurs by nucleophilic addition of 4-chloroaniline to guaiacol-derived dimers. Free-radical reactions were thought to be responsible for the appearance of the remaining three cross-coupled products. Three reaction pathway schemes are proposed that describe initial stages for the incorporation of the aniline into the guaiacol-derived oligomers. Conclusions drawn from this study can be applied in the further investigation of the incorporation of substituted anilines into humus materials.

Introduction

Aniline-based herbicides are readily degraded in soil via chemical and microbial hydrolysis (1), and the environmental fate of the resulting substituted anilines has been the focus of numerous investigations. It has been established that a major pathway of transformation of the substituted anilines in soil involves binding of the residue to soil humic materials (2-5). The nature of binding can range from sorptive forces such as charge-transfer complexation, hydrogen bonding, and hydrophobic interactions

to irreversible covalent bonds that are resistant to acid or base hydrolysis (3, 6), thermal treatment (7), and microbial degradation (3, 6, 8).

Model systems have been used in investigations that have sought to characterize binding sites and the mechanisms involved in the incorporation of substituted anilines into soil organic matter. Anilines were reacted with humus constituents, or humus analogues, and some of the reaction products were structurally identified (9-13). Results indicated that the anilines were involved in Michael addition to quinonoid rings of the humuslike compounds, with subsequent tautomerization and oxidation to yield stable aminoquinone adducts (9, 10, 12). Other investigators have found that cross-coupling of substituted anilines with a monomeric humus constituent occurred when a solution of the two substrates was incubated with an enzyme of a soil fungus (11) or with a soil-water slurry (13). The benzoquinone monoimine dimeric structure of the resulting products suggests that free-radical coupling had occurred. Cyclization of bound aniline residues with adjacent humic quinonoid groups could result in nitrogen heterocycle formation, which would further alter the character of the bound aniline by multiplying the bonds between the residue and the soil organic matter (9). However, nitrogen heterocyclic product structures have not been isolated from reactions of substituted anilines with humus analogues or with natural humus materials.

We reported previously about studies of the initial products formed from 4-chloroaniline alone (14, 15) and

from guaiacol (16) after incubation with oxidoreductases. The goal of the investigation presented here was to more clearly characterize the incorporation of an aniline, 4-chloroaniline, into humuslike oligomers. Oxidative polymerization of 4-chloroaniline and guaiacol was catalyzed by enzymes, and the resulting co-oligomers were isolated and structurally identified. In conclusion, from these data we propose reaction pathways that account for the formation of the identified co-oligomeric products.

Materials and Methods

Chemicals. Guaiacol (2-methoxyphenol) was purchased from Fluka Chemical Corp. (Ronkonkoma, NY) and 4-chloroaniline from Aldrich Chemical Co. (Milwaukee, WI). Guaiacol and 4-chloroaniline were 98% pure as confirmed by thin-layer chromatography (TLC) and high-performance liquid chromatography (HPLC).

Reaction Conditions. All reactions were conducted at 24 °C in citrate/phosphate buffers of pH 7.3 or 5.5, with guaiacol and/or 4-chloroaniline, each at concentrations of 1 $\mu\text{mol/mL}$. The catalyst was added, and at the specified incubation time, the enzymatic reactions were stopped by adjusting the solution to pH 2.5 with acetic acid. Boiled enzymes were used in control samples. HPLC was used in the analysis of the reaction product mixtures.

Manganese Dioxide. Manganese dioxide was purchased from Sigma Chemical Co. (St. Louis, MO), and 0.025 g/mL was added to the reaction solution of pH 5.5. The manganese dioxide catalyzed reaction was allowed to proceed for 10 min before acidification and filtration of the solution.

Tyrosinase. Tyrosinase, with an activity of 3300 tyrosinase units/mg, was purchased from Sigma. A tyrosinase unit is defined as the amount of enzyme that will cause an increase in absorption (at 280 nm) of 0.001 unit/min at 25 °C in a 3-mL reaction mixture (pH 5.5) containing L-tyrosine. Tyrosinase (0.41 tyrosinase unit/mL) was added to the reaction solution, pH 5.5, and incubated for 15 min.

Peroxidase. Horseradish peroxidase, with a Reinheitszahl of 0.43 and an activity of 45 purpurogallin units/mL, was obtained from Sigma. A purpurogallin unit is defined as the amount of enzyme that forms 1.0 mg of purpurogallin from pyrogallol in 20 s at pH 6.0 and 25 °C. (Purpurogallin concentration is measured by its absorption at 420 nm.) Peroxidase reactions were conducted at pH 5.5, and hydrogen peroxide was added at a concentration of 2.5 $\mu\text{mol/mL}$. The reaction was stopped after 2 min.

Laccases. The extracellular laccases of *Rhizoctonia praticola* and *Trametes versicolor* were isolated from culture filtrates and purified as previously described (17). The activity of the laccases was expressed as DMP (2,6-dimethoxyphenol) units, which are defined as the amount of enzyme that causes a change in absorbance of 1.0 unit/min at 468 nm for a 3.5-mL aliquot (pH 4.2) containing 3.24 μmol of DMP.

The reaction catalyzed by the laccase of *R. praticola* (0.05 DMP unit/mL) was conducted at pH 7.3 for 15 min. The laccase of *T. versicolor* was incubated with the substrates at pH 5.5 for 2 min at an enzyme concentration of 0.37 DMP unit/mL.

Thin-Layer Chromatography (TLC). TLC was used to isolate the co-oligomers produced in 25-mL reaction solutions (pH 5.5) in which guaiacol and 4-chloroaniline were incubated with the peroxidase (0.36 purpurogallin unit/mL) and hydrogen peroxide (2.5 $\mu\text{mol/mL}$) for 5 min. Enzyme activity was halted by adjusting the pH of the solution to 2.5, and the products were extracted by using a PrepSep C₁₈ column (Fisher Scientific Co., Fairlawn, NJ),

which had been wetted with methanol. After application of the reaction solution, the column was dried under vacuum. The products were removed from the column with 1.0 mL of ethyl acetate, and the ethyl acetate extract was applied to a silica gel 60F-254 plate (EM Science, Darmstadt, West Germany). The plate was developed with a mobile phase of 30/70 (v/v) ethyl acetate/hexane. Individual product bands were extracted from the silica gel with ethyl acetate and were further purified by TLC with a mobile phase of 40/60 (v/v) ethyl acetate/hexane. Additional purification steps were performed by HPLC.

Mass Spectrometry. Molecular weights of products obtained following the oxidation of the combined guaiacol and 4-chloroaniline substrates were determined by electron ionization (70 eV) mass analysis. A Kratos MS 9/50 double-focusing mass spectrometer was used for the analyses, and sample introduction was by direct-insertion probe with the source temperature between 250 and 350 °C.

Nuclear Magnetic Resonance. Product structures were confirmed with proton nuclear magnetic resonance (NMR) spectroscopy. A Bruker WM-360 instrument was used with acetone-*d*₆ as solvent, and decoupling experiments were performed to determine ortho and meta coupling of protons on aromatic rings.

High-Performance Liquid Chromatography. The disappearance of substrates and formation of products were monitored by HPLC. A 40-mL aliquot of the reaction solution was acidified and filtered through a 0.45- μm pore size Nylon 66 membrane (Fisher). The filter was rinsed with 1.0 mL of methanol, which was added to the sample. The sample was immediately analyzed by injecting 200 μL onto a Waters Associates (Milford, MA) high-performance liquid chromatograph, consisting of a U6K injector, M45 and 6000A pumps run by a Model 720 Systems Controller, a Lambda Max 450 LC spectrometer set at 280 nm (0.05 AUFS), and a Model 730 Data Module.

Reverse-phase separation was achieved on a 15 cm \times 4.6 mm Supelcosil LC-18 (bonded octadecylsilane) column of 5- μm particle size from Supelco, Inc. (Bellefonte, PA). The mobile phase at a flow rate of 1.5 mL/min was a mixture of an aqueous component A (2% acetic acid/0.018 M ammonium acetate in water, pH 3.3) and an organic component B (2% acetic acid/0.018 M ammonium acetate in methanol). The initial mobile-phase composition of 68/32 A/B was held for 3 min and was then brought to 48/52 A/B by 12 min and held at 48/52 A/B for 3 min. Between 15 and 28 min, the composition was brought from 48/52 A/B to 20/80 A/B, and this final composition was held for 16 min. The column was equilibrated at initial conditions for 10 min before each injection. Retention times were reproducible to 0.1 min.

HPLC retention times for the co-oligomers formed following the oxidative coupling of guaiacol and 4-chloroaniline were obtained from coinjecting the reaction solution samples with pure isolates of the individual compounds. The co-oligomers were labeled compounds B–F, in order of their elution from the HPLC column.

Quantitation of guaiacol and 4-chloroaniline was achieved by using calibration curves that were constructed from injections of standard solutions of the pure substrates. All quantitative data points are averages obtained from injections of triplicate samples.

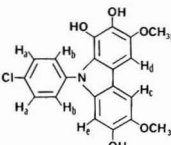
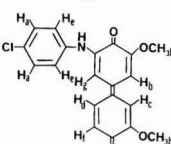
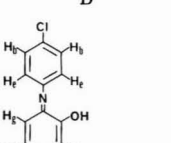
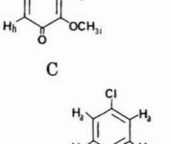
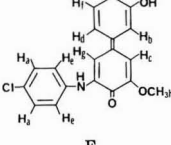
HPLC was also used to purify the TLC-isolated co-oligomers for structural analysis. The isolate was dissolved in 80/20 (v/v) buffer (pH 5.5)/methanol and 1.5 mL was injected onto the column. A mobile-phase composition of 40/60 A/B, at 1.5 mL/min, was used. The eluted peak

Table I. Characterization of Co-Oligomers Derived from Guaiacol and 4-Chloroaniline

compound	TLC R_f	MW		
		calcd	measd ^a	formula ^a
B trimer [9-(4-chlorophenyl)-3,6-dimethoxy-1,2,7-trihydroxycarbazole]	0.19	385.0718	385.0713	C ₂₀ H ₁₆ NO ₅ Cl
C trimer [3-hydroxy-3'-methoxy-N-(4-chlorophenyl)-4-imino-4'-diphenoquinone]	0.36	341.0820	341.0808	C ₁₉ H ₁₆ NO ₃ Cl
D trimer [5-(4-chloroanilino)-3,3'-dimethoxy-4,4'-diphenoquinone]	0.45	369.0769	369.0736	C ₂₀ H ₁₆ NO ₄ Cl
E trimer [6-chloro-3-hydroxy-3'-methoxy-N-(4-chlorophenyl)-4-imino-4'-diphenoquinone]	0.61	375.0244	375.0241	C ₁₉ H ₁₃ NO ₃ Cl ₂
F tetramer [3-(4-chloroanilino)-3'-hydroxy-5-methoxy-N-(4-chlorophenyl)-4'-imino-4-diphenoquinone]	0.76	464.0696	464.0666	C ₂₅ H ₁₈ N ₂ O ₃ Cl ₂

^a Values obtained with high-resolution electron ionization mass spectrometry.

Table II. Proton NMR Data for Co-Oligomeric Products from the Oxidation of Guaiacol and 4-Chloroaniline

compound	chem shift, ppm	splitting ^a (integral)	proton assignmt	coupling const, Hz	
	6.91	d (2 H)	H _a	8.8	
	6.78	d (2 H)	H _b	8.8	
	6.52	s (1 H)	H _c		
	6.51	s (1 H)	H _d		
	6.05	s (1 H)	H _e		
	3.90	s (3 H)	H _f		
	3.62	s (3 H)	H _g		
	7.45	d (2 H)	H _a	8.8	
	7.26	d (1 H)	H _b	2.4	
	7.24	d (1 H)	H _c	2.5	
	7.13	dd (1 H)	H _d	8.3, 2.5	
	6.99	d (2 H)	H _e	8.8	
	6.90	d (1 H)	H _f	8.3	
	6.28	d (1 H)	H _g	2.4	
	3.90	s (6 H)	H _h		
	7.24	m (1 H)	H _a		
	7.23	d (2 H)	H _b	8.6	
	7.14	m (1 H)	H _c		
	7.13	m (1 H)	H _d		
	7.10	d (2 H)	H _e	8.6	
	7.02	m (1 H)	H _f		
	6.98	d (1 H)	H _g	8.0	
	6.86	d (1 H)	H _h	8.0	
	3.91	s (3 H)	H _i		
		7.43	d (4 H)	H _a	8.6
		7.29	d (1 H)	H _b	2.0
7.27		d (1 H)	H _c	2.5	
7.18		dd (1 H)	H _d	8.3, 2.0	
6.98		d (4 H)	H _e	8.6	
6.92		d (1 H)	H _f	8.3	
6.38		m (1 H)	H _g		
3.92		s (3 H)	H _h		
					

^a s, singlet; d, doublet; dd, doublet of doublets; m, multiplet.

was collected, combined fractions were diluted with 200 mL of water, and the resulting solution was extracted twice with 50 mL of methylene chloride. The extract solvent was removed by rotary evaporation at 35 °C, and the purity of the residue was confirmed by HPLC.

Results

Oxidoreductases were used to catalyze the co-oligomerization of 4-chloroaniline and guaiacol. Horse-radish peroxidase is readily available, so it was used to produce the co-oligomers on a preparatory scale as needed for the structural studies. The laccase of *T. versicolor*, which was isolated and purified in our laboratory, catalyzes

the co-oligomerization reactions without inhibition effects and was therefore used in the analytical studies. Although the mechanisms of substrate oxidation are different, both enzymes catalyze the one-electron oxidation of 4-chloroaniline and guaiacol.

Guaiacol and 4-chloroaniline were incubated with the peroxidase, and the resulting products were isolated by solid-phase extraction and separated with TLC, and their structures were determined by mass spectrometry and proton NMR. Table I lists chemical names, molecular weights, molecular formulas, and TLC R_f values for the five co-oligomeric products. Table II lists the proton NMR data for four of the products.

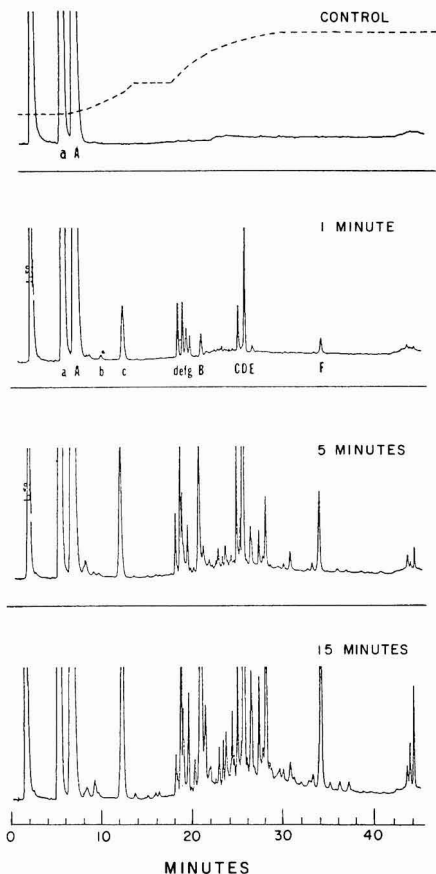


Figure 1. HPLC chromatograms of product mixtures obtained with a boiled enzyme control (after 15 min) and after a 1-, 5-, and 15-min incubation of guaiacol (peak a) and 4-chloroaniline (peak A) with the laccase of *T. versicolor*. Compounds b-g are guaiacol-derived oligomers and compounds B-F are co-oligomers. The dashed curve in the control chromatogram represents the mobile-phase gradient.

The laccase of *T. versicolor* (0.83 DMP unit/mL) was used to catalyze the transformation of a guaiacol and 4-chloroaniline in aqueous solution, and product formation was monitored by HPLC. The chromatograms for 0-, 1-, 5-, and 15-min enzyme incubations are shown in Figure 1. The first five co-oligomers (peaks B-F) were detected after 1 min of incubation with the enzyme. Five guaiacol-derived oligomers (peaks a-g), which have been identified previously (16), also appear in the same chromatogram. Additional peaks are observed after 5 and 15 min of incubation time, but the structures of these compounds were not determined.

Various inorganic and biological soil components were examined for their ability to initiate the co-oligomerization of guaiacol and 4-chloroaniline. The same five co-oligomers produced in the *T. versicolor* laccase-mediated reaction were also found in reaction solutions where manganese dioxide, peroxidase, laccase of *R. praticola*, and tyrosinase were used as oxidants. HPLC chromatograms of the five reaction product mixtures are shown in Figure 2. Reaction conditions are listed under Materials and Methods.

The disappearances of 4-chloroaniline and guaiacol were monitored by HPLC. When 4-chloroaniline was incubated at pH 5.5 with the laccase of *T. versicolor* (0.76 DMP unit/mL) or with horseradish peroxidase (0.023 purpuro-

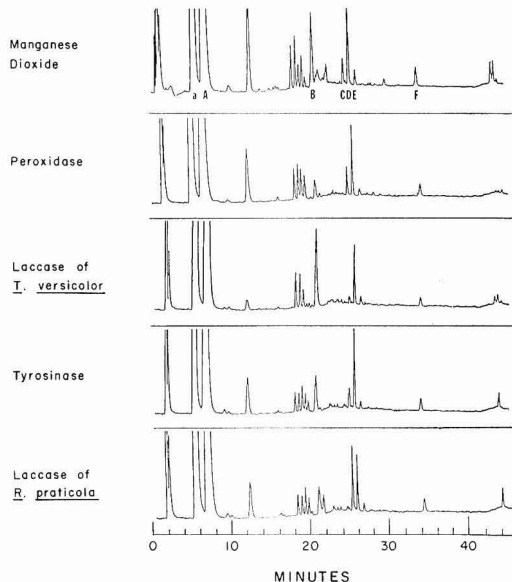


Figure 2. HPLC chromatograms of product mixtures containing various soil components as reaction initiators for the co-oligomerization of guaiacol (peak a) and 4-chloroaniline (peak A). Compounds B-F are identified in Table I.

gallin unit/mL), very little substrate disappearance was noted. However, when 4-chloroaniline was incubated with the laccase of *T. versicolor* in the presence of guaiacol, the 4-chloroaniline disappearance was considerably enhanced (Figure 3). Guaiacol was easily transformed by the oxidoreductases as evidenced by its disappearance in the *Trametes* laccase and the peroxidase assays. When guaiacol was incubated with the peroxidase in the presence of 4-chloroaniline, guaiacol disappearance was notably less relative to the transformation observed with guaiacol as the sole substrate (Figure 3). These observations show that guaiacol is a better substrate than 4-chloroaniline for the aforementioned enzyme-mediated reactions, that the transformation of 4-chloroaniline in the laccase solution is enhanced by the presence of guaiacol, and that the disappearance of guaiacol in the peroxidase assay is inhibited by the presence of 4-chloroaniline.

Discussion

Oxidative copolymerization of guaiacol and 4-chloroaniline resulted in the formation of five co-oligomers during the initial stages of the reaction. Because the initially formed co-oligomers were of interest in this investigation, only small amounts of catalysts and short incubation times were used in order to limit the oligomerization reactions. With longer incubation times, additional products were formed which indicates continuation of the polymerization process (Figure 1).

While the product mixture contained six guaiacol-derived oligomers (16), no 4-chloroaniline-derived oligomers (14) were found. Guaiacol is more readily oxidized than 4-chloroaniline, and therefore, it is not surprising that—under the reaction conditions used—only guaiacol-derived oligomers were observed.

The structures of the co-oligomers B-D and F were identified by mass spectrometric and proton NMR analyses. Compound E was isolated, but was rapidly converted to compound C; it was not possible to isolate a sufficient quantity of compound E for proton NMR analysis. On the basis of the conversion of compound E to compound D,

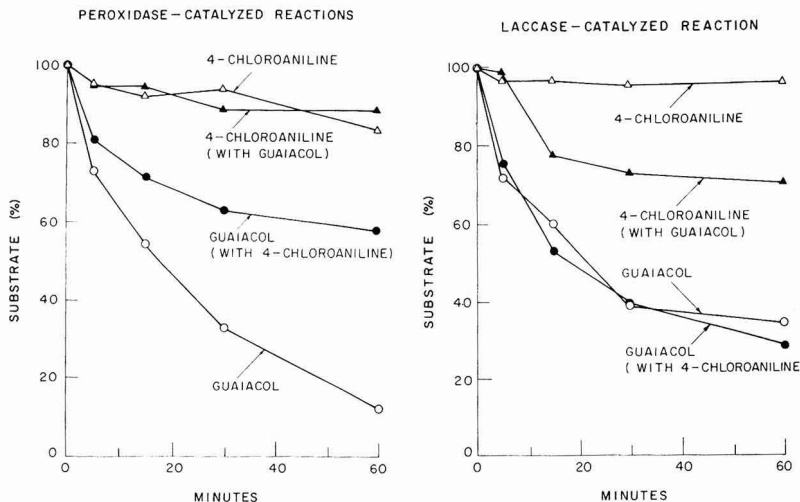


Figure 3. Substrate disappearance curves for peroxidase- and laccase-catalyzed reactions of guaiacol and 4-chloroaniline for solutions of the separate and combined substrates. [The curves labeled "4-chloroaniline" and "guaiacol" present the respective disappearance when used as the only substrate. The curves labeled "4-chloroaniline (with guaiacol)" and "guaiacol (with 4-chloroaniline)" present the disappearance of each substrate when incubated together.]

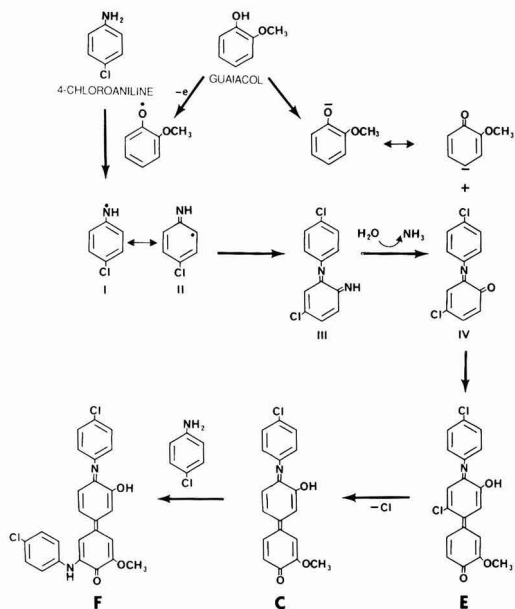


Figure 4. Reaction pathway scheme for the formation of compounds E, C, and F.

and on the high-resolution mass spectrometric data obtained for compounds C and E, compound E is believed to have the same structure as compound C with an ad-

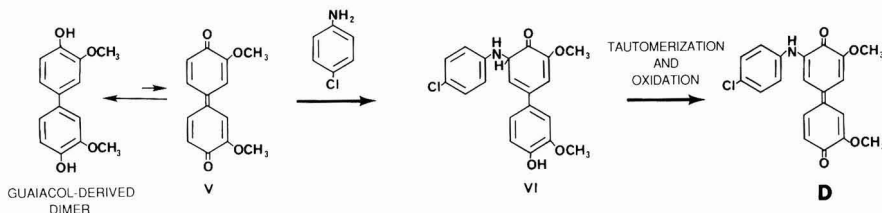


Figure 5. Reaction pathway scheme for the formation of compound D.

ditional chlorine substituent at a position para to the hydroxyl group of the central ring system.

The proposed reaction pathway leading to the formation of compounds E, C, and F (Figure 4) appears to be initiated by the coupling of two anilino free radicals (I and II). Formation of these radicals most likely occurs through the abstraction of an electron from 4-chloroaniline by a guaiacol free radical. Compounds C, E, and F were found in reaction mixtures of guaiacol and 4-chloroaniline which were incubated with tyrosinase and the laccase of *R. praticola* (Figure 2). Neither of these enzymes was found to effect 4-chloroaniline transformation in the absence of guaiacol. Therefore, abstraction of electrons by guaiacol free radicals and not the enzyme-catalyzed oxidation of 4-chloroaniline was probably responsible for the formation of the anilino free radicals shown in Figure 4.

Coupling of the anilino free radicals (I and II) could result in a diimine dimeric intermediate (III), which has been previously implicated in the formation of 4-chloroaniline-derived oligomers (15). Hydrolysis of the intermediate (III) would produce a substituted quinone dimer (IV), and subsequent condensation of that dimer with a resonance-stabilized guaiacol anion, followed by oxidation, could result in the formation of compound E. Spontaneous chlorine loss from compound E would form compound C, and addition of 4-chloroaniline to compound C then leads to the formation of compound F.

It appears that compound D, a trimer, is formed by the nonenzymatic addition of 4-chloroaniline to a guaiacol-derived benzoquinone dimer (V) (Figure 5). Addition of the aniline would result in the formation of an intermediate trimer (VI) which undergoes tautomerization and oxidation

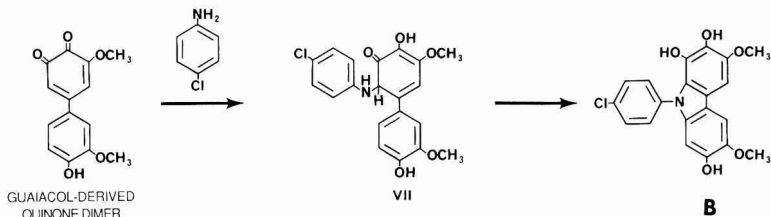


Figure 6. Reaction pathway scheme for the formation of compound B.

to yield the stable aminoquinone trimer (D). In previous studies, only the reduced form of intermediate V was isolated, and therefore the quinone dimer was suggested as a likely precursor in the formation of four guaiacol-derived oligomers (16). The incorporation of 4-chloroaniline apparently stabilizes the oxidized quinonoid form of the para-para guaiacol-coupled dimer, as indicated by the structure of compound D.

Another co-oligomeric trimer, compound B, is thought to be formed by the addition of 4-chloroaniline to an *o*-quinone guaiacol-derived dimer (Figure 6), whose formation is discussed elsewhere (16). Addition of 4-chloroaniline results in a substituted cyclohexadienone intermediate (VII) which likely forms the stable nitrogen heterocyclic compound B through an intramolecular reaction much like that of a dienone-phenol rearrangement (18). The driving force for this rearrangement is the formation of stable aromatic rings (19), such as those found in compound B.

Compound B was also formed when 4-chloroaniline was added to a solution (pH 5.5) of the orange-colored *o*-quinone dimer (observation was not reported under results). The reaction solution changed color from orange to purple within minutes, and the purple reaction product was isolated and found to be compound B.

In our study we examined various inorganic and biological soil components for their ability to co-oligomerize 4-chloroaniline and guaiacol. The addition of manganese dioxide, horseradish peroxidase, tyrosinase, or the laccase of either *T. versicolor* or *R. praticola* to a solution of guaiacol and 4-chloroaniline resulted in the formation of the same five co-oligomeric products (Figure 2).

Since neither the laccase of *R. praticola* nor tyrosinase were found to effect the transformation of 4-chloroaniline alone, and since all the soil components were found to produce guaiacol-derived oligomers (16), it can be assumed that the oxidation of guaiacol is essential to the formation of the co-oligomers described.

Figures 4-6 show chemically rational pathways for the formation of the five co-oligomers found during the initial stages of the guaiacol and 4-chloroaniline reactions. The pathway models can be used to better understand binding of substituted anilines to humus structures. The aniline could be bound to humus materials through nucleophilic addition to humus quinonoid groups, or through free-radical coupling reactions. The nucleophilic additions resulting in aminoquinone and nitrogen heterocycle formations might occur at existing humus core sites, whereas the free-radical reactions are likely to be induced during phenol polymerization, which is an important process during humification.

It has been reported that the addition of ferulic acid, a lignin derivative, to 3,3'-dichlorobenzidine-contaminated soil enhanced the binding of the xenobiotic to soil organic matter (20). The effect was thought to have resulted from an increase in oxidative coupling as mediated by indigenous soil peroxidases. We report analogous results in that,

during laccase-mediated reactions, the transformation of 4-chloroaniline was enhanced in the presence of guaiacol (Figure 3).

The transformation of organic compounds by enzymatic oxidative coupling and polymerization has been suggested for the detoxication of waste water (21-23), and the binding of xenobiotic compounds to humus materials has been discussed as a method of soil decontamination (24). Clearly, further investigations are necessary to evaluate the feasibility of enhancing in situ the enzyme-catalyzed binding of xenobiotics to humic matter or polymerization as a means of soil or waste water decontamination.

Registry No. B, 117309-64-5; C, 117309-65-6; D, 117309-66-7; E, 117309-67-8; F, 117309-68-9; guaiacol-4-chloroaniline polymer, 117309-63-4.

Literature Cited

- (1) Cripps, R. E.; Roberts, T. R. In *Pesticide Microbiology*, Hill, I. R., Wright, S. J. L., Eds.; Academic: New York, 1978; pp 667-730.
- (2) Hsu, T.-S.; Bartha, R. *Soil Sci.* **1974**, *116*, 444-452.
- (3) Bollag, J.-M.; Blattmann, P.; Laanio, T. *J. Agric. Food Chem.* **1978**, *26*, 1302-1306.
- (4) Bartha, R. *ASM News* **1980**, *46*, 356-360.
- (5) Freitag, D.; Scheunert, I.; Klein, W.; Korte, F. *J. Agric. Food Chem.* **1984**, *32*, 203-207.
- (6) Hsu, T.-S.; Bartha, R. *Soil Sci.* **1974**, *118*, 213-220.
- (7) Helling, C. S.; Krivonak, A. E. *J. Agric. Food Chem.* **1978**, *26*, 1156-1163.
- (8) Saxena, A.; Bartha, R. *Soil Biol. Biochem.* **1983**, *15*, 59-62.
- (9) Parris, G. E. *Environ. Sci. Technol.* **1980**, *14*, 1099-1106.
- (10) You, I.-S.; Jones, R. A.; Bartha, R. *Bull. Environ. Contam. Toxicol.* **1982**, *29*, 476-482.
- (11) Bollag, J.-M.; Minard, R. D.; Liu, S.-Y. *Environ. Sci. Technol.* **1983**, *17*, 72-80.
- (12) Saxena, A.; Bartha, R. *Bull. Environ. Contam. Toxicol.* **1983**, *30*, 485-491.
- (13) Liu, S.-Y.; Minard, R. D.; Bollag, J.-M. *J. Environ. Qual.* **1987**, *16*, 48-53.
- (14) Simmons, K. E.; Minard, R. D.; Freyer, A. J.; Bollag, J.-M. *Int. J. Environ. Anal. Chem.* **1986**, *26*, 209-227.
- (15) Simmons, K. E.; Minard, R. D.; Bollag, J.-M. *Environ. Sci. Technol.* **1987**, *21*, 999-103.
- (16) Simmons, K. E.; Minard, R. D.; Bollag, J.-M. *Soil Sci. Soc. Am. J.* **1988**, *52*, 1356-1360.
- (17) Bollag, J.-M.; Sjoblad, R. D.; Liu, S.-Y. *Can. J. Microbiol.* **1979**, *25*, 229-233.
- (18) Shine, H. J. In *Reaction Mechanisms in Organic Chemistry*; Earborn, C., Chapman, N. B., Eds.; Elsevier: New York, 1967; Vol. 6, pp 55-63.
- (19) March, J. *Advanced Organic Chemistry. Reactions, Mechanisms, and Structure*, 2nd Ed.; McGraw-Hill: New York, 1977; pp 962-1072.
- (20) Berry, D. F.; Boyd, S. A. *Environ. Sci. Technol.* **1985**, *19*, 1132-1133.
- (21) Duguet, J. P.; Dussert, B.; Bruchet, A.; Mallevalle, J. *Ozone: Sci. Eng.* **1986**, *8*, 247-260.
- (22) Klibanov, A. M.; Morris, E. D. *Enzyme Microb. Technol.* **1981**, *3*, 119-122.
- (23) Maloney, S. W.; Manem, J.; Mallevalle, J.; Flessinger, F. *Environ. Sci. Technol.* **1986**, *20*, 249-253.

(24) Bollag, J.-M. In *Chemical and Biochemical Detoxification of Hazardous Waste*; J. A. Glaser, Ed.; Lewis: Chelsea, MI, in press.

Office of Research and Development, Environmental Protection Agency (EPA; Grant No. R-811518). The EPA does not necessarily endorse any commercial products used in the study, and the conclusions represent the views of the authors and do not necessarily represent the opinions, policies, or recommendations of EPA. Additional funding was provided by the Pennsylvania Agricultural Experimental Station (journal series no. 7774).

Received for review April 6, 1988. Accepted July 25, 1988. Primary funding for this research project was provided by the

Physical and Chemical Behavior of Stabilized Sewage Sludge Blocks in Seawater

Chih-Shin Shieh*

Department of Oceanography and Ocean Engineering, Florida Institute of Technology, Melbourne, Florida 32901

Frank J. Roethel

Marine Sciences Research Center, State University of New York at Stony Brook, Stony Brook, New York 11794

■ Dewatered sewage sludge (20% solids) was successfully stabilized into block form by using fly ash, gypsum, lime, and Portland cement. Physical and chemical properties, including leachate test, of selected mixes were determined to evaluate the effectiveness of stabilization. The permeability of the stabilized blocks decreased from $\sim 1.0 \times 10^{-5}$ to 4.5×10^{-6} cm s⁻¹ over 330 h and compressive strength ranged between 2000 and 2600 kPa and was found to increase with time after submerging in seawater. Cd, Pb, Cr, and As were found in the EP leachate, but their concentrations were lower than the maximum regulatory concentrations established by the U.S. Environmental Protection Agency. Concentrations of Al, Cu, Zn, and Pb in the exterior portions (<1 cm) of the sewage sludge blocks increased with time after exposure to seawater, suggesting readsorption of Al, Cu, Zn, and Pb onto the seawater submerged stabilized blocks. The concentration of Cd, however, decreased with time. The results indicated that the stabilized sewage sludge blocks maintain their structural integrity in seawater and would be classified as a nonhazardous material.

ocean disposal of sewage sludge should be sought, developed, and evaluated.

A potentially new method for waste management in the ocean is to stabilize wastes into block forms and then to place the blocks at sea to form an artificial structure. Stabilization of energy wastes (coal ash, flue gas desulfurization sludge, and oil ash) has been demonstrated for ocean disposal of these solid wastes generated by electric power plants (10). Stabilized coal wastes, in block form, were used as materials for artificial reef construction in the Atlantic Ocean near Long Island, NY (11), and also in Chesapeake Bay (12); a similar reef constructed with stabilized oil ash blocks has been placed in the coastal water off central Florida (13). This practice not only provided a method for waste disposal but also resulted in a beneficial utilization of the waste materials.

In the present study, dewatered sewage sludge was stabilized within a fly ash matrix to form solid blocks. Test samples with satisfactory properties (e.g., a minimum compressive strength of 2000 kPa) were subjected to physical and chemical tests to determine the effectiveness of the stabilization process. A primary goal of the investigation was to assess, on a laboratory scale, the environmental acceptability of stabilized sewage sludge-fly ash (SS-FA) blocks in the sea. There is potential for using such blocks for construction of artificial reefs. Recent studies investigating stabilized coal ashes in marine applications have shown the blocks to be structurally strong and a potential substrate for marine organisms (11). A provision in the U.S. Ocean Dumping Regulation would permit the utilization of solid "materials" for the purpose of developing, maintaining, or harvesting fisheries resources (14).

Methodology

Test Samples. Test blocks were solid cylinders (11.9 by 10.2 cm) of a sewage sludge-fly ash mixture and were fabricated following the guidelines of ASTM method D698-78 (15). The blocks were compacted in three layers with 25 compactions per layer by use of a 2500-g rammer falling 30 cm; experimental error in compressive strength was ± 150 kPa.

Sewage sludges used in this study were from the Cedar Creek Wastewater Treatment Facility of the County of Nassau, Wantagh, Long Island, NY, and from the Cedarhurst Wastewater Treatment Facility, Cedarhurst (also Nassau County), Long Island. Both facilities produce a

Introduction

Sewage sludge, a concentrated semisolid material resulting from sewage treatment, is currently disposed of in landfills or in the ocean. Alternatives to current disposal practices include utilization (composting or soil additive) and incineration. In the Federal Republic of Germany, for example, composted sewage sludge is applied to agricultural land to improve crop production (1). Sludge incineration is carried out in order to reduce the volume of solids and to provide sterilization (2). Both land and ocean disposal actions have induced considerable argument regarding the potential for pollution and environmental degradation. Disposal of sewage sludge in landfill is in part becoming more difficult in urban areas, due to the scarcity of vacant land, the high costs of disposal operation, and the possibility of groundwater contamination. Incineration of sewage sludge may cause an air pollution problem (2). In the New York/New Jersey region, and also in the United Kingdom, ocean disposal of sludge from sea-going barges has been the preferred method of disposal; off southern California, ocean outfalls are used for sludge disposal (3). At sludge dumpsites, the diversity of organisms has decreased (4-8) and the organisms have experienced an increase in various diseases (4, 9). Because of these effects, other alternatives to the present practice of

Table I. Elemental Concentrations in Sewage Sludge and Fly Ash Prior to Stabilization^a

element	sewage sludge		fly ash
	Cedar Creek	Cedarhurst	
Ca	2.1% (±0.6)	0.5% (±0.1)	2.1% (±0.1)
Al	1.9% (±0.2)	1.2% (±0.2)	9.3% (±0.1)
Si	6.6% (±0.3)	11.9% (±0.5)	18.6% (±0.3)
Cd	19.4 (±0.9)	10.4 (±0.6)	3.8 (±0.5)
Cu	1066 (±32)	748 (±28)	160 (±14)
Zn	1492 (±49)	1300 (±118)	504 (±25)
Pb	262 (±25)	259 (±11)	148 (±11)
Ni	128 (±5)	48 (±9)	217 (±5)
Hg	0.39 (±0.09)	0.14 (±0.03)	0.16 (±0.05)

^aConcentrations expressed in micrograms per gram except where noted. Values in parentheses denote standard deviation ($n = 3$).

Table II. Formulation and Physical Properties of the Mixes^a

	mix types	
	A	B
composition, %		
sewage sludge		
Cedar Creek plant	16	0
Cedarhurst plant	0	16
Ca(OH) ₂	6	6
CaSO ₄ ·2H ₂ O	6	6
Portland cement (type I)	3	3
fly ash	65	66
H ₂ O added	4	3
	100	100
solid contents in sludge, %	27	19
moisture in mix, %	16	16
curing temperature, °C	49	49
curing time, day	7	7
compressive strength, kPa	2500	2600
density, g/cm ³	1.7	1.7

^aAnother set of mixes using CaSO₄·1/2H₂O instead of CaSO₄·2H₂O was also prepared. The physical and engineering properties of the CaSO₄·1/2H₂O mixes were the same, within experimental error, as those for the CaSO₄·2H₂O mixes (21).

secondary anaerobic digested sludge. The sludges had 2% solid content and were dewatered by using a plate and frame press accompanied with air drying to achieve desired solids contents of ~20%. Fly ash used in the research was from the Petersburg power station of the Indianapolis Power and Light Co., Petersburg, IN, and was obtained from Conversion Systems, Inc., Horsham, PA. Lime [Ca(OH)₂], gypsum (CaSO₄·2H₂O), and Portland cement (type I) were the stabilization additives used in this study. Type II cement is recommended for longer term studying in order to minimize sulfate attack by seawater. All additives were certified reagent grade chemicals obtained from Fisher Scientific, Inc., Pittsburgh, PA, except for the Portland cement (type I) which was obtained from a local supplier. The elemental concentrations in sewage sludge and fly ash were determined prior to stabilization (Table I). Samples were freeze-dried and then digested by the HF-H₃BO₃ technique (16, 17). In this method, ~1 g of dry powdered samples were digested by 100 mL of distilled, deionized water-HF-H₃BO₃ (0.5:0.5:90) solution for 24 h; the digests were then filtered through 0.4-μm Millipore filter paper and then analyzed by Atomic absorption spectrophotometry (AAS).

Formulations of the stabilized mixes selected for the physical and chemical testing are shown in Table II. The samples were cured in a kiln set at 49 °C and 98–100%

Table III. Elemental Composition of the Stabilized Sewage Sludge Blocks Prior to Submersing in Seawater^a

elements	mix types ^b	
	A	B
Ca, %	8.5 (±0.1)	8.4 (±0.1)
Al, %	4.2 (±0.1)	4.9 (±0.3)
Si, %	12.1 (±1.1)	11.7 (±0.01)
Cd, μg/g	8.4 (±0.7)	9.7 (±0.4)
Cu, μg/g	182 (±8)	189 (±4)
Zn, μg/g	353 (±6)	358 (±20)
Pb, μg/g	69 (±7)	68 (±3)
Ni, μg/g	168 (±9)	171 (±11)
Hg, μg/g	0.16 (±0.01)	0.13 (±0.01)

^aMix types are described in Table II. ^bValues in parentheses denote standard deviation ($n = 6$, three samples were taken from two blocks with the same mix design).

relative humidity for 7 days. Following removal from the kiln, the samples were air dried at room temperature (23 ± 1 °C) for 3 days before testing. A minimum unconfined compressive strength (18) of 2000 kPa (300 psi) for these test blocks was the criterion for an acceptable block (19). For the chemical studies, SS-FA blocks were ground to fine powder with a porcelain mortar and pestle and then analyzed for Ca, Al, Si, Cd, Cu, Zn, Pb, Ni, and Hg (Table III) by AAS techniques (16, 17).

Physical Tests. (a) Permeability. Permeability of the stabilized solid cylinders was determined by the Darcy falling-head method (20, 21). Seawater (salinity 25–28%) from the Flax Pond Laboratory at the State University of New York, which is adjacent to Long Island Sound, was filtered through 0.4-μm Millipore filter paper and was added to test columns in which the specimens were emplaced. Elutriate from the permeability columns was collected, with starting and finish times and height of the water column recorded. The coefficient of permeability was then calculated based on amount of elutriates, height of the water column at successive intervals, and duration of each measurement (20, 21).

(b) Block Strength. Variation of block strength with time in seawater was studied by using submerged block samples in a flow-through seawater aquarium system at the Flax Pond Laboratory. One block of each mix type was removed from the aquarium each month and tested for unconfined compressive strength with a Riehle Universal testing machine (Model FA160) with a loading rate of 0.064 cm/min.

(c) Morphology of the Block. Scanning electron microscopy (SEM) was used to determine the microscopic morphology of stabilized block materials and to observe crystal growth in order to infer chemical processes that may be occurring in the stabilized mixes both prior to and following submersion in seawater. All test samples for SEM study were freeze-dried prior to placement on a stainless steel stub and gold plating. The analysis was carried out on a JOEL Model 35C (Tokyo, Japan) scanning electron microscope with resolution capability of 100 Å.

Chemical Tests. (a) Leachate Test. U.S. EPA Extraction Procedure (EP). A chemical leachate test on the stabilized blocks was carried out (22). Different portions of each stabilized block were crushed, and a 100-g sample was mixed with 1600 mL of distilled, deionized water in a polypropylene container. The pH of the liquid was measured and adjusted to pH 5.0 by adding 0.5 N acetic acid to the solution. The mixture was shaken for 24 h and then filtered through a 0.45-μm glass-fiber filter. The filtered solution was collected and analyzed for Cd, Pb, Cu, Ni, Co, Cr, Mn, Sr, Ti, As, Hg, Mg, K, and Ca by

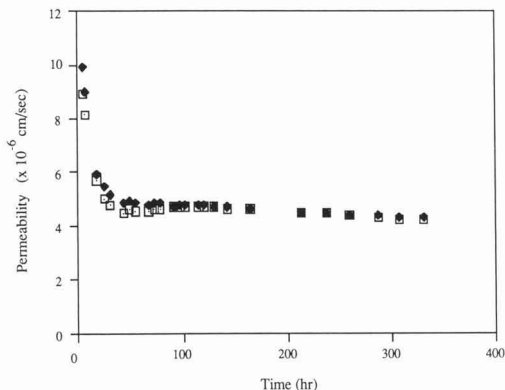


Figure 1. Variation of permeabilities of the stabilized sewage sludge-fly ash blocks in seawater (◆) mix A; (□) mix B.

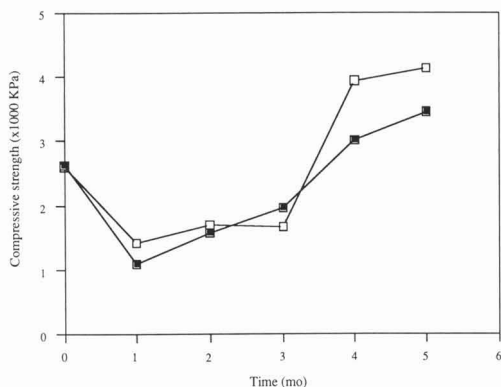


Figure 2. Variation of compressive strength of the stabilized sewage sludge-fly ash blocks in seawater. (□) mix A; (■) mix B.

flame and furnace AAS techniques.

(b) **Elemental Variation in Reacted Blocks.** Variation in elemental concentration at the exterior portion (<1 cm) of the exposed blocks was examined to determine whether chemical dissolution or precipitation processes were occurring on the surfaces of the stabilized blocks exposed to seawater. In this experiment, samples were placed in a tank containing flowing seawater at Flax Pond Laboratory. One sample of each mix type was removed from the tank each month and exterior portions, no thicker than 1 cm, of test samples were digested by the HF-H₃BO₃ digestion technique (16, 17) and analyzed for Cd, Cu, Zn, Pb, and Al by both flame and furnace AA. These results were then compared to elemental concentrations in unreacted blocks.

Results and Discussion

Permeability. Permeability of the stabilized blocks (mixes A and B, see Table III) decreased rapidly from $\sim 1.0 \times 10^{-5}$ to 4.5×10^{-6} cm s⁻¹ within the first 30 h of the experiment and then decreased slowly with time after ~ 40 h (Figure 1). The rapid change may be due to one or a combination of the following possibilities: (1) saturation by seawater of the permeable pore spaces in the block, (2) precipitation and/or cementation occurring in the pore spaces, or (3) disaggregation, at the microscopic level, of the test samples causing blockage of the pore spaces.

Compressive Strength. Figure 2 shows the changes in compressive strength of test samples that had been

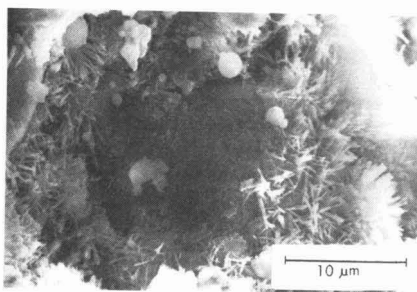
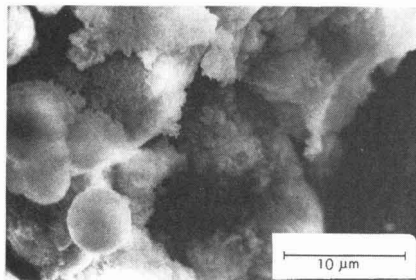


Figure 3. Scanning electron micrographs of (top) unreacted block and (bottom) reacted block.

submerged in a seawater tank at the Flax Pond Laboratory for up to 5 months. Prior to submersion, block strengths ranged between 1850 and 2600 kPa. In the first month after submersion, compressive strength decreased to ~ 1000 kPa. After the initial decline, the strength of the blocks began to increase and surpassed the initial values after 5 months of submersion.

Morphology. Scanning electron micrographs (SEM) of unreacted and reacted blocks (relative to seawater exposure for 4 months; Figure 3) revealed small, needle-shaped crystals dominating the interior of the reacted blocks. The needle-shaped crystal formations, which developed when the blocks were in seawater, were not observed in unreacted blocks. The presence of these crystals in the reacted block supports the hypothesis that cemental precipitation is an important process leading to decreased permeability and increased compressive strength. Double and Hellaway (23) indicate that needle formations in cement may be the hydration products (hydrated silicates) in the reaction responsible for the solidification of concrete. Also, needle formations, in stabilized coal waste blocks have been attributed as the cause for the improvement of the compressive strength of these blocks in seawater (24, 25).

Leachate Test. Although the goal of the study was to understand the behavior of the stabilized sewage sludge-fly ash blocks in seawater, the EPA leachate test was conducted because it is the currently accepted standard criterion for recognizing hazardous wastes. The results of leachate analyses are given in Table IV. Calcium was the major component of the leachate followed by potassium and magnesium. The high Ca leachate was the result of the presence of the Ca(OH)₂ and CaSO₄·2H₂O in excess of that needed in stabilization.

The elements Cd, Pb, Cr, and As, for which the U.S. EPA has established maximum concentration limits in

Table IV. EPA Leachate Composition of Stabilized Sewage Sludge-Fly Ash Blocks^a

element	leachate concn, $\mu\text{g/g}$	EPA max concn, $\mu\text{g/g}$	element	leachate concn, $\mu\text{g/g}$	EPA max concn, $\mu\text{g/g}$
Cd	0.0 (± 0.003)	1.0	Sr	7.05 (± 1.00)	
Pb	0.02 (± 0.009)	5.0	Ti	19.40 (± 2.90)	
Cu	21.87 (± 0.56)		As	2.01 (± 0.88)	5.0
Ni	2.15 (± 0.10)		Hg	0.00	0.2
Co	0.54 (± 0.06)		Mg	110 (± 10)	
Cr	1.45 (± 0.03)	5.0	K	1000 (± 30)	
Mn	0.08 (± 0.02)		Ca	37000 (± 470)	

^a Values in parentheses denote standard deviation ($n = 3$).

Table V. Variation of Elemental Concentration of Exposed Blocks Surfaces

element	time, month	mix types ^a	
		A	B
Al, %	0	4.2 (± 0.1)	4.9 (± 0.3)
	1	4.6 (± 0.0)	6.7 (± 0.2)
	2	6.6 (± 0.2)	8.0 (± 0.3)
	3	7.8 (± 0.0)	7.8 (± 0.3)
Cd, $\mu\text{g/g}$	0	8.4 (± 0.7)	9.7 (± 0.4)
	1	7.8 (± 0.4)	7.8 (± 0.4)
	2	5.8 (± 0.3)	6.3 (± 0.3)
	3	3.6 (± 0.2)	4.2 (± 0.3)
Cu, $\mu\text{g/g}$	0	$r = 0.85$	$r = 0.95$
	1	182 (± 8)	189 (± 4)
	2	247 (± 9)	189 (± 13)
	3	224 (± 14)	215 (± 10)
Zn, $\mu\text{g/g}$	0	279 (± 4)	234 (± 25)
	1	$r = 0.85$	$r = 0.95$
	2	353 (± 6)	358 (± 20)
	3	432 (± 4)	390 (± 6)
Pb, $\mu\text{g/g}$	0	435 (± 5)	413 (± 1)
	1	447 (± 8)	456 (± 27)
	2	$r = 0.86$	$r = 0.99$
	3	69.0 (± 7.0)	68.0 (± 3.0)
	1	80.2 (± 3.5)	81.5 (± 5.2)
	2	93.1 (± 2.3)	94.6 (± 4.4)
	3	91.4 (± 4.9)	100.8 (± 4.4)
		$r = 0.98$	$r = 0.99$

^a Mix types are described in Table II. r represents the correlation coefficient.

leachates, were also found in the leachate (Table IV). None of the maximum concentration limits for these elements were exceeded in the leachate from the crushed samples. Thus, the stabilized blocks used in this study would not be classified as hazardous materials according to EPA criteria.

Variation in Elemental Concentration in Reacted Blocks. Concentrations of Al, Cu, Zn, and Pb in the exterior portions (<1 cm) of the blocks increased with time during exposure to seawater; a steady decrease of Cd was also observed (Table V). Linear regressions, fitted by the method of least squares (26) to the series of concentration measurements versus duration of immersion, showed significant positive slopes for Al, Cu, Zn, and Pb and a significant negative slope for Cd. (Correlation coefficients ranged from $r = 0.92$ to $r = 0.99$ for Pb and Al; from $r = 0.77$ to $r = 0.99$ for Zn and Cu, and from $r = -0.97$ to $r = -0.99$ for Cd.) The increased concentration of Al is likely due to changes in the fly ash/sewage sludge ratio. The Al concentration in the samples appears to be approaching that measured in fly ash, indicating that the test samples experienced a decline in sludge content. This alteration

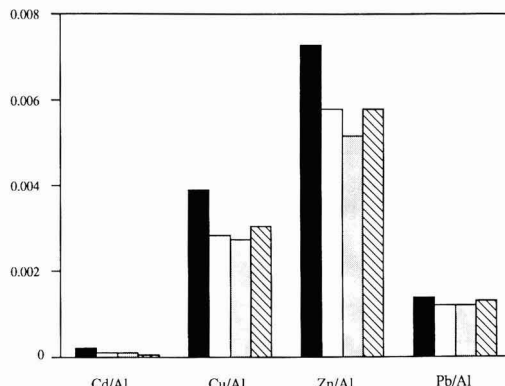


Figure 4. Variation of the ratio of Cd, Cu, Zn, and Pb to Al of exposed sewage sludge-fly ash blocks. (■) initial ratio prior to submersion; (□) 1-month submersion; (▨) 2-month submersion; (▩) 3-month submersion.

is likely due to decomposition of sewage sludge contained on the outer shell of the blocks that were directly exposed to seawater. The ratios of metals relative to Al, a fairly conservative element, were calculated (Figure 4). Only the Cd/Al ratio showed a linear decline with time ($r = -0.96$ to $r = -0.99$), suggesting that leaching of Cd was a function of the decomposition of sludge. Decomposition of sewage sludge in the exterior of the blocks should also result in the decrease in concentrations of Pb, Zn, and Cu, because these elements were very enriched in the sewage sludge. However, ratios of Zn/Al, Pb/Al, and Cu/Al showed fluctuations with time (Figure 4), indicating the possibility that readsorption of these ions back onto the blocks was occurring or the blocks were removing trace elements from seawater.

Conclusions

The results of this investigation have shown that sewage sludge can be stabilized into block form by using fly ash, lime, gypsum, and cement. The stabilized sewage sludge blocks maintain their structural integrity following submersion in seawater and would be classified as nonhazardous material according to the U.S. EPA leachate test. The stabilization of sewage sludge and fly ash into solid blocks may provide an acceptable option for artificial reef construction. Further investigations should consider bioassays, assessment of the fate of sewage-sludge-derived carbon, and processing, in trial runs, large quantities of sewage sludge-fly ash mixes by using concrete block machines.

Acknowledgments

We thank the Marine Sciences Research Center, the Department of Materials Science and Engineering, and the Department of Biology for the use of their facilities. We also thank Iver W. Duedall for valuable suggestions and discussions.

Registry No. Cd, 7440-43-9; Pb, 7439-92-1; Cu, 7440-50-8; Ni, 7440-02-0; Co, 7440-48-4; Cr, 7440-47-3; Mn, 7439-96-5; Sr, 7440-24-6; Ti, 7440-32-6; As, 7440-38-2; Hg, 7439-97-6; Mg, 7439-95-4; K, 7440-09-7; Ca, 7440-70-2; gypsum, 13397-24-5.

Literature Cited

- Blickwedel, P. T.; Mach, R. *Forum Stadte-Hyg.* 1983, 34, 122-124.
- Burd, R. S. Water Pollution Control Research Series Pub. No. WP-20-4, U.S. Department of the Interior, 1968.

- (3) Brooks, N. H.; Arnold, R. G.; Koh, R. C. Y.; Jackson, G. A.; Faisst, W. K. In *Oceanic Processes in Marine Pollution*; Krieger Publishing Co.: Melbourne, FL, 1987; Vol. 2, pp 99-115.
- (4) Rees, E. I. S.; Walker, A. J. M.; Ward, A. R. In *Out of Sight Out of Mind, Report of a Working Party on Sludge Disposal in Liverpool Bay*; Department of the Environment, Her Majesty's Stationery Office: London, 1972; Vol. 2, pp 297-343.
- (5) Bascom, W. *Environ. Sci. Technol.* 1982, 16, 226A-236A.
- (6) Read, P. A.; Anderson, K. J.; Matthews, J. E.; Watson, P. G.; Halliday, M. C.; Shiells, G. M. *Mar. Pollut. Bull.* 1983, 14, 12-16.
- (7) Lyons, W. B.; Armstrong, P. B.; Gaudette, H. E. *Mar. Pollut. Bull.* 1983, 14, 65-68.
- (8) Lear, D. W.; O'Malley, M. L. In *Wastes in the Ocean*; Duedall, I. W., Ketchum, B. H., Park, P. K., Kester, D. R., Eds.; Wiley-Interscience: New York, 1983; Vol. 1, pp 293-312.
- (9) Jenkins, S. H. *Mar. Pollut. Bull.* 1982, 13, 37-39.
- (10) Duedall, I. W.; Roethel, F. J.; Seligman, J. D.; O'Connors, H. B.; Parker, J. H.; Woodhead, P. M. J.; Dayal, R.; Chezar, B.; Roberts, B. K.; Mullen, H. In *Ocean Dumping of Industrial Wastes*; Ketchum, B. H., Kester, D. R., Park, K., Eds.; Plenum: New York, 1981; pp 315-346.
- (11) Woodhead, P. M. J.; Parker, J. H.; Duedall, I. W. *Mar. Fish. Rev.* 1982, 44, 16-23.
- (12) Duedall, I. W.; Humphries, E. M., final report to Power Plant Siting Program, State of Maryland, Annapolis, MD, 1982.
- (13) Kalajin, E. H.; Duedall, I. W.; Shieh, C. S.; Wilcox, J. R. Fourth International Conference on Artificial Habitats for Fisheries, Miami, FL, 1987.
- (14) *Fed. Regist.* 1977, 42, No. 220.
- (15) *Ann. Book ASTM Stand.* 1980, Part 19, 201-207.
- (16) Heaton, M. G.; Buyer, J. S.; Hershey, J. P.; Duedall, I. W. *Environ. Technol. Lett.* 1982, 3, 529-540.
- (17) Silberman, D.; Fisher, G. L. *Anal. Chim. Acta* 1979, 106, 299-307.
- (18) *Ann. Book ASTM Stand.* 1979, Part 14, 24-27.
- (19) Parker, J. H.; Woodhead, P. M. J.; Duedall, I. W. In "Coal Waste Artificial Reef Program", EPRI CS-2009, Vol. 2, Project 1341-1, interim report, prepared for Electric Power Research Institute, Palo Alto, CA, 1981; pp 51-77.
- (20) Verbeck, G. J. *ASTM Spec. Tech. Publ.* 169a, 1968, 211-219.
- (21) Shieh, C. S. MS. Thesis, Marine Sciences Research Center, State University of New York at Stony Brook, 1984.
- (22) *Fed. Regist.* 1977, 43, No. 222.
- (23) Double, D. D.; Hellaway, A. *Sci. Am.* 1977, 237, 79-90.
- (24) Roethel, F. J. Ph.D. Dissertation, Marine Sciences Research Center, State University of New York at Stony Brook, 1981.
- (25) Duedall, I. W.; Buyer, J. S.; Heaton, M. G.; Oakley, S. A.; Okubo, A.; Dayal, R.; Tatro, M.; Roethel, F.; Wilke, R. J.; Hershey, J. P. In *Wastes in the Ocean*; Duedall, I. W., Ketchum, B. H., Park, P. K., Kester D. R., Eds. Wiley-Interscience: New York, 1983, Vol. 1, pp 375-395.
- (26) Sokal, R. R.; Rohlf, F. J. In *Biometry: The Principles and Practice of Statistics in Biological Research*; Freeman: San Francisco, CA, 1969.

Received for review December 16, 1986. Accepted July 25, 1988. This research was funded by the Ocean Assessments Division of National Oceanic and Atmospheric Administration and Nassau County, Long Island, NY.

Theoretical and Experimental Evidence for Artifact Particulate Matter Formation in Electrical Aerosol Analyzers

Arthur W. Stelson

Dolphus E. Milligan Science Research Institute, Atlanta University Center, Inc., Atlanta, Georgia 30310

■ An artifact signal was observed in an electrical aerosol analyzer (EAA) when sulfur dioxide was introduced into a filtered aerosol inlet gas stream. This signal is explainable by hydroxyl radical-sulfur dioxide chemistry leading to sulfuric acid formation. Theoretical expressions are derived for the amount of sulfuric acid formed based on inlet sulfur dioxide concentration and measured channel currents. The experimental data and predictions agree within an order of magnitude. Exact agreement is obtainable by allowing the aerosol size to vary within channel 2 of the EAA. Calculated sulfur dioxide concentrations large enough to cause a measurable current change in each channel of the electrical aerosol analyzer indicate artifact particulate matter formation will mainly be a problem with combustion source characterization where sulfur dioxide concentrations are in excess of 1000 ppm; though care may be necessitated with ambient measurements.

Introduction

Since its development, the electrical aerosol analyzer (EAA) has proven to be a valuable tool in appraising aerosol size distributions for submicron aerosols. In addition to many ambient air applications, the EAA has been used to appraise source aerosol size characteristics (1, 2). In ambient air and smog chamber applications, doubt has arisen concerning measured size distribution quality and the possibility of artifact particulate formation within the EAA (3, 4). If artifact aerosol formation is causing a

problem with ambient air measurements, then an increased concern should exist for source level measurements in effluents containing a greater abundance of aerosol precursors.

Marlow attributed variation in aerosol size distribution measurement in the presence of sulfur dioxide to nonideal aerosol diffusion charging (5, 6). He accounted for variance by particle dielectric constant and ion mobility distribution effects in addition to ion and aerosol polydispersities. Liu and Pui performed very careful experiments to show sulfur dioxide at 0.52 ppm had little effect on aerosol measurement with the EAA (7). This paper will demonstrate, by comparing theoretical predictions with experimental measurements, that the EAA can form artifact particulate matter under certain conditions, and this artifact can cause a significant interference in source measurements.

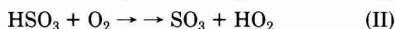
Theoretical Analysis

The operation of the EAA and the analysis of data measured with it is described in detail by Liu and Pui (8). The instrument consists of three sections: an aerosol charger, a mobility analyzer, and an electrometer current sensor. The aerosol charger is based on diffusion charging from a positive corona discharge. In analysis of the possible sources of artifact aerosol formation, the corona discharge seemed a likely source. After analysis of the literature concerning the chemistry of positive corona discharges in the presence of oxygen, nitrogen, and water

vapor, all papers indicated hydroxyl radicals were formed in equal concentrations to secondary ions (9-12). For example, one positive nitrogen molecule in the presence of water would form one secondary ion and a hydroxyl radical. Positively charged oxygen and water molecules would have the same results. Thus, hydroxyl radicals are generated within the aerosol charger of the EAA.

Since previous researchers had indicated sulfur dioxide caused an interference within the EAA, a simple experiment was performed. A total filter was placed over the aerosol inlet, and sulfur dioxide was introduced into the aerosol inlet through the total filter. A large interference was observed in channels 2 and 3 of the EAA. From this experiment, it was hypothesized that sulfur dioxide was reacting with oxygen, hydroxyl radicals, and water to form sulfuric acid aerosol which was subsequently charged causing a current in the electrometer current sensor.

The chemistry of sulfuric acid formation is outlined as follows:



Reaction I is the rate-controlling step in this sequence so

$$d[\text{H}_2\text{SO}_4]/dt = k_1[\text{OH}][\text{SO}_2] \quad (1)$$

Since only a small amount of sulfuric acid is formed in comparison to the sulfur dioxide concentration, the sulfur dioxide concentration can be assumed to be constant. The hydroxyl radical concentration would also be constant because the charging rate is constant. Thus, eq 1 can be integrated to yield

$$[\text{H}_2\text{SO}_4] = k_1[\text{OH}][\text{SO}_2]t \quad (2)$$

But the hydroxyl radical concentration-time product, $[\text{OH}]t$, is equal to the ion concentration times the charger residence time, Nt , so

$$[\text{H}_2\text{SO}_4] = k_1[\text{SO}_2]Nt \quad (3)$$

The amount of sulfuric acid formed within the EAA can be predicted from known quantities; the EAA's charger Nt , the sulfur dioxide concentration, and the reaction rate coefficient, k_1 .

The reaction rate coefficient can be taken from a compilation of reaction rate coefficients of atmospheric interest similar to the one edited by Hampson and Garvin (12). From Hampson and Garvin, the ratio of the hydroxyl radical-sulfur dioxide reaction rate coefficient to the hydroxyl radical-carbon monoxide reaction rate coefficient was taken as 4.3 (Castelman and Tang's value). Their recommendation for the hydroxyl radical-carbon monoxide reaction rate coefficient in air at 1 atm is $3.0 \times 10^{-13} \text{ cm}^3 \text{ molecule}^{-1} \text{ s}^{-1}$. Thus, the hydroxyl radical-sulfur dioxide reaction rate coefficient is $\sim 1.29 \times 10^{-13} \text{ cm}^3 \text{ molecule}^{-1} \text{ s}^{-1}$.

By substituting appropriate quantities and conversions in eq 3, an expression for the amount of sulfuric acid formed as a function of sulfur dioxide formed is obtained;

$$[\text{H}_2\text{SO}_4]_M = 3.18 \times 10^8 [\text{SO}_2]_p \quad (4)$$

where $[\text{H}_2\text{SO}_4]_M$ has units of molecules per cubic centimeter and $[\text{SO}_2]_p$ has units of ppm.

The amount of sulfuric acid formed can be also predicted from the measured instrument response;

$$[\text{H}_2\text{SO}_4]_M = \sum_i \left(\frac{\Delta N}{\Delta I} \right)_i d_{pi}^3 \Delta I_i (\rho_i x_i / M_{sa}) N_{AVG} \pi / 6 \quad (5)$$

where $(\Delta N / \Delta I)_i$ is the EAA channel sensitivity as measured by Liu and Pui (8) (in particles $\text{cm}^{-3} \text{ V}^{-1}$), d_{pi} is the

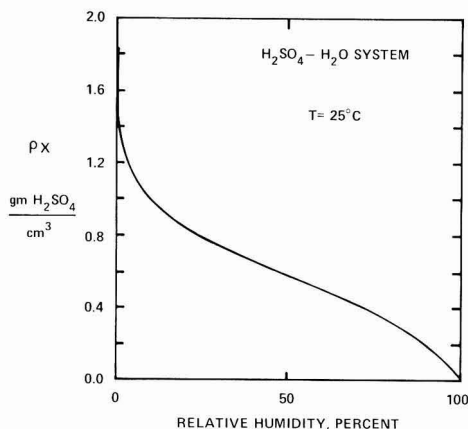


Figure 1. Solution density-mass fraction H_2SO_4 product versus relative humidity for H_2SO_4 - H_2O system at 25°C .

EAA channel log mean diameter (in cm), ΔI_i is the EAA channel current (in V), ρ_i is the sulfuric acid aerosol density (in g cm^{-3}), x_i is the mass fraction sulfuric acid in the aerosol, M_{sa} is the molecular mass of sulfuric acid (in g g^{-1}), and N_{AVG} = Avogadro's number (in molecules g^{-1}). Note the EAA channel current has units of volts because the current is being measured by an electrometer. For the EAA used in this study, the conversion of the electrometer voltage to current is 1 V/pA . Since signals were observed in channels 2 and 3 in the simple experiment with filtered air and sulfur dioxide, eq 5 reduces to

$$[\text{H}_2\text{SO}_4]_M = \left(\frac{\Delta N}{\Delta I} \right)_2 d_{p2}^3 \Delta I_2 (\rho_2 x_2 / M_{sa}) N_{AVG} \pi / 6 + \left(\frac{\Delta N}{\Delta I} \right)_3 d_{p3}^3 \Delta I_3 (\rho_3 x_3 / M_{sa}) N_{AVG} \pi / 6 \quad (6)$$

Substituting values into eq 6 results in

$$[\text{H}_2\text{SO}_4]_M = 1.29 \times 10^{10} \rho_2 x_2 \Delta I_2 + 3.15 \times 10^9 \rho_3 x_3 \Delta I_3 \quad (7)$$

where $[\text{H}_2\text{SO}_4]_M$ has units of molecules per cubic centimeter, ρ_2 and ρ_3 have units of grams per cubic centimeter, and ΔI_2 and ΔI_3 have units of volts.

In Figure 1, ρx is shown as a function of relative humidity for the sulfuric acid-water system at 25°C . This figure was constructed with water activities from Robinson and Stokes and density data from Beattie et al. (14, 15). Figure 1 applies for flat solution surfaces, and this application involves small aqueous droplets with a large curvature. Thus, the Kelvin equation must be used.

The generalized Kelvin equation for water in the sulfuric acid-water droplet can be written as

$$RT \ln \frac{\text{RH}_d}{\text{RH}_s} = \frac{4\sigma v_w}{d_p} - \frac{6x_s v}{d_p} \frac{d\sigma}{dx_s} \quad (8)$$

where R = the ideal gas constant (in $\text{erg g}^{-1} \text{ K}^{-1}$), T = the temperature (in K), RH_d = the relative humidity over the droplet, RH_s = the relative humidity over a flat surface, σ = the solution surface tension (in dyn cm^{-1}), v_w = the partial molar volume of water (in $\text{cm}^3 \text{ g}^{-1}$), d_p = the droplet diameter (in cm), x_s = the mole fraction of sulfuric acid, and v = the molar volume of the solution (in $\text{cm}^3 \text{ mol}^{-1}$) (16). For the concentration region studied by this work, $d\sigma/dx_s$ is approximately zero or very small, so eq 8 can be approximated by

$$RT \ln \frac{\text{RH}_d}{\text{RH}_s} = \frac{4\sigma v_w}{d_p} \quad (9)$$

Table I. EAA Response to Various Sulfur Dioxide Concentrations

SO ₂ concn, ppm	analyzer current step point voltages ^a			av RH, %
	2	3	4	
0	<0.002	<0.002	<0.002	~46
70	5.1	0.26	0.003	~46
88	6.1	0.30	0.001	~46
145	7.9	0.52	0.003	~46
390	10.5	1.3	0.003	~46
1050	13.5	2.2	0.006	~46
1570	13.8	2.0	0.010	~46

^a Analyzer current for channel 2 is equal to analyzer current step point voltage 2 - analyzer current step point voltage 3.

Table II. Theoretical Predictions and Experimental Evidence for Sulfuric Acid Formation within the EAA

[SO ₂] _p ppm	[H ₂ SO ₄] _M , molecules cm ⁻³				(5) ^b	(6) ^c
	eq 4 (1)	channel 2 (2)	channel 3 (3)	eq 7 (4) ^a		
70	2.22 (10)	4.40 (10)	5.39 (8)	4.45 (10)	0.499	1.2
88	2.80 (10)	5.18 (10)	6.26 (8)	5.24 (10)	0.534	1.2
145	4.62 (10)	6.71 (10)	1.08 (9)	6.82 (10)	0.677	1.6
390	1.24 (11)	8.39 (10)	2.71 (9)	8.66 (10)	1.43	3.1
1050	3.34 (11)	1.03 (11)	4.60 (9)	1.08 (11)	3.09	4.3
1570	5.00 (11)	1.07 (11)	4.19 (9)	1.11 (11)	4.50	3.8

^a Column 4 is defined as the sum of columns 2 and 3. ^b (1)/(4). ^c (3)/(4) × 100.

Note recent theoretical study indicates eq 8 should not include the second term on the right-hand side (17). If this work is correct, then eq 9 is more readily derived.

The physical constants for eq 9 are obtainable from the literature (15, 18). By using eq 9 and Figure 1 and knowing the mean diameter of each EAA channel and the relative humidity of the air entering the EAA, $\rho_i x_i$ can be determined and [H₂SO₄]_M becomes a function of the measured currents in each channel.

Thus, the amount of sulfuric acid formed within the EAA can be predicted two ways: one by knowing the sulfur dioxide concentration in the aerosol inlet stream and another by knowing the relative humidity of the air entering the EAA and the measured EAA channel current differences.

Experimental Description

The responses of the EAA in channels 2 and 3 was measured as a function of sulfur dioxide concentration over the range of 70–1570 ppm. A cylinder containing 0.921% sulfur dioxide in nitrogen was blended with filtered line air (dew point ~-40 °C) to make dilute sulfur dioxide mixtures. A rotameter dilution system was used for blending in which the rotameters were calibrated by using bubble flowmeters. The sulfur dioxide-nitrogen-air

mixtures were simultaneously flowed into the aerosol inlet of a Thermo Systems, Inc. Model 3030 Electrical Aerosol Analyzer (EAA), and an Environment One Rich 100 Condensation Nuclei Monitor (CNC). Excess gas mixture was vented into the room. The EAA charger sheath air and the mobility analyzer clean air were taken from the room. The room air was 24.1–24.9 °C and ~50% relative humidity as taken by a sling psychrometer. The maximum nuclei concentration measured by the CNC was ~1000 particles cm⁻³, indicating the majority of particulate matter was removed by the filter. The EAA response in absence of sulfur dioxide was ~0.000 V.

The results of this experimental study are shown in Table I. With this data, the theoretical expressions previously derived can be examined. It should be noted that the instrument response varied with time, and these values are the initial values after subjecting the filtered aerosol inlet gas stream to sulfur dioxide. The instrument response gradually decreased with a half-life between 20 and 40 min. The reason for this decrease is undetermined at this time, but indications are the aerosol charger was producing less hydroxyl radicals. After the instrument was purged with clean air, the initial response was again obtained.

The actual sulfate concentration was inferred instead of measured because only a small amount of material is formed within the EAA, 1.5 µg of sulfate/m³ at 1570 ppm sulfur dioxide. For sampling at the EAA total flow rate, ~11 h would be required to reach the sensitivity of an ion chromatograph without preconcentration columns. This time was too long considering the variable instrument response.

Discussion

The theoretical predictions for sulfuric acid formation based on eq 4 are compared with predictions based on eq 7 in Table II. Table II, column 5, shows both predictions are of the same order of magnitude. This agreement indicates the validity of the theoretical analysis. Also, Table II, column 6, shows the majority (>95%) of the aerosol is deposited in channel 2.

Since the sensitivity of the EAA is a strong function of aerosol diameter in channel 2, an additional calculation was performed. The amount of sulfuric acid monomer formed was calculated by using eq 4, this value was equated to the first term of eq 6, and the EAA sensitivity was calculated. By use of the expression for EAA sensitivity of Richards, the diameter corresponding to the calculated sensitivity was determined (19). Table III summarizes the results. The density-mass fraction product was calculated by an iterative process, but Table III shows that approximating the product as the product corresponding to the log mean channel diameter leads to minimal error. Also, Table III shows the calculated particle diameter decreases as the sulfur dioxide concentration increases. This result is as expected because a higher sulfur

Table III. Calculated Aerosol Diameter Based on Variable Sensitivity within Channel 2

[SO ₂] _p , ppm	[H ₂ SO ₄] _M (eq 4), molecule cm ⁻³	$d_p^3(\Delta N/\Delta I)$, µm ³ cm ⁻³ V ⁻¹	d_p^a , µm	RH _s , %	ρx , g of H ₂ OSO ₄ cm ⁻³	d_p^b , µm
70	2.22 (10)	2.04	0.0088	36	0.685	0.0089
88	2.80 (10)	2.18	0.0087	36	0.685	0.0088
145	4.62 (10)	2.78	0.0082	35	0.695	0.0082
390	1.24 (11)	5.99	0.0068	33	0.710	0.0068
1050	3.34 (11)	13.1	0.0056	31	0.730	0.0056
1570	5.00 (11)	18.8	0.0051	30	0.740	0.0050
		4.02	0.0075	34	0.705	

^a First iterative calculation of aerosol diameter. ^b Second iterative calculation of aerosol diameter.

Table IV. Maximum Sulfur Dioxide Concentration for Measurable Analyzer Current Change (0.001 V) in Each Channel

channel	$(\Delta N/\Delta I)_i^a$ $\text{cm}^{-3} \text{V}^{-1}$	d_{pi}^a , μm	$(\Delta N/\Delta I)_i d_{pi}^3$ $\mu\text{m}^3 \text{cm}^{-3} \text{V}^{-1}$	$[\text{SO}_2]_p$, ppm
2	9.52 (6)	0.0075	4.02	0.074
3	4.17 (5)	0.0133	0.981	0.018
4	1.67 (5)	0.0237	2.22	0.041
5	8.70 (4)	0.0422	6.54	0.121
6	4.44 (4)	0.075	18.7	0.346
7	2.41 (4)	0.133	56.7	1.05
8	1.23 (4)	0.237	164	3.02
9	6.67 (3)	0.422	501	9.25
10	3.51 (3)	0.750	1480	27.3

^aReference 8.

dioxide concentration would result in a smaller nucleation diameter for the aerosol or higher sulfuric acid supersaturation. Additional proof to the theoretical analysis is the range of diameters calculated from the sensitivities. The calculated range is 0.0050–0.0089 μm , which closely corresponds to the EAA channel 2 range of 0.0056–0.01 μm measured by Liu and Pui (8).

A question of concern when operating an EAA is "What sulfur dioxide concentration will cause a measurable difference in the EAA signal?" The answer to this question is dependent on the prevailing relative humidity within the EAA, the EAA channel of interest, the amount and size of aerosol present, and the host gas composition. For illustrative purposes, the relative humidity will be assumed to be approximately zero so $\rho_i x_i = 1.8255$. This hypothetical case will yield the maximum sulfur dioxide concentration for a measurable current change in each channel. Equating eq 4 with each term of eq 5 yields the desired expression

$$[\text{SO}_2]_p = 1.85 \times 10^{-2} d_{pi}^3 (\Delta N/\Delta I)_i \quad (10)$$

where d_{pi} has units of microns. By using the sensitivities and log mean diameters from Liu and Pui, the maximum sulfur dioxide concentration corresponding to a measurable current change in each channel (0.001 V) can be calculated (8). The results are summarized in Table IV.

Note the results in Table IV illustrate the problem associated with appraising the effect of artifact aerosol formation on a measured size distribution. The effect of artifact material will be dependent on preexisting aerosol size and the amount of aerosol or scavenging. As relative humidity increases, the effect of sulfur dioxide should become more dramatic ($\rho_i x_i$ decreases). An additional problem is the host gas or aerosol surface could scavenge hydroxyl radicals, making the interference more variable. This discussion shows the complexity of this interference. Table IV should be used as a general guide to the order of magnitude of sulfur dioxide concentrations at which artifact aerosol formation presents a problem. This table indicates extreme care should be used when measuring aerosol from combustion sources, and even with ambient applications, problems may exist.

Conclusions

The feasibility of artifact aerosol formation from sulfur dioxide within the EAA was theoretically and experi-

mentally demonstrated. The artifact signal will be dependent on the amount of water vapor, sulfur dioxide concentration, and preexisting aerosol loading. Care should be exercised when applying the EAA to characterization of combustion sources, but calculations indicate minimal problems exist for ambient applications where the sulfur dioxide loading is much smaller.

Acknowledgments

I thank Joe Leone and Dale Warren for performing the experiments while students at the California Institute of Technology.

Registry No. SO_2 , 7446-09-5; H_2SO_4 , 7446-03-9.

Literature Cited

- (1) Markowski, G. R.; Filby, R. *Environ. Sci. Technol.* **1985**, *19*, 796–804.
- (2) Dittenhoefer, A. C.; De Pena, R. G. *Atmos. Environ.* **1978**, *12*, 297–306.
- (3) Marlow, W. H.; Reist, P. C.; Dwiggin, G. A. *J. Aerosol Sci.* **1976**, *7*, 457–462.
- (4) Su, J. Experimental Studies on Aerosol Formation in the NH_3 -HCl and NH_3 - SO_2 Systems at ppm Concentration Levels. M.S. Thesis, Department of Chemical Engineering, University of Kentucky, 1979.
- (5) Marlow, W. H. *J. Colloid Interface Sci.* **1978**, *64*, 543–548.
- (6) Marlow, W. H. *J. Colloid Interface Sci.* **1978**, *64*, 549–554.
- (7) Liu, B. Y. H.; Pui, D. Y. H. *J. Aerosol Sci.* **1979**, *10*, 103–106.
- (8) Liu, B. Y. H.; Pui, D. Y. H. *J. Aerosol Sci.* **1975**, *6*, 249–264.
- (9) Young, C. E.; Falconer, W. E. *J. Chem. Phys.* **1972**, *57*, 918–929.
- (10) Good, A.; Durden, D. A.; Kebarle, P. *J. Chem. Phys.* **1970**, *52*, 222–229.
- (11) Shahin, M. M. *J. Chem. Phys.* **1967**, *47*, 4392–4398.
- (12) Shahin, M. M. *J. Chem. Phys.* **1965**, *45*, 2600–2605.
- (13) Hampson, R. F., Jr.; Garvin, D. Eds. *Reaction Rate and Photochemical Data for Atmospheric Chemistry—1977*. NBS Spec. Publ. (U.S.) **1978**, No. 513.
- (14) Robinson, R. A.; Stokes, R. H. *Electrolyte Solutions; The Measurement and Interpretation of Conductance, Chemical Potential and Diffusion in Solutions of Simple Electrolytes*, Butterworths: London, 1959; p 477.
- (15) Beattie, J. A.; Brooks, B. T.; Gillespie, L. J.; Scatchard, G.; Schumb, W. C.; Tefft, R. F. Density (Specific Gravity) and Thermal Expansion (Under Atmospheric Pressure) of Aqueous Solutions of Inorganic Substances and of Strong Electrolytes. In *International Critical Tables of Numerical Data: Physics, Chemistry and Technology*; McGraw-Hill: New York, 1928; Vol. III, pp 25, 56–57.
- (16) Seinfeld, J. H. *Atmospheric Chemistry and Physics of Air Pollution*; Wiley: New York, 1986; p 366.
- (17) Wilemski, G. *J. Chem. Phys.* **1984**, *80*, 1370–1372.
- (18) Young, T. F.; Harkins, W. D. Surface-Tension Data for Certain Pure Liquids between 0 and 360 °C and for All Types of Solutions at All Temperatures. In *International Critical Tables of Numerical Data: Physics, Chemistry and Technology*; McGraw-Hill: New York, 1928; Vol. IV, p 464.
- (19) Richards, L. W. The Reduction of Data from the Electrical Aerosol Analyzer. Presented at the Aerosol Measurement Workshop, University of Florida, March, 1976.

Received for review March 23, 1988. Revised manuscript received July 11, 1988. Accepted July 28, 1988. This work was partially supported by the California Institute of Technology and the Pittsburgh Energy Technology Center of the U.S. Department of Energy through Grant No. DE-FG22-87PC79911.



COPYRIGHT STATUS FORM

Name of American Chemical Society Publication

Author(s)

Ms No.

Ms Title

Received

This manuscript will be considered with the understanding you have submitted it on an exclusive basis. You will be notified of a decision as soon as possible.

[THIS FORM MAY BE REPRODUCED]

For
the
author's
use and
address

COPYRIGHT TRANSFER

The undersigned, with the consent of all authors, hereby transfers, to the extent that there is copyright to be transferred, the exclusive copyright interest in the above cited manuscript (subsequently referred to as the "work") to the American Chemical Society subject to the following (Note: if the manuscript is not accepted by ACS or if it is withdrawn prior to acceptance by ACS, this transfer will be null and void and the form will be returned.):

- A. The undersigned author and all coauthors retain the right to revise, adapt, prepare derivative works, present orally, or distribute the work provided that all such use is for the personal noncommercial benefit of the author(s) and is consistent with any prior contractual agreement between the undersigned and/or coauthors and their employer(s).
B. In all instances where the work is prepared as a "work made for hire" for an employer, the employer(s) of the author(s) retain(s) the right to revise, adapt, prepare derivative works, publish, reprint, reproduce, and distribute the work provided that all such use is for the promotion of its business enterprise and does not imply the endorsement of the American Chemical Society.
C. Whenever the American Chemical Society is approached by third parties for individual permission to use, reprint, or republish specified articles (except for classroom use, library reserve, or to reprint in a collective work) the undersigned author's or employer's permission will also be required.
D. No proprietary right other than copyright is claimed by the American Chemical Society.
E. For works prepared under U.S. Government contract or by employees of a foreign government or its instrumentalities, the American Chemical Society recognizes that government's prior nonexclusive, royalty-free license to publish, translate, reproduce, use, or dispose of the published form of the work, or allow others to do so for noncommercial government purposes. State contract number:

SIGN HERE FOR COPYRIGHT TRANSFER [Individual Author or Employer's Authorized Agent (work made for hire)]

Print Author's Name

Print Agent's Name and Title

Original Signature of Author on Behalf of All Authors (in Ink)

Date

Original Signature of Agent (in Ink)

CERTIFICATION AS A WORK OF THE U.S. GOVERNMENT

This is to certify that ALL authors are or were bona fide officers or employees of the U.S. Government at the time the paper was prepared, and that the work is a "work of the U.S. Government" (prepared by an officer or employee of the U.S. Government as a part of official duties), and, therefore, it is not subject to U.S. copyright. (This section should NOT be signed if the work was prepared under a government contract or coauthored by a non-U.S. Government employee.)

INDIVIDUAL AUTHOR OR AGENCY REPRESENTATIVE

Print Author's Name

Print Agency Representative's Name and Title

Original Signature of Author (in Ink)

Date

Original Signature of Agency Representative (in Ink)

FOREIGN COPYRIGHT RESERVED (NOTE: If your government permits copyright to be transferred, refer to section E and sign this form in the top section.)

If ALL authors are employees of a foreign government that reserves its own copyright as mandated by national law, DO NOT SIGN THIS FORM. Please check this box as your request for the FOREIGN GOVERNMENT COPYRIGHT FORM (Blue Form) which you will be required to sign. If you check this box, mail this form to: Copyright Administrator, Books and Journals Division, American Chemical Society, 1155 Sixteenth Street, N.W., Washington, D.C. 20036, U.S.A.

13th
SYMPOSIUM ON
AQUATIC
TOXICOLOGY
and
RISK ASSESSMENT

April 16-18, 1989 Atlanta, Georgia

For a free program booklet, contact:

Tina Battista, ASTM
1916 Race Street
Philadelphia, PA 19103
215/299-5461.



INVITATION AND CALL FOR ABSTRACTS

FIRST ANNUAL MEETING OF THE
INTERNATIONAL SOCIETY FOR
ENVIRONMENTAL EPIDEMIOLOGY (ISEE)

September 13-15, 1989

This symposium will be held at Brookhaven National Laboratory, Upton, Long Island, New York. Papers on all aspects of environmental epidemiology are invited. One day of the conference will be dedicated to health effects of water disinfection.

Deadline for submission of abstracts: April 1989. For information and abstract forms contact:

Leonard D. Hamilton, M.D., Ph.D., Head
Biomedical and
Environmental Assessment Division
Building 475
Brookhaven National Laboratory
Upton, New York 11973-5000 U.S.A.

Phone: (516) 282-2003/2004
Telex: 6852516 BNL DOE

ENVIRONMENTAL SCIENCE & TECHNOLOGY

ES&T



**The premiere
research
publication in the
environmental
field.**

Environmental science continues to be one of the fastest growing fields. And ES&T has grown right along with it!

ES&T continues to give you the practical, hard facts you need on this science . . . covering research, techniques, feasibility, products and services.

Essential reading for environmental scientists both in the business and academic world . . . ES&T has increased its emphasis on peer-reviewed research dealing with water, air, and waste chemistry in addition to adding critical reviews of important environmental science issues—all relevant to understanding the management of our natural environment.

Also included are discussions on environmental analyses, governmental regulations, current environmental lab activities, and much more!

For rate information, and to subscribe, call toll free:

(800) 424-6747